

<https://doi.org/10.15388/vu.thesis.724>

<https://orcid.org/0000-0003-0822-8651>

VILNIUS UNIVERSITY

Martyna Koplūnaitė

# Chemoenzymatic Synthesis of Nucleoside 5'-Monophosphates

**DOCTORAL DISSERTATION**

Natural Sciences,  
Biochemistry (N 004)

VILNIUS 2025

The dissertation was prepared between 2020 and 2024 at the Department of Molecular Microbiology and Biotechnology, Institute of Biochemistry, Life Sciences Center, Vilnius University. The research was partially funded by Research Council of Lithuania (LMTLT) (projects 01.2.2-LMT-K-718-03-0082; 09.3.3.-LMT-K-712-15-0108; S-MIP-22-6; and 01.2.2-CPVA-K-703-03-0023) and Vilnius University (scholarship for academic accomplishments).

**Academic Supervisors** – Prof. Dr. Rolandas Meškys [Vilnius University, Natural Sciences, Biochemistry – N 004] (2021–2024), Dr. Daiva Tauraitė [Vilnius University, Natural Sciences, Chemistry – N 003] (2020–2021).

This doctoral dissertation will be defended in a public meeting of the Dissertation Defence Panel:

**Chairman** – Dr. Julija Armalytė [Vilnius University, Natural Sciences, Biology – N 010].

**Members:**

Dr. Renata Gudiukaitė [Vilnius University, Natural Sciences, Biology – N 010],

Dr. Mantas Mališauskas [Lundbeck, Denmark, Natural Sciences, Biochemistry – N 004],

Prof. Dr. Saulius Serva [Vilnius University, Natural Sciences, Biochemistry – N 004],

Dr. Asta Zubrienė [Vilnius University, Natural Sciences, Biochemistry – N 004].

The dissertation shall be defended at a public meeting of the Dissertation Defence Panel at 2 p.m. on 21 February 2025 in Room R401 of the Life Sciences Center, Vilnius University.

Address: Sauletekio av. 7, Vilnius, LT-10257, Lithuania.

Tel. +37052234420; e-mail: [info@gmc.vu.lt](mailto:info@gmc.vu.lt)

The text of this dissertation can be accessed at Martynas Mažvydas National Library of Lithuania or the Lithuanian Academic Electronic Library, as well as on the website of Vilnius University:

[www.vu.lt/lt/naujienos/ivykiu-kalendorius](http://www.vu.lt/lt/naujienos/ivykiu-kalendorius)

<https://doi.org/10.15388/vu.thesis.724>

<https://orcid.org/0000-0003-0822-8651>

VILNIAUS UNIVERSITETAS

Martyna Koplūnaitė

# Chemofermentinė nukleozidų 5'-monofosfatų sintezė

**DAKTARO DISERTACIJA**

Gamtos mokslai,  
Biochemija (N 004)

VILNIUS 2025

Disertacija rengta 2020–2024 metais Vilniaus universiteto Gyvybės mokslų centro Biochemijos instituto Molekulinės mikrobiologijos ir Biotechnologijos skyriuje.

Mokslinius tyrimus dalinai rėmė Lietuvos mokslo taryba (projektai 01.2.2-LMT-K-718-03-0082; 09.3.3.-LMT-K-712-15-0108; S-MIP-22-6; ir 01.2.2-CPVA-K-703-03-0023) ir Vilniaus universitetas (stipendija už akademinis pasiekimus).

**Moksliniai vadovai** – prof. dr. Rolandas Meškys [Vilniaus universitetas, gamtos mokslai, biochemija – N 004] (2021–2024), dr. Daiva Tauraitė [Vilniaus universitetas, gamtos mokslai, chemija – N 003] (2020–2021).

Gynimo taryba:

**Pirmininkė** – dr. Julija Armalytė – [Vilniaus universitetas, gamtos mokslai, biologija – N 010].

**Nariai:**

dr. Renata Gudiukaitė [Vilniaus universitetas, gamtos mokslai, biologija – N 010],

dr. Mantas Mališauskas [Lundbeck, Danija, gamtos mokslai, biochemija – N 004],

prof. dr. Saulius Serva [Vilniaus universitetas, gamtos mokslai, biochemija – N 004],

dr. Asta Zubrienė [Vilniaus universitetas, gamtos mokslai, biochemija – N 004].

Disertacija ginama viešame Gynimo tarybos posėdyje 2025 m. vasario mėn. 21 d. 14 val. Vilniaus universiteto Gyvybės mokslų centro R401 auditorijoje. Adresas: Saulėtekio al. 7, Vilnius, LT-10257, Lietuva.

Tel. +37052234420; el. paštas: [info@gmc.vu.lt](mailto:info@gmc.vu.lt)

Disertaciją galima peržiūrėti Lietuvos nacionalinėje Martyno Mažvydo bibliotekoje, Lietuvos akademinėje elektroninėje bibliotekoje ir VU interneto svetainėje adresu:

*<https://www.vu.lt/naujienos/ivykiu-kalendorius>*

## CONTENTS

LIST OF ABBREVIATIONS .....	8
INTRODUCTION.....	10
1. LITERATURE OVERVIEW .....	15
1.1. Nucleosides and their derivatives .....	15
1.2. Nucleotide biosynthesis in living cells .....	20
1.3. Chemical nucleoside phosphorylation .....	23
1.4. Enzymatic nucleoside monophosphate synthesis .....	26
1.4.1. Phosphoribosyltransferases.....	27
1.4.2. Non-specific acid phosphatases .....	28
1.4.3. Nucleoside kinases.....	29
1.4.3.1. <i>Drosophila melanogaster</i> deoxynucleoside kinase .....	35
1.4.3.2. <i>Bacillus subtilis</i> deoxycytidine kinase.....	40
1.5. Phosphate donor regeneration.....	42
2. EXPERIMENTAL .....	46
2.1. General information.....	46
2.1.1. Chemicals.....	46
2.1.2. Purification and analysis of synthesized compounds .....	46
2.1.3. Gene sources and bacterial strains .....	47
2.1.4. Reagents for plasmid construction.....	47
2.1.5. Computer software.....	47
2.2. Chemical synthesis of modified nucleosides .....	48
2.2.1. Synthesis of $N^4$ amino acid-acylated nucleosides.....	48
2.2.2. Synthesis of <i>N</i> -4-(2'-deoxycytidinyl)amino acid amides.....	48
2.3. Enzymatic synthesis of modified nucleoside 5'-monophosphates .....	49
2.3.1. Cloning of target genes .....	49
2.3.2. Site-Directed Mutagenesis.....	49
2.3.3. Expression of target genes and purification of the enzymes .....	50

2.3.4. Optimization of reaction conditions catalysed by <i>DmdNK</i> -WT and <i>BsdCK</i> -WT.....	51
2.3.4.1. Optimal reaction duration .....	51
2.3.4.2. Optimal temperature.....	51
2.3.4.3. Optimal pH.....	52
2.3.4.4. Optimal nucleoside concentration.....	52
2.3.4.5. Optimal phosphate donor concentration .....	52
2.3.4.6. Optimal nucleoside kinase concentration.....	52
2.3.5. Substrate specificities of the nucleoside kinases .....	53
2.3.6. Larger-scale syntheses of nucleoside 5'-monophosphates.....	54
3. RESULTS AND DISCUSSION .....	56
3.1. Synthesis of $N^4$ amino acid-acylated nucleosides.....	56
3.2. Synthesis of <i>N</i> -4-(2'-deoxycytidinyl)amino acid amides.....	60
3.3. Production of target proteins.....	64
3.4. Optimization of reaction conditions catalysed by <i>DmdNK</i> -WT and <i>BsdCK</i> -WT.....	65
3.5. Substrate specificity of <i>DmdNK</i> -WT .....	68
3.6. Exploring <i>DmdNK</i> active site mutations .....	79
3.6.1. Synthesis and application of the mutant <i>DmdNK</i> variants .....	79
3.6.2. Substrate selection .....	81
3.6.3. Mutations in the hydrophobic cavity of <i>DmdNK</i> active site .....	82
3.6.4. Significance of the Q81 residue in the active centre of <i>DmdNK</i> .....	86
3.6.5. Significance of the W57 residue in the active site of <i>DmdNK</i> .....	88
3.6.6. Differences in phosphorylation of $N^4$ -amino acid modified nucleosides bearing amide and carboxyl functional groups .....	89
3.7. Substrate specificity of <i>BsdCK</i> -WT .....	91
3.8. Enhancing <i>BsdCK</i> substrate diversity via single-site mutagenesis ..	102
3.8.1. Synthesis and application of the mutant <i>BsdCK</i> variants .....	102
3.8.2. Impact of the <i>BsdCK</i> active site mutations.....	102
3.9. Application of <i>DmdNK</i> -WT and <i>BsdCK</i> -WT for a larger-scale synthesis of nucleoside monophosphates .....	107

Final remarks.....	110
CONCLUSIONS.....	112
REFERENCES.....	113
APPENDICES.....	140
SANTRAUKA .....	153
ACKNOWLEDGEMENTS .....	161
LIST OF PUBLICATIONS .....	162
SCIENTIFIC PARTICIPATION .....	163
CURRICULUM VITAE.....	164

## LIST OF ABBREVIATIONS

- ACK – Acetate kinase  
ADK – Adenosine kinase  
AZT – Azidothymidine  
Boc – *tert*-Butyloxycarbonyl  
Boc<sub>2</sub>O – Di-*tert*-butyl dicarbonate  
BsdCK – *Bacillus subtilis* deoxycytidine kinase  
BsdCK-WT – Wild-type *Bacillus subtilis* deoxycytidine kinase  
CDI – 1,1'-Carbonyldiimidazole  
DCC – *N,N'*-Dicyclohexylcarbodiimide  
dAK – Deoxyadenosine kinase  
dCK – Deoxycytidine kinase  
dGK – Deoxyguanosine kinase  
dK – 2,4-Diamino-5-(1'-β-D-2'-deoxyribofuranosyl)-pyrimidine  
DmdNK – *Drosophila melanogaster* deoxynucleoside kinase  
DmdNK-WT – Wild-type *Drosophila melanogaster* deoxynucleoside  
kinase  
DMF – Dimethylformamide  
dNDP – 2'-Deoxynucleoside 5'-diphosphate  
dNMP – 2'-Deoxynucleoside 5'-monophosphate  
dNTP – 2'-Deoxynucleoside 5'-triphosphate  
dK – 2,4-Diamino-5-(1'-β-D-2'-deoxyribofuranosyl)-pyrimidine  
dP – 2-Amino-8-(1'-β-D-2'-deoxyribofuranosyl)-imidazo[1,2-*a*]-1,3,5-  
triazin-4(8H)-one  
dX – 8-(1'-β-D-2'-Deoxy-ribofuranosyl)imidazo[1,2-*a*]-1,3,5-triazine-  
2(8H)-4(3H)-dione  
dZ – 6-Amino-3-(1'-β-D-2'-deoxyribofuranosyl)-5-nitro-1H-pyridin-2-  
one  
*Ec*ACK – *Escherichia coli* acetate kinase  
*Hsd*AK – *Homo sapiens* deoxyadenosine kinase  
*Hsd*CK – *Homo sapiens* deoxycytidine kinase  
*Hsd*GK – *Homo sapiens* deoxyguanosine kinase  
*Hs*TK2 – *Homo sapiens* thymidine kinase 2  
HSV-1 – Herpes simplex type-1 virus  
IMP – Inosine 5'-monophosphate  
IPTG – Isopropyl β-D-1-thiogalactopyranoside  
Mol. eq. – Molar equivalent  
NA – Nucleoside analogue  
NGS – Next-generation sequencing



NHS – *N*-Hydroxysuccinimide  
NDP – Nucleoside 5'-diphosphate  
NDPK – Nucleoside 5'-diphosphate kinase  
NMP – Nucleoside 5'-monophosphate  
NMPK – Nucleoside 5'-monophosphate kinase  
NSAP – Non-specific acid phosphatase  
NTP – Nucleoside 5'-triphosphate  
PEP – Phosphoenolpyruvate  
PolyP – Inorganic polyphosphate  
PP<sub>i</sub> – Inorganic pyrophosphate  
PPK – Polyphosphate kinase  
PRPP – 5-Phosphoribosyl-1-pyrophosphate  
PRT – Phosphoribosyltransferase  
rNK – Ribonucleoside kinase  
SDS-PAGE – Sodium dodecyl sulphate–polyacrylamide gel  
electrophoresis  
TK – Thymidine kinase  
TLC – Thin-layer chromatography  
UCK – Uridine-cytidine kinase  
VZV – Varicella zoster virus  
WT – Wild-type

## INTRODUCTION

Nucleosides and nucleotides are a fundamental class of molecules that play vital roles in the function, regulation, and structure of cells. In addition to storage and transmission of genetic information, nucleotides participate in cell signalling, act as cofactors, serve as an energy source for countless cellular processes, and are crucial in various metabolic pathways (Illes et al., 2000; Rudolph, 1994). The significance of the compounds makes them an interesting study subject in the fields of molecular biology, biotechnology, and pharmacology. Nucleoside and nucleotide analogues are often utilized in enzymatic reactions, where they play roles of substrates or inhibitors to certain enzymes, such as kinases, polymerases, hydrolases or reverse transcriptases (Holec et al., 2018; Jakubovska et al., 2018; Solaroli et al., 2008; Urbelienė et al., 2023). Radio- or fluorescently labelled nucleotides are applied as probes in nucleic acid research (Morgenroth et al., 2011; Saito and Hudson, 2018). In addition, certain nucleoside and nucleotide analogues are known to possess anticancer or antiviral properties, while others are key building blocks in modern RNA vaccines (Arevalo et al., 2022; Guinan et al., 2020; Zenchenko et al., 2021).

Traditionally, modified nucleotides are obtained via chemical phosphorylation (Roy et al., 2016). However, synthetic approaches are far from being perfect and must be chosen wisely depending on the starting nucleoside. Chemical synthesis usually relies on immensely reactive phosphochloride agents, such as phosphorylchloride or salicylic acid phosphorochloridate cyclic anhydride (Burgess and Cook, 2000). The compounds are known to be extremely reactive, hygroscopic, and harmful to the environment. Such reactions generally take multiple steps to complete, require protecting group chemistry, and quite often result in low to medium product yields. A promising alternative to chemical phosphorylation is the application of phosphorylating enzymes. Nucleosides can be converted into the corresponding nucleoside monophosphates by nucleoside kinases, which catalyse a phosphate group transfer from a nucleoside 5'-triphosphate, primarily ATP or GTP, to the 5'-hydroxy group of a nucleoside (Sandrini and Piškur, 2005). Nucleoside kinases are typically substrate-specific enzymes, and their specificities are determined by key amino acid residues in their substrate recognition pocket. The substrate binding is influenced by the size and polarity of these residues, as binding occurs only when favourable interactions between the residues and the nucleoside form. Most nucleoside kinases feature relatively tight substrate binding sites and can accommodate only canonical or modestly modified nucleosides, such as with methylated or

fluorinated nucleobases (Piškur et al., 2004). Thymidine kinase (TK), which is active towards thymidine and 2'-deoxyuridine, is ubiquitous in eukaryotes and prokaryotes (Piškur et al., 2004; Sandrini et al., 2006). However, other deoxynucleoside kinases (dNKs), such as deoxyguanosine kinase (dGK), deoxycytidine kinase (dCK) or deoxyadenosine kinase (dAK), are only present in certain genera. For example, four dNKs with slightly overlapping specificities, TK1, TK2, dCK and dGK, are present in mammalian cells (Johansson et al., 2001). In contrast, insects, such as *Drosophila melanogaster*, possess a single multisubstrate dNK, capable of phosphorylating all canonical deoxynucleosides as well as nucleoside analogues with various substitutions at nucleobase or sugar (Johansson et al., 1999; Knecht et al., 2009; Serra et al., 2014). Furthermore, most bacteria are known to lack dCK, dAK, and dGK activities (Bockamp et al., 1991; Sandrini et al., 2007). Only *Lactobacilli* and *Bacilli* have been documented to phosphorylate all four canonical deoxynucleosides (Ives and Ikeda, 1997; Møllgaard, 1980). For example, dCK from *Bacillus subtilis* has been shown to phosphorylate nucleosides of cytosine and adenine bearing various sugar-moieties (Andersen and Neuhard, 2001). While the substrate selectivity of the kinases can be a limiting factor, the mild reaction conditions and high regioselectivity still makes enzymatic phosphorylation a compelling alternative to chemical nucleotide synthesis.

**The aim of this study** was to explore the nucleoside kinases *DmdNK* and *BsdCK* for the enzymatic synthesis of nucleoside 5'-monophosphates. To attain the aim, the following tasks have been formulated:

- To chemically synthesize  $N^4$ -amino acid-modified 2'-deoxycytidine nucleosides to be utilized as substrates for nucleoside kinases.
- To determine the optimal reaction conditions for *DmdNK* and *BsdCK*.
- To determine the substrate specificities of wild-type *DmdNK* and *BsdCK*.
- To determine the impact of mutations at the active site of *DmdNK*.
- To expand the substrate scope of *BsdCK* via site-directed mutagenesis.
- To scale up an enzymatic synthesis of nucleoside 5'-monophosphates.

### **Scientific novelty and practical value**

In the last few decades nucleoside analogues (NAs) have been receiving ample attention as tools for various enzymatic or nucleic acid research, many are being researched as potential prodrugs (Lapponi et al., 2016; Pruijssers and Denison, 2019; Sinokrot et al., 2017). Alterations of canonical

nucleosides provide a chance to improve the properties of the existing molecules or even give them completely new characteristics. Modifications of nucleobases are usually performed at the C5 position of pyrimidines or C7 position on 7-deazapurines, hence, less is known about the effects of alterations at other nucleobase positions such as  $N^4$  and  $O^4$  of pyrimidines and  $N^6$  and  $O^6$  of purines (Hulpia et al., 2018; Shanmugasundaram et al., 2019). Herein we present a synthesis of novel amino acid and 2'-deoxycytidine conjugates:  $N^4$ -amino acid-acylated 2'-deoxycytidine derivatives and  $N$ -(4-(2'-deoxycytidinyl))amino acid amides. The addition of amino acids to 2'-deoxycytidine enhances the functional diversity of the nucleoside and broadens its potential applications. The compounds expand the existing library of NAs and can serve as substrates for the study of numerous enzymes, such as nucleoside phosphorylases, deaminases, or  $N$ -deoxyribosyl-transferases. Furthermore, they can be utilized as intermediates for chemical or enzymatic synthesis of nucleotides.

The  $N^4$ -amino acid modified deoxycytidines, together with an addition of canonical and modified nucleosides, were employed for the characterisation of two nucleoside kinases: *DmdNK*-WT and *BsdCK*-WT. While there is a fair amount of information on the substrate specificity of *DmdNK*-WT, a major share of the research has been done using canonical nucleosides or nucleoside prodrugs, most of which are fluorinated at the nucleobase or bear modified sugar-moieties, hence, little is known of the enzyme's activity towards  $N^4/O^4$  position modified pyrimidine nucleosides (Johansson et al., 1999; Knecht et al., 2009; Ma et al., 2011; Mikkelsen et al., 2008). In contrast to *DmdNK*-WT, information on the substrate specificity of *BsdCK*-WT is very limited. It is known that the enzyme favours 2'-deoxy- and ribonucleosides of adenine and cytosine, however, there is no data on its activity towards NAs (Andersen and Neuhard, 2001). The pool of NAs, selected for the study of the kinases, contained pyrimidine nucleosides bearing varying size and polarity alterations at the nucleobase- or sugar-moieties.

It was discovered that *DmdNK*-WT is highly active towards pyrimidine nucleosides with small- to medium-sized modifications, such as acetyl or glycinoyl, at the  $N^4/O^4$  positions of the nucleobase, while phosphorylation of pyrimidine nucleosides with altered C5 position is less efficient. Furthermore, small substitutions at ribose 2'- and 3'-positions were found to be also acceptable. The substrate scope of *BsdCK*-WT was revealed to be more inclusive than initially believed. The kinase, in addition to all canonical nucleosides, exhibited high activity towards pyrimidine nucleosides with small  $N^4/O^4$ -substitutions, whereas C5-substituted nucleosides were

phosphorylated less efficiently. Small alterations at ribose 2'- and 3'-positions were also tolerated.

While the substrate specificities of the kinases exceeded expectations, there still were limitations regarding the size and polarity of the accepted nucleoside modifications. *In silico* analysis of the active centres together with site-directed mutagenesis was utilized to create mutant variants of *DmdNK* and *BsdCK* with expanded scopes of accepted substrates. Certain mutations at the substrate binding sites of the kinases, especially V84A, V84G, and A110G in the case of *DmdNK* and R70M together with D93A in the case of *BsdCK*, were found to increase their activity towards *N*<sup>4</sup>-modified cytosine nucleosides that were otherwise phosphorylated very inefficiently or not at all by the wild-type variants.

To explore a more practical side of the nucleoside kinases, *DmdNK*-WT and *BsdCK*-WT were applied for the phosphorylation of three nucleosides: 2'-deoxycytidine, *N*<sup>4</sup>-acetyl-2'-deoxycytidine, and 2-thiouridine. The syntheses of the NMPs were executed at a milligram-scale and were made even more sustainable by utilizing acetate kinase to regenerate depleted GTP.

The findings combined are of significant importance from an industrial viewpoint, as such enzymes can be applied for large-scale manufacturing of nucleotides and their analogues. Chemical nucleoside phosphorylation methods are infamous for their harsh conditions and waste production, are laborious, and often result in low to medium product yields (Burgess and Cook, 2000; Roy et al., 2016). Hence, the high regio- and stereoselectivity, high product yields and mild reaction conditions offered by the nucleoside kinase catalysed reactions pave a new way towards nucleotide production (Ding et al., 2020; Serra et al., 2014; Tao and Xu, 2009). In addition to industrial applications, nucleoside kinases have their place in therapeutics (Saeb et al., 2022; Tamura et al., 2021). For years, suicide gene therapy has been attracting attention as an option for cancer treatment that involves introducing specific genes into tumour cells (Duarte et al., 2012). The genes encode enzymes, in many cases nucleoside kinases, that convert non-toxic prodrugs into toxic metabolites that selectively kill cancer cells but leave healthy tissues unaffected. HSV-1 TK is one of the most common kinases applied in suicide gene therapy (Wang et al., 2011; Fillat et al., 2003). However, the broad substrate range of *DmdNK* and *BsdCK* suggests that these enzymes could have therapeutic potential, as well. Finally, altering the active sites of the nucleoside kinases via site-directed mutagenesis provides a way to enhance the efficiency of the enzymes or even tailor them to suit a desired substrate (Hult and Berglund, 2003).

## Thesis statements

1. Boc-protected  $N^4$ -amino acid-modified deoxycytidines can be attained via a three-step synthesis.
2.  $N$ -4-(2'-Deoxycytidinyl)amino acid amides form during a deprotection reaction of  $N^4$ -amino acid-modified deoxycytidines.
3. Despite their mesophilic nature, *DmdNK*-WT and *BsdCK*-WT retain high enzymatic activities at temperatures as high as 60–70 °C.
4. *DmdNK*-WT and *BsdCK*-WT phosphorylate nucleobase- and sugar-modified pyrimidine nucleosides.
5. Mutations in the active centres of *DmdNK* and *BsdCK* increase their activity towards pyrimidine nucleoside analogues.
6. *DmdNK*-WT and *BsdCK*-WT coupled with a GTP regeneration system can be utilized for a milligram-scale synthesis of NMPs.

# 1. LITERATURE OVERVIEW

## 1.1. Nucleosides and their derivatives

Nucleosides and nucleotides are a group of organic molecules, that can be considered as the backbone of all things living. The compounds serve numerous vital functions in living organisms, from storing and transferring genetic information, to being an energy source for countless cellular processes. Nucleosides are comprised of two main components (**Figure 1**): a nucleobase and a five-carbon sugar molecule, ribose or 2'-deoxyribose, which is attached to the nucleobase via a  $\beta$ -N-glycosidic bond. Nucleobases are further divided into pyrimidines, such as cytosine (C), uracil (U), and thymine (T), and purines, such as adenine (A) and guanine (G). While T and U are usually found as 2'-deoxy- and ribonucleosides, respectively, both forms of C, A, and G are abundant in cells. Nucleosides, that have one or more phosphate groups attached to the sugar-moiety, are known as nucleotides. Nucleotides are the monomeric units of DNA, which encodes genetic information, and RNA, which is required for protein synthesis (Nelson et al., 2021).

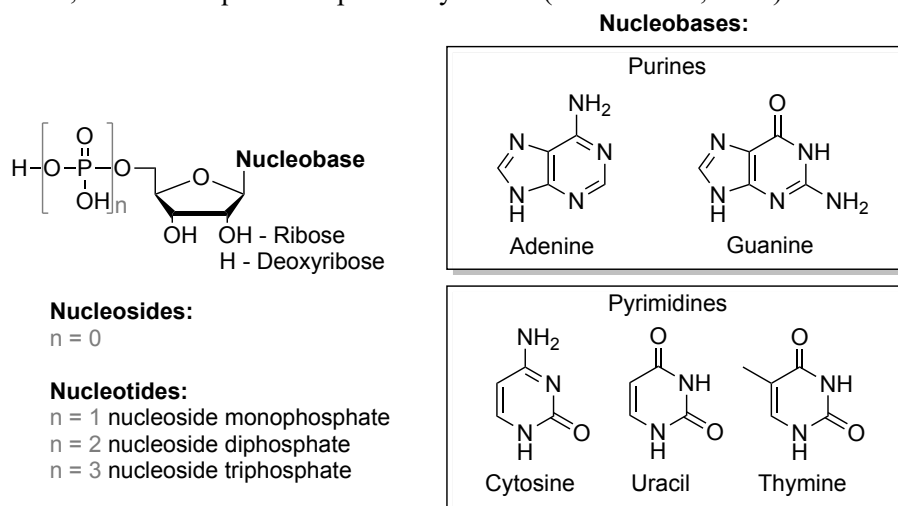


**Figure 1.** Structures of canonical nucleosides and nucleotides.

In addition to being the building blocks of nucleic acids, nucleotides play a pivotal role in cellular metabolism. Nucleoside triphosphates, mainly ATP, are the dominant energy currency in living organisms. Hydrolysis of the high-energy phosphodiester bond between the  $\beta$ - and  $\gamma$ -phosphate groups releases a high amount of free energy that drives almost all cellular processes, including but not limited to biosynthesis, intracellular and extracellular signalling, active transport, and muscle contraction (Akola and Jones, 2003;

Dunn and Grider, 2023; Higgins and Linton, 2004; Holmes and Geeves, 2000). Adenine nucleotides are structural components of some cofactors, including NAD, NADP, FAD, and CoA, while glycosylated nucleotides act as activated intermediates in the biosynthesis oligosaccharides and polysaccharides (Mikkola, 2020; Veech et al., 2019). Furthermore, cyclic nucleotides, such as cAMP and cGMP, and newly discovered cCMP and cUMP, function as secondary signalling molecules in numerous pathways (Gomelsky, 2011; Seifert, 2015).

In addition to the five canonical nucleobases A, T, G, C, and U, nucleic acids contain a variety of modified nucleotides (**Figure 2**), that provide additional informational content. To date, more than 300 modified nucleosides and nucleotides have been discovered in cells (Cappannini et al., 2024). Modifications of procaryotic and eukaryotic DNA are rather conservative and are usually limited to methylation or hydroxymethylation, however, formyl- and carboxyl-modifications were discovered in higher organisms, as well (Moore et al., 2013; Neri et al., 2015). The modified nucleobases encode epigenetic data necessary for the developmental processes of a cell (Dahl et al., 2011; Khavari et al., 2010).

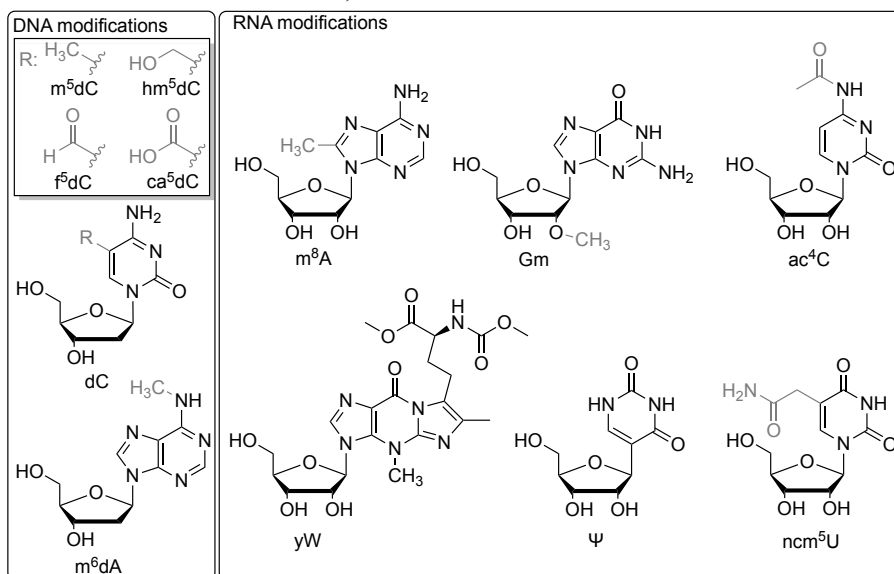


**Figure 2.** Examples of modified nucleosides found in DNA and RNA.  $\text{m}^5\text{dC}$  – 5-methyldeoxycytidine;  $\text{hm}^5\text{dC}$  – 5-hydroxymethyldeoxycytidine;  $\text{f}^5\text{dC}$  – 5-formyldeoxycytidine;  $\text{ca}^5\text{dC}$  – 5-carboxyldeoxycytidine;  $\text{N}^6$ -methyldeoxyadenosine;  $\text{m}^8\text{A}$  – 8-methyladenosine;  $\text{Gm}$  – 2'-O-methylguanosine;  $\text{ac}^4\text{C}$  –  $\text{N}^4$ -acetylcytidine;  $\text{yW}$  – wybutosine;  $\Psi$  – pseudouridine;  $\text{ncm}^5\text{U}$  – 5-carbamoylmethyluridine.



Bacteriophage DNA, however, has been reported to contain more atypical modifications compared to DNA of cellular organisms. Various modified purines and pyrimidines, including but not limited to  $N^6$ -carbamoyl-methyladenine, deoxyarchaeosine, 5-hydroxy-methyldeoxyuracil, and 5-dihydroxypentauracil, have been discovered in bacteriophages (Weigele and Raleigh, 2016). Furthermore, DNA sugar hypermodifications, such as heptoses, hexoses, *N*-acetylhexosamines, or ketodeoxyoctonic acid covalently linked to 5-hydroxymethylcytosine, have been recently identified, as well (Pyle et al., 2024). The roles of bacteriophage DNA modifications are not fully understood. They are believed to protect the DNA from cleavage by host restriction enzymes, take part in the regulation of gene expression and initiation of DNA packaging into the viral capsid (Krüger and Bickle, 1983; Scraba et al., 1983; Sternberg and Coulby, 1990).

RNA, on the other hand, is known to be abundant in modified nucleotides (Carell et al., 2012). There is not a single position of pyrimidine or purine nucleosides that has not been discovered to have a modification, including the ribose moiety (Cappannini et al., 2024). The largest diversity of RNA modifications is found in tRNA. It is estimated that around 10–15% of tRNA nucleotides are modified. The modifications include methylation, acetylation, thiolation, transglycosylation, amino acid addition, deamination, isomerisation and so forth (Phizicky and Alfonzo, 2010). Furthermore, alternative nucleosides are also present, such as pseudouridine, inosine, or wybutosine (Dutta et al., 2022; Fandilolu et al., 2019; Li et al., 2016). The modifications of RNA play numerous cellular roles, including but not limited to proliferation, senescence, cell death, autophagy, and differentiation (Wilkinson et al., 2022).

The involvement of nucleosides does not end in natural cellular processes. Nucleosides and their derivatives are extensively utilised in the fields of biotechnology, biochemistry, and pharmacology (**Figure 3**). Some of the broadly employed research techniques revolve around the use of nucleosides and their phosphates. For example, deoxynucleoside triphosphates are used as the building blocks for DNA amplification during PCR (Garibyan and Avashia, 2013). The first-generation sequencing, also known as Sanger sequencing, is based on the use of radio- or fluorescently labelled dideoxynucleotides, which, when incorporated into an oligonucleotide, terminate further extension of the chain and allow determination of the original DNA sequence (Sanger et al., 1977). In addition, next-generation sequencing (NGS) techniques also rely on nucleotides. For example, Illumina NGS technology, which is known as sequencing by synthesis, uses

fluorescently labelled nucleotides, which, when incorporated into the growing DNA chain, provide a distinct fluorescent signal and allow identification of the added nucleobase (Heather and Chain, 2016). In addition, labelled nucleotides can be applied as probes for the detection and visualisation of DNA and RNA, and other compounds such as proteins, various small molecules, or metal ions (Rist and Marino, 2002; Xu et al., 2017).

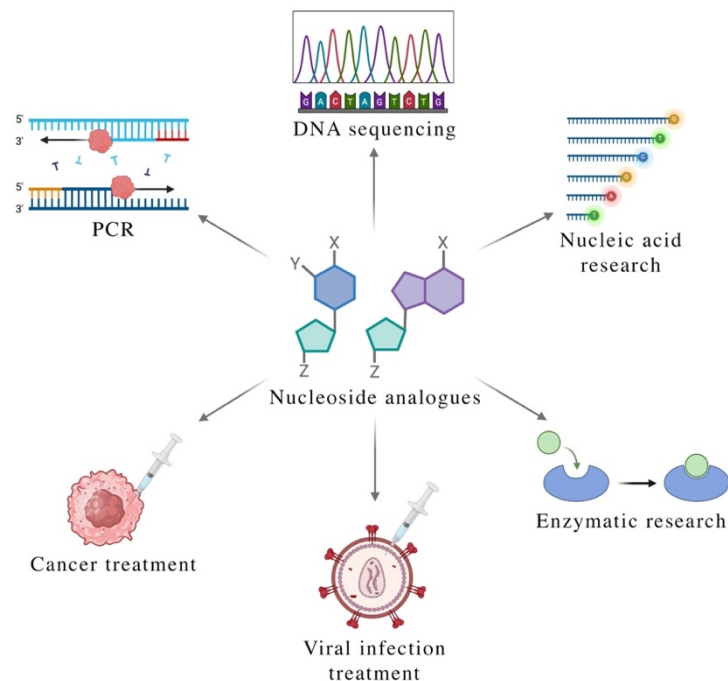


**Figure 3.** Applications of nucleosides and their derivatives. Created with BioRender.com

The importance of nucleosides and their derivatives in the field of enzymatic research should not be understated, as well. The compounds are indispensable research tools that, when utilized as substrates or inhibitors, provide insight into structure, substrate specificity, mechanism and kinetics of enzymes, involved in nucleic acid metabolism, such as kinases, polymerases, deaminases, or reverse transcriptases (Hazra et al., 2010; Hottin and Marx, 2016; Menéndez-Arias et al., 2014; Urbelienè et al., 2023).

Analogues of nucleosides and nucleotides, known as nucleoside prodrugs, are widely recognized as therapeutics for their antiviral, antibacterial, antifungal, anticancer, and antiparasitic properties (**Figure 4**) (Barnadas-Carceller et al., 2023; Shelton et al., 2016; Stauffer et al., 2007; Zenchenko et al., 2021).

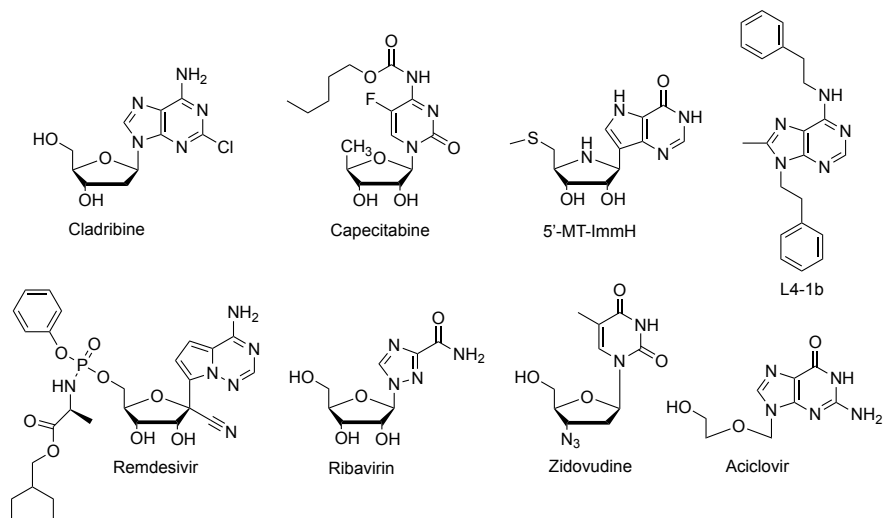


**Figure 4.** Examples of nucleoside derived prodrugs. Cladribine – treatment of hairy cell leukaemia (Hoffman et al., 1997); capecitabine – treatment of metastatic breast and colorectal cancers (Walko and Lindley, 2005); 5'-MT-ImmH – 5-methylthio-immucillin-H, targeted against *Plasmodium falciparum* (Ting et al. 2005); L4-1b – purine nucleoside analogue, targeted against *Trypanosoma cruzi* (Barnadas-Carceller et al., 2023); remdesivir – treatment of SARS-CoV-2 infection (Beigel et al., 2020); ribavirin – treatment of hepatitis C and hepatitis E viral infections (Crotty et al., 2000); zidovudine – treatment of HIV infection (Gulick et al., 1997); aciclovir – treatment of herpes simplex virus infection (Kesson, 1998).

Nucleoside-based drugs are designed to mimic natural nucleosides; hence, they utilize the same metabolic pathways as their natural counterparts. Upon entering a tumour or a virus/microorganism-infected cell, nucleoside analogues undergo activation – a three-step phosphorylation performed by various kinases, which leads to accumulation of mono-, di-, and triphosphate forms of the nucleoside. Incorporation of such triphosphates into DNA or RNA can lead to termination of chain elongation. In addition, nucleoside and nucleotide analogues can inhibit numerous cellular and viral enzymes, such as DNA or RNA polymerases, DNA methyltransferases, kinases, ribonucleotide reductase, or purine and pyrimidine nucleoside phosphorylase (Jordheim et al., 2013). The first nucleoside analogues to be approved by U. S. Food and Drug Administration were cytarabine, applied for the treatment of acute myeloid leukaemia, and edoxudine, which acted as an antiviral agent (Chu and Fischer, 1962; De Clercq and Shugar, 1975). Since these initial approvals in 1969, dozens of new nucleoside analogues have been approved and applied for treatment of cancer and viral or microorganism infections (Geraghty et al., 2021; Shelton et al., 2016).

Nucleosides and their derivatives are crucial for numerous cellular processes ranging from storage and transfer of genetic information to metabolic regulation. They are also integral in the fields of biotechnology, biochemistry, and pharmacology, where nucleoside-based compounds are widely utilized as research tools or therapeutic agents.

## 1.2. Nucleotide biosynthesis in living cells

As highlighted in the previous section, nucleosides and nucleotides are essential components of life. In addition to being the building blocks of DNA and RNA, nucleosides and their derivatives engage in various metabolic pathways, from providing energy to countless biochemical reactions and being messenger molecules to constituting cofactors and acting as intermediate compounds in biosynthesis. Nucleoside and nucleotide metabolism is strictly controlled and is imperative for the homeostasis of cells. Most organisms use two routes for the synthesis of nucleotides: *de novo* and salvage pathways (**Figure 5**) (Kamatani et al., 2021).

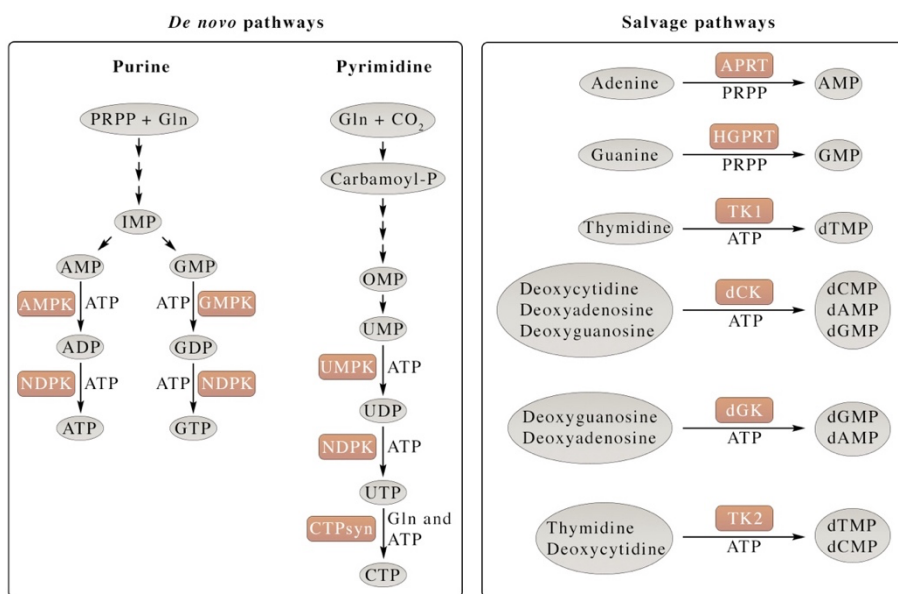


**Figure 5.** *De novo* and salvage nucleotide synthesis pathways. PRPP – 5-phosphoribosyl-1-pyrophosphate; Gln – glutamine; AMPK – adenylate kinase; GMPK – guanylate kinase; NDPK – nucleoside diphosphate kinase; UMPK – uridylate kinase; CTPsyn – CTP synthetase; APRT – adenine phosphoribosyltransferase; HGPRT – hypoxanthine-guanine phosphoribosyltransferase; TK1 – thymidine kinase 1; dCK – deoxycytidine kinase; dGK – deoxyguanosine kinase; TK2 – thymidine kinase 2.

Nucleotides, produced via the *de novo* pathway, are synthesized using precursor compounds derived from glucose and amino acid metabolism, and ammonia and carbon dioxide. The *de novo* synthesis is further divided into the purine and pyrimidine pathways. Purine synthesis begins with a transfer of glutamine-derived amine group to 5-phosphoribosyl-1-pyrophosphate (PRPP). The formed 5-phosphoribosylamine undergoes a series of subsequent reactions to produce inosine 5'-monophosphate (IMP). The IMP biosynthesis from PRPP is a very energy-intensive process, as 5 of the 10 reactions require hydrolysis of ATP or GTP. The final step of the *de novo* purine pathway is the conversion of IMP into AMP or GMP, that also involves hydrolysis of GTP or ATP, respectively (Zalkin and Dixon, 1992). The *de novo* synthesis of pyrimidine nucleotides, that is also known as the orotate-pathway, constitutes of 6 subsequent reactions that result in UMP. In comparison with *de novo* purine synthesis, pyrimidine pathway is slightly less energy-intensive, as only 2 ATP molecules are essential to synthesize the pyrimidine nucleotide precursor UMP. The orotate-pathway starts with the formation of carbamoyl phosphate from glutamine and carbon dioxide. A pyrimidine ring, formed in three additional reactions, is then coupled with a PRPP molecule resulting in orotidine 5'-monophosphate (OMP). The monophosphate is decarboxylated and a first canonical pyrimidine UMP is formed. The UMP is subsequently phosphorylated by kinases into UDP and UTP. Utilizing energy from ATP hydrolysis, an amino group from glutamine is transferred onto the latter and a CTP molecule is formed, which can be dephosphorylated into CMP if needed (Huang and Graves, 2003; Mathews, 2015).

Deoxynucleotides, essential for DNA synthesis and repair, are obtained through the action of ribonucleotide reductase (**Figure 6**). The enzyme reduces the 2'-position of nucleoside 5'-diphosphates (NDPs) to produce nucleoside 2'-deoxy-5'-diphosphates (dNDPs), which are further phosphorylated into dNTPs or dephosphorylated to dNMPs or deoxynucleosides, depending on cellular needs (Mathews, 2015). In addition, methylation of dUMP leads to formation of dTMP (Anderson et al., 2011).

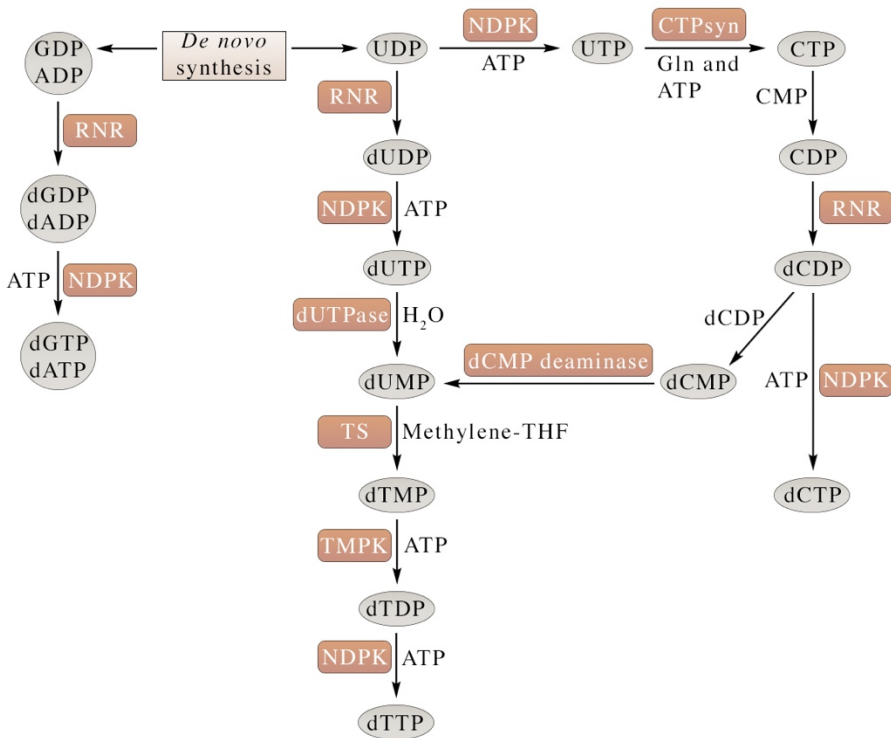


**Figure 6.** *De novo* dNTP synthesis pathways. RNR – ribonucleotide reductase; NDPK – nucleoside diphosphate kinase; dUTPase – dUTP nucleotidohydrolase; TS – thymidylate synthase; THF – tetrahydrofolate; TMPK – thymidylate kinase; CTPsyn – CTP synthetase. CTP and CMP are converted into two CDP, and two dCDP are converted into dCTP and dCMP via myokinase-type reactions. Adapted from Mathews 2015.

The salvage pathway is based on recovering nucleobases or nucleosides derived from DNA or RNA degradation. The pathway is considerably more energy-efficient than the *de novo* synthesis and is driven by various enzymes to obtain nucleoside monophosphates. Majority of purine mononucleotides are obtained from phosphoribosyltransferase catalysed reactions, where purine nucleobases are coupled with PRPP (Nyhan, 2014). However, phosphorylation by nucleoside kinases is also present (Zhulai et al., 2022). In addition, deamination of adenosine results in inosine, which is converted into hypoxanthine and subsequently into IMP (Cristalli et al., 2001). Pyrimidine nucleotides are mostly salvaged through direct phosphorylation by nucleoside kinases, although some bacteria contain phosphoryltransferases that convert free uracil into UMP (Andersen et al., 1992; Nyhan, 2014). Moreover, cytosine and cytidine deaminases catalyse cytosine nucleobase or nucleoside conversions to uracil or its nucleosides (Micozzi et al., 2014).

Tight regulation of nucleoside and nucleotide metabolism is critical for maintaining cellular homeostasis. A multitude of human health issues, such as anaemia, slowed growth, immunodeficiency, autism, gout, or arthritis, are associated with dysregulation of the *de novo* or salvage pathways (Kamatani et al., 2021; Nyhan, 2014). Furthermore, abnormal deoxynucleotide metabolism has been shown to contribute to random DNA mutagenesis, that is linked with cancer development (Ma et al., 2021; Mathews, 2015). One of the most thoroughly researched nucleotide metabolism disorder, the Lesch-Nyhan disease, is caused by a deficiency of hypoxanthine-guanine phosphoribosyltransferase, which is an enzyme from the purine salvage pathway that catalyses the conversion of hypoxanthine and guanine into their corresponding monophosphates. Insufficient activity of the phosphoribosyltransferase promotes accelerated *de novo* purine synthesis and accumulation of uric acid, which leads to multiple health problems such as delayed physical and intellectual development, gout and kidney stones (Nyhan, 1973; Torres and Puig, 2007). Furthermore, a deficiency in thymidine kinase 2 (TK2), which phosphorylates deoxythymidine and deoxycytidine, is known to cause impairments in mitochondrial DNA replication. TK2-deficient patients present with muscle weakness, hepatic failure, respiratory insufficiency, and death within the first two years (Domínguez-González et al., 2019).

### 1.3. Chemical nucleoside phosphorylation

To this day chemical nucleoside phosphorylation is still the preferred option for the synthesis of modified nucleoside 5'-phosphates, however, a universal method, satisfactory for all nucleosides is yet to exist. It is crucial to choose a protocol that is suitable for a particular nucleoside since a method that works for one substrate might not work for another. Protocol selection mainly depends on the functional groups of the substrate and an unwisely chosen method will result in low nucleoside phosphate yields. To date, dozens of nucleotide preparation methods exist and more will be discovered. There are many excellent reviews on the topic, thus only the most popular phosphorylation methods will be elaborated on (Burgess and Cook, 2000; Roy et al., 2016).

Chemical synthesis of the first nucleoside 5'-phosphate dates as far back as 1948, when an adenosine 5'-triphosphate molecule was synthesized using adenosine benzyl phosphate and dibenzyl chlorophosphonate as reactants as displayed in **Figure 7a** (Baddiley et al., 1948). The synthesis was a multistep

process that was laborious and time consuming. Early nucleotide synthesis was often performed using nucleoside 5'-monophosphates (NMPs) as precursors (**Figures 7b** and **7c**). During such synthesis, the substrate's phosphate group was activated by a coupling agent such as *N,N'*-dicyclohexylcarbodiimide (DCC) or 1,1'-carbonyldiimidazole (CDI) (Hoard and Ott, 1965; Moffatt and Khorana, 1961). The formed intermediate was then treated with tributylammonium pyrophosphate, and a nucleoside 5'-triphosphate (NTP) was formed. These early methods often resulted in medium to high product yields, however, a major drawback was that a 5'-monophosphate form was necessary as the precursor molecule.

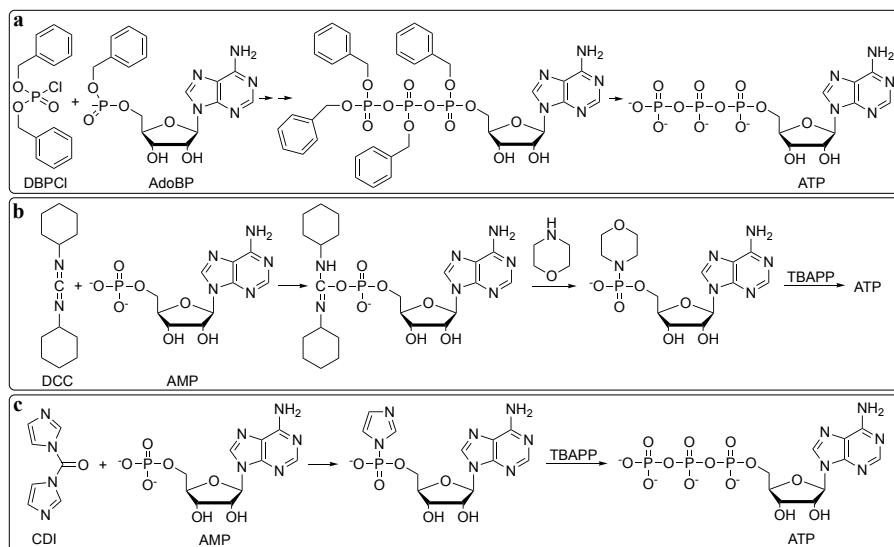


**Figure 7.** Early methods of nucleotide synthesis. **a** ATP synthesis from dibenzyl chlorophosphonate (DBPCI) and adenosine benzyl phosphate (AdoBP). **b** ATP synthesis from AMP and *N,N'*-dicyclohexylcarbodiimide (DCC). **c** ATP synthesis from AMP and 1,1'-carbonyldiimidazole (CDI). TBAPP – tributylammonium pyrophosphate.

As time went on, the interest in nucleosides and nucleotides only grew fonder, various modifications at nucleoside's base or sugar were being introduced, thus new, more advanced nucleoside phosphorylation methods had to be developed. One of the earliest methods for the phosphorylation of nucleoside 5'-hydroxyl group was based on the use of phosphoryl chloride. The phosphorylation, however, was plagued by lack of regioselectivity as immensely reactive phosphoryl chloride reacted not only with the desired 5'-position but with 2'- and 3'-hydroxyl groups, also. Additional protection of 2'- and 3'-positions was necessary to avoid the undesired by-product



formation. A breakthrough happened in 1967 when Yoshikawa and colleagues discovered that the use of trimethyl phosphate or another trialkyl phosphate as a solvent promotes phosphorylation of 5'-position (Yoshikawa et al., 1967). The formed intermediate phosphorodichloridate nucleoside can be hydrolysed to obtain a nucleoside 5'-monophosphate or be used for the synthesis of nucleoside 5'-triphosphates. In 1981, Ludwig and colleagues reported that treatment of the phosphorodichloridate intermediate with bis(tri-*n*)-butylammonium)pyrophosphate in dry dimethylformamide results in a cyclic NTP, which, when hydrolysed, produces NTP with 80–90% yield (**Figure 8a**) (Ludwig, 1981).

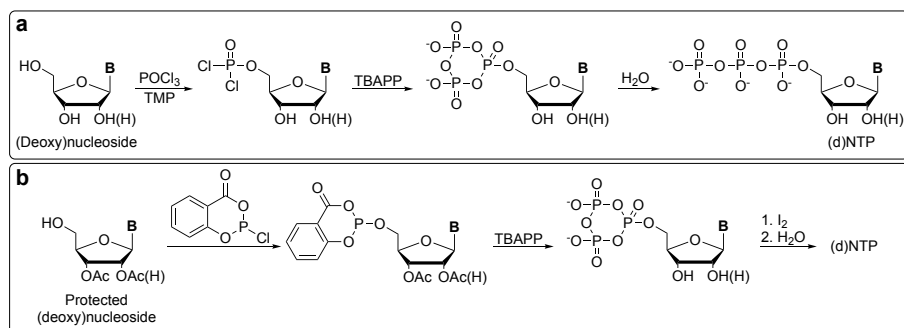


**Figure 8.** Most common (d)NTP synthesis methods. **a** Ludwig procedure. **b** Ludwig-Eckstein approach. **B** – natural or modified nucleobase;  $\text{POCl}_3$  – phosphoryl chloride; TMP – trimethyl phosphate; TBAPP – tributylammonium pyrophosphate.

To date, the Ludwig procedure is still the most commonly used method for the preparation of natural and modified NTPs, however, the product yields can be highly varying depending on the nature of the substrate. Over time certain alterations have been applied to the procedure to increase the phosphorylation efficiency. It was discovered that the use of a proton sponge and execution at a lower temperature increases the rate of phosphorylation during the first step of the synthesis (Gillerman and Fischer, 2010; Kovács and Ötvös, 1988). In addition, replacing dimethylformamide with acetonitrile prevents the formation of Vilsmeier-Haack complex and increases the overall yield of NTP (Kore et al., 2012; Su et al., 2010). Notwithstanding the advancements, Gillerman and Fischer have identified that an abundance of by-products forms during ATP synthesis via Ludwig procedure as displayed in **Figure 9** (Gillerman and Fischer, 2010). Unwanted by-product formation further complicates purification process and decreases the final yield of the product.

Another traditional approach for the synthesis of NTPs involves phosphites and was first described by Ludwig and Eckstein (**Figure 8b**) (Ludwig and Eckstein, 1989). The “one-pot, three-step” procedure starts with treatment of

2',3'-protected nucleoside with salicyl phosphorochloridite in pyridine/dioxane mixture. The reaction mixture is then supplemented with bis(tri-*n*-butylammonium)pyrophosphate in dry dimethylformamide. The resultant cyclic triphosphite is oxidized with iodine in aqueous media and a nucleoside triphosphate is formed. The synthesis was reported to result in 10–50% yields of natural nucleotides (Caton-Williams et al., 2011).

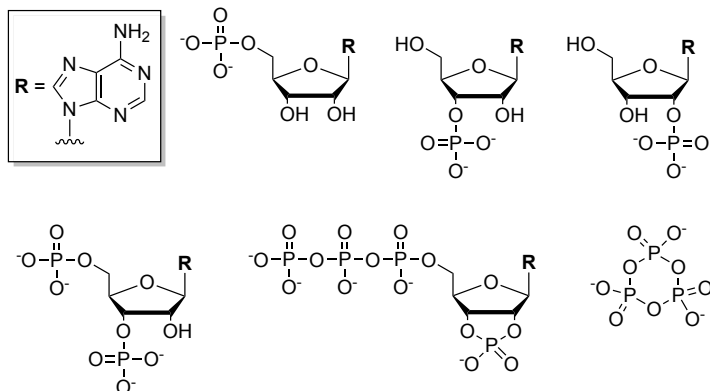


**Figure 9.** By-products formed during ATP synthesis via Ludwig procedure. High reactivity of  $\text{POCl}_3$  leads to indiscriminate phosphorylation of the ribose moiety.

Although many chemical methods for the preparation of NTPs exist, none of them are perfect. The harsh reaction conditions, hydrophobicity of the reagents, inevitable by-product formation, and cumbersome purification of the product are problems with which organic chemists must face. A more efficient and less laborious procedure, applicable for a large diversity of substrates, would be a welcome addition to the existing arsenal of nucleoside phosphorylation methods.

#### 1.4. Enzymatic nucleoside monophosphate synthesis

The immense interest in nucleosides and their derivatives has spurred a search for more effective and sustainable methods for nucleoside phosphorylation. As green chemistry is gaining more and more traction, enzymatic nucleoside phosphate synthesis is considered as a viable alternative to chemical methods. Enzymatic reactions offer many advantages, such as higher final product yield, shorter reaction duration, and enhanced stereo-, regio- and enantioselectivity. Industrial production of naturally occurring ribo- and deoxynucleoside monophosphates is traditionally achieved by enzymatic hydrolysis of RNA and DNA (Bird et al., 2023; Ledesma-Amaro et al., 2013). However, alternative strategies are required to obtain nucleotide

analogues, that bear modifications at their nucleobase or sugar. Various enzymes, that participate in nucleotide metabolism, are being explored as biocatalysts for the biosynthesis of NMPs, such as nucleoside phosphoribosyltransferases, acid phosphotransferases, or nucleoside kinases.

### 1.4.1. Phosphoribosyltransferases

Purine and pyrimidine phosphoribosyltransferases (PRTs) catalyse a reversible phosphoribosyl transfer from PRPP to purine or pyrimidine nucleobase forming nucleoside monophosphate and inorganic pyrophosphate (PP<sub>i</sub>) as displayed in **Figure 11a**. PRTs are crucial in both *de novo* and salvage biosynthesis pathways (Villela et al., 2011; del Arco and Fernandez-Lucas, 2018; Leija et al., 2016). The enzymes have been applied for multiple syntheses of nucleoside monophosphate analogues (**Figures 11b-11d**).

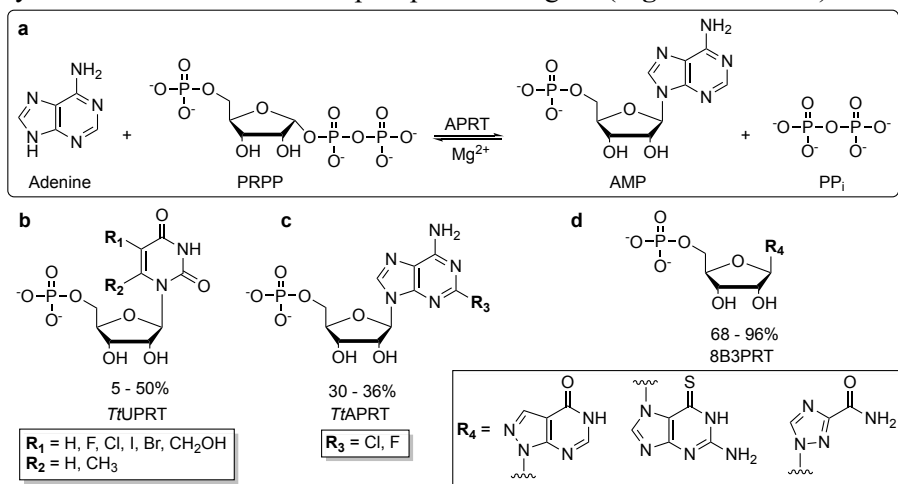


**Figure 11.** Examples of PRT catalysed reactions. **a** Reaction performed by APRT (adenine phosphoribosyltransferase). **b** UMP analogues synthesized using *T. thermophilus* uracil PRT (del Arco et al., 2018). **c** AMP analogues synthesized using *T. thermophilus* adenine PRT (Esipov et al., 2016). **d** Nucleotide analogues synthesized using a mutant variant of *E. coli* hypoxanthine PRT (Scism et al., 2007).

For example, a mutant variant of *Escherichia coli* hypoxanthine PRT was reported to successfully synthesize various base-modified nucleotide monophosphates from purine base analogues and PRPP, with conversion rates of up to 96% (Scism et al., 2007). Moreover, both soluble and immobilized forms of uracil PRT from *Thermus thermophilus* have been applied for the synthesis of non-natural NMPs, using 5- and 6-position modified uracil analogues and PRPP as precursors (del Arco et al., 2020; del Arco et al.,

2018). Furthermore, a multi-enzymatic system, containing a ribokinase from *Thermus* sp. 2.9, and PRPP-synthetase and adenine PRT from *T. thermophilus*, was utilized to synthesise modified NMPs. Hence, 2-chloroadenosine and 2-fluoroadenosine monophosphates were obtained using *D*-ribose and appropriate nucleobases as precursors in the presence of ATP with final conversion rates of around 30% (Esipov et al., 2016).

Majority of the research on nucleoside PRTs is currently focused on their potential as therapeutic agents for the treatment of cancer or viral and bacterial infections, however, as discussed previously, PRTs can be efficient biocatalysts for the synthesis of NMPs, too (Naesens et al., 2013; Parker et al., 2011). Although employing nucleoside PRTs for NMP synthesis can seem like an appealing approach, there are some concerns that should be taken into careful consideration. Firstly, nucleoside PRTs are known to be substrate specific, hence, it is crucial to choose an appropriate one for the substrate used (del Arco and Fernandez-Lucas, 2018). Secondly, as the PRT catalysed reaction is reversible, it is important to find optimal conditions to shift the equilibrium towards nucleotide formation as opposed to its cleavage (Giacomello and Salerno, 1978). Thirdly, PRPP is a high-cost and unstable reagent, thus utilizing nucleoside PRT in a multi-enzymatic cascade, where PRPP is synthesized from inexpensive precursors, might be more fitting (Gross et al., 1983).

#### 1.4.2. Non-specific acid phosphatases

Non-specific acid phosphatases (NSAPs) catalyse a reversible dephosphorylation of organic phosphoesters in acidic conditions (**Figure 12a**). As the name suggests, the enzymes do not exhibit a strict substrate specificity and accept a wide array of substrates, ranging from nucleotides and sugar phosphates to phytic acid. The main cellular role of NSAPs is the free phosphate acquisition, however, they are also known to be involved in the regulation of cellular metabolism and signal transduction (Carmany et al., 2003; Rossolini et al., 1998). Investigation of NSAPs as potential NMP biocatalysts began after discovering that NSAPs from certain bacteria, such as *Morganella morganii*, possess specific activity towards 5'-position of nucleosides. The enzyme can utilize  $PP_i$ , carbamoyl phosphate or acetylphosphate as phosphate donors (Asano et al., 1999). Using *E. coli* cells that overexpressed a mutated NSAP from *M. morganii* was reported to produce IMP with 88% molar yield utilizing  $PP_i$  as a phosphate source (Mihara et al., 2000). In addition, a mutated NSAP from *Escherichia blattae*

was applied for the synthesis of IMP reaching a molar yield of 45% (**Figure 12b**) (Liu et al., 2012).

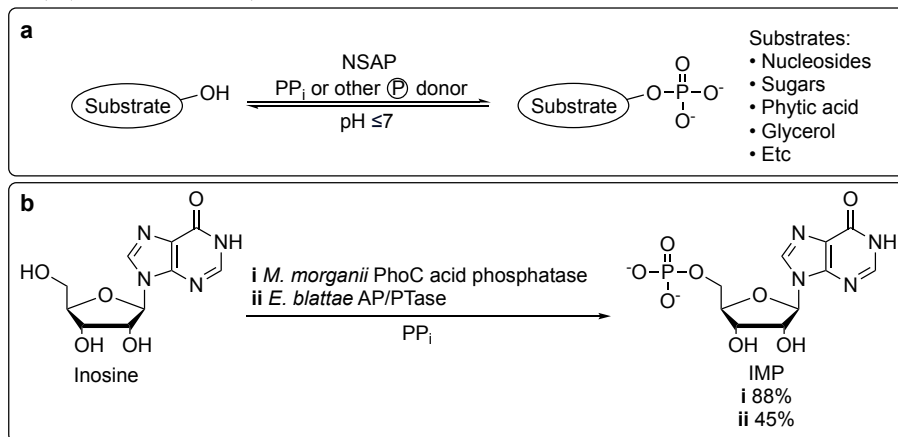


**Figure 12.** Reactions catalysed by NSAPs. **a** General scheme of NSAP catalysed reaction. **b** Examples of NSAPs applied for the biosynthesis of nucleotides (Liu et al., 2012; Mihara et al., 2000).

The main advantage of using NSAPs as biocatalysts in NMP synthesis is that inorganic pyrophosphate can be used as a phosphate donor, which is an inexpensive, readily available and non-toxic reagent. On the other hand, NSAPs are characterised as hydrolases, thus, a thorough reaction optimisation is essential to minimize dephosphorylation of produced NMP. In addition, substrate specificity should also be considered, as NSAPs were shown to favour ribonucleosides over 2'- and 3'-deoxyribonucleosides (Asano et al., 1999).

### 1.4.3. Nucleoside kinases

Ribonucleoside kinases (rNKs) and deoxynucleoside kinases (dNKs) are enzymes that catalyse an irreversible  $\gamma$ -phosphate group transfer from a donor nucleoside 5'-triphosphate, usually ATP or GTP, to an acceptor ribonucleoside or 2'-deoxynucleoside, respectively, resulting in ribonucleoside or 2'-deoxynucleoside 5'-monophosphate and nucleoside 5'-diphosphate as displayed in **Figure 13**. Divalent metal ions, usually magnesium, are crucial for the activity of nucleoside kinases (Suzuki et al., 2004; Yu et al., 2011). In addition to catalysing the initial step in nucleotide salvage pathway, rNKs and dNKs are also responsible for *in vivo* activation of various antiviral and antitumour agents (Deville-Bonne et al., 2010; Slot Christiansen et al., 2015; Van Rompay et al., 2001).

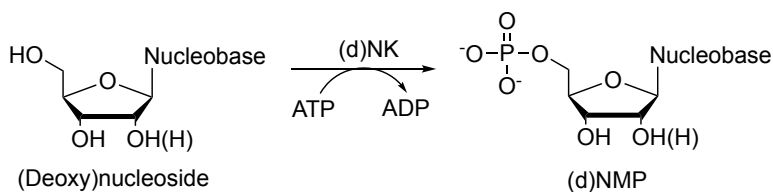


**Figure 13.** Nucleoside phosphorylation reaction catalysed by (deoxy)nucleoside kinase.

With the exception of fungi, all living organisms are known to possess at least one dNK (Vernis, 2003). Mammalian cells contain four dNKs, that have defined, but overlapping specificities. Deoxycytidine kinase (dCK) is the most efficient towards deoxycytidine, although deoxyadenosine, deoxyguanosine and a handful of nucleoside analogues such as cytarabine, gemcitabine, or fludarabine are also its substrates (Eriksson et al., 1991; Sabini et al., 2003). Thymidine kinase 2 (TK2) phosphorylates canonical nucleosides deoxythymidine, deoxycytidine, and deoxyuridine, but certain pyrimidine analogues are also accepted (Barroso et al., 2003). For example, azidothymidine, 3'-fluoro-2',3'-deoxythymidine, 5-(2-bromovinyl)-2'-deoxyuridine, 1-(2'-deoxy-2'-fluoro-1-β-D-arabinofuranosyl)-5-iodouracil, and 5-(2-chloroethyl)-2'-deoxycytidine are known substrates of TK2 (Eriksson et al., 1991; Munch-Petersen et al., 1991; Wang et al., 1999). Deoxyguanosine kinase (dGK) phosphorylates natural purine deoxyribonucleosides, such as deoxyguanosine, deoxyadenosine, and deoxyinosine, and purine analogues, such as 9-β-D-arabinofuranosylguanine, 2',2'-difluorodeoxyguanosine, and 2-chloro-2'-arabino-fluoro-2'-deoxyadenosine (Sjöberg et al., 1998; Wang et al., 1993). Thymidine kinase 1 (TK1) is known to be the most restricted in its substrate scope, as it only accepts deoxythymidine, deoxyuridine, azidothymidine, and 5-halogenated deoxyuridines as substrates (Eriksson et al., 1991; Hanan et al., 2012).

As opposed to mammals, only one dNK, that phosphorylates all natural deoxyribonucleosides, is found in insect cells. For example, *Anopheles gambiae* contains a multisubstrate kinase that phosphorylates all four canonical deoxynucleosides with a preference towards purines. Besides natural substrates, the kinase has displayed activity towards nucleoside analogues, such as stavudine, 5-fluoro-2'-deoxyuridine, 2-chloro-2'-deoxyadenosine, and 5-bromo-vinyl-2'-deoxyuridine (Knecht, 2003). In contrast, dNKs from *Drosophila melanogaster* and *Bombyx mori* exhibit preference towards pyrimidine nucleosides, but purines are also phosphorylated. In addition to natural deoxynucleosides, the aforementioned dNKs are also

active towards various nucleoside analogues, including but not limited to 5-fluoro-2'-deoxyuridine, 2',3'-dideoxycytidine, arabinosylcytosine, 3'-deoxyadenosine, 2-chloro-2'-deoxyadenosine, and fludarabine (Knecht et al., 2002; Munch-Petersen et al., 2000).

Most bacteria mainly exhibit TK activity, although certain species are known to phosphorylate all canonical nucleosides. For example, *Lactobacillus acidophilus* strain R26, that has lacking ribonucleotide reductase activity, has two additional dNKs to satisfy cellular deoxynucleotide requirements (Durham and Ives, 1971). Heterodimeric dAK/dGK and dAK/dCK are highly specific enzymes, that are responsible for the biosynthesis of deoxyadenosine, deoxyguanosine, and deoxycytidine (Ives and Ikeda, 1997). Furthermore, *Bacillus subtilis*, in addition to TK, contains dGK and dACK/dCK enzymes, that are active towards deoxyguanosine and deoxyinosine, and deoxyadenosine and deoxycytidine, respectively (Andersen and Neuhard, 2001).

Certain DNA-containing viruses, such as poxviruses and herpes viruses, contain a TK. Additionally to the activity towards deoxythymidine, TKs from Herpes simplex type-1 (HSV-1) and varicella zoster (VZV) viruses possess a thymidylate kinase activity and phosphorylate dTMP into dTDP (Bird et al., 2003; Fyfe, 1982). Compared to mammalian TK1, HSV-1 TK is active towards a much broader range of nucleosides. For example, canonical cytosine and guanine 2'-deoxyribonucleosides are known substrates of the kinase (Gentry, 1992). Furthermore, various nucleoside analogues, including idoxuridine, azidothymidine, brivudine, acyclovir, and ganciclovir are also phosphorylated (Balzarini et al., 2002; Fyfe et al., 1978; Spadari et al., 1992). Similarly to HSV-1, VZV TK exhibits a broad substrate acceptance and phosphorylates pyrimidine and purine analogues with small substitutions at nucleobase or sugar, including acyclovir (Roberts et al., 1993). Vaccinia TK displays a stricter substrate specificity, much like mammalian TK1, and in addition to deoxythymidine phosphorylates deoxycytidine and azidothymidine (El Omari et al., 2006; Prichard et al., 2007). The broad substrate range of viral TKs makes viruses susceptible to antiviral prodrugs that are otherwise non-toxic to human cells.

Based on their amino acid sequences, dNKs can be separated into two large groups: TK1-like and non-TK1-like kinases (Clausen et al., 2012). However, the classification is yet to be final, and sometimes viral dNKs can be designated as a third group (Eriksson et al., 2002). Kinases that belong to TK1-like group are homologs to human thymidine kinase-1 (*HsTK1*) such as eukaryotic TK1s and thymidine kinases from Gram-negative bacteria (Sandrini and Piškur, 2005). TK1s are homodimers, in a quiescent state, or

homotetramers, in an active state, and each monomer consists of two domains (Munch-Petersen et al., 1995; Welin et al., 2004). The fold of human TK1 monomer can be seen in **Figure 14a**. The larger  $\alpha/\beta$  domain has a six-stranded parallel  $\beta$ -sheet which is adjoined by a long  $\alpha 1$  helix and a flexible P-loop on one side, and three shorter  $\alpha$  helices on the other side. Even though the P-loop is highly conserved and is similar to the P-loop found in non-TK1-like kinases, structurally the  $\alpha/\beta$  domain of TK1 resembles ATP binding domain of RecA-F<sub>1</sub> ATPase. The smaller domain is called the lasso loop. It consists of two  $\beta$ -sheets linked by a zinc ion and covers substrate site. The active site of the TK1 monomer is located between the  $\alpha/\beta$  domain and the lasso loop. The phosphate donor molecule binds to the  $\alpha/\beta$  domain where it is coordinated by the P-loop and a magnesium ion. As opposed to non-TK1-like kinases, TK1-like kinases do not have a substrate binding site. The substrate therefore binds in a narrow hydrophobic pocket between the two domains of TK1, which explains why TK1 kinases can efficiently phosphorylate only deoxythymidine and deoxyuridine (Welin et al., 2004).

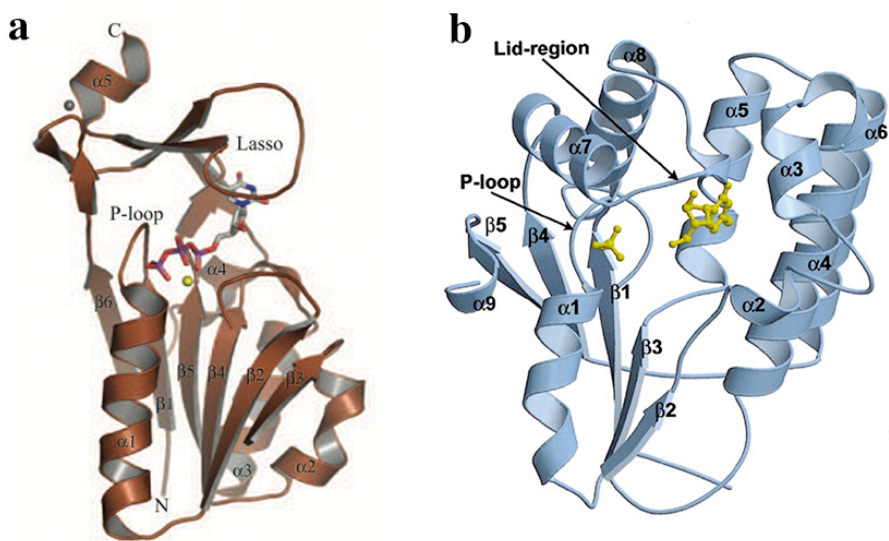


**Figure 14.** Tertiary structures of TK1-like and non-TK1-like deoxynucleoside kinases. **a** *HsTK1* (TK1-like) with dTTP and Mg<sup>2+</sup> (yellow). Adapted from (Welin et al., 2004); **b** *DmdNK* (non-TK1-like) with dT and sulfate (yellow). Adapted from (Johansson et al., 2001).

Non-TK1-like kinases, on the other hand, are not as strict as TK1 and can phosphorylate a wider range of nucleosides with partially overlapping specificities (Slot Christiansen et al., 2015; Sandrini and Piškur, 2005). Non-TK1-like group includes bacterial non-TK1-like kinases, such as dAK, dGK,



and dCK, and eukaryotic kinases (TK2-like) with examples being *Homo sapiens* dAK (*HsdAK*), dGK (*HsdGK*), dCK (*HsdCK*), and TK2 (*HsTK2*), and multisubstrate dNKs from insects such as *B. mori* or *D. melanogaster* (Clausen et al., 2012). Structurally non-TK1-like kinases are similar to thymidylate kinases. The kinases possess a similar fold and are found as homodimers. Each monomer consists of a five-stranded parallel  $\beta$  sheet surrounded by 8–10  $\alpha$  helices (**Figure 14b**). Phosphate donor is bound to the enzyme with the help of three distinct motifs: P-loop, which is located right after  $\beta$ 1 and is similar in all nucleoside and nucleotide kinases; LID domain, which is comprised of three arginine residues, and closes onto the phosphate donor molecule and participates in catalysis; and Glu-Arg-Ser motif that assists in magnesium ion binding and catalysis. Phosphate acceptor molecule is anchored into the active site of the enzyme by several conservative amino acid residues that interact with the nucleoside via hydrogen bonding: a glutamine residue interacts with the nucleobase, Glu-Tyr pair forms hydrogen bonds with 3'-hydroxyl group, and a Glu-Arg couple bonds with the 5'-OH of the deoxyribose moiety (Johansson et al., 2001; Sandrini and Piškur, 2005).

While there is an exhaustive number of studies on dNKs, comparatively, rNKs have received less attention. There are three rNKs found in human cells: uridine-cytidine kinase 1 (UCK1), uridine-cytidine kinase 2 (UCK2), and adenosine kinase (ADK) (Van Rompay et al., 2003). Both UCK1 and UCK2 phosphorylate uridine and cytidine, with UCK2 having a higher catalytic efficiency compared to that of UCK1. Neither kinase accepts 2'-deoxy-nucleosides or purine nucleosides as substrates, however, they have been shown to phosphorylate various pyrimidine ribonucleoside analogues, such as 6-azauridine, 5-fluorouridine, and  $N^4$ -acetylcytidine (Van Rompay et al., 2001). UCKs display a broad phosphate donor specificity, including dNTPs, however, UTP and CTP have been shown to inhibit their activity (Van Rompay et al., 2001). In contrast, ADK phosphorylates both ribo- and 2'-deoxy- forms of adenosine, although its affinity towards Ado is >1000-fold higher compared to that of dAdo (Hurley et al., 1986). Both ATP and GTP are suitable phosphate donors to the kinase (Yamada et al., 1981). There is no evidence of a guanosine kinase in mammalian cells, however, the enzyme has been discovered in certain bacteria and plant cells (Ashihara et al., 1997; Harlow et al., 1995). Guanosine kinase exhibits phosphorylating activity towards inosine and guanosine, and can utilize ATP, dATP, and UTP as phosphate donors (Mori et al., 1995).

The crystal structures of the three human rNKs have been solved (**Figure 15**) (Koizumi et al., 2001; Mathews et al., 1998; Van Rompay et al., 2001). Based on their sequence similarity, UCKs belong to NMP kinase fold family

and are found as homotetramers (Suzuki et al., 2004). In contrast, ADK shows little sequence resemblance to other human rNKs. Structurally, it is similar to microbial ribokinases and fructokinases, and bacterial guanosine kinase (Spychala et al., 1996). The question of whether ADK developed ribose and ATP binding sites through convergent evolution or if it evolved as a sugar kinase instead of a nucleoside kinase remains unresolved.

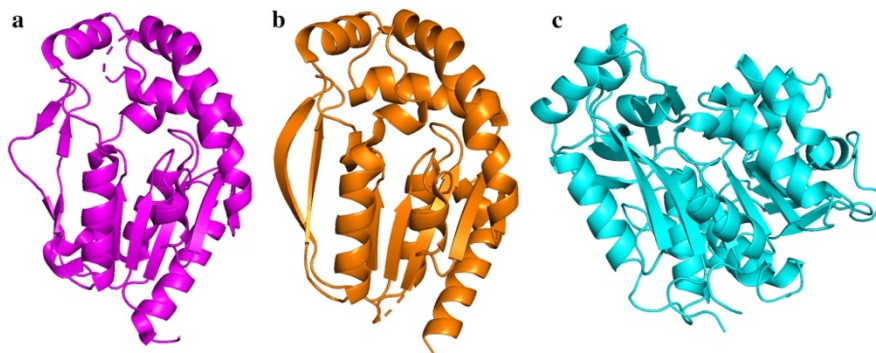


**Figure 15.** Tertiary structures of human rNKs. **a** *HsUCK1* monomer. PDB ID: 2JEO. **b** *HsUCK2* monomer. PDB ID: 1UDW. **c** *HsADK* monomer. PDB ID: 1BX4. *HsUCK1* and *HsUCK2* share a similar fold, while *HsADK* is different.

Nucleoside kinases are generally the superior choice when it comes to enzymatic NMP synthesis as they offer many advantages over acid phosphatase or phosphoribosyltransferase catalysed reactions. Although rNKs and dNKs are substrate-specific enzymes, their variety and partially overlapping specificities provide options to choose from to suit the target substrate. While reactions, catalysed by NSAPs or PRTs are reversible and result in an equilibrium of precursors and a mononucleotide, reactions, catalysed by rNKs and dNKs, are directed towards nucleotide formation and, depending on the substrate, can result in high product yields (Ding et al., 2020; Eriksson et al., 1991; Hellendahl et al., 2019; Serra et al., 2014). In addition, nucleoside triphosphates, required as phosphate donors in nucleoside kinase catalysed reactions, are readily available and relatively stable under normal conditions (Hulett, 1970).

Multiple nucleoside kinases have been successfully applied for the enzymatic synthesis of various NMPs. For example, *Homo sapiens* dCK was utilized as a biocatalyst in fludarabine 5'-monophosphate synthesis using fludarabine and GTP as precursors (Hellendahl et al., 2019). The synthesis has been executed using both soluble and immobilized forms of the kinase, with conversion efficiencies reaching 60% and 55%, respectively, when using 12 mM of starting nucleoside. Furthermore, an immobilized form of dAK from a soil-dwelling amoeba *Dictyostelium discoideum* has been applied for

the biosynthesis of multiple adenine 5'-arabinonucleotides (Serra et al., 2017). Production of vidarabine and fludarabine monophosphates has been shown to reach as high as 99%. In addition, nucleoside kinases are frequently utilized as constituents of multi-enzymatic cascades. For example, a system, containing *Clostridium perfringens* uridine phosphorylase, *Aeromonas hydrophila* purine nucleoside phosphorylase and *Dictyostelium discoideum* dAK has been applied for the synthesis of vidarabine monophosphate in a millilitre-scale using 25 mM arabinosyluracil as a starting substrate (Robescu et al., 2020). Vidarabine monophosphate production efficiency has been reported to reach 95.5% after 81 h. In another publication, a cytidine kinase from *Phorcysia thermohydrogeniphila* has been coupled together with a polyphosphate kinase from *Acidibacillus sulfuroxidans* to synthesize CMP in industrial scale (Li et al., 2020). The cytidine kinase transformed cytidine into cytidine monophosphate using ATP as a phosphate donor, while the polyphosphate kinase performed ATP regeneration role. The system has been reported to result in 96 mM of CMP produced within 6 h, which comes to an efficiency of almost 100%. A guanosine-inosine kinase from *Exiguobacterium acetylicum* has been explored as a biocatalyst for the production of guanosine and inosine 5'-monophosphates. The kinase, coupled together with an ATP regenerating system, reached guanosine and inosine phosphorylation efficiencies of 16% and 81%, respectively (Kawasaki et al., 2000). Furthermore, *HsdCK* and *HsUCK2* have been successfully applied in cell-specific metabolic labelling of RNA, where the kinases phosphorylated 2'-azidocytidine and 2'-azidouridine, respectively, into their monophosphate forms, which were then subsequently phosphorylated into NTPs by cellular NMP and NDP kinases. Incorporation of these NTPs by RNA polymerases allowed for effective RNA probing with low cytotoxicity (Nainar et al., 2020; Wang et al., 2020). In addition, *D. melanogaster* dNK and *B. subtilis* dCK have also been utilized as biocatalysts in enzymatic synthesis of various mononucleotide analogues, however, these will be discussed in more detail in the following sections.

#### 1.4.3.1. *Drosophila melanogaster* deoxynucleoside kinase

In contrast to mammals, insects have a single deoxynucleoside kinase which is responsible for the phosphorylation of all four natural deoxynucleosides to their corresponding monophosphates. Deoxynucleoside kinase from *Drosophila melanogaster* (*DmdNK*) is a unique multisubstrate kinase with a high catalytic efficiency and a broad substrate range. It is known to have a preference towards pyrimidine deoxynucleosides, with thymidine

being the best substrate, although purines are also acceptable substrates (Johansson et al., 1999). In addition to natural nucleosides, *DmdNK* is able to phosphorylate numerous nucleoside analogues (NAs) with noncanonical nucleobases or sugars (**Figure 16**). Antineoplastic and antiviral agents such as floxuridine, azidothymidine, zalcitabine, brivudine, or gemcitabine are known substrates of the kinase (Knecht et al., 2009; Mikkelsen et al., 2003). Surprisingly, even unnatural nucleosides, based on isocarbostyryl or 7-azaindole rings, were found to be suitable substrates for the kinase (Wu et al., 2002).

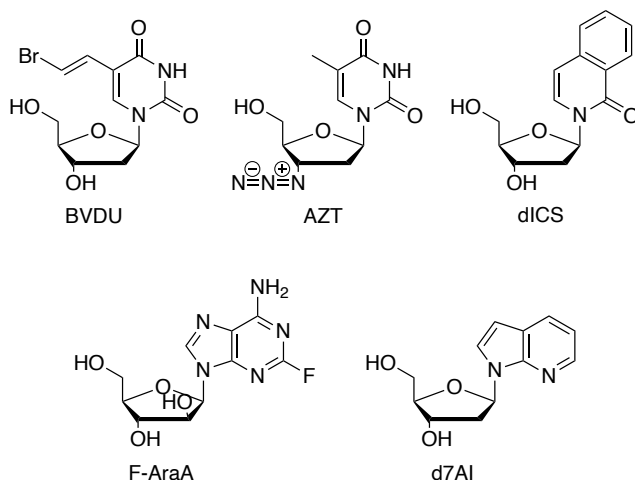


**Figure 16.** Nucleoside analogues accepted as substrates by *DmdNK*. BVDU – brivudine; AZT – azidothymidine; dICS – isocarbostyryl-based deoxyribonucleoside (Wu et al., 2002); F-AraA – fludarabine; d7AI – 7-azaindole-based deoxyribonucleoside (Wu et al., 2002).

In addition, an immobilized form of *DmdNK* has been applied for the biosynthesis of adenine arabinosylnucleotides in preparatory scale (Serra et al., 2014). Vidarabine monophosphate and its fluorinated analogue fludarabine monophosphate were produced from 12 mM of starting nucleosides with 98% and 91% conversions, respectively. Furthermore, a multi-enzymatic system exhibited in **Figure 17**, consisting of *Drosophila melanogaster* dNK, and commercially obtained UMP-CMP kinase, NDP kinase, and pyruvate kinase, has been applied for the synthesis of natural and modified nucleoside triphosphates (Fehlau et al., 2020). *DmdNK* phosphorylated cytidine, deoxycytidine, arabinosylcytosine, and 5-fluorocytidine into corresponding monophosphates, while UMP-CMP kinase and NDP kinase subsequently converted them into diphosphate and triphosphate forms, respectively. The system has been supplemented with a

pyruvate kinase, which regenerated consumed ATP, by transferring a phosphate group from phosphoenolpyruvate onto ADP. Final formation of the pyrimidine triphosphates was calculated to be 75–99%.

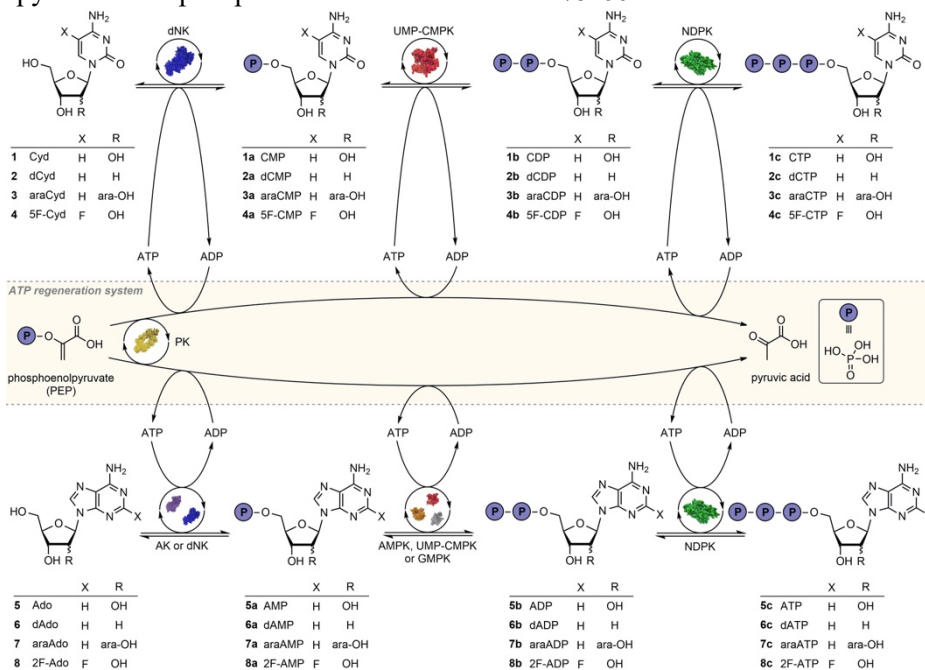


**Figure 17.** Multi-enzymatic synthesis of natural and modified dNTPs with an ATP regeneration system. dNK – *D. melanogaster* deoxynucleoside kinase; AK – adenosine kinase; UMP-CMPK – uridylylate-cytidylylate kinase; GMPK – guanylate kinase; AMPK – adenylate kinase; NDPK – nucleoside diphosphate kinase; PK – pyruvate kinase. Adapted from (Fehlau et al., 2020).

Based on sequence similarity *DmdNK* belongs to non-TK1-like group and shares a similar fold with human deoxynucleoside kinases. Sequence analysis has revealed that *DmdNK* is 44% identical to *HsTK2*, whereas identities with *HsdCK* and *HsdGK* are 31% and 34%, respectively (Munch-Petersen et al., 2000). *DmdNK* crystallizes as a dimeric protein with 29 kDa in mass, and each monomer is comprised of eight  $\alpha$ -helices and a central five-strand parallel  $\beta$ -sheet (**Figure 18a**). Crystal structures of *DmdNK* with deoxycytidine, thymidine, dCTP, dGTP, dTTP, and various NAs have been solved (Egeblad-Welin et al., 2007; Johansson et al., 2001; Knecht et al., 2009; Mikkelsen et al., 2003, 2008). The substrate site of the kinase is an elongated cavity, that has hydrophobic residues on its top and bottom, it is located near the C-terminus of the  $\beta$ -sheet. Crystallographic data of *DmdNK* with a bound deoxycytidine has revealed that the cytosine is stabilized by  $\pi$ -stacking

interactions with F114 on one side, and W57 and F80 on the other side of the base as can be seen in **Figure 18b**.

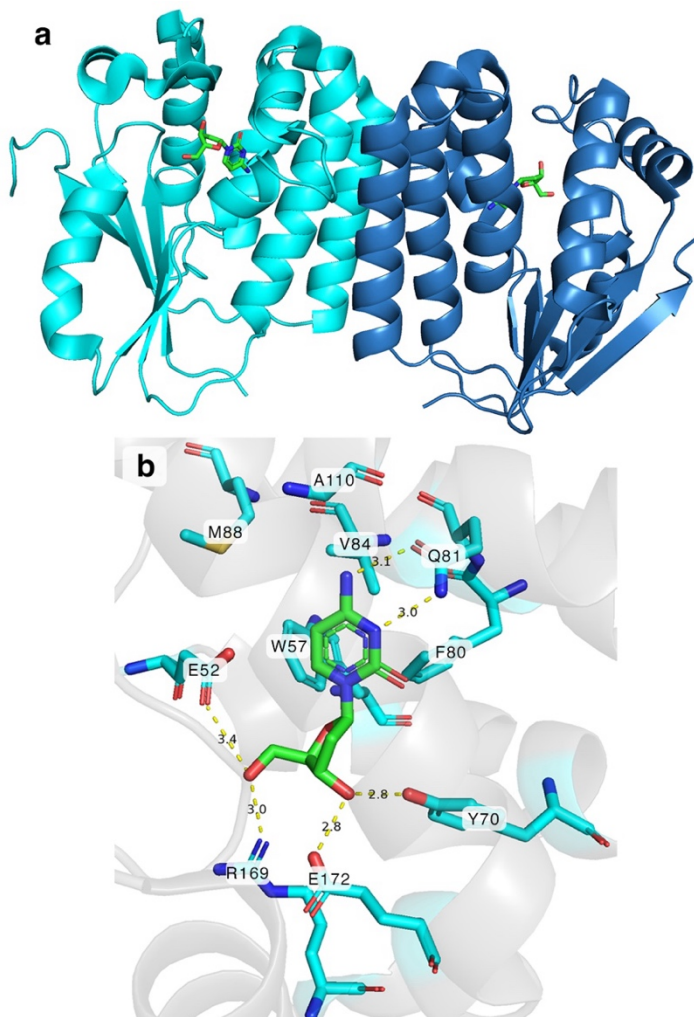


**Figure 18.** Crystal structure of *D. melanogaster* dNK. PDB ID: 1j90. **a** Dimer form of *D. melanogaster* dNK with 2'-deoxycytidine molecules (green) bound in the active centres. Each monomer is coloured in different shades of blue. **b** Amino acid residues (cyan) found in the active site of *D. melanogaster* dNK. 2'-Deoxycytidine molecule is green; yellow dashed lines represent hydrogen bonds. Residue F114 is omitted for a clearer view.

The  $N^3$  and  $N^4$  atoms of cytosine are bonded with Q81, and the oxygen atom at C2 forms hydrogen bonds with two water molecules. On the other side of the base, near the C5-position, there is a deep cavity dominated by hydrophobic residues V84, M88, A110. The hydrophobic cleft provides a possible explanation why *DmdNK* accepts such a wide range of nucleosides

with modifications at positions 4 and 5 of pyrimidine ring. The deoxyribose moiety is anchored in the active site by few polar residues. The oxygen atom of the 3'-hydroxy group interacts with Y70 and E172, while 5'-oxygen forms hydrogen bonds with E52, R169 and a water molecule. (Johansson et al., 2001). Functional studies of *DmdNK* mutants have revealed that E52 initiates the phosphorylation reaction by deprotonating the 5'-hydroxy group of ribose, and R105 stabilizes the transitional state (Egeblad-Welin et al., 2007).

The substrate specificity of *DmdNK* can be modulated by replacing certain amino acids in the active centre. Knecht and colleagues have successfully altered the specificity of *DmdNK* and made it more similar to eukaryotic dCK and dGK (Knecht, 2002). The amino acids V84, M88 and A110, that line the substrate pocket, were replaced to corresponding amino acids typical for dCK and dGK, which was later replicated in several other studies (Knecht et al., 2007; Solaroli et al., 2007). It was discovered that triple *DmdNK* mutants V84S/M88R/A110D and V84A/M88R/A110D, which resemble the active sites of dGK and dCK, respectively, gained substrate preferences similar to the kinases. The mutants demonstrated greater catalytic efficiency for dGuo and dAdo compared to Thd. The mutated variants have also obtained the ability to phosphorylate certain nucleoside analogues that were not acceptable substrates to wild-type *DmdNK* (*DmdNK*-WT). The compounds include ganciclovir, an acyclic guanosine analogue, stavudine, which is a thymidine analogue, and even 2'-deoxyribose without a nucleobase moiety.

The residues lining the hydrophobic pocket of *DmdNK* are not the only ones of interest. Asparagine in position 64 was discovered during random *in vitro* mutagenesis (Knecht et al., 2000). A *DmdNK* mutant, bearing N64D mutation, was found to have lower activity towards natural nucleosides compared to the wild-type kinase, however the activity towards 3'-modified nucleosides such as azidothymidine (AZT) remained fairly the same. Further studies have identified the residue to stabilize E172, which forms hydrogen bonds with 3'-hydroxyl group of the ribose moiety (Welin et al., 2005). Replacing the N64 with aspartate creates a negative charge which in turn electrostatically repels E172. The distance between the glutamate residue and the 3'-position of ribose increases, which allows for more space for a substrate with a bulkier substitute, such as 3'-azide group.

Another residue that has received attention is glutamine in position 81. The two hydrogen bonds formed between Q81 and a pyrimidine nucleobase are important for substrate binding. In one study the glutamine was replaced with asparagine, and such variant was found to prefer purine nucleosides over pyrimidines (Solaroli et al., 2003). In two other ones, *DmdNK*-Q81E mutant

has been utilized for the phosphorylation of unnatural nucleosides 2-amino-8-(1'- $\beta$ -D-2'-deoxyribofuranosyl)-imidazo[1,2-a]-1,3,5-triazin-4(8H)-one (dP), 6-amino-3-(1'- $\beta$ -D-2'-deoxyribofuranosyl)-5-nitro-1H-pyridin-2-one (dZ), 8-(1'- $\beta$ -D-2'-deoxy-ribofuranosyl)imidazo[1,2-a]-1,3,5-triazine-2(8H)-4(3H)-dione (dX), and 2,4-diamino-5-(1'- $\beta$ -D-2'-deoxyribofuranosyl)-pyrimidine (dK) whose structures are presented in **Figure 19** (Chen et al., 2017; Matsuura et al., 2017). Replacement of the glutamine's positive charge with the negative charge of glutamate enabled phosphorylation of the beforementioned unnatural nucleosides whereas wild-type kinase phosphorylated them extremely inefficiently or not at all.

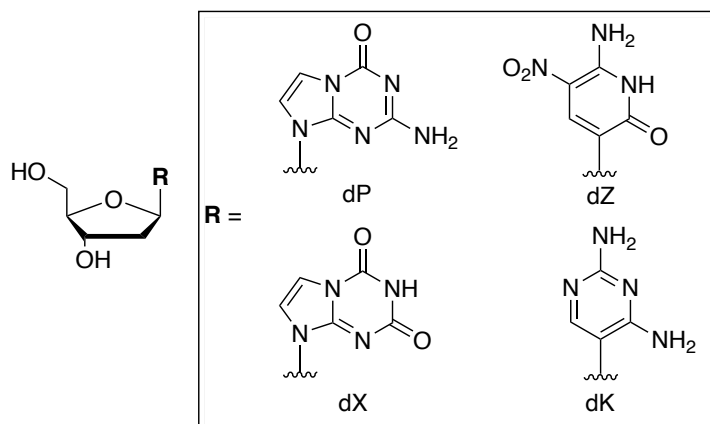


**Figure 19.** Structures of unnatural nucleosides dP, dZ, dX, and dK, that are phosphorylated by *DmdNK*-Q81E variant (F. Chen et al., 2017; Matsuura et al., 2017).

The broad substrate scope of *DmdNK*-WT allows phosphorylation of various canonical nucleosides and their derivatives. Additionally, the efficiency of kinase can be improved by selective substitution of specific amino acid residues in its active site, which further enhances the activity of the kinase towards certain compounds.

#### 1.4.3.2. *Bacillus subtilis* deoxycytidine kinase

Deoxycytidine kinase (*BsdCK*) from *Bacillus subtilis* is a bacterial deoxynucleoside kinase, that belongs to the non-TK1-like kinase family together with *HsdCK*, *HsdGK*, and *DmdNK* (Sandrini and Piškur, 2005). Contrary to the aforementioned kinases, *BsdCK* has not received as much attention. Crystal structure of the enzyme has yet to be solved, however, based on sequence analysis it is 25.6% and 25.3% identical to *DmdNK* and *HsdCK*,



respectively. It is known the enzyme is a homodimer, with a monomer size of 25.4 kDa.

The kinase was first characterized in 1980 (Møllgaard, 1980). Its specificity towards nucleobases was discovered to be quite strict and only nucleosides of cytosine and adenine are known to be suitable substrates. The sugar moiety, however, is not as important. Even though 2'-deoxyribo-nucleosides are favoured, nucleosides bearing ribose or arabinose moieties are also accepted (Andersen and Neuhard, 2001). While research on the topic is limited, a paper from 2013 reported on the application of *BsdCK* as a biocatalyst for the synthesis of nucleoside 5'-monophosphates (Zou et al., 2013). The authors presented a one-pot synthesis, where *BsdCK* together with *N*-deoxyribosyltransferase from *Lactobacillus delbrueckii* and acetate kinase from *Escherichia coli* were applied for the production of dNMPs (**Figure 20**).

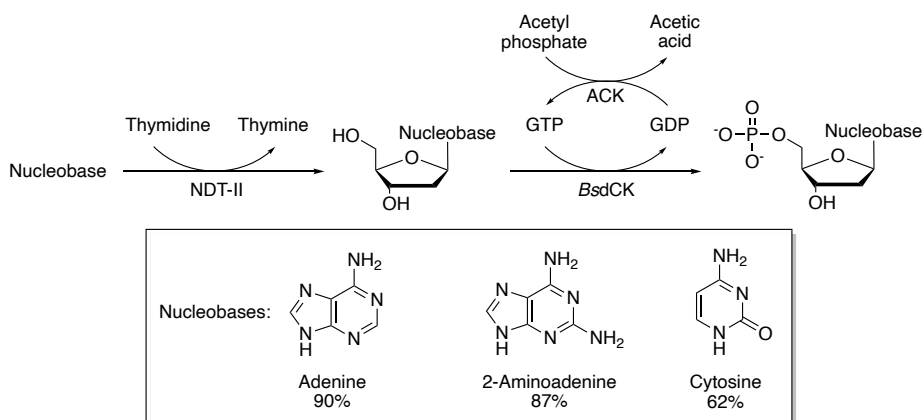


**Figure 20.** Multi-enzymatic synthesis of NMPs from thymidine and nucleobases. NDT-II – *N*-deoxyribosyltransferase II; ACK – acetate kinase. Adapted from (Zou et al., 2013).

*N*-Deoxyribosyltransferase catalysed a deoxyribose transfer from deoxythymidine to adenine, 2-aminoadenine, or cytosine. The formed nucleoside was phosphorylated by *BsdCK* using GTP as a phosphate donor, while acetate kinase performed GTP regeneration using acetyl phosphate. The production efficiencies of deoxyadenosine monophosphate, 2-aminodeoxyadenosine monophosphate, and deoxycytidine monophosphate were 90%, 87%, and 62%, respectively. *BsdCK* phosphorylates adenine and cytosine nucleosides with various sugar moieties, suggesting that it may possess a wider substrate range than originally thought. Coupled with its high nucleoside conversion rates, this makes *BsdCK* a promising candidate for

enzymatic NMP synthesis. However, further research is necessary to fully assess its potential.

### 1.5. Phosphate donor regeneration

Enzymatic nucleoside phosphorylation, carried out by nucleoside kinases, requires NTPs (typically ATP or GTP) as phosphate donors, and this approach has certain disadvantages. Firstly, NTPs are relatively expensive reagents. While this may not be a matter of concern in analytical scale experiments, preparatory scale syntheses can get rather costly. Secondly, NTP depletion during phosphorylation reactions results in NDP accumulation, which can suppress enzymatic activity and complicate final product purification. Implementing a phosphate donor regeneration system is a way to rectify the issues and make enzymatic NMP synthesis more efficient and sustainable. Most commonly, ATP regeneration is executed by various kinases, that facilitate a  $\gamma$ -phosphate transfer from adenosine triphosphate to an acceptor molecule. The reversible action of such kinases is often exploited to regenerate ATP from ADP and inexpensive materials (Andexer and Richter, 2015; Chen and Zhang, 2021).

To date, one of the most popular enzymes for *in vitro* ATP regeneration is acetate kinase. The kinase catalyses a reversible phosphate group transfer from acetyl phosphate to ADP and has been proven to be an effective strategy in ATP regeneration (Nakajima et al., 1984). Acetate kinase/acetyl phosphate system has been successfully coupled with UCK to synthesize UMP and CMP in very high conversion yields (Qian et al., 2014). Furthermore, the system has been utilized to regenerate GTP in a one-pot enzymatic cascade, containing *N*-deoxyribosyltransferase II and deoxycytidine kinase, to produce adenosine, 2-aminoadenosine and cytidine 5'-monophosphates (Zou et al., 2013). In another paper, *E. coli* cells with surface-displayed NMP kinases and acetate kinase were reported to be applied for the synthesis of CTP, dCTP, ATP, dATP, dTTP, and dUTP from their corresponding monophosphates with conversion yields reaching 80–96%. In addition to regenerating the ATP, necessary for NMP kinases, acetate kinase performed the subsequent phosphorylation by converting produced NDPs into NTPs (Ding et al., 2020).

Acetyl phosphate is an inexpensive starting material, that, if needed, can be simply synthesized (Crans and Whitesides, 1983). However, a considerable drawback is that it is rather unstable and tends to breakdown into acetate and inorganic phosphate (Lipmann and Tuttle, 1944). Coupling the reaction with pyruvate oxidase, that synthesizes acetyl phosphate from pyruvate, oxygen,

and inorganic phosphate as displayed in **Figure 21**, can make the regeneration more sustainable; however, an addition of catalase is necessary to eliminate  $H_2O_2$ , which is a toxic byproduct of pyruvate oxidase catalysed reaction (Kim and Swartz, 1999).

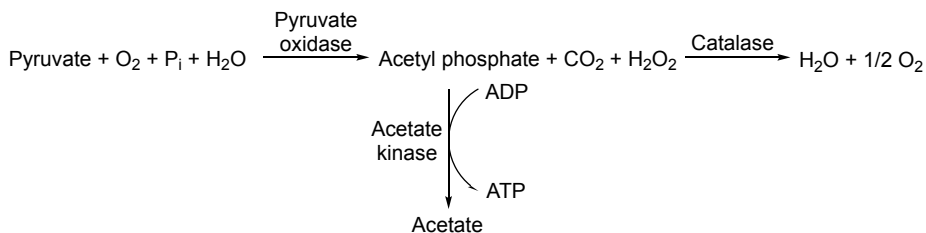


**Figure 21.** ATP regeneration system consisting of acetate kinase, pyruvate oxidase, and catalase. Adapted from (Kim and Swartz, 1999).

Pyruvate kinase together with phosphoenolpyruvate (PEP) is another example of ATP regenerating systems (**Figure 22a**), however, its main limitation is its cost. PEP is one of the most expensive phosphate donors and while it can be synthesized from less costly precursors, such as pyruvate, the additional complexity makes the system less appealing (An et al., 2017; Hirschbein et al., 1982). Pyruvate kinase/PEP ATP regeneration system has been utilized in various nucleotide preparations. Fluorinated nucleotide analogues 5F-UTP and 5F-CTP were synthesized from 5-fluorouracil and 5-fluorocytidine, respectively, in enzymatic cascades, where ATP was regenerated by pyruvate kinase using PEP as a donor (Hennig et al., 2007). Pyruvate kinase has been also applied for ATP regeneration in enzymatic one-pot phosphorylation of various cytidine and adenosine analogues into their corresponding triphosphate forms (Fehlau et al., 2020).

Creatine kinase, whose main responsibility *in vivo* is the maintenance of the ADP homeostasis, together with creatine phosphate (**Figure 22b**), is not as popular for ATP regeneration as acetate kinase/acetyl phosphate or pyruvate kinase/PEP systems. However, creatine kinase's low  $K_M$  value for ADP and relatively low-cost of creatine phosphate might make it an approach worth exploring (Sahlin and Harris, 2011). The creatine kinase/creatine phosphate synthesis has been successfully applied to regenerate ATP in cell-free syntheses of glycoconjugates and proteins (Kigawa et al., 1999; Zhang et al., 2003).

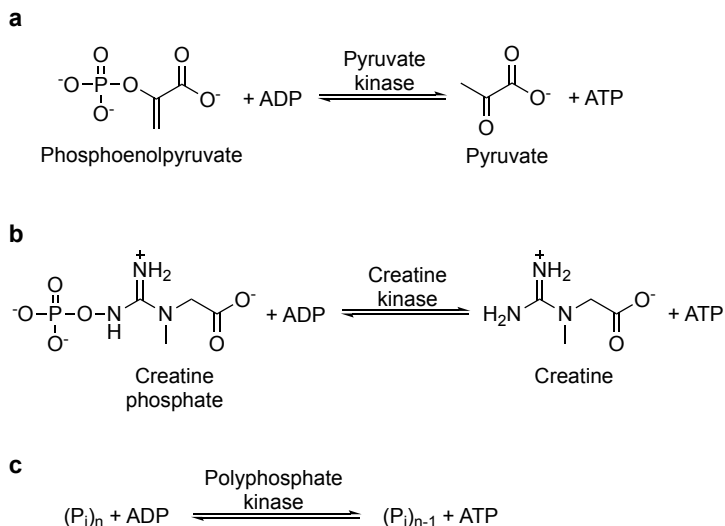


**Figure 22.** Examples of ATP regeneration systems. **a** ATP regeneration using pyruvate kinase/phosphoenolpyruvate system; **b** ATP regeneration using creatine kinase/creatine phosphate system; **c** ATP regeneration using polyphosphate kinase/polyphosphate system.

Polyphosphate kinases (PPK) are becoming increasingly popular as candidates for *in vitro* ATP regeneration. The enzymes catalyse a reversible  $\gamma$ -phosphate transfer from ATP to inorganic polyphosphate (polyP) (**Figure 22c**), which is a readily available, low-cost and highly stable in a broad pH range material (Ahn and Kornberg, 1990; Rao et al., 2009). Based on their sequences, PPKs are classified into two families: PPK1 and PPK2 (Neville et al., 2022). PPK1s have been utilized in multiple enzymatic syntheses where ATP regeneration was required, such as production of amorphadiene from mevalonate, 5-aminolevulinic acid from glycine and succinate, and NTPs from NDPs (Meng et al., 2016; Noguchi and Shiba, 1998; Shimane et al., 2012). Even though PPK1s have been successfully applied in enzymatic syntheses, there are a few drawbacks that are hard to overlook. Firstly, reaction equilibrium of PPK1 enzymes is shifted towards polyP synthesis over ATP synthesis (Tzeng and Kornberg, 2000). Secondly, PPK1s are membrane-bound proteins, thus purification and solubility are something to be considered (Akiyama et al., 1992). In contrast to PPK1, PPK2 enzymes are water-soluble and favour ATP synthesis over degradation (Ishige et al., 2002). They share no sequence similarities with PPK1 enzymes and are further classified into three subfamilies (Motomura et al., 2014). PPK2-I and PPK2-II catalyse phosphorylation of NDPs and NMPs, respectively, while PPK2-III phosphorylates both nucleoside mono- and diphosphates into their

triphosphate forms. In recent years, PPK2 catalysed ATP regeneration was utilized in numerous biosyntheses. For example, PPK2 from *Corynebacterium glutamicum* was applied for ATP regeneration in enzymatic glutathione production, while PPK2-III from *Deinococcus geothermalis* was used to regenerate ATP from AMP in chemoenzymatic synthesis of *N*-methylbutyrylamide and similar amides (Cao et al., 2018; Lelièvre et al., 2020). Furthermore, PPK2 from *Meiothermus cerbereus* has been coupled together with UCK from *Lactobacillus helveticus* to manufacture CMP in high titre (143 mM) from cytidine (Teng et al., 2023).

There are numerous nucleoside triphosphate regeneration systems available, each with its own set of advantages and disadvantages. Acetyl phosphate, utilized by acetate kinase, is relatively affordable but tends to be unstable in prolonged reaction times. In contrast, pyruvate kinase/PEP system does not share the instability issue but is one of the most expensive choices for ATP regeneration. Creatine kinase/creatine phosphate system is not as thoroughly studied for *in vitro* ATP regeneration as the beforementioned systems; however, the low cost and high stability of creatine phosphate makes it an attractive option. Finally, PPK catalysed ATP regeneration appears to be a reasonable choice, as it uses inexpensive and stable polyP as a phosphate donor.

### Takeaway

Nucleosides and their derivatives are essential in numerous scientific fields, including molecular biology, biochemistry, and pharmacology. Beyond countless cellular functions, their significance extends to therapeutic applications, such as antiviral and anticancer treatments, making them prominent research objects. Notwithstanding their importance, chemical nucleoside phosphorylation presents considerable challenges. Chemical nucleotide synthesis often involves complex and laborious multi-step reactions, that often lead to low product yields. Additional complications arise if specific stereochemistry is required. Enzymatic nucleoside phosphate synthesis is extensively explored as an alternative to traditional chemical phosphorylation methods. Enzymatic phosphorylation offers many advantages, such as greater specificity, milder reaction conditions, higher product yields and is overall a more sustainable and environmentally conscious approach. While significant progress in the enzymatic nucleotide synthesis has been made, many of the approaches are not yet fully optimized and further advancements are necessary for a widespread application.

## 2. EXPERIMENTAL

### 2.1. General information

#### 2.1.1. Chemicals

Chemicals and solvents were purchased from Sigma-Aldrich (Germany), Alfa Aesar (Germany), Honeywell (Germany), Fluka (Germany), Merck (Germany), and GE Healthcare (Germany). They were of analytical grade or higher and were used without further purification. Acetyl phosphate was prepared in the laboratory based on a method previously described by Crans and Whitesides (Crans and Whitesides, 1983).

#### 2.1.2. Purification and analysis of synthesized compounds

Thin-layer chromatography (TLC) was carried out on 25 TLC aluminium sheets coated with silica gel 60 F254 (Merck, Germany). Column chromatography was performed on silica gel 60 (0.063–0.200 nm) (Merck, Germany) and reverse-phase chromatography on Grace flash cartridges C-18 (Fisher Scientific, Germany). Ion exchange chromatography was performed on DEAE Sephadex A-25 (GE Healthcare, Germany).

Melting points were determined with a MEL-TEMP (Electrothermal, Germany) melting apparatus in capillary tubes and are not corrected. NMR spectra were recorded in DMSO- $d_6$  and D<sub>2</sub>O on a Bruker Ascend 400 (Bruker BioSpin, Germany) <sup>1</sup>H NMR–400 MHz, <sup>13</sup>C NMR–101 MHz, <sup>31</sup>P–202 MHz. Chemical shifts are reported in ppm relative to the solvent resonance signal as an internal standard. UV spectra were recorded on a Lambda 25 Perkin Elmer UV/VIS spectrometer (PerkinElmer, UK). HPLC-MS analyses were performed using a high-performance liquid chromatography system, equipped with a photo diode array detector (SPD-M20A) and a mass spectrometer (LCMS-2020, Shimadzu, Japan) equipped with an ESI source. The chromatographic separation was conducted using a YMC Pack Pro column, 3×150 mm (YMC, Japan) at 40°C and a mobile phase that consisted of 0.1% formic acid water solution (solvent A), and acetonitrile (solvent B). Mass spectrometry data was acquired in both positive and negative ionization mode and analysed using the LabSolutions LCMS software (version 5.42 SP6).

### 2.1.3. Gene sources and bacterial strains

Plasmid pOpen-dromedNK, that encoded *D. melanogaster* deoxynucleoside kinase (*DmdNK*-WT) gene was kindly provided by Drew Endy and Jennifer Molloy and FreeGenes Project (Addgene plasmid #165579; <http://n2t.net/addgene:165579>; RRID:Addgene\_165579; Watertown, MA, USA; accessed on 12 October 2021), *B. subtilis* deoxycytidine kinase (*BsdCK*-WT) and *E. coli* acetate kinase (*EcACK*) genes were cloned from *Bacillus subtilis* 168 (from laboratory stock of Department of Molecular Microbiology and Biotechnology, Institute of Biochemistry, Life Sciences Center, Vilnius University, Lithuania) and *Escherichia coli* DH5 $\alpha$  (Novagen, Germany), respectively. *Escherichia coli* DH5 $\alpha$  was used for plasmid amplification, and *Escherichia coli* BL21 (DE3) (Novagen, Germany) and *Escherichia coli* KRX (Promega, Austria) were used for the expression of the target proteins.

### 2.1.4. Reagents for plasmid construction

The expression vector pLATE31 was purchased from ThermoFisher Scientific (Lithuania) as a part of aLICator LIC cloning and expression set. Phusion High-Fidelity PCR Master Mix and Phusion Plus PCR Master Mix, utilized for gene amplification, were purchased from ThermoFisher Scientific (Lithuania). Restriction enzyme DpnI (10 U/ $\mu$ L) was purchased from ThermoFisher Scientific (Lithuania). GeneJet PCR purification kit was purchased from ThermoFisher Scientific (Lithuania). ZR Plasmid MiniPrep, used for plasmid isolation, was purchased from Zymo Research (Germany).

### 2.1.5. Computer software

Protein structures were visualized using PyMOL Molecular Graphics System, Version 3.0 Schrödinger, LLC. Protein structure models were generated by ColabFold v1.5.5 software (Mirdita et al., 2022). Molecular docking was performed utilizing DiffDock software (<https://huggingface.co/spaces/reginabarzilaygroup/DiffDock-Web>; accessed on 12 August 2024).

## 2.2. Chemical synthesis of modified nucleosides

### 2.2.1. Synthesis of $N^4$ amino acid-acylated nucleosides

An appropriate amino acid (L-alanine, L-glycine,  $\beta$ -alanine, L-leucine, L-isoleucine, L-methionine, L-phenylalanine, or L-tyrosine, 6.66 mmol) was dissolved in 24 mL of 1,4-dioxane and water mixture (1:1). 13.3 mL of 1 M NaOH (2 mol. eq.) was slowly added. After cooling the mixture in the freezer for 20 min, 2.183 g (10 mmol) of di-*tert*-butyl dicarbonate (Boc<sub>2</sub>O) was added and the reaction was stirred for 3 h at room temperature (Krapcho and Kuell, 1990). After the reaction had taken place, the mixture was reduced to a volume of 2–5 mL using a rotary evaporator. Aqueous solution of citric acid (10%) was added to the mixture until pH reached 2.0. The mixture was extracted using ethyl acetate. Ethyl acetate fractions were pooled, dried with anhydrous sodium sulphate, filtered, and reduced using a rotary evaporator to recover a Boc-protected amino acid.

The protected amino acid, 7.33 mmol of *N*-hydroxysuccinimide (NHS) and 7.33 mmol of *N,N'*-dicyclohexylcarbodiimide (DCC) were dissolved in 30 mL of ethyl acetate (Barré et al., 2016). The reaction mixture was stirred at room temperature. After 24 hours had passed, the formed white precipitate was separated from reaction mixture by filtration, and ethyl acetate was removed using a rotary evaporator. The formed *N*-Boc protected and NHS-activated amino acid together with 6.66 mmol of 2'-deoxycytidine was dissolved in 8–10 mL of dimethylformamide (DMF) and stirred for 5 days at room temperature. DMF was removed under reduced pressure, the obtained residue was purified by column chromatography (silica gel, chloroform/methanol mixture, 100:0 to 85:15). Structures of the synthesized nucleosides were confirmed by NMR spectroscopy and HPLC-MS analysis (provided in **Appendix 1**).

### 2.2.2. Synthesis of *N*-4-(2'-deoxycytidinyl)amino acid amides

*N*-4-(2'-Deoxycytidinyl)amino acid amides were obtained by removing the Boc-protecting group from the synthesized  $N^4$ -acylated-2'-deoxycytidine compounds. The deprotection reaction was performed by dissolving a selected deoxycytidine derivative (1.0–1.3 mmol) in 10–15 mL of water and boiling the solution for 45–70 min (J. Wang et al., 2009). The course of the deprotection reaction was monitored by TLC. After the deprotection took place, water was removed using a rotary evaporator. The remaining reaction



mixture was purified by reverse phase chromatography (GRACE C-18 column, water/methanol mixture, 5:0 to 4:1, as eluent). Fractions containing the products were pooled and reduced under pressure to afford *N*-4-(2'-deoxycytidinyl)amino acid amides. The synthesized nucleoside derivatives were characterized by NMR spectroscopy and HPLC-MS analysis (provided in **Appendix 2**).

### 2.3. Enzymatic synthesis of modified nucleoside 5'-monophosphates

#### 2.3.1. Cloning of target genes

The target genes encoding *DmdNK*-WT, *BsdCK*-WT and *EcACK* were amplified from pOpen-dromedNK plasmid, *B. subtilis* 168 genomic DNA, and *E. coli* DH5 $\alpha$  genomic DNA, respectively. The amplification was done by PCR using Phusion polymerase with synthetic primers (**Appendix 4**). The amplified genes were purified from 1% agarose gel using a GeneJET PCR purification kit and cloned into pLATE31 plasmid according to manufacturer's protocols. The plasmids were electroporated into electro-competent *E. coli* DH5 $\alpha$  cells (Dower et al., 1988). Transformants were selected on LB agar plates that contained 0.1 mg/mL ampicillin. The recombinant plasmids were isolated using ZR Plasmid Miniprep kit, sequenced and named pLATE31-dNK, pLATE31-dCK, and pLATE31-ACK.

#### 2.3.2. Site-Directed Mutagenesis

Site-directed mutagenesis was utilized for the creation of sixteen *D. melanogaster* dNK and three *B. subtilis* dCK mutant variants. Plasmids pLATE31-dNK and pLATE31-dCK were used as starting templates. Full list of templates and primers utilized in the mutagenesis of the kinases is provided in **Appendix 5**. The target genes were synthesised by PCR using Phusion Plus polymerase. *DmdNK* variants V84A, V84A+A110D, V84A+M88A, M88A, M88R, M88R+A110D, and A110D, and *BsdCK* variants R70M, R70M+D93M, and D93M were synthesized traditionally, utilizing a forward and a reverse primer, both carrying the same mutation. Synthesis of *DmdNK* variants W57F, W57V, Q81A, Q81A+V84G, Q81A+M88G, Q81A+A110G, V84G, M88G, and A110G was based on a single-primer site-directed mutagenesis protocol (Huang and Zhang, 2017). After completion of PCR, template DNA was removed by treating reaction mixtures with 1  $\mu$ L of DpnI.

The products were purified from 1% agarose gel and cloned into pLATE31 plasmid according to manufacturer's protocol. The obtained plasmids were chemically transformed into competent *E. coli* DH5 $\alpha$  cells. Transformants were selected on LB agar plates (0.1 mg/mL ampicillin). The plasmids were isolated and sequenced to confirm that the desired mutations were present. The plasmids with correct sequences were named pLATE31-dNK-W57F, pLATE31-dNK-W57V, pLATE31-dNK-Q81A, pLATE31-dNK-Q81A+V84G, pLATE31-dNK-Q81A+M88G, pLATE31-dNK-Q81A+A110G, pLATE31-dNK-V84A, pLATE31-dNK-V84G, pLATE31-dNK-V84A+M88A, pLATE31-dNK-V84A+A110D, pLATE31-dNK-M88A, pLATE31-dNK-M88G, pLATE31-dNK-M88R, pLATE31-dNK-M88R+A110D, pLATE31-dNK-A110D, pLATE31-dNK-A110G, pLATE31-dCK-R70M, pLATE31-dCK-R70M+D93M, and pLATE31-dCK-D93M.

### 2.3.3. Expression of target genes and purification of the enzymes

The recombinant plasmids (except for *DmdNK-Q81A+V84G*, *DmdNK-Q81A+M88G*, *DmdNK-Q81A+A110G*, *DmdNK-V84G*, *DmdNK-M88G*, and *DmdNK-A110G*, for which *E. coli* KRX strain was used) were transformed into *E. coli* BL21 (DE3) by electroporation. Transformants were selected on LB agar plates that contained 0.1 mg/mL ampicillin and inoculated into two flasks containing 200 mL of LB medium with 0.1 mg/mL ampicillin. The inoculates were incubated at 37 °C and 180 rpm for 2–5 h. After OD<sub>600</sub> reached 0.6, gene expression was induced by supplementing the medium with 1 mM of isopropyl  $\beta$ -D-1-thiogalactopyranoside (IPTG) and continuing incubation for additional 3 h at the same conditions. In case of *E. coli* KRX transformants, at an OD<sub>600</sub> of 0.6, the temperature was decreased to 20 °C and gene expression was induced with 0.5 mM of IPTG and 0.1% of L-rhamnose for 20 h. The cells were harvested by centrifugation at 4,000  $\times$  g at 4 °C for 10 min. After separation from supernatant, the cells were resuspended in 10 mL of buffer A (50 mM potassium phosphate, pH 7.5) and lysed by sonication (5 min total time; 2 s disruption; 8 s cooling; 22 kHz at 40% amplitude) on ice using a Branson SFX 250 sonicator (Emerson, Missouri, USA). Cell-free supernatant was recovered by centrifugation at 4,000  $\times$  g at 4 °C for 10 min. The collected soluble fractions were loaded onto 5 mL Ni<sup>2+</sup> HiTrap chelating HP column (Cytiva, USA), equilibrated with buffer A, and mounted on an AKTA pure (Cytiva, USA) protein purification system. Protein purification was performed at room temperature at 1 mL/min flow rate. The

enzymes were eluted using buffer B (50 mM potassium phosphate, 0.5 M imidazole, pH 7.5) gradient from 0% to 100% over 10 min. Protein purification was monitored using 14% sodium dodecyl sulphate–polyacrylamide gel electrophoresis (SDS-PAGE). Fractions with target proteins were pooled, placed into dialysis bags, and dialyzed for 18 h at 4 °C in buffer A. The precipitated proteins were removed by centrifugation at  $16,000 \times g$  at 4 °C for 10 min. Solutions of the purified enzymes were stored at –20 °C until further use.

#### 2.3.4. Optimization of reaction conditions catalysed by *DmdNK*-WT and *BsdCK*-WT

The influence of various factors such as reaction duration, temperature, pH, substrate concentration, and enzyme concentration, was assessed. The effects of these factors were determined by HPLC-MS analysis based on the conversion of 2'-deoxycytidine (dCyd) to 2'-deoxycytidine 5'-monophosphate (dCMP).

##### 2.3.4.1. Optimal reaction duration

The generation of dCMP was measured at 1 min, 2 min, 5 min, 10 min, 15 min, 30 min, 1 h, 2 h, and 4 h. The reaction mixtures were of 300  $\mu$ L of volume and consisted of 10 mM dCyd, 15 mM GTP, 15 mM  $MgCl_2$ , 50 mM potassium phosphate buffer (pH 7.5), and 0.69 nmol/mL of *DmdNK*-WT or 9.45 nmol/mL of *BsdCK*-WT. The syntheses were performed at 37 °C and 500 rpm. Samples of 20  $\mu$ L were quenched with 60  $\mu$ L of acetonitrile, centrifuged at  $16,000 \times g$  at 4 °C for 10 min, and analysed with HPLC-MS.

##### 2.3.4.2. Optimal temperature

The influence of temperature to the phosphorylation of 2'-deoxycytidine was measured at 4 °C, 20 °C, 30 °C, 37 °C, 45 °C, 50 °C, 60 °C, 70 °C, and 80 °C. Total reaction volumes were 50  $\mu$ L and consisted of 10 mM dCyd, 15 mM GTP, 15 mM  $MgCl_2$ , 50 mM potassium phosphate buffer (pH 7.5), and 0.69 nmol/mL of *DmdNK*-WT or 9.45 nmol/mL of *BsdCK*-WT. The reactions were performed at 500 rpm for a duration of 5 min. Samples were quenched with 150  $\mu$ L of acetonitrile, centrifuged at  $16,000 \times g$  at 4 °C for 10 min, and analysed with HPLC-MS.

#### 2.3.4.3. Optimal pH

Two buffers with ranging acidities were used to evaluate reaction mixture's pH effect on dCMP synthesis: 50 mM potassium phosphate buffer with pH values of 5.5, 6.0, 6.5 and 7.0, and 50 mM Tris-HCl buffer with pH values of 7.0, 7.5, 8.0, 8.5 and 9.0. Each buffer contained 10 mM dCyd, 15 mM GTP, 15 mM MgCl<sub>2</sub>, and 0.69 nmol/mL of *DmdNK*-WT or 9.45 nmol/mL of *BsdCK*-WT, with the total volume being 50  $\mu$ L. The reactions were executed at 37 °C and 500 rpm for 5 min. The syntheses were stopped by adding 150  $\mu$ L of acetonitrile. The samples were centrifuged at 16,000  $\times$  g at 4 °C for 10 min, and analysed with HPLC-MS.

#### 2.3.4.4. Optimal nucleoside concentration

To evaluate the effect of nucleoside concentration to the phosphorylation reaction, 7 different 2'-deoxycytidine concentrations were utilized: 1 mM, 2.5 mM, 5 mM, 10 mM, 20 mM, 30 mM, and 50 mM. In addition to the nucleoside, reaction mixtures contained 30 mM GTP, 15 mM MgCl<sub>2</sub>, and 0.69 nmol/mL of *DmdNK*-WT or 9.45 nmol/mL of *BsdCK*-WT, and 50 mM potassium phosphate buffer (pH 7.5) with the total volume being 50  $\mu$ L. The dCMP syntheses were executed at 37 °C and 500 rpm and quenched with 150  $\mu$ L of acetonitrile after 5 min. The samples were centrifuged at 16,000  $\times$  g at 4 °C for 10 min, and analysed with HPLC-MS.

#### 2.3.4.5. Optimal phosphate donor concentration

The effect of GTP concentration to the synthesis of 2'-deoxycytidine 5'-monophosphate was evaluated by using 8 different GTP:dCyd molar ratios: 1:4, 1:2, 1:1, 3:2, 2:1, 5:2, 3:1, and 5:1. The reaction mixtures of 50  $\mu$ L consisted of 10 mM dCyd, 2.5 mM, 5 mM, 10 mM, 15 mM, 20 mM, 25 mM, 30 mM, or 50 mM GTP, 15 mM MgCl<sub>2</sub>, 50 mM potassium phosphate buffer (pH 7.5), and 0.69 nmol/mL *DmdNK*-WT or 9.45 nmol/mL *BsdCK*-WT. The reactions were performed for 5 min at 37 °C and a mixing speed of 500 rpm. The syntheses were halted by adding 150  $\mu$ L of acetonitrile, centrifuged at 16,000  $\times$  g at 4 °C for 10 min, and analysed with HPLC-MS.

#### 2.3.4.6. Optimal nucleoside kinase concentration

To determine how effectively the recombinant enzymes phosphorylated dCyd, a range of different kinase concentrations were employed. The reaction mixtures made up 50  $\mu$ L and consisted of 10 mM dCyd, 15 mM GTP, 15 mM MgCl<sub>2</sub>, 50 mM potassium phosphate buffer (pH 7.5), and 0.07 nmol/mL,

0.14 nmol/mL, 0.34 nmol/mL, 0.69 nmol/mL, 1.37 nmol/mL, 2.06 nmol/mL (for *DmdNK*-WT) or 1.89 nmol/mL, 4.72 nmol/mL, 9.45 nmol/mL, 18.9 nmol/mL, 56.7 nmol/mL, 94.5 nmol/mL, 189 nmol/mL (for *BsdCK*-WT) kinase. The reactions were executed for 5 min at 37 °C and 500 rpm. Phosphorylations were quenched by adding 150  $\mu$ L of acetonitrile, mixtures were centrifuged at 16,000  $\times$  g at 4 °C for 10 min, and analysed with HPLC-MS.

### 2.3.5. Substrate specificities of the nucleoside kinases

The substrate specificities of the recombinant nucleoside kinases *DmdNK* and *BsdCK* were performed in reaction mixtures with a total volume of 50  $\mu$ L that consisted of 10 mM of nucleoside, 15 mM of GTP, 15 mM MgCl<sub>2</sub>, 50 mM potassium phosphate buffer (pH 7.5), and 0.69 nmol/mL of wild-type or mutant *DmdNK*, or 9.45 nmol/mL wild-type *BsdCK* or 2.69 nmol/mL mutant *BsdCK*. The phosphorylation reactions were executed at 37 °C and 300 rpm for the duration of 24 h. The reactions were stopped by adding 150  $\mu$ L of acetonitrile. The samples were centrifuged at 16,000  $\times$  g at 4 °C for 10 min, and analysed with TLC and HPLC-MS.

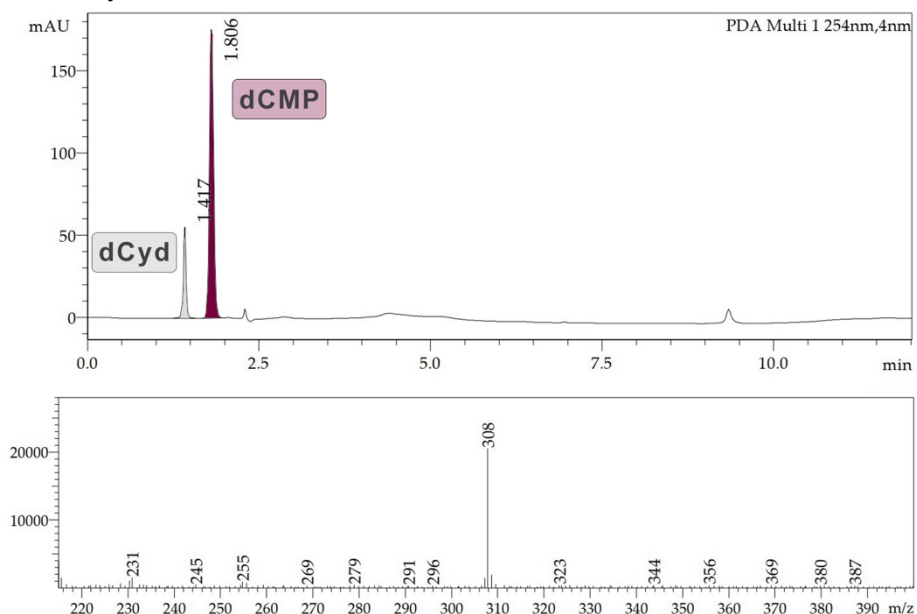


**Figure 23.** HPLC-MS analysis of dCyd phosphorylation reaction catalysed by *DmdNK*-WT. Higher – HPLC chromatogram, where dCyd area is coloured in gray and dCMP area is coloured in burgundy. Retention times – 1.417 min (dCyd); 1.806 min (dCMP). Below – MS spectrum, where the peak at 308 m/z corresponds to dCMP (307 g/mol) in positive ionisation ( $[M+H]^+$ ).

The specificities of the enzymes were determined based on the generation of corresponding nucleoside 5'-monophosphates. Reaction efficiencies were calculated by chromatogram areas of HPLC-MS analyses. An example of such analysis is provided in **Figure 23** above. The equation used to calculate the phosphorylation efficiencies (%):  $100\% \times \frac{NMP \text{ area}}{Nucleoside \text{ area} + NMP \text{ area}}$ . The substrates used for the experiments are listed in **Tables 3–6, 8–10**.

### 2.3.6. Larger-scale syntheses of nucleoside 5'-monophosphates

The conditions for the larger-scale synthesis of nucleoside 5'-monophosphates were based on the previously described optimization assays. Nucleosides, chosen for the phosphorylation, were 2'-deoxycytidine and *N*<sup>4</sup>-acetyl-2'-deoxycytidine for *BsdCK*-WT, and 2-thiouridine for *DmdNK*-WT. The reactions were started using these conditions: 50 mM nucleoside, 5 mM GTP, 15 mM MgCl<sub>2</sub>, 100 mM acetyl phosphate, 0.46 nmol/mL *EcACK*, and 9.45 nmol/mL *BsdCK*-WT or 0.34 nmol/mL *DmdNK*-WT in 15 mL of 50 mM potassium phosphate buffer (pH 7.5). Phosphorylation reactions were carried out in round-bottom flasks at 37 °C and mixed gently by hand every few hours. After 24 h and 48 h, mixtures were supplemented with 1.5 mL of 1 M acetyl phosphate, 15 μL of 462 nmol/mL *EcACK*, and 150 μL of 472 nmol/mL *BsdCK*-WT or 34 nmol/mL *DmdNK*-WT. After a total duration of 72 h, reactions were quenched with 15 mL of acetonitrile and centrifuged at 16,000 × g at 4 °C for 10 min. Soluble fractions were dried in a rotary evaporator. The remaining precipitate that contained synthesized nucleoside monophosphate was dissolved in 5 mL of water and loaded onto a chromatography column filled with 30 mL DEAE Sephadex A-25 equilibrated with water. The ion-exchange chromatography started with 150 mL of water which was used to wash out the unphosphorylated nucleoside. Then, 200 mL of 50 mM NaCl solution was used to elute the nucleoside monophosphate. Fractions containing nucleotides were pooled and dried using a rotary evaporator. Additional purification using reverse-phase chromatography was performed. The dry material was dissolved in 5 mL of water and loaded onto a Grace C-18 (12 g) column equilibrated with water. The synthesized nucleoside monophosphate was eluted using water. Fractions, containing product, were pooled and dried using a rotary evaporator. The mononucleotide syntheses and purification processes were monitored using TLC analysis. Yields of purified nucleotides were calculated using UV spectra of corresponding nucleosides. Structures of

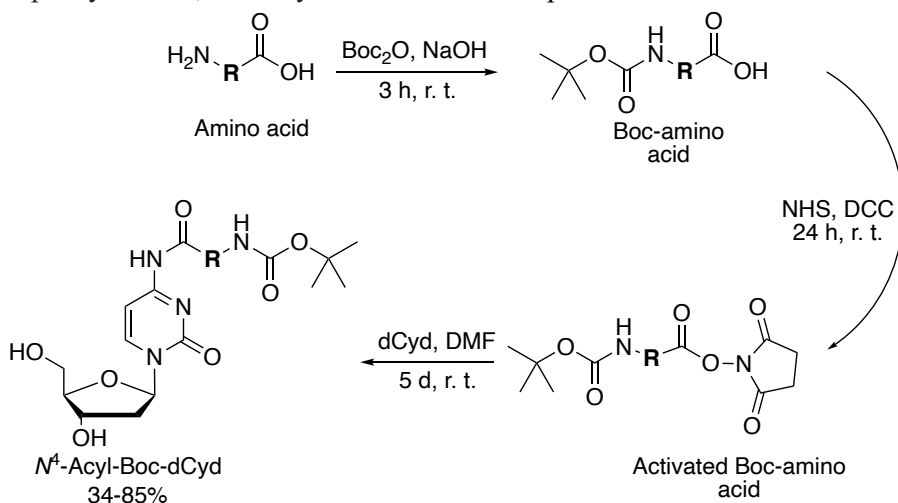
nucleoside 5'-monophosphates were confirmed by HPLC-MS and NMR analyses (provided in **Appendix 3**).

### 3. RESULTS AND DISCUSSION

During this work, sixteen novel amino acid and deoxycytidine conjugates were synthesized. Eight of the compounds were Boc-protecting group bearing  $N^4$ -amino acid-acylated 2'-deoxycytidines, and eight of them were  $N$ -4-(2'-deoxycytidinyl)amino acid amides, that were obtained by deprotecting the beforementioned nucleosides. The amino acids were chosen to have varying length and polarity side chains to ensure heterogeneity. The addition of amino acids to 2'-deoxycytidine improves the functional diversity by giving the nucleoside new properties and, therefore, expanding the list of its potential applications. In addition to broadening the current library of nucleoside analogues, the synthesized compounds serve as potential substrates to nucleic acid-related enzymes, including but not limited to deaminases, nucleoside phosphorylases or  $N$ -deoxyribosyltransferases. Furthermore, the produced nucleosides can serve as intermediate compounds for chemical or enzymatic synthesis of nucleoside phosphates.

#### 3.1. Synthesis of $N^4$ amino acid-acylated nucleosides

Synthesis of the Boc-protected  $N^4$ -amino acid-modified nucleosides was performed in three steps, as exhibited in **Figure 24**, and 2'-deoxycytidine and glycine, L-alanine,  $\beta$ -alanine, L-leucine, L-isoleucine, L-methionine, L-phenylalanine, and L-tyrosine were used as precursors.

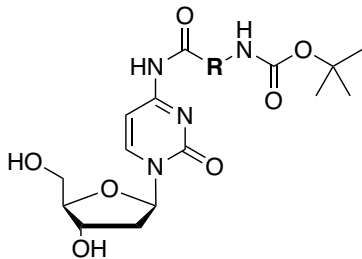
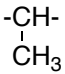
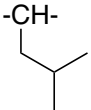
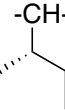
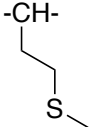
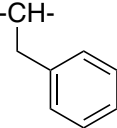
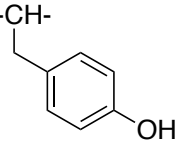


**Figure 24.** General scheme of  $N^4$ -acyl-Boc-2'-deoxycytidine nucleoside synthesis.  $\text{Boc}_2\text{O}$  – di-*tert*-butyl dicarbonate;  $\text{NHS}$  – *N*-hydroxysuccinimide;  $\text{DCC}$  – dicyclohexylcarbodiimide;  $\text{dCyd}$  – 2'-deoxycytidine;  $\text{DMF}$  – dimethylformamide.



In total eight  $N^4$ -acyl-Boc-2'-deoxycytidine nucleosides were synthesized. The compounds with their final yields are provided in **Table 1** below.

**Table 1.** Synthesized  $N^4$ -acyl-Boc-2'-deoxycytidine nucleosides.

Nucleoside	R	Amount, g	Yield, %
	-CH <sub>2</sub> -	1.36	53
		1.32	50
	-CH <sub>2</sub> CH <sub>2</sub> -	1.55	59
		1.91	65
		1.17	40
		1.03	34
		2.66	85
		1.72	53

The synthesis began by protecting an amine group of the selected amino acid using di-*tert*-butyl dicarbonate (Jahani et al., 2011). The protection reactions were executed for 3 h at room temperature in a prechilled mixture of 1 M NaOH, 1,4-dioxane, and water (1.1:1:1). The mechanism of the amine protection reaction is provided in **Figure 25**. The amine group of the amino acid performs a nucleophilic attack on carboxylic carbon atom of di-*tert*-butyl dicarbonate. An intermediate compound with a protonated nitrogen atom and *tert*-butyl carbonate, which further breaks down into CO<sub>2</sub> and *tert*-butoxide, form. Base deprotonates the intermediate compound, and *N*-Boc-protected

amino acid forms. The protected amino acids were extracted with ethyl acetate with yields reaching 90–95%.

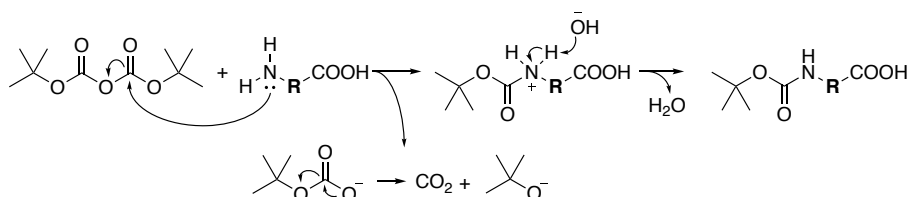


**Figure 25.** Reaction mechanism of an amine coupling with Boc-protecting group (Viswanadham et al., 2017).

The second step of the synthesis – carboxyl group activation – was performed by treating the protected amino acid with NHS and DCC in ethyl acetate for 24 h at room temperature (Barré et al., 2016). The activation is a two-step process, as shown in **Figure 26**, in which the carboxyl group of the protected amino acid first reacts with DCC to form a very reactive *O*-acylisourea intermediate. Then the intermediate further reacts with NHS and forms a more stable NHS-ester and *N,N'*-dicyclohexylurea as a byproduct, which is removed by filtration.

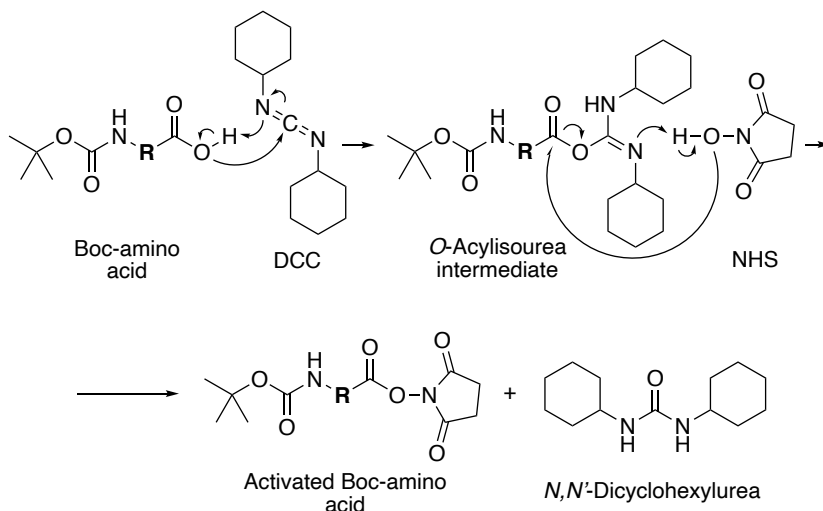


**Figure 26.** Boc-protected amino acid activation with NHS and DCC (Barré et al., 2016). DCC – dicyclohexylcarbodiimide; NHS – *N*-hydroxysuccinimide.

Coupling reaction of 2'-deoxycytidine and a selected activated amino acid proceeded in DMF and took 5 days at room temperature to complete. During the reaction  $N^4$  nitrogen atom of the cytosine nucleobase performs a nucleophilic attack on carboxylic carbon of the activated amino acid (Fischer,

2010). Reaction results in a modified 2'-deoxycytidine nucleoside and NHS as displayed in **Figure 27**.

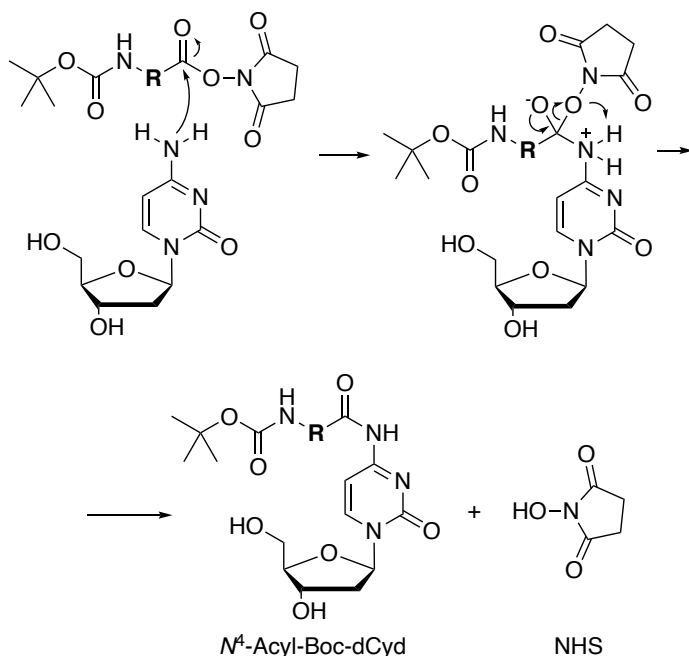


**Figure 27.** Coupling reaction of an activated Boc-protected amino acid and 2'-deoxycytidine (Fischer, 2010). NHS – *N*-hydroxysuccinimide.

The synthesized compounds were purified by column chromatography (solid phase: silica gel, liquid phase: chloroform-methanol, 100:0 to 85:15). The structures were confirmed by NMR and HPLC-MS analyses. An example of HPLC-MS analysis of purified Boc-protected L-tyrosine-modified 2'-deoxycytidine is provided in **Figure 28**, while full analyses can be found in **Appendix 1**.

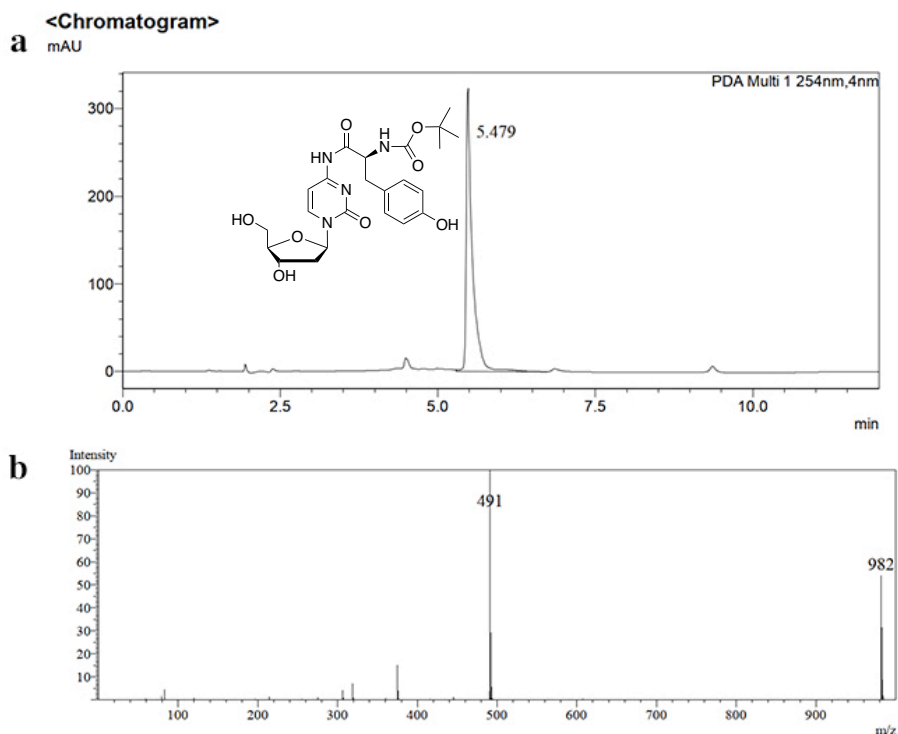


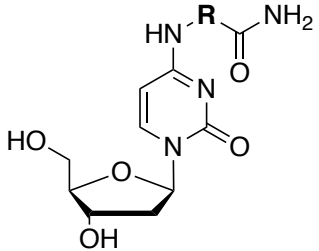
**Figure 28.** HPLC-MS analysis of purified *tert*-butyl ((*S*)-1-((1-((2*R*,4*S*,5*R*)-4-hydroxy-5-(hydroxymethyl)tetrahydrofuran-2-yl)-2-oxo-1,2-dihydropyrimidin-4-yl)amino)-3-(4-hydroxyphenyl)-1-oxopropan-2-yl)carbamate. **a** HPLC chromatogram. The largest peak at 5.479 min represents the compound. **b** MS spectrum of nucleoside at 5.507 min. The peak at 491 *m/z* represents the nucleoside ( $M=490$  g/mol) in positive ionisation ( $[M+H]^+$ ).

The novel Boc-protected amino acid and 2'-deoxycytidine conjugates (**Table 1**) were obtained in 34–85% final yields. The yields are comparable to those of previously reported  $N^4$ -acyl-modified 2'-deoxycytidine nucleosides (40–84%) (Jakubovska et al., 2018).

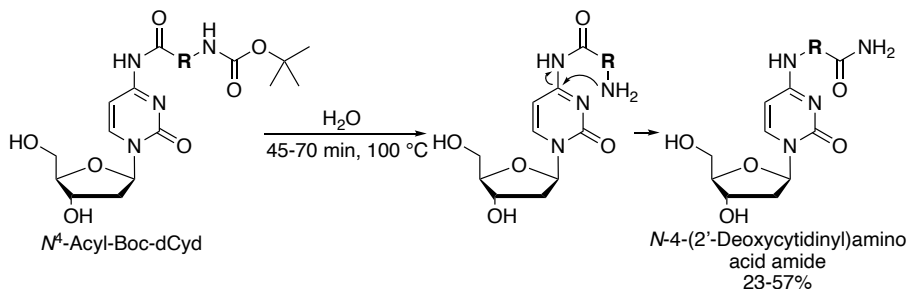
### 3.2. Synthesis of *N*-4-(2'-deoxycytidinyl)amino acid amides

The synthesis of *N*-4-(2'-deoxycytidinyl)amino acid amides was performed using Boc-protected amino acid-modified 2'-deoxycytidine nucleosides, described in the previous chapter. In total, eight novel 2'-deoxycytidine derivatives were obtained with final yields of 23–57% (**Table 2**). The resulting yields were similar, albeit slightly lower, to previously reported yields of *N*-(4-cytidinyl)amino acid amides (38–81%) (Zhang et al., 2008).

**Table 2.** Synthesized *N*-4-(2'-deoxycytidinyl)amino acid amides.

Nucleoside	R	Amount, g	Yield, %
	-CH <sub>2</sub> -	0.18	48
	-CH-   CH <sub>3</sub>	0.11	37
	-CH <sub>2</sub> CH <sub>2</sub> -	0.17	57
	-CH-   CH <sub>2</sub>   CH <sub>3</sub>	0.10	29
	-CH-   CH <sub>2</sub>   CH <sub>2</sub>   CH <sub>3</sub>	0.09	26
	-CH-   CH <sub>2</sub>   S-CH <sub>3</sub>	0.21	51
	-CH-   CH <sub>2</sub>   C <sub>6</sub> H <sub>5</sub>	0.09	23
	-CH-   CH <sub>2</sub>   C <sub>6</sub> H <sub>4</sub> -OH	0.18	46

For the removal of the *N*-Boc protecting group a catalyst-free method with mild and neutral conditions was chosen (J. Wang et al., 2009). The deprotection was accomplished by heating the *N*<sup>4</sup>-acylated deoxycytidines at reflux in water for 45–70 min, the reaction is provided in **Figure 29** below.

**Figure 29.** Rearrangement of *N*<sup>4</sup>-acyl-Boc-2'-deoxycytidines to *N*-4-(2'-deoxycytidinyl)amino acid amides during *N*-Boc deprotection reaction (Zhang et al., 2008).

The reaction is based on water's ability to self-ionize (Arcis et al., 2020). At higher temperatures, up to a certain point, the ionization of water increases and both  $\text{H}_3\text{O}^+$  and  $\text{OH}^-$  ions are more abundant, which are believed to act as a dual acid/base catalyst at the *N*-Boc deprotection reaction whose mechanism is displayed in **Figure 30**. Firstly, the carbonyl oxygen atom is protonated by a hydronium ion. Water molecule attacks the protonated carboxylic carbon and an intermediate tetrahedral diol forms. Hydroxide ion deprotonates one of the hydroxyl groups, the following N-C bond breakage results in a primary amine and *tert*-butylcarboxylic acid.

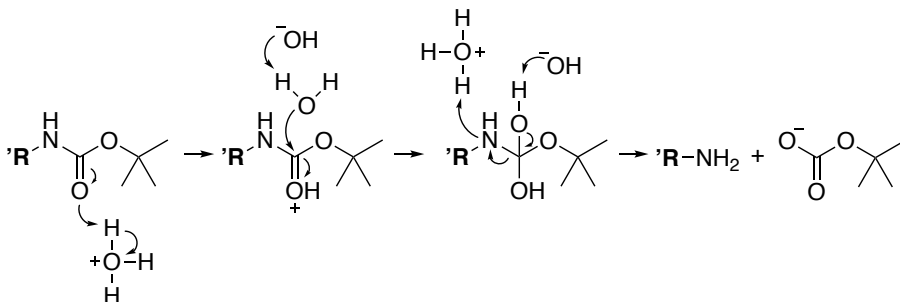


**Figure 30.** Mechanism of *N*-Boc deprotection (B. Li et al., 2019).

Notwithstanding, the formed aminoacyl intermediate is unstable in aqueous solution and, thus, is not a final product. As proposed by Zhang and co-workers, the primary amine undergoes a rearrangement where the  $\alpha$ -amine performs a nucleophilic attack to the C4 atom of the cytosine nucleobase, N-C bond breaks and a significantly more stable acylamide derivative is formed (Zhang et al., 2008). The rearrangement occurred for all 8 of the synthesized nucleosides during the deprotection and was confirmed by a shift of the NH signal in  $^1\text{H-NMR}$  spectroscopy. An example of the spectrum is provided in **Figure 31** below. The  $N^4$  hydrogen atom of the *N*-Boc protected  $N^4$ -acylated nucleosides appeared as a singlet at 11 ppm, however, since after the rearrangement the  $N^4$  hydrogen atom did not have a carbonyl group nearby, the NH signal shifted to around 7.8 ppm and split into a doublet, triplet or multiplet depending on the amino acid residue. In addition, two singlets of the primary amide  $\text{NH}_2$  appeared at around 7.0 and 7.5 ppm.

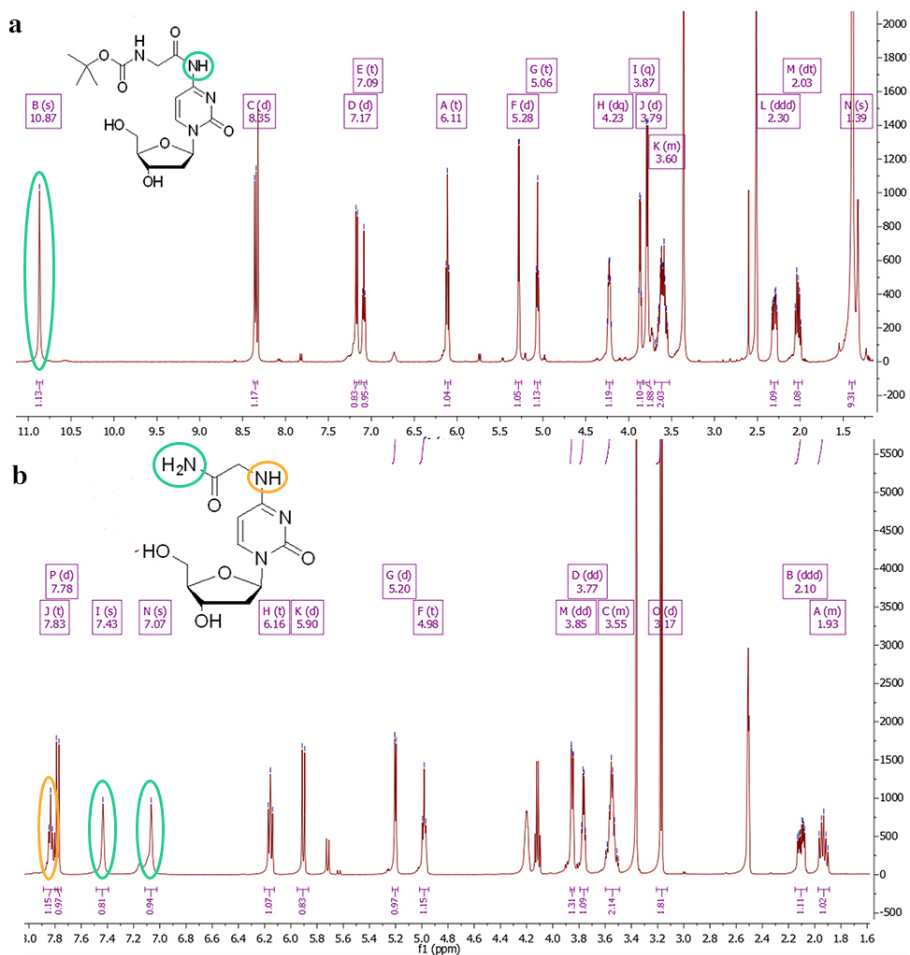


**Figure 31.**  $^1\text{H-NMR}$  spectra of synthesized nucleosides. **a**  $^1\text{H-NMR}$  spectrum of *tert*-butyl(2-((1-((2*R*,4*S*,5*R*)-4-hydroxy-5-(hydroxymethyl)tetrahydrofuran-2-yl)-2-oxo-1,2-dihydropyrimidin-4-yl)amino)-2-oxoethyl)carbamate. The singlet at 10.87 ppm marked in green colour represents the  $N^4$  hydrogen atom of the *N*-Boc protected nucleoside. **b**  $^1\text{H-NMR}$  spectrum of 2-((1-((2*R*,4*S*,5*R*)-4-hydroxy-5-(hydroxymethyl)tetrahydrofuran-2-yl)-2-oxo-1,2-dihydropyrimidin-4-yl)amino)acetamide. The triplet at 7.83 ppm marked in yellow represents the  $N^4$  hydrogen atom, while two singlets at 7.07 ppm and 7.43 ppm marked in green represent hydrogens of the primary amide  $\text{NH}_2$ .

The acylamides were purified using reverse phase chromatography (solid phase: C18 column, liquid phase: water-methanol, 100:0 to 80:20) and isolated in 23–57% yields. Deprotection reactions took 45–70 min. HPLC-MS analyses of the reaction mixtures confirmed that reactions that took longer than 45 min contained 2'-deoxycytidine as an impurity. The byproduct formation can be explained by cleavage of the  $N^4$ -amide bond. Most of the time the aforementioned impurity did not cause any major issues as

2'-deoxycytidine could be easily separated from the synthesized *N*-4-(2'-deoxycytidinyl)amino acid amides during the purification process. The only exception was *N*-4-(2'-deoxycytidinyl)glycinamide which possessed similar retention time as 2'-deoxycytidine and could not be separated from it during the reverse-phase chromatography. The problem was overcome by taking an extra synthesis step. The *N*-4-(2'-deoxycytidinyl)glycinamide with 2'-deoxycytidine impurity was treated with acetyl-NHS ester in DMF. The reaction occurred only between the acetyl-NHS ester and 2'-deoxycytidine, and the resulting *N*<sup>4</sup>-acetyl-2'-deoxycytidine was successfully separated from *N*-4-(2'-deoxycytidinyl)glycinamide by purification.

### 3.3. Production of target proteins

Expression of the target genes and purification of the corresponding proteins is described in Section 2.3.2. Since the genes, encoding the enzymes, were cloned into pLATE31 vector, all the proteins were purified with *C*-terminal (His)<sub>6</sub>-tags and were used without further removal of the tags.

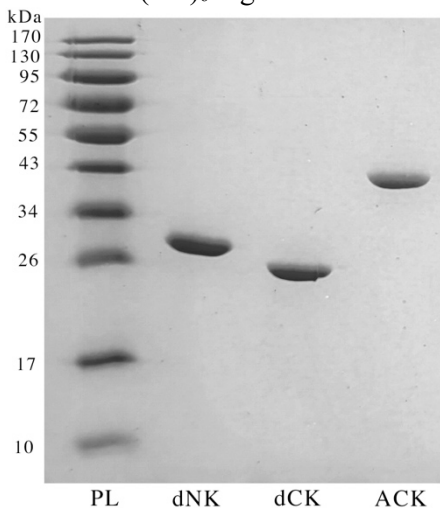


**Figure 32.** SDS-PAGE (14%) of the purified enzymes. PL – Fisher BioReagents EZ-Run Prestained Rec Protein Ladder; dNK – *D. melanogaster* deoxynucleoside kinase (29.1 kDa); dCK – *B. subtilis* deoxycytidine kinase (25.4 kDa); ACK – *E. coli* acetate kinase (43.3 kDa).

As can be seen from the SDS-PAGE analysis of purified *DmdNK*-WT, *BsdCK*-WT, and *EcACK* provided in **Figure 32**, the recombinant proteins were of high purity. The obtained concentrations were as follows: 34 nmol/mL *DmdNK*-WT, 472 nmol/mL *BsdCK*-WT, and 462 nmol/mL *EcACK*.



### 3.4. Optimization of reaction conditions catalysed by *DmdNK*-WT and *BsdCK*-WT

After purification of the nucleoside kinases, the following task was to find reaction conditions in which *DmdNK*-WT and *BsdCK*-WT phosphorylate substrates optimally. The parameters that were evaluated were reaction duration, temperature, pH, nucleoside concentration, GTP concentration, and enzyme concentration. The assessments were done using HPLC-MS chromatogram area sizes of formed nucleoside monophosphate. Unless stated otherwise, the reactions were performed in 37 °C and 300 rpm for 5 min and consisted of 10 mM dCyd, 15 mM GTP, 15 mM MgCl<sub>2</sub>, and 0.69 nmol/mL *DmdNK*-WT or 9.45 nmol/mL *BsdCK*-WT in 50 mM potassium phosphate buffer (pH 7.5).

The influence of reaction duration was evaluated by utilizing 1 µL of kinase in a total volume of 50 µL, which equates to 0.69 nmol/mL *DmdNK*-WT or 9.45 nmol/mL *BsdCK*-WT, for 1–120 min. As illustrated in **Figure 33a**, reactions catalysed by *DmdNK*-WT and *BsdCK*-WT start slowing down at around 30 min and reach a maximum dCMP production efficiency of almost 100% at around 60 min. The reaction duration, necessary for optimal nucleoside phosphorylation by *DmdNK*-WT and *BsdCK*-WT, agrees with previously reported data, where reaction durations range from 30 min to 10 h, depending on the substrate and its amount (Johansson et al., 1999; Zou et al., 2013).

The effect of temperature on the activities of the kinases was measured at a range of 4–80 °C (**Figure 33b**). As expected, the phosphorylation efficiencies of the enzymes rose up to a particular temperature and fell sharply after. Both *DmdNK*-WT and *BsdCK*-WT exhibited the lowest catalytic efficiencies at 4–20 °C range, with dCyd conversions reaching only 10–20% after 5 min. The activities of the kinases increased until 60 °C where conversion efficiencies of dCyd were almost at 100% after 5 min. It was discovered that *DmdNK*-WT tolerates slightly higher temperatures than *BsdCK*-WT, as the former retained maximum catalytic efficiency even at 70 °C, where the activity of *BsdCK*-WT has already started plummeting. At the temperature of 80 °C, efficiencies of both enzymes declined sharply: phosphorylation activity of *DmdNK*-WT decreased to around 70%, and activity of *BsdCK*-WT sunk to 20%.

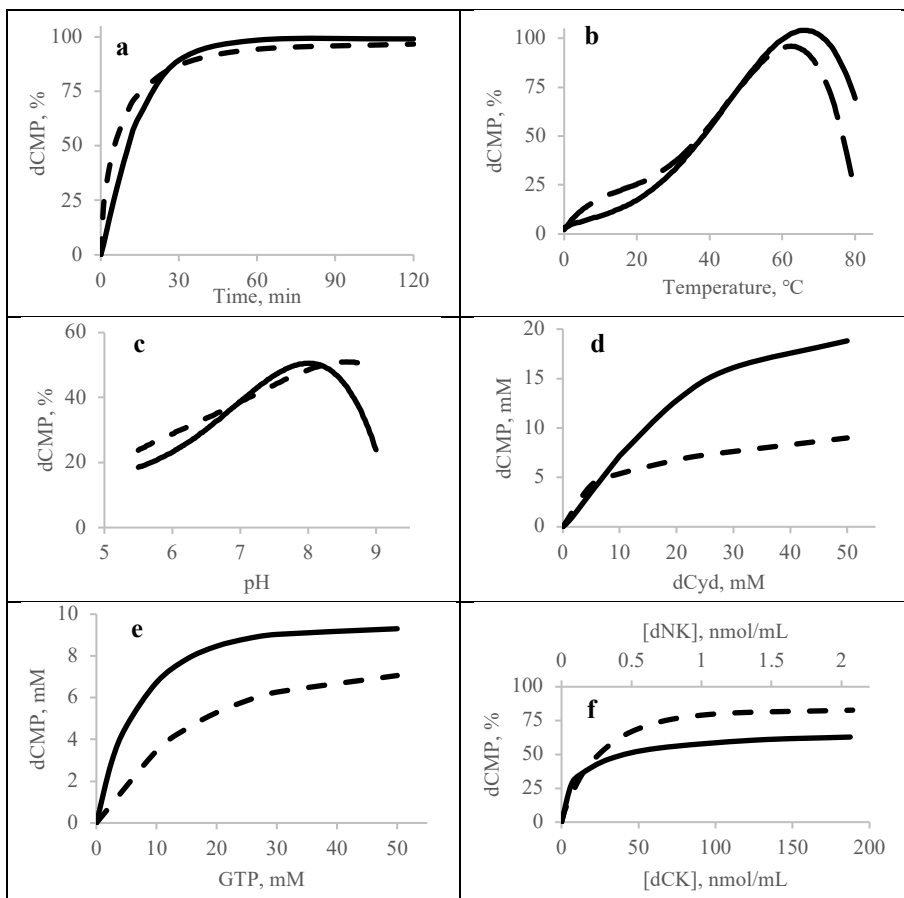


**Figure 33.** Influence of various parameters on the phosphorylation effectiveness of dCyd by *DmdNK*-WT and *BsdCK*-WT. The solid line represents *DmdNK*-WT and the dashed line represents *BsdCK*-WT. **a** Effect of reaction duration on the dCMP production; **b** influence of temperature on reaction efficiency; **c** dependency of reaction efficiency on medium pH; **d** impact of dCyd concentration on phosphorylation efficiency; **e** influence of GTP concentration on reaction efficiency; **f** effect of kinase concentration on the reaction efficiency.

The results might indicate that the optimal temperature for the enzymes studied is significantly higher than the moderate range of 20–40 °C that is typical for mesophilic organisms like *B. subtilis* and *D. melanogaster* (Partridge et al., 1994; van de Vossenberg et al., 1999). However, it is important to recognize that enzymatic activity is also influenced by the duration of the reaction (Daniel et al., 2008). Although the highest enzymatic activities for *BsdCK*-WT and *DmdNK*-WT were recorded at 60–70 °C, these reactions were conducted for only 5 minutes; hence, lower temperatures may be optimal for longer reaction durations.

The optimal pH of the reaction medium was evaluated utilizing two 50 mM buffers: potassium phosphate buffer with a pH range of 5.5–7.0 and Tris-HCl buffer with a pH range of 7.0–9.0. As can be seen from a solid line, which represents *DmdNK*-WT, in **Figure 33c**, the kinase reaches the highest catalytic efficiency when reaction solution pH is 8.0, however similar results are observed in the pH range of 7.5–8.5, which correlates with previously reported data (Chen et al., 2017; Johansson et al., 1999; Solaroli et al., 2003). The activity of *DmdNK*-WT plummets when pH reaches 9.0. Dashed line, which represents *BsdCK*-WT, in the same chart tells a slightly different story. *BsdCK*-WT is a little less sensitive to pH variations overall as it retains more activity at both lower and higher pH, and compared to *DmdNK*-WT favours a slightly more alkaline environment. *BsdCK*-WT reaches the highest conversion of dCyd at pH 8.5, although comparable activity is observed at pH 8.0–9.0, which agrees with previously reported data that the enzyme is the most active at pH 8.6 (Møllgaard, 1980).

The effect of nucleoside concentration was evaluated by applying 0.69 nmol/mL (34 pmol or 10 µg) *DmdNK*-WT or 9.45 nmol/mL (470 pmol or 120 µg) *BsdCK*-WT for the phosphorylation of 2'-deoxycytidine with concentrations ranging from 1 to 50 mM in the 5 min timeframe. As can be seen from the curves in **Figure 33d**, higher deoxycytidine concentrations correlated with higher deoxycytidine monophosphate concentrations and no inhibitory effects were observed. The highest concentration of dCMP was detected when reaction mixtures contained 50 mM of dCyd. However, it is feasible that even higher dCMP concentrations could be obtained given higher dCyd concentration was used. During these conditions 34 pmol of *DmdNK*-WT converted 18 mM of dCyd into dCMP, while *BsdCK*-WT was more sluggish as 470 pmol of the enzyme was capable of phosphorylating only 8 mM of deoxycytidine. This equates to 26.2 pmol and 0.85 pmol of nucleoside converted by 1 pmol of *DmdNK*-WT and *BsdCK*-WT, respectively, making *DmdNK*-WT around 30 times more efficient at phosphorylating deoxycytidine than *BsdCK*-WT. The results were used to calculate specific activities of the kinases, which equated to 35.9 and 1.6 µmol min<sup>-1</sup> mg<sup>-1</sup> for *DmdNK*-WT and *BsdCK*-WT, respectively. The measured specific activity of *DmdNK*-WT for dCyd is greater than the previously reported value of 370 nmol h<sup>-1</sup> µg<sup>-1</sup> (equivalent to 6.17 µmol min<sup>-1</sup> mg<sup>-1</sup>), possibly due to variations in experimental conditions (Johansson et al., 1999). Specific activity data on *BsdCK*-WT, to the best of our knowledge, is not currently available.

The influence of GTP concentration on dCMP production was measured by using 0.25–5 mol. eq. of GTP in the dCyd phosphorylation mixtures. As

depicted in **Figure 33e**, *DmdNK*-WT reached highest dCMP conversions utilizing slightly less GTP than *BsdCK*-WT, however *BsdCK*-WT was not far off. At least 1.5 mol. eq. of GTP was necessary for the reactions to run optimally, however, 2 or 2.5 mol. eq., especially in case of *BsdCK*-WT, might allow for the reactions to be even more efficient. Using higher concentrations of GTP (3–5 mol. eq.) had almost no further effect on dCMP production. *DmdNK*-WT and *BsdCK*-WT have been shown to phosphorylate substrates with phosphate donor (ATP or GTP) amounts ranging from 1 mol. eq. up to 20 mol. eq.; however, an optimal amount of phosphate donor for the kinases has not been established (Chen et al., 2017; Egeblad-Welin et al., 2007; Johansson et al., 1999; Møllgaard, 1980; Zou et al., 2013).

The optimal enzyme concentrations for the phosphorylation of 10 mM of deoxycytidine were measured using 0.07–2.06 nmol/mL *DmdNK*-WT or 1.89–189 nmol/mL *BsdCK*-WT. As previously calculated, the kinases differ in phosphorylating efficiencies, thus diverging results were to be expected (**Figure 33f**). The optimal concentration of *DmdNK*-WT was determined to be 0.34 nmol/mL. Far greater amount of *BsdCK*-WT was needed for the reactions to run at an optimal speed. It was noted that 47 nmol/mL of *BsdCK*-WT was a point where dCMP formation started to taper off and higher concentration of the enzyme had no additional benefit.

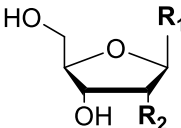
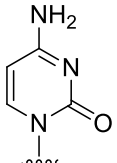
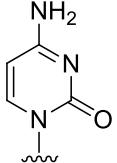
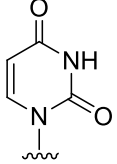
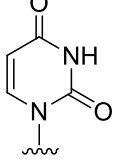
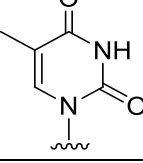
To summarize, phosphorylation of 10 mM deoxycytidine with 1.5 mol. eq. GTP and 0.69 nmol/mL *DmdNK*-WT or 9.45 nmol/mL *BsdCK*-WT in the reaction mixture takes up to an hour to complete. The highest phosphorylation efficiencies were observed at the temperatures of 70 °C for *DmdNK*-WT and 60 °C for *BsdCK*-WT. Both enzymes best perform at a slightly alkaline reaction solution: pH of 8.0 is optimal for *DmdNK*-WT, and pH of 8.5 – for *BsdCK*-WT. However, due to sensitive nature of synthesized nucleoside monophosphates, and a possibility of denaturing of kinases during prolonged reaction times, as a precaution, 37 °C and pH 7.5 were chosen for further experiments.

### 3.5. Substrate specificity of *DmdNK*-WT

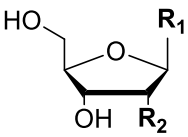
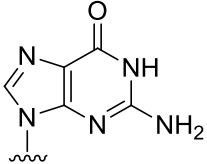
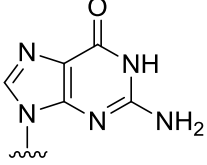
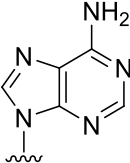
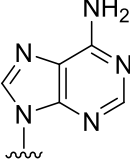
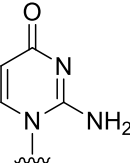
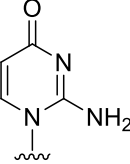
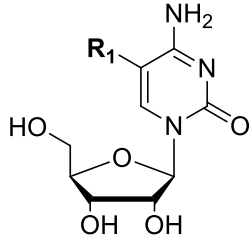
To expand the knowledge on the substrate specificity of *DmdNK*-WT, an assortment of 57 nucleosides was chosen to be tested as substrates, amongst which were both canonical and modified compounds (**Tables 3–5**). The utilized nucleoside analogues included pyrimidine nucleosides bearing small to moderately sized modifications at nucleobase's 4<sup>th</sup> or 5<sup>th</sup> positions, or at sugar's 2' or 3' positions. A large part of the tested compounds, 43 to be

precise, were found to be suitable substrates for the nucleoside kinase. The conditions for the phosphorylation reactions were based on the optimization assay described in Section 3.4. Nucleoside concentration was 10 mM and the concentrations of both GTP and MgCl<sub>2</sub> were 15 mM. Since the reactions were executed for 24 h, 1 μL of kinase was added to the mixtures, which equated to 0.69 nmol/mL in 50 mM potassium phosphate buffer. Gentle conditions of 37 °C and pH 7.5 were chosen due to possible enzyme denaturation and sensitive nature of utilized nucleosides and corresponding monophosphates.

**Table 3.** Efficiency of synthesis of canonical nucleoside monophosphates and cytidine derivative monophosphates by *DmdNK*-WT. HPLC-MS analysis of the reaction mixtures was performed after incubation at 37 °C for 24 h.

Nucleoside	No.	R <sub>1</sub>	R <sub>2</sub>	NMP, %
	1		-H	98
	2		-OH	78
	3		-H	61
	4		-OH	78
	5		-H	64

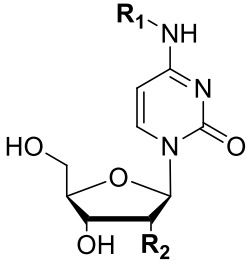
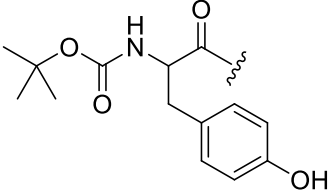
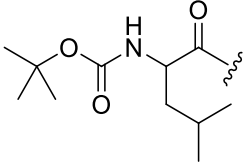
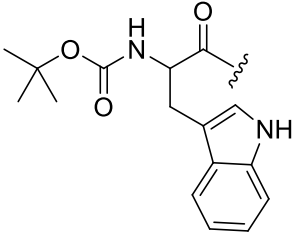
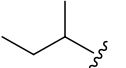
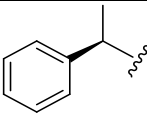
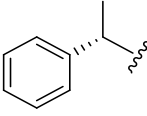
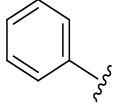
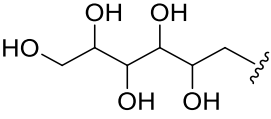
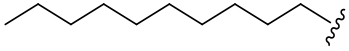
**Table 3 continued.** Efficiency of synthesis of canonical nucleoside monophosphates and cytidine derivative monophosphates by *DmdNK*-WT. HPLC-MS analysis of the reaction mixtures was performed after incubation at 37 °C for 24 h.

Nucleoside	No.	R <sub>1</sub>	R <sub>2</sub>	NMP, %
	6		-H	94
	7		-OH	21
	8		-H	26
	9		-OH	35
	10		-OH	62
	11		-H	82
	12	-F	-	8
	13	-CH <sub>3</sub>	-	22

**Table 3 continued.** Efficiency of synthesis of canonical nucleoside monophosphates and cytidine derivative monophosphates by *DmdNK*-WT. HPLC-MS analysis of the reaction mixtures was performed after incubation at 37 °C for 24 h.

Nucleoside	No.	R <sub>1</sub>	R <sub>2</sub>	NMP, %
	14		-H	100
	15		-H	0
	16	-OH	-OH	46
	17		-H	0
	18		-H	0
	19		-H	3
	20		-H	0
	21		-H	31
	22		-H	0
23		-H	0	

**Table 3 continued.** Efficiency of synthesis of canonical nucleoside monophosphates and cytidine derivative monophosphates by *DmdNK*-WT. HPLC-MS analysis of the reaction mixtures was performed after incubation at 37 °C for 24 h.

Nucleoside	No.	R <sub>1</sub>	R <sub>2</sub>	NMP, %
	24		-H	0
	25		-H	0
	26		-H	0
	27		-H	93
	28		-H	5
	29		-H	11
	30		-H	74
	31		-H	0
	32		-H	0



As can be seen from **Table 3**, *DmdNK*-WT successfully converted all canonical 2'-deoxy- and ribonucleosides into their 5'-monophosphate forms. The highest nucleoside conversion rates were noticed when 2'-deoxycytidine (**1**) and 2'-deoxyguanosine (**6**) were utilized as substrates (94–98%), however, cytidine (**2**), 2'-deoxyuridine (**3**), uridine (**4**), and 2'-deoxythymidine (**5**) were phosphorylated efficiently (64–78%), as well. Out of all tested canonical nucleosides, guanosine (**7**), 2'-deoxyadenosine (**8**), and adenosine (**9**) were the least suitable substrates as their phosphorylation efficiencies hovered around 21–35%. The results mostly agree with previously reported data, where it is stated that *DmdNK*-WT favours pyrimidine nucleosides over purines, and 2'-deoxyribonucleosides over ribonucleosides (Johansson et al., 1999).

In addition to canonical nucleosides, *DmdNK*-WT phosphorylates a wide array of cytosine nucleosides. Both isocytidine (**10**) and its 2'-deoxy- form (**11**) were converted into corresponding monophosphates with efficiency of 62–82%. Modifications at the C5-position of cytidine were found to be less tolerated. 5-Fluorocytidine (**12**) and 5-methylcytidine (**13**) were phosphorylated up to ten times less efficiently compared to canonical cytidine, as conversion efficiencies reached only 8–22%.

A considerable part of tested cytosine nucleosides contained modifications at the  $N^4$ -position. It was discovered that certain modifications at the said position are acceptable. For example,  $N^4$ -acetyl-2'-deoxycytidine (**14**) was converted into its monophosphate form completely, whereas bulkier  $N^4$ -isobutyryl-2'-deoxycytidine (**15**) was not phosphorylated at all. A hydroxyl modification at the  $N^4$ -position of cytidine lowered the phosphorylation efficiency of the  $N^4$ -hydroxycytidine (**16**) almost twice compared to canonical cytidine: it was converted into a monophosphate with a 46% efficiency. Two structurally similar deoxycytidines bearing  $N^4$ -benzoyl- (**17**) and  $N^4$ -isonicotinoyl- (**18**) modifications were found to be unsuitable substrates to the wild-type enzyme as no monophosphate formation after 24h was detected.

The synthesized  $N^4$ -aminoacid modified deoxycytidines were tested as substrates for *DmdNK*-WT, as well. Out of the eight tested nucleosides (**19-26**) only two were accepted by the kinase. The smallest modifications carrying  $N^4$ -alaninoyl- (**19**) and  $N^4$ -glycinoyl-2'-deoxycytidine (**21**) were phosphorylated with efficiencies of 3% and 31%, respectively. Bulkier nucleoside analogues, such as  $N^4$ -tyrosinoyl-2'-deoxycytidine (**23**), and Boc-protecting group bearing aminoacid-modified 2'-deoxycytidines (**20**, **22**, **24**, **25**, **26**) were not phosphorylated by the enzyme.

*DmdNK*-WT displayed tolerance towards  $N^4$ -hydrophobic modifications bearing deoxycytidines. A *sec*-butyl modification bearing deoxycytidine (**27**) was converted into a monophosphate exceptionally well, as conversion was

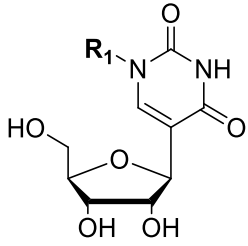
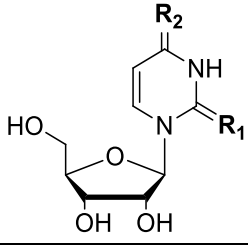
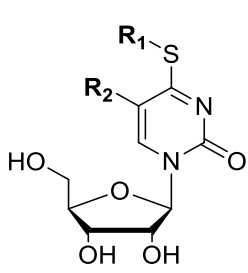
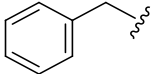
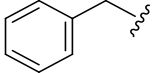
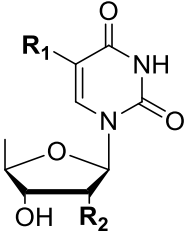
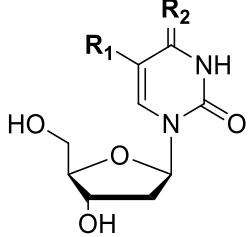
93%. Benzene ring carrying nucleosides were phosphorylated, as well. Even though the efficiencies were low (5–11%), *o*-methylbenzyl-modified nucleoside enantiomers (**28** and **29**) were accepted as substrates. In addition, the kinase exhibited high activity towards *N*<sup>4</sup>-phenyl-modified deoxycytidine (**30**), as 74% of the compound was turned into the monophosphate form.

Deoxycytidines bearing long-chain modifications at the *N*<sup>4</sup>-position were found to be unsuitable substrates to the kinase. Monophosphate formation of D-glucose-modified deoxycytidine (**31**) or *N*<sup>4</sup>-decyl-2'-deoxycytidine (**32**) was not detected.

As was suggested in the current literature, *DmdNK*-WT exhibited a broad substrate acceptance and successfully phosphorylated ribo- and 2'-deoxycytidine nucleosides with various substitutions at *N*<sup>4</sup> and C5 positions (Johansson et al., 1999; Knecht et al., 2009; Mikkelsen et al., 2008). *N*<sup>4</sup>-Modifications of varying sizes and polarities, such as *N*<sup>4</sup>-acetyl-, *N*<sup>4</sup>-glycinoyl, and *N*<sup>4</sup>-phenyl were tolerated by the kinase. In contrast, the findings from phosphorylation reactions involving C5-substituted cytidines suggest that alterations at this position are less compatible with *DmdNK*-WT. Even small modifications such as fluoro or methyl significantly reduced phosphorylation efficiency compared to that of unmodified cytidine. To determine, whether uracil nucleobase bearing nucleosides could serve as suitable substrates to *DmdNK*-WT, various uridine derivatives were evaluated as substrates for the kinase (**Table 4**).

Pseudouridine (**33**) was converted into a monophosphate with 80% efficiency, however, a twofold decrease in phosphorylation efficiency was observed when *N*<sup>1</sup>-methylpseudouridine (**34**) was used as a substrate. Thiouridines were accepted as substrates, as well. 2-Thiouridine (**35**) was superior to 4-thiouridine (**36**) as a substrate, as phosphorylation efficiency of the compound was 91% compared to 49% of 4-thiouridine. Moreover, *DmdNK*-WT was active towards compounds bearing small substitutions at nucleobase positions 4 and 5. 4-Methylthiouridines, both with (**37**) and without 5-fluoro-moiety (**38**), were converted into their corresponding monophosphates with 29–57% efficiencies. The slightly bulkier 4-ethylthiouridine (**40**) was successfully phosphorylated (70% efficiency), however, the additional fluorine atom in 5-fluoro-4-ethylthiouridine (**39**) almost completely halted phosphorylation: only a trace (0.4%) of monophosphate was detected in the reaction mixture. Benzyl-moiety bearing nucleosides were likely too bulky to the kinase. 5-Fluoro-4-benzylthiouridine (**41**) and 4-benzylthiouridine (**42**) were not phosphorylated by *DmdNK*-WT.

**Table 4.** Efficiency of synthesis of uridine derivative monophosphates by *DmdNK*-WT. HPLC-MS analysis of the reaction mixtures was performed after incubation at 37 °C for 24 h.

Nucleoside	No.	R <sub>1</sub>	R <sub>2</sub>	R <sub>3</sub>	NMP, %
	33	-H	-	-	80
	34	-CH <sub>3</sub>	-	-	40
	35	-S	-O	-	91
	36	-O	-S	-	49
	37	-CH <sub>3</sub>	-F	-	29
	38	-CH <sub>3</sub>	-H	-	57
	39	-CH <sub>2</sub> CH <sub>3</sub>	-F	-	0.4
	40	-CH <sub>2</sub> CH <sub>3</sub>	-H	-	70
	41		-F	-	0
	42		-H	-	0
	43	-F	-OH	-	0
	44	-H	-H	-	0
	45	-OH	-O	-	94
	46	-H	-S	-	49

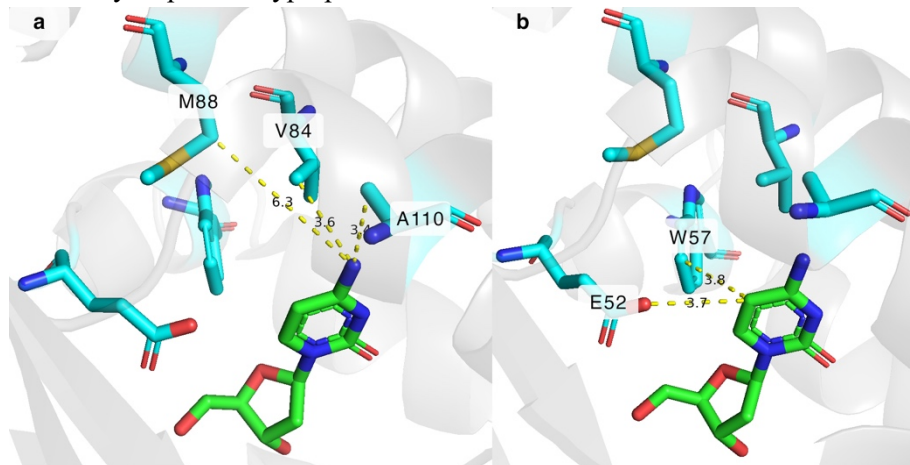
As expected, nucleosides that lacked a 5'-hydroxyl group to attach a phosphate to, such as 5-fluoro-5'-deoxyuridine (**43**) and 2',5'-dideoxyuridine (**44**), were not phosphorylated by the kinase. An additional hydroxyl group in 5-hydroxy-2'-deoxyuridine (**45**) did not hinder phosphorylation in any way, as the conversion efficiency reached 94%. Moreover, 2'-deoxy-4-thiouridine (**46**) was phosphorylated as efficiently as its ribo-equivalent: 49% of the compound was converted into a monophosphate.

The results lead to conclude that *DmdNK*-WT is quite tolerant of modifications at the 4<sup>th</sup> position of cytidine or uridine nucleobase. In addition to relatively small modifications such as acetyl-, in case of *N*<sup>4</sup>-acetyl-2'-deoxycytidine (**14**), hydroxy-, in case of *N*<sup>4</sup>-hydroxycytidine (**16**), or thio-, in case of 4-thiouridine (**36**), kinase presented with high activity towards nucleosides with bulkier substitutions. Examples being 2'-deoxycytidines bearing *sec*-butyl- (**27**), or phenyl-modifications (**30**), or 4-ethylthiouridine (**40**). Modifications at the 5<sup>th</sup> position of the nucleobase, however, were less tolerated. Even small substitutions, such as fluoro-, in case of 5-fluorocytidine (**12**), or methyl, in case of 5-methylcytidine (**13**), decreased the phosphorylation efficiencies up to 10-fold, compared to that of 5-position unmodified equivalent cytidine (**2**).

Analysis of the crystal structure of *DmdNK*-WT with a 2'-deoxycytidine molecule bound in its active site (PDB ID: 1j90) provides some clarification. As depicted in **Figure 34a**, the *N*<sup>4</sup> atom of deoxycytidine is situated near the voluminous cavity of *DmdNK*-WT, that is lined with hydrophobic residues (Mikkelsen et al., 2008). The residues V84 and A110 are located in close proximity, 3.6 Å and 3.4 Å, respectively, to the *N*<sup>4</sup> atom of cytosine nucleobase and do not provide much space for substitutions at the 4<sup>th</sup> position. However, the distance between the residue M88 and the nitrogen atom is 6.3 Å, which is enough to allow accommodation of pyrimidine nucleosides with modified 4<sup>th</sup> position. In addition to space, interactions between the nucleobase and the residues of the active centre are also important. Since the residues, that line the empty cavity, are hydrophobic in nature, hydrophobic substitutions of a nucleoside form favourable interactions and positively impact the activity of the kinase towards the substrate. This explains why a relatively bulky *sec*-butyl modification at the *N*<sup>4</sup>-position of deoxycytidine was well tolerated by *DmdNK*-WT.

The C5 carbon of the cytosine nucleobase is located 3.7 Å and 3.8 Å from residues E52 and W57, respectively, as shown in **Figure 34b**. The distances explain why a relatively small substitution, such as a methyl group or a fluorine atom, have such a great impact on phosphorylation efficiencies. In addition to steric hindrance, provided by the glutamate and tryptophan

residues, polar interactions also play a role. The significant decrease in phosphorylation of 5-fluoro-modified pyrimidine nucleosides can be partially explained by unfavourable repelling interactions between the fluorine atom and the hydrophobic tryptophan.

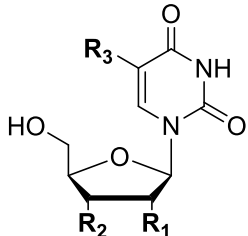
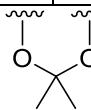
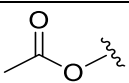
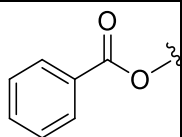
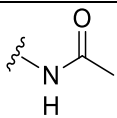


**Figure 34.** The active site of *DmdNK*-WT with bound deoxycytidine. **a** Distances between  $N^4$  atom of deoxycytidine and V84, M88, and A110 residues of *DmdNK*-WT. **b** Distances between C5 atom of deoxycytidine and E52 and W57 residues of *DmdNK*-WT. PDB ID: 1j90.

Since *DmdNK*-WT accepted pyrimidine nucleosides with various modifications at nucleobase, we have decided to test whether sugar modifications were tolerated, as well. Hence, uridine nucleosides, bearing modified ribose moieties, were chosen (**Table 5**). The small methyl substitution bearing 2'-*O*-methyluridine (**47**) and 3'-*O*-methyluridine (**48**) were accepted as substrates by the kinase, however, the phosphorylation efficiency decreased 3- to 5-fold compared to that of uridine and reached 16-24%. Similarly, 2'-*O*-methyl-5-methyluridine (**49**) was phosphorylated with 21% efficiency. A slightly bulkier allyl modification bearing 2'-(*O*-allyl)-uridine (**50**) and 3'-(*O*-allyl)-uridine (**51**) were phosphorylated by *DmdNK*-WT, as well. Although modification at 3'-position was tolerated better, as conversion efficiencies were 14% and 39%, respectively. In addition, phosphorylation efficiency of 2',3'-*O*-isopropylideneuridine (**52**) reached 14%. Substrates with bulkier modifications at 3'-position of ribose were found to be unsuitable to the kinase. Neither 3'-*O*-acetyluridine (**53**) nor 3'-*O*-benzoyl-2'-deoxyuridine (**54**) were phosphorylated. Moreover, 2'-amino-modification bearing nucleosides 2'-amino-2'-deoxyuridine (**55**) and 2'-*N*-acetyl-2'-amino-2'-deoxyuridine (**56**) were phosphorylated with 32–56%

efficiency, while conversion of 2',3'-hydroxyl group lacking 2',3'-di-deoxyuridine (**57**) was even more efficient and reached 65%.

**Table 5.** Efficiency of synthesis of sugar-modified uridine monophosphates by *DmdNK*-WT. HPLC-MS analysis of the reaction mixtures was performed after incubation at 37 °C for 24 h.

Nucleoside	No.	R <sub>1</sub>	R <sub>2</sub>	R <sub>3</sub>	NMP, %
	47	-OCH <sub>3</sub>	-OH	-H	24
	48	-OH	-OCH <sub>3</sub>	-H	16
	49	-OCH <sub>3</sub>	-OH	-OCH <sub>3</sub>	21
	50	-OCH <sub>2</sub> CHCH <sub>2</sub>	-OH	-H	14
	51	-OH	-OCH <sub>2</sub> CHCH <sub>2</sub>	-H	39
	52			-H	14
	53	-OH		-H	0
	54	-H		-H	0
	55	-NH <sub>2</sub>	-OH	-H	56
	56		-OH	-H	32
57	-H	-H	-H	65	

The tolerance of ribose modifications can be explained by looking at the active site of *DmdNK*-WT with a bound deoxycytidine molecule (PDB ID: 1j90). The C2' and C3' atoms of deoxyribose moiety are located near residues I29, Y70, and E172. When a deoxyribonucleoside is bound, its C2' atom is 3.7 Å away from tyrosine and isoleucine residues (**Figure 35a**). The distance is sufficient to allow accommodation of small substitutions, such as methoxy or amino, at the C2' position.

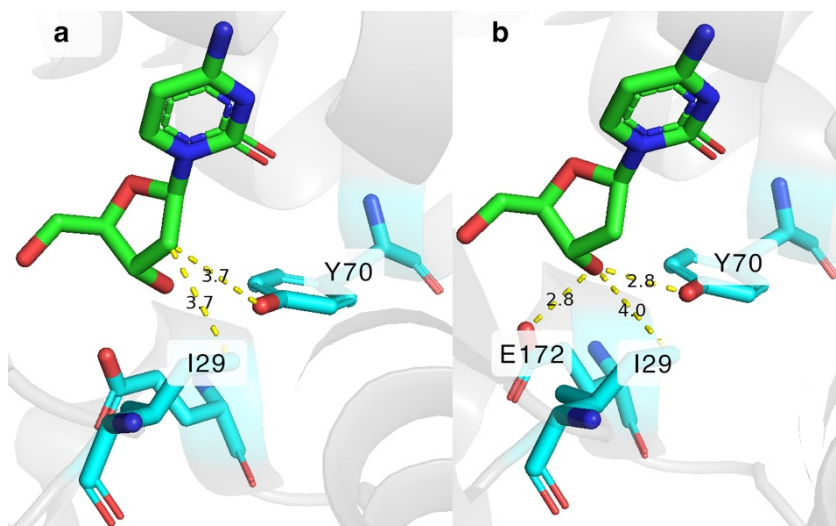


**Figure 35.** The active site of *DmdNK*-WT with bound deoxycytidine. **a** Distances between the 2' carbon atom of deoxycytidine and I29 and Y70 residues of *DmdNK*-WT. **b** Distances between 3'-hydroxyl group of deoxycytidine and I29, Y70, and E172 residues of *DmdNK*-WT. PDB ID: 1j90.

The hydroxyl group of C3' atom is situated 2.8 Å from the hydroxy groups of tyrosine and glutamate residues, and 4.0 Å away from isoleucine residue (**Figure 35b**). Small substitutions are acceptable, however, nucleosides bearing bulkier modifications, such as benzoyl, cannot bind the active site due to spatial limitations.

### 3.6. Exploring *DmdNK* active site mutations

The study on substrate specificity of *DmdNK*-WT has affirmed that the kinase can phosphorylate a wide array of pyrimidine nucleoside analogues bearing modifications at the nucleobase or sugar. However, certain compounds were found to be not accepted as substrates. To expand the substrate scope of *DmdNK*, we have created 16 mutant variants and tested them towards various  $N^4$ -modified cytosine nucleosides.

#### 3.6.1. Synthesis and application of the mutant *DmdNK* variants

For the creation of *DmdNK* mutants single-site mutagenesis was utilized. In total, sixteen *DmdNK* mutant variants, that carried a single or a double mutation, were created (**Table 6**). Positions for mutagenesis were chosen

based on the active centre of *DmdNK*-WT, focusing on amino acids that are involved in nucleoside binding. Residues V84, M88, and A110 line the hydrophobic cavity of the kinase and are considered to be the reason for the broad substrate acceptance of the kinase (Mikkelsen et al., 2008). The amino acids were replaced with smaller alanine and glycine to expand the hydrophobic cavity and remove hydrophobic side chains that could potentially create unfavourable interactions with substrates. Glutamine in position 81 forms hydrogen bonds with pyrimidine nucleobase and stabilizes the nucleoside in the active site of the enzyme (Johansson et al., 2001). The residue was replaced with alanine to remove the stabilizing forces and allow for additional flexibility of the nucleobase in the active centre of the kinase. Furthermore, residue W57 assists in nucleoside binding by forming stacking interactions with the nucleobase (Johansson et al., 2001). To determine whether removal of the stabilizing interaction would allow binding of bulkier nucleosides in the active site, W57 was replaced with hydrophobic phenylalanine and valine.

**Table 6.** Generated *DmdNK* mutant variants.

No.	Mutant variant
1	<i>DmdNK</i> -W57F
2	<i>DmdNK</i> -W57V
3	<i>DmdNK</i> -Q81A
4	<i>DmdNK</i> -Q81A+V84G
5	<i>DmdNK</i> -Q81A+M88G
6	<i>DmdNK</i> -Q81A+A110G
7	<i>DmdNK</i> -V84A
8	<i>DmdNK</i> -V84A+M88A
9	<i>DmdNK</i> -V84A+A110D
10	<i>DmdNK</i> -V84G
11	<i>DmdNK</i> -M88A
12	<i>DmdNK</i> -M88G
13	<i>DmdNK</i> -M88R
14	<i>DmdNK</i> -M88R+A110G
15	<i>DmdNK</i> -A110D
16	<i>DmdNK</i> -A110G

The enzymes were generated with (His)<sub>6</sub>-tags at the *C*-termini and used for the phosphorylation of nucleosides without further removal of the tags. The preparation of the kinases is described in Section 2.3.2. Variants *DmdNK*-Q81A+V84G, *DmdNK*-Q81A+M88G, *DmdNK*-Q81A+A110G, *DmdNK*-V84G, *DmdNK*-M88G, and *DmdNK*-A110G were found to be unstable and precipitated after an overnight dialysis. The solubility of those proteins was partially overcome by replacing *E. coli* BL-21(DE3) with *E. coli* KRX strain for gene expression and cultivation of the transformants at 20 °C instead of 37 °C for 20 h instead of 3 h. Electrocompetent *E. coli* KRX cells



feature a chromosomal T7 RNA polymerase that is driven by a rhamnose promoter (*rhaP<sub>BAD</sub>*), which allows for a precisely controlled protein expression (Egan and Schleif, 1993; Studier and Moffatt, 1986). In this *E. coli* K12-derived strain, target protein expression levels are higher compared to those of *E. coli* BL-21(DE3)-derived strains (Ishido et al., 2011). Hence, more soluble *DmdNK* mutants were obtained.

The generated *DmdNK* mutants were applied for the phosphorylation of cytosine nucleosides, provided in Section 3.6.2. The conditions for the phosphorylation reactions are provided in Section 2.3.5.

### 3.6.2. Substrate selection

To explore the effects of mutations on the activity of *DmdNK*, 14 nucleosides, which are provided in **Figure 36**, were chosen.

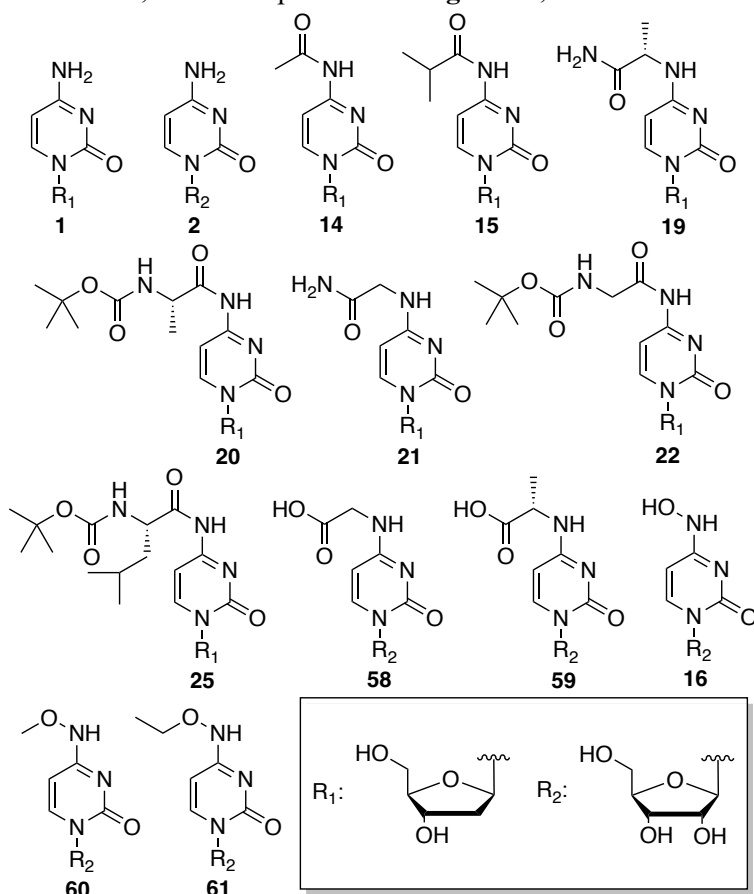


**Figure 36.** Structures of the canonical and *N*<sup>4</sup>-modified cytosine nucleosides exploited in the study.

Canonical 2'-deoxycytidine and cytidine were picked to evaluate the overall activity of generated mutants, since these compounds are known to be efficiently phosphorylated by the wild-type variant (Johansson et al., 1999). The remaining 12 compounds were cytosine nucleosides, that had modifications at the  $N^4$ -position. The substrates were chosen to be as diverse as possible and had modifications that ranged from small to bulky, and from hydrophobic to polar. Nucleosides **1**, **2**, **14**, **15** were obtained commercially, while the rest were synthesized in our laboratory. Preparation of the  $N^4$ -amino acid modified nucleosides (**19**, **20**, **21**, **22**, and **25**) is a part of this work and is described in Section 2.2, while syntheses of the cytidine nucleosides **16**, **58-61** were executed by a colleague K. Butkutė and are provided in our collaborative publication (Koplūnaitė et al., 2024).

### 3.6.3. Mutations in the hydrophobic cavity of *DmdNK* active site

The broad substrate specificity of *DmdNK*-WT is largely influenced by the presence of the hydrophobic cavity in its active site, that provides enough space to accommodate cytosine nucleosides, bearing various modifications at  $N^4$  or C5 positions, or uracil nucleosides, modified at  $O^4$  and C5 positions. The residues, that line the hydrophobic cavity are V84, M88, and A110 (Mikkelsen et al., 2008). To explore how mutations at the cavity affect the activity of *DmdNK* towards  $N^4$ -position modified cytosine nucleosides, single-site mutagenesis was utilized for the creation of *DmdNK* variants with mutations at positions V84, M88, and A110, respectively. The hypothesis was that replacing these residues with smaller ones, such as alanine or glycine, would increase the space required to accommodate nucleoside analogues with bulkier modifications. In total, seven single-mutation variants with modifications at the hydrophobic pocket were created. V84 was replaced with alanine (*DmdNK*-V84A) and glycine (*DmdNK*-V84G); M88 was replaced with alanine (*DmdNK*-M88A), glycine (*DmdNK*-M88G), and arginine (*DmdNK*-M88R); A110 was replaced with aspartate (*DmdNK*-A110D) and glycine (*DmdNK*-A110G). In addition, three double mutants were created (*DmdNK*-V84A+M88A, *DmdNK*-V84A+A110D, and *DmdNK*-M88R+A110G) to investigate whether any synergistic effects were present. The data on the activity of the generated mutant *DmdNK* variants is presented in **Table 7**.

**Table 7.** Phosphorylation efficiencies of pyrimidine nucleosides by *DmdNK* wild-type and mutant variants. Number is the phosphorylation efficiency (%) calculated using HPLC-MS chromatogram areas. Cells are coloured based on mutant performance in comparison to the wild-type kinase with the particular substrate (a margin of error of  $\pm 3$  was applied). Rose – phosphorylation efficiency decreased  $\geq 2$ -fold compared to *DmdNK*-WT; orange – phosphorylation efficiency decreased  $\geq 1.5$ -fold but  $< 2$ -fold compared to *DmdNK*-WT; lime – phosphorylation efficiency increased  $\geq 1.5$ -fold but  $< 2$ -fold compared to *DmdNK*-WT; green – phosphorylation efficiency increased  $\geq 2$ -fold compared to *DmdNK*-WT; white – phosphorylation efficiency was similar to *DmdNK*-WT.

Substrate <i>DmdNK</i>	1	2	14	15	19	20	21	22	25	58	59	16	60	61
WT	98	78	100	0	3	0	31	0	0	0	0	46	5	0
W57F	89	51	27	1	0	0	1	0	0	0	0	6	0	0
W57V	89	6	4	0	0	0	0	0	0	0	0	0	0	0
Q81A	88	14	100	9	0	0	20	0	0	0	0	2	11	4
Q81A+V84G	92	2	88	61	31	0	82	0	0	0	0	0	4	3
Q81A+M88G	94	4	93	3	1	0	7	0	0	0	0	0	6	1
Q81A+A110G	93	13	100	87	55	0	98	0	0	0	0	11	30	30
V84A	97	75	100	68	75	0	95	0	0	0	0	24	8	2
V84A+M88A	98	71	100	0	56	0	60	0	0	0	0	1	3	2
V84A+A110D	22	1	0	0	0	0	0	0	0	0	0	0	0	0
V84G	88	41	100	94	84	0	98	0	0	0	0	4	6	2
M88A	79	47	54	4	1	0	14	0	0	0	0	9	0	0
M88G	87	30	29	2	1	0	5	0	0	0	0	6	0	0
M88R	34	5	0	0	0	0	1	0	0	0	0	0	0	0
M88R+A110G	91	4	0	0	0	0	0	0	0	0	0	0	0	0
A110D	96	10	27	0	0	0	11	0	0	0	0	0	0	0
A110G	89	65	100	30	33	0	98	0	0	0	0	8	4	0

When canonical 2'-deoxycytidine (**1**) was utilized as a substrate, most of the generated mutant variants displayed similar performance to that of *DmdNK*-WT and converted the compound into a 5'-monophosphate form with 79–98% efficiency. However, a couple of mutants (*DmdNK*-V84A+A110D and *DmdNK*-M88R) displayed up to 5-fold lower activity towards the nucleoside as the phosphorylation efficiencies reached 22–34%. Variants *DmdNK*-V84A, *DmdNK*-V84A+M88A, and *DmdNK*-A110G maintained similar activities towards cytidine (**2**) as *DmdNK*-WT and phosphorylated the

nucleoside with 65–75% efficiencies, while the activities of the remaining mutants decreased to 1–41%.

As can be deduced from the green cells in **Table 7**, replacing bulky valine in position 84 with a smaller alanine or glycine in the active centre of *DmdNK* positively impacted the kinase's ability to phosphorylate *N*<sup>4</sup>-modified cytosine nucleosides. Variants *DmdNK*-V84A and *DmdNK*-V84G retained the same activity towards *N*<sup>4</sup>-acetyl-2'-deoxycytidine (**14**) as *DmdNK*-WT and phosphorylated the compound with an efficiency of 100%. However, phosphorylation efficiencies of *N*<sup>4</sup>-isobutyryl- (**15**), *N*<sup>4</sup>-alaninoyl- (**19**), and *N*<sup>4</sup>-glycinoyl-2'-deoxycytidine (**21**) more than doubled compared *DmdNK*-WT and reached 60–98%, whereas the wild-type enzyme phosphorylated the compounds with 0–31% efficiency.

Mutations in position 88 did not provide a boost in activity towards the tested nucleosides. Variants, where methionine in position 88 was replaced with either alanine (*DmdNK*-M88A), or glycine (*DmdNK*-M88G), displayed 2- to 6-fold lower phosphorylation efficiencies of nucleosides **14**, **19**, and **21** compared to those of *DmdNK*-WT. Mutant *DmdNK*-V84A+M88A, however, performed slightly better. Compared to *DmdNK*-WT, the double mutant displayed a significant increase in activity towards *N*<sup>4</sup>-amino-acid modified deoxycytidines **19** and **21**, as the phosphorylation efficiencies rose from 3–31% to 56–60%. None of the *DmdNK* variants with a mutated M88 position were able to efficiently phosphorylate *N*<sup>4</sup>-isobutyryl-modified nucleoside **15**. In addition to alanine and glycine, M88 was also replaced with arginine (*DmdNK*-M88R), as is natively found in many deoxyguanosine kinases (Johansson et al., 2001). The mutant displayed a complete absence of activity towards the tested *N*<sup>4</sup>-modified cytidines, as did the double mutant *DmdNK*-M88R+A110D.

Another residue, that lines the hydrophobic cavity of *DmdNK*-WT, is alanine in position 110. Even though the residue is already small, it was replaced with an even smaller glycine residue to investigate whether absence of alanine's methyl group would make a difference in the activity of the kinase. As can be seen from **Table 7**, the mutant *DmdNK*-A110G presented with a significantly higher activity towards *N*<sup>4</sup>-modified deoxycytidines **15**, **19**, and **21** compared to that of *DmdNK*-WT: the mutant reached phosphorylation efficiencies of up to 98%, whereas the efficiencies of *DmdNK*-WT were up to 31%. The alanine in position 110 was also replaced with an aspartate residue, which is found in the active sites of *HsdGK* and *HsdCK* (Johansson et al., 2001). Even though the mutant *DmdNK*-A110D retained the same activity towards canonical deoxycytidine as *DmdNK*-WT, a substantial decrease in phosphorylation of *N*<sup>4</sup>-modified cytidines was

observed: phosphorylation of  $N^4$ -acetyl-2'-deoxy-cytidine (**14**) and  $N^4$ -glycinoyl-2'-deoxycytidine (**21**) declined from 31–100% to 11–27%. Additionally, the double mutant *DmdNK*-V84A+A110D was incapable of phosphorylating any of the  $N^4$ -modified nucleosides.

Neither of the created *DmdNK* mutant variants were proficient at phosphorylating  $N^4$ -amino acid-modified deoxycytidines, that had a Boc-protecting group (**20**, **22**, and **25**). Presumably, the active centre of *DmdNK* is not spacious enough to accommodate nucleosides with such bulky substitutions. Furthermore, mutations at positions V84, M88, and A110 did not increase the activity of the kinase towards the acidic cytidines **58** and **59**, and  $N^4$ -hydroxy- (**16**) and  $N^4$ -alkoxy-modified cytidines (**60**, **61**). Phosphorylation efficiencies of the compounds were up to 24% compared to up to 46% of *DmdNK*-WT, however, in most cases the substrates were not converted into the corresponding monophosphates at all. Substitutions of the aforementioned nucleosides are relatively small-sized, thus unfavourable interactions are believed to be the cause of poor phosphorylation, and not a lack of space as is in the case of Boc-protected nucleosides.

Analyses of the active sites of *DmdNK*-WT with a bound deoxycytidine (PDB ID: 1j90) and *in silico* generated mutant models provide some insight on how the mutations impacted phosphorylation efficiencies of the kinase (Mirdita et al., 2022). As can be seen in **Figure 37a**, there is an empty pocket near the positions C5 and  $N^4$  of deoxycytidine. Residue M88 is 6.3 Å away from the  $N^4$ -position of cytosine nucleobase which provides some space for the kinase to bind cytidine substrates with certain modifications at the  $N^4$ -position. Replacing the residue with a more compact one, such as alanine (*DmdNK*-M88A) or glycine (*DmdNK*-M88G), or a positively charged arginine (*DmdNK*-M88R), does not improve the phosphorylation efficiency of *DmdNK* – the activity of all M88 mutants towards the tested nucleosides has decreased 2- to 3-fold compared to that of *DmdNK*-WT.

The V84 and A110 residues, however, are 3.4–3.6 Å away from the  $N^4$  atom (**Figure 37a**) and might spatially limit certain substrates from binding the active site. As depicted in **Figure 37b**, replacing the residues with a smaller glycine expands the hydrophobic pocket, as the distances from the  $N^4$  atom to the V84 and A110 residues are expected to become 3.7 Å and 6.0 Å, respectively. In addition to the capacity of the cavity, non-covalent interactions between the substrate and the residues of the active site are important. Removal of the hydrophobic side chain of valine in case of *DmdNK*-V84A or *DmdNK*-V84G, or methyl in case of *DmdNK*-A110G, increases the affinity of the kinase towards substrates with polar modifications

such as  $N^4$ -alaninoyl-2'-deoxycytidine (**19**) or  $N^4$ -glycinoyl-2'-deoxycytidine (**21**).

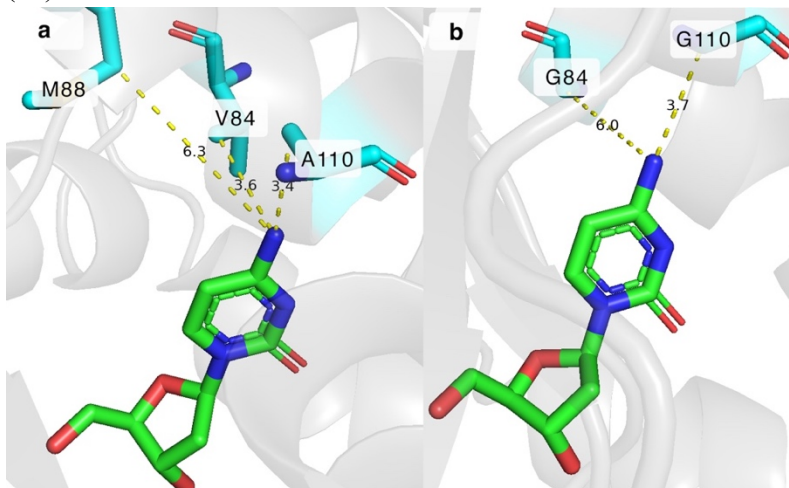


**Figure 37.** The active site of *DmdNK* with bound deoxycytidine. **a** Distances between  $N^4$  atom of deoxycytidine and V84, M88, and A110 residues of *DmdNK*-WT. PDB ID: 1j90. **b** Predicted distances between  $N^4$  atom of deoxycytidine and residues at the positions 84 and 110, where V84 and A110 are replaced by glycine. Model generated by ColabFold v1.5.5.

To sum up, mutating the residues of the hydrophobic cavity of *DmdNK*-WT can be utilized as a strategy to expand the substrate scope of the enzyme. Residues V84 and A110 are relatively close to the  $N^4$ -position of cytosine nucleoside, thus replacing them with less bulky non-polar amino acids eliminates some of the spatial, as well as polar, limitations and allow for accommodation of substrates, that were otherwise not accepted by *DmdNK*-WT. The residue M88 is rather far away from the  $N^4$  atom and replacing it with a smaller residue had a negative effect on the activity of the kinase: a decrease in phosphorylation efficiency of  $N^4$ -modified cytidines was observed.

#### 3.6.4. Significance of the Q81 residue in the active centre of *DmdNK*

In the active site of *DmdNK*-WT, residue Q81 forms two hydrogen bonds with the  $N^3$  and  $N^4$  atoms of cytosine nucleobase and the interactions are known to stabilize the substrate in the active site of the kinase (Johansson et al., 2001). To evaluate whether the removal of the hydrogen bonding would allow for more flexibility of the nucleobase moiety in the active centre and, in

turn, enable binding of nucleosides with bulkier modifications, a *DmdNK* mutant, where the glutamine residue was replaced with a residue of alanine (*DmdNK*-Q81A), was created. In the wild-type kinase, the distances between the  $N^3$  and  $N^4$  atoms of deoxycytidine and Q81 are 3.0 Å and 3.1 Å, respectively (**Figure 38a**). When Q81 is replaced by alanine (*DmdNK*-Q81A), those distances are expected to increase to over 6.2 Å (**Figure 38b**), and the hydrogen bonding between the nucleobase and the residue in position 81 should no longer be present.

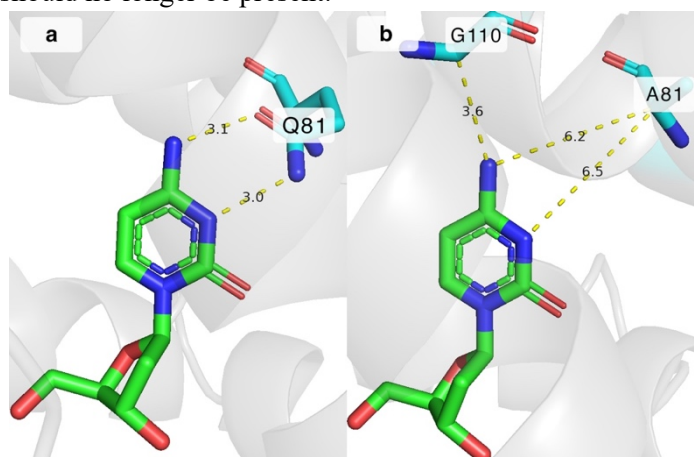


**Figure 38.** The active site of *DmdNK* with bound deoxycytidine. **a** Hydrogen bonds between  $N^3$  and  $N^4$  atoms of deoxycytidine and Q81 residue in *DmdNK*-WT. PDB ID: 1j90. **b** Predicted distances between deoxycytidine and the residues at the positions 81 and 110, where Q81 is replaced by alanine, and A110 is replaced by glycine. Model generated by ColabFold v1.5.5.

As is evident from **Table 7**, replacing the Q81 residue with alanine did not have an extreme effect on the activity of the kinase. Mutant *DmdNK*-Q81A remained similarly active towards 2'-deoxycytidine (**1**) and  $N^4$ -acetyl-2'-deoxycytidine (**14**) as *DmdNK*-WT, although the activity towards cytidine decreased more than 5-fold. In addition, phosphorylation of  $N^4$ -modified deoxycytidines **15**, **19**, and **21** remained fairly similar to that of *DmdNK*-WT and reached up to 20%. In the same manner as the wild-type enzyme, *DmdNK*-Q81A did not phosphorylate the Boc-protected deoxycytidines (**20**, **22**, and **25**) or the acidic cytidine nucleosides **58** and **59**. Compared to *DmdNK*-WT, phosphorylation efficiency of  $N^4$ -hydroxycytidine (**16**) decreased more than 20-fold (from 46% to 2%), although a slight increase in phosphorylation of  $N^4$ -methoxy- (**60**) and  $N^4$ -ethoxycytidine (**61**) was observed: conversions rose up to 11%, whereas conversion efficiencies of *DmdNK*-WT were up to 5%.

To investigate, whether any cumulative effects were present, Q81A mutation was paired with previously characterized mutations V84G, M88G, and A110G. Compared to single mutants *DmdNK-V84G*, *DmdNK-M88G*, and *DmdNK-A110G*, in most cases, double-mutation carrying variants *DmdNK-Q81A+V84G*, *DmdNK-Q81A+M88G*, and *DmdNK-Q81A+A110G* did not display an increase in activity towards the tested substrates. However, variant *DmdNK-Q81A+A110G* did exhibit an improved phosphorylation efficiency of *N*<sup>4</sup>-alkoxy-modified nucleosides. Conversions of *N*<sup>4</sup>-methoxy- (**60**) and *N*<sup>4</sup>-ethoxycytidine (**61**) surged to 30%, whereas *DmdNK-WT* or *DmdNK-A110G* phosphorylated the compounds with efficiencies of 0–5%. A possible explanation for the observed results could be positive intragenic epistasis (Parera and Martinez, 2014). Individual mutations Q81A and A110G did not have as significant of effect on *DmdNK* activity as the combination of both mutations did. Analysis of the active site of the kinase suggests that the extra space, provided by A110G mutation, and the additional mobility of the nucleobase, provided by the Q81A mutation, lead to an overall increase in activity (**Figure 38b**).

### 3.6.5. Significance of the W57 residue in the active site of *DmdNK*

Aromatic-aromatic interactions play an important role in positioning substrates in the active sites of enzymes (Makarov et al., 2021). As mentioned previously, in *DmdNK-WT*, the residues, that stabilize cytosine nucleobase in the active centre, are W57, F80, and F114 (Johansson et al., 2001). To investigate how significant such interactions are for the activity of *DmdNK*, we have chosen the W57 residue, which interacts with C5 and C6 atoms of cytosine, and replaced it with hydrophobic residues, phenylalanine (*DmdNK-W57F*) or valine (*DmdNK-W57V*). As can be seen in **Table 7**, both mutants retained similar activity towards canonical deoxycytidine (**1**) as *DmdNK-WT*, however, phosphorylation efficiencies of cytidine and all *N*<sup>4</sup>-modified nucleosides decreased at least 2-fold (from 0–100% to 0–51%). To understand why the drastic decline in activity occurred, we have utilized ColabFold v1.5.5 software to generate models of the mutants (Mirdita et al., 2022). As depicted in **Figure 39b**, replacing W57 with a valine residue is expected to increase the distances between the cytosine nucleobase and the residue to over 7.0 Å, whereas in *DmdNK-WT* the distances are 3.5–3.8 Å (**Figure 39a**).



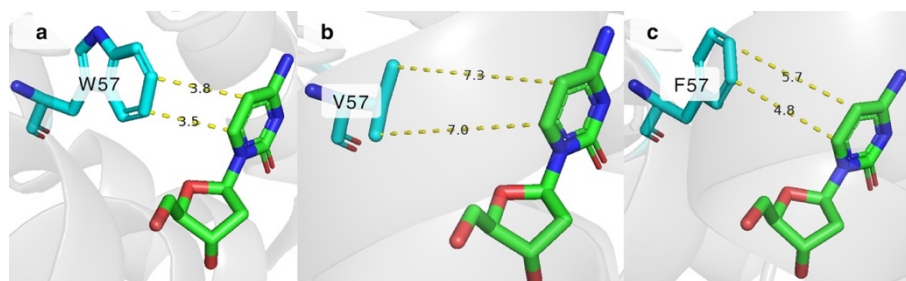


**Figure 39.** The active site of *DmdNK* with bound deoxycytidine. **a** Stacking interaction between W57 and cytosine atoms. PDB ID: 1j90. **b** Predicted distances between C5 and C6 atoms of deoxycytidine and residue at the position 57, where W57 is replaced by valine. Model generated by ColabFold v1.5.5. **c** Possible interactions between C5 and C6 atoms of deoxycytidine and residue at the position 57, where W57 is replaced by phenylalanine. Model generated by ColabFold v1.5.5.

Generally, aromatic-aromatic interactions occur at distances of 3.5–4.5 Å, however, weaker interactions are still possible at larger distances of up to 6.0 Å (Headen et al., 2010; Kuš et al., 2020). The predicted 7.0 Å distance between V57 and cytosine nucleobase is too grand for any kind of stabilizing interactions to occur. In case of mutant *DmdNK*-W57F, the distance between the cytosine nucleobase and the phenylalanine residue is predicted to be around 4.8–5.7 Å (**Figure 39c**) which is sufficient for weaker stacking interactions to occur. This explains why the mutant *DmdNK*-W57F, that had a phenylalanine residue, exhibited slightly higher activity towards cytidine (**2**), *N*<sup>4</sup>-acetyl-2'-deoxycytidine (**14**), and *N*<sup>4</sup>-hydroxycytidine (**16**) compared to *DmdNK*-W57V variant, that had a valine residue. The results lead to conclude that the stabilizing aromatic-aromatic interactions between the nucleobase and the W57 residue are essential for the overall performance of *DmdNK*-WT.

### 3.6.6. Differences in phosphorylation of *N*<sup>4</sup>-amino acid modified nucleosides bearing amide and carboxyl functional groups

Intriguingly, acidic cytidines **58** and **59**, which are analogues of nucleosides **19** and **21**, were not accepted as substrates by either *DmdNK* mutant variant. The main difference between the compounds is that the acidic nucleosides have an exposed carboxyl group, whereas nucleosides **19** and **21** bear an exposed amide group as shown in **Figure 40**.

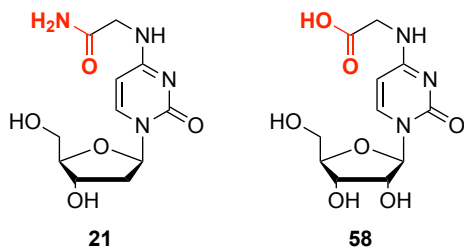


**Figure 40.** Structures of  $N^4$ -amino acid modified cytosine nucleosides bearing amide (**21**) and carboxyl (**58**) functional groups.

The carboxyl and amide groups are similarly sized, which suggests that the differences in phosphorylation were due to unfavourable interactions between the substrates and the residues of the active site, rather than a lack of space. To uncover what might be causing such contrasting results, molecular docking was performed where *DmdNK*-WT (PDB ID: 1j90) was docked with its substrate  $N^4$ -glycinoyl-2'-deoxycytidine (**21**) and the unphosphorylated  $N^4$ -glycine-modified acidic nucleoside (**58**) (**Figure 41**).

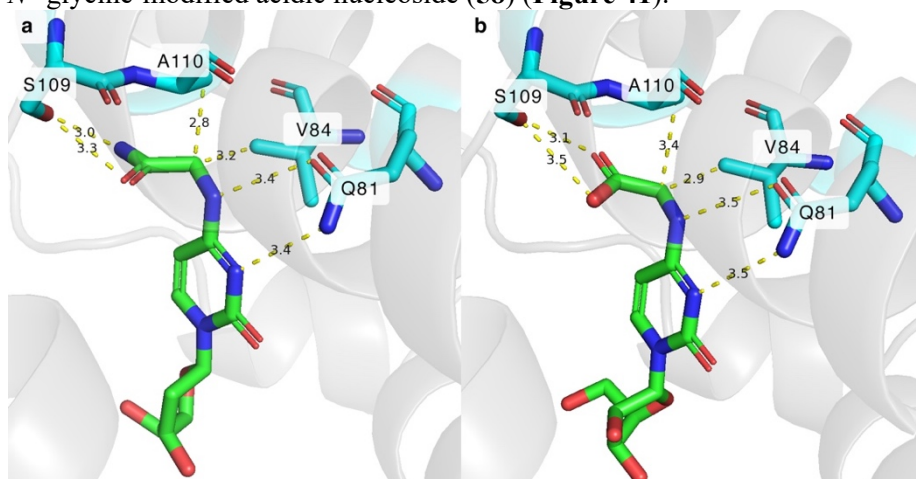


**Figure 41.** Molecular docking of  $N^4$ -amino acid modified cytosine nucleosides bearing amide and carboxyl functional groups in the active site of *DmdNK*-WT. **a** Molecular docking of  $N^4$ -glycinoyl-2'-deoxycytidine (**21**) in the active centre of *DmdNK*-WT. **b** Molecular docking of  $N$ -[1-( $\beta$ -D-ribofuranosyl)-2-oxo-4-pyrimidinyl]-glycine (**58**) in the active centre of *DmdNK*-WT. PDB ID: 1j90. Molecular docking performed by DiffDock software (<https://huggingface.co/spaces/reginabarzilaygroup/DiffDock-Web>; accessed on 13 August 2024).

As depicted in **Figures 41a** and **41b**, both nucleosides form similar interactions with neighbouring residues Q81, V84, and A110. However, an additional residue in the substrate pocket of *DmdNK*-WT was discovered and

it might be the deciding factor in whether an  $N^4$ -modified nucleoside is phosphorylated or not. Serine in position 109 is located approximately 3-3.5 Å away from the amide or carboxyl groups of the  $N^4$ -amino acid modified nucleosides. The amide group of  $N^4$ -glycinoyl-2'-deoxycytidine (**21**) forms hydrogen bonds with the hydroxy group of S109 and is effectively phosphorylated by certain *DmdNK* mutants. On the other hand, at physiological pH the carboxyl group of nucleoside **58** is expected to be deprotonated and carry a negative charge, which in turn forms unfavourable repulsive interactions with the same S109 residue (Larsen, 1980). The repulsive force creates disadvantageous environment for nucleoside binding; hence, the acidic nucleosides are not accepted as substrates by the kinase.

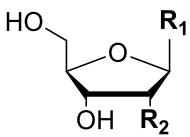
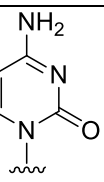
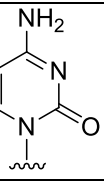
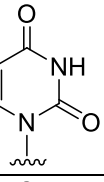
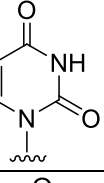
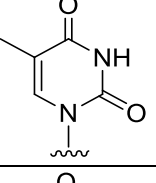
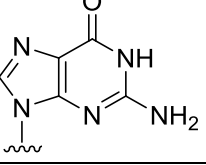
### 3.7. Substrate specificity of *BsdCK*-WT

Deoxycytidine kinase from *B. subtilis* is not as thoroughly examined as *DmdNK* or *HsdCK* (Bohman and Eriksson, 1988; Eriksson et al., 1991; Hellendahl et al., 2019; Johansson et al., 1999; Knecht et al., 2000, 2009; Ma et al., 2011; Sabini et al., 2007; Serra et al., 2014). The data on its substrate specificity is quite sparse, however, as mentioned previously, it is known to phosphorylate nucleosides of cytosine and adenine (Andersen and Neuhard, 2001). To gain a deeper understanding of the substrate spectre of wild-type *BsdCK* (*BsdCK*-WT), we have applied the kinase for the phosphorylation of 57 nucleosides, amongst which were both canonical and modified compounds (**Tables 8–10**). The study utilized the same nucleosides, that were used for the substrate specificity investigation of *DmdNK*-WT (Section 3.5). Out of the 57 tested substrates, 34 were phosphorylated by the kinase. The conditions for the phosphorylation reactions were based on optimization assay, that is detailed in Section 3.4.

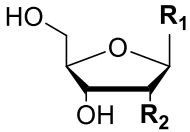
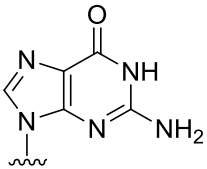
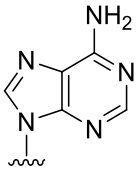
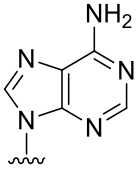
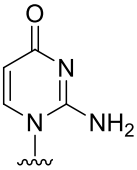
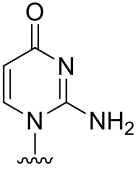
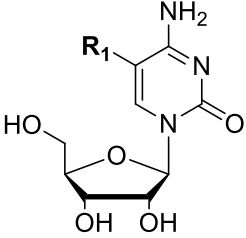
As can be seen from the results provided in **Table 8**, *BsdCK*-WT was very efficient at phosphorylating ribo- and 2'-deoxy-forms of cytosine and uracil nucleosides (**1–4**); the compounds were converted into the corresponding 5'-monophosphates with 92–100% efficiency. Activity towards 2'-deoxy-thymidine (**5**), on the other hand, was significantly lower: phosphorylation efficiency reached only 31%. In addition to canonical pyrimidine nucleosides, *BsdCK*-WT exhibited relatively high affinity towards purine nucleosides. 2'-Deoxyguanosine (**6**) and 2'-deoxyadenosine (**8**) were converted into their monophosphate forms with efficiencies of up to 98%, however, their ribo-counterparts guanosine (**7**) and adenosine (**9**) were phosphorylated slightly less efficiently (43–63%). Activities towards isocytidine (**10**) and 2'-deoxy-

isocytidine (**11**) were low compared to that of 2'-deoxycytidine. Phosphorylation of the ribonucleoside (**10**) was only 7%, while its 2'-deoxy-counterpart (**11**) was phosphorylated with 37% efficiency. A fluorine substitution at the C5 position of cytidine had little effect on the activity of *BsdCK*-WT, as 5-fluorocytidine (**12**) was converted into its monophosphate with 98% efficiency. A methyl group, however, reduced the phosphorylation efficiency of 5-methylcytidine (**13**) down to 5%.

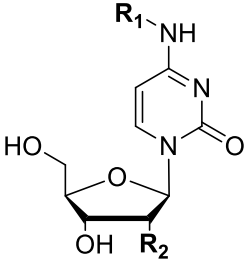
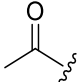
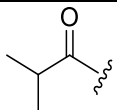
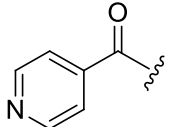
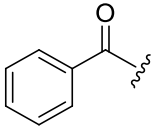
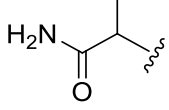
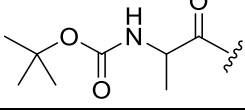
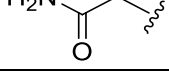
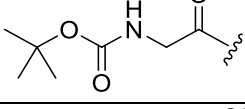
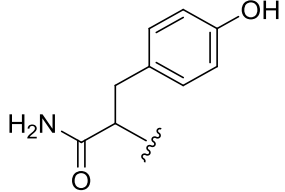
**Table 8.** Efficiency of synthesis of canonical nucleoside monophosphates and cytidine derivative monophosphates by *BsdCK*-WT. HPLC-MS analysis of the reaction mixtures was performed after incubation at 37 °C for 24 h.

Nucleoside	No.	R <sub>1</sub>	R <sub>2</sub>	NMP, %
	1		-H	100
	2		-OH	93
	3		-H	97
	4		-OH	97
	5		-H	31
	6		-H	98

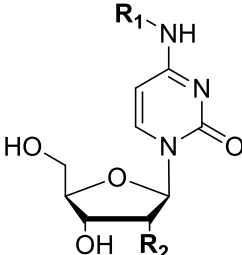
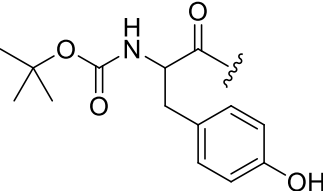
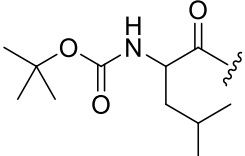
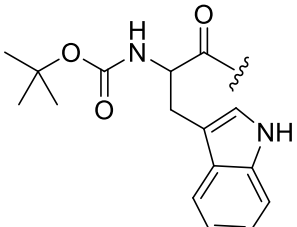
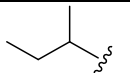
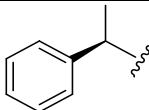
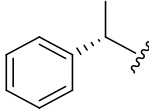
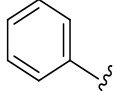
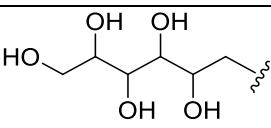
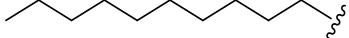
**Table 8 continued.** Efficiency of synthesis of canonical nucleoside monophosphates and cytidine derivative monophosphates by *BsdCK*-WT. HPLC-MS analysis of the reaction mixtures was performed after incubation at 37 °C for 24 h.

Nucleoside	No.	R <sub>1</sub>	R <sub>2</sub>	NMP, %
	7		-OH	43
	8		-H	88
	9		-OH	63
	10		-OH	7
	11		-H	37
	12	-F	-	98
	13	-CH <sub>3</sub>	-	50

**Table 8 continued.** Efficiency of synthesis of canonical nucleoside monophosphates and cytidine derivative monophosphates by *BsdCK*-WT. HPLC-MS analysis of the reaction mixtures was performed after incubation at 37 °C for 24 h.

Nucleoside	No.	R <sub>1</sub>	R <sub>2</sub>	NMP, %
	14		-H	95
	15		-H	2
	16	-OH	-OH	18
	17		-H	37
	18		-H	0
	19		-H	0
	20		-H	0
	21		-H	11
	22		-H	0
23		-H	0	

**Table 8 continued.** Efficiency of synthesis of canonical nucleoside monophosphates and cytidine derivative monophosphates by *BsdCK*-WT. HPLC-MS analysis of the reaction mixtures was performed after incubation at 37 °C for 24 h.

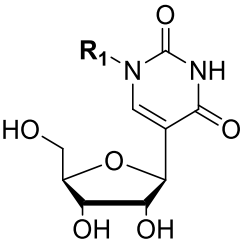
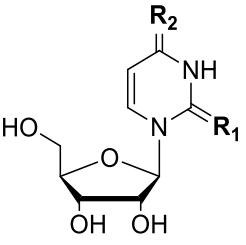
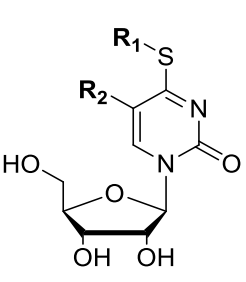
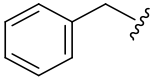
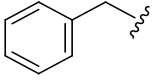
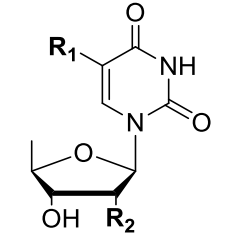
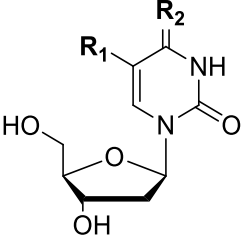
Nucleoside	No.	R <sub>1</sub>	R <sub>2</sub>	NMP, %
	24		-H	0
	25		-H	0
	26		-H	0
	27		-H	34
	28		-H	27
	29		-H	16
	30		-H	60
	31		-H	0
	32		-H	0

*BsdCK*-WT proved to be tolerant towards certain modifications at the  $N^4$ -position of cytosine nucleobase. Deoxycytidine nucleoside, bearing acetyl substitution at the  $N^4$ -position (**14**) was phosphorylated almost as efficiently as canonical deoxycytidine, as conversion reached 95%.  $N^4$ -Isobutyryl-2'-deoxycytidine (**15**) monophosphate formation, however, was barely detected and reached 2%. Hydroxyl substitution decreased phosphorylation efficiency of  $N^4$ -hydroxycytidine (**16**) 5-fold compared to that of cytidine (18% versus 93%). While  $N^4$ -isonicotinoyl-modification bearing deoxycytidine (**17**) was phosphorylated with 37% efficiency, structurally almost identical  $N^4$ -benzoyl-2'-deoxycytidine (**18**) was not accepted as a substrate by *BsdCK*-WT. Out of all synthesized  $N^4$ -aminoacid modified deoxycytidines (**19–26**),  $N^4$ -glycinoyl-2'-deoxycytidine (**21**) was the only one that was phosphorylated by the kinase, although the conversion rate was very low (11%). In addition, *BsdCK*-WT displayed activity towards relatively bulky deoxycytidines, bearing  $N^4$ -hydrophobic substitutions:  $N^4$ -*sec*-butyl-2'-deoxycytidine (**27**), *R* and *S* enantiomers of *a*-methylbenzyl-modified 2'-deoxycytidines (**28** and **29**), and  $N^4$ -phenyl-substituted 2'-deoxycytidine (**30**) were phosphorylated with efficiencies of 16–60%. Finally, the largest modifications bearing D-glucose-modified deoxycytidine (**31**), and  $N^4$ -decyl-2'-deoxycytidine (**32**) were not accepted as substrates by *BsdCK*-WT, as no formation of their monophosphates was observed.

Application of *BsdCK*-WT for the phosphorylation of canonical nucleosides and nucleobase-modified cytidine derivatives has revealed that the kinase possesses a much broader substrate acceptance than initially believed (Møllgaard, 1980). To determine, whether uracil nucleosides would be suitable substrates as well, we have employed the kinase for the phosphorylation of uridine derivatives, bearing modifications at the nucleobase (**Table 9**). The kinase displayed high activity towards  $N^1$ -methylpseudouridine (**34**), 2-thiouridine (**35**) and 4-thiouridine (**36**), as conversion rates reached 88–98%. However, phosphorylation efficiency of pseudouridine (**33**) was 2-fold lower and reached 44%. In addition, *BsdCK*-WT was able to phosphorylate the least bulky thiouridine derivatives 5-fluoro-4-methylthiouridine (**37**) and 4-methylthiouridine (**38**) with 8–11% efficiency, but bulkier thiouridines (**39–42**) were not accepted as substrates.



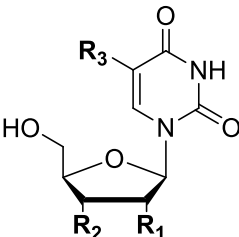
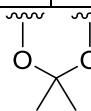
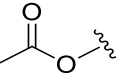
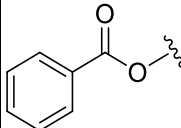
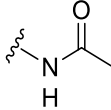
**Table 9.** Efficiency of synthesis of nucleobase-modified uridine derivative monophosphates by *BsdCK*-WT. HPLC-MS analysis of the reaction mixtures was performed after incubation at 37 °C for 24 h.

Nucleoside	No.	R <sub>1</sub>	R <sub>2</sub>	R <sub>3</sub>	NMP, %
	33	-H	-	-	44
	34	-CH <sub>3</sub>	-	-	93
	35	-S	-O	-	98
	36	-O	-S	-	88
	37	-CH <sub>3</sub>	-F	-	8
	38	-CH <sub>3</sub>	-H	-	11
	39	-CH <sub>2</sub> CH <sub>3</sub>	-F	-	0
	40	-CH <sub>2</sub> CH <sub>3</sub>	-H	-	0
	41		-F	-	0
	42		-H	-	0
	43	-F	-OH	-	0
	44	-H	-H	-	0
	45	-OH	-O	-	99
	46	-H	-S	-	0

As to be expected, 5-fluoro-5'-deoxyuridine (**43**) and 2',5'-dideoxyuridine (**44**), were not converted into monophosphates as they had no 5'-hydroxyl group to attach a phosphate to. The kinase exhibited extremely high activity towards 2'-deoxyuridine, bearing a hydroxyl group at C5-position (**45**) and phosphorylated the compound almost fully (99%). 2'-Deoxy-4-thiouridine (**46**), however, was not accepted as a substrate by the kinase, whereas its ribo-equivalent 4-thiouridine was phosphorylated very efficiently.

The available literature suggests that *BsdCK*-WT is not excessively strict on nucleoside sugar-moiety, as it was shown to phosphorylate nucleosides bearing ribose, 2'-deoxyribose, and arabinose (Møllgaard, 1980). To investigate whether alternative sugars were acceptable, an assortment of uridine derivatives bearing modified sugar-moiety were tested as substrates for the kinase (**Table 10**).

**Table 10.** Efficiency of synthesis of sugar-modified uridine derivative monophosphates by *BsdCK*-WT. HPLC-MS analysis of the reaction mixtures was performed after incubation at 37 °C for 24 h.

Nucleoside	No.	R <sub>1</sub>	R <sub>2</sub>	R <sub>3</sub>	NMP, %
	<b>47</b>	-OCH <sub>3</sub>	-OH	-H	18
	<b>48</b>	-OH	-OCH <sub>3</sub>	-H	0
	<b>49</b>	-OCH <sub>3</sub>	-OH	-OCH <sub>3</sub>	0
	<b>50</b>	-OCH <sub>2</sub> CHCH <sub>2</sub>	-OH	-H	21
	<b>51</b>	-OH	-OCH <sub>2</sub> CHCH <sub>2</sub>	-H	0
	<b>52</b>			-H	70
	<b>53</b>	-OH		-H	0
	<b>54</b>	-H		-H	0
	<b>55</b>	-NH <sub>2</sub>	-OH	-H	40
	<b>56</b>		-OH	-H	54
<b>57</b>	-H	-H	-H	29	

Phosphorylation results of ribose-modified uridines suggest that *BsdCK*-WT is more tolerant of modifications at ribose 2'- rather than

3'-position. The kinase converted 2'-modified 2'-*O*-methyluridine (**47**) and 2'-(*O*-allyl)-uridine (**50**) into the corresponding monophosphates with 18-21% efficiency. Meanwhile, 3'-*O*-methyluridine (**48**), 2'-*O*-methyl-5-methyluridine (**49**), 3'-(*O*-allyl)-uridine (**51**), 3'-*O*-acetyluridine (**53**), and 3'-*O*-benzoyl-2'-deoxyuridine (**54**) were not accepted as substrates. Moreover, *BsdCK*-WT was active towards 2',3'-*O*-isopropylideneuridine (**52**), 2'-amino-2'-deoxy-uridine (**55**), 2'-*N*-acetyl-2'-amino-2'-deoxyuridine (**56**), and 2',3'-di-deoxyuridine (**57**), as the compounds were phosphorylated with 29–70% efficiency.

As mentioned previously, the crystal structure of *BsdCK*-WT has not been solved. To gain additional insight, a model of a *BsdCK*-WT monomer was generated utilizing protein structure prediction software ColabFold v1.5.5 (Mirdita et al., 2022). The created model was superimposed on the crystal structure of *DmdNK*-WT with a 2'-deoxycytidine molecule bound in its active site (PDB ID: 1j90).

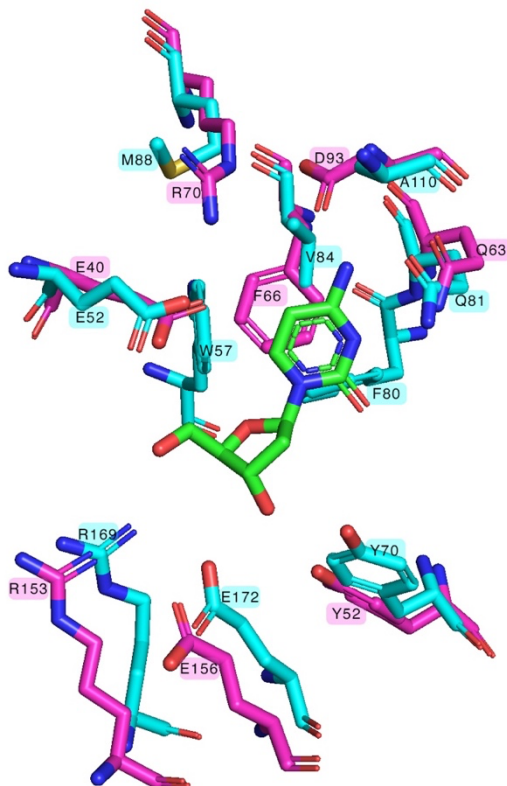


**Figure 42.** Superimposition of *BsdCK*-WT (magenta) on *DmdNK*-WT (cyan) with a bound 2'-deoxycytidine (green). Residues F97 (*BsdCK*-WT) and F114 (*DmdNK*-WT) are omitted for a clearer view. *BsdCK*-WT model generated by ColabFold v1.5.5; *DmdNK*-WT PDB ID: 1j90.

As can be seen in **Figure 42**, the active centres of *BsdCK*-WT and *DmdNK*-WT look very similar and share a lot of the same residues. The main difference between the two kinases is that *BsdCK*-WT lacks the empty cavity that *DmdNK*-WT has (Johansson et al., 2001). Instead of the hydrophobic residues V84, M88, and A110 of *DmdNK*-WT, *BsdCK*-WT has residues F66, R70, and D93, respectively. In addition, the nucleobase in the active centre of *DmdNK*-WT is stabilised by aromatic residues W57, F80, and F114, whereas in the case of *BsdCK*-WT the residues are F66 and F97.

According to the created *in silico* model, when deoxycytidine is bound in the active centre of *BsdCK*-WT, the  $N^3$  and  $N^4$  atoms of the nucleobase form hydrogen bonds with Q63 residue (**Figure 43a**). In addition, the nucleobase is stabilized in place by stacking interactions, provided by hydrophobic residues F66 and F97. The  $N^4$ - and C5-positions of cytosine nucleobase are in close proximity to polar residues R70 and D93. As is shown in **Figure 43a**, residue D93 is expected to be 2.2 Å away from the  $N^4$  atom of deoxycytidine and the arginine in position 70 should be located 4.9 Å and 4.2 Å away from the  $N^4$  and C5 atoms, respectively. The closeness of these polar residues provides some clarity on the observed substrate specificity of *BsdCK*-WT. While certain pyrimidine nucleosides, bearing modifications at positions  $N^4$  or C5, such as  $N^4$ -acetyl-2'-deoxycytidine or 5-methylcytidine, were accepted as substrates by the kinase, the spatial limitations provided by residues R70 and D93 prevented bulkier nucleosides, such as  $N^4$ -alaninoyl-2'-deoxycytidine or 4-ethylthiouridine, from fitting in the active site. In addition to limited space, polar interactions should also be considered. Both aforementioned residues are polar in nature and are ionized in physiological pH, thus nucleosides with hydrophobic substitutions are likely repelled by unfavourable interactions (Larsen, 1980). For example, as mentioned previously, phosphorylation efficiencies of two similarly sized nucleosides, 5-fluorocytidine (Van der Waals radius of fluorine is 1.47 Å) and 5-methylcytidine (Van der Waals radius of methyl group is 2.00 Å), differed 2-fold (Batsanov, 2001). Presumably, the polar fluorine substitution of 5-fluorocytidine formed favourable polar interactions with the guanidino group of R70 and was phosphorylated as efficiently as canonical cytidine. However, the observed decrease in activity towards 5-methylcytidine was most likely caused by repulsive forces between the hydrophobic methyl group and the R70 residue.

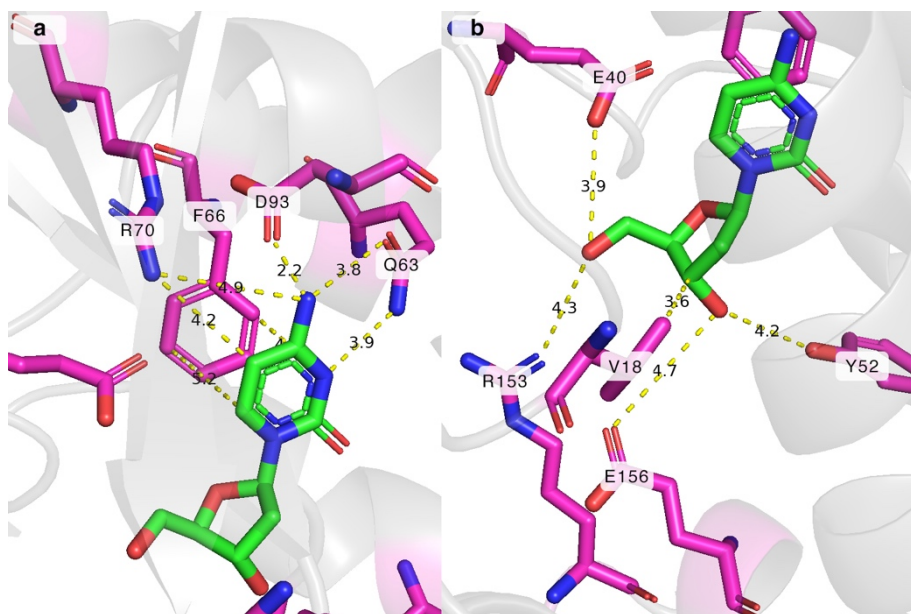


**Figure 43.** Predicted active site of *BsdCK*-WT. *BsdCK*-WT model generated by ColabFold and superimposed onto the active site of *DmdNK*-WT (PDB ID: 1j90) (residues not shown) with a bound 2'-deoxycytidine molecule (green). **a** Predicted interactions between the residues of *BsdCK*-WT and the nucleobase of 2'-deoxycytidine (residue F97 removed for a clearer view). **b** Predicted interactions between the residues of *BsdCK*-WT and the 2'-deoxyribose moiety of 2'-deoxycytidine.

The *in silico* active site model of *BsdCK*-WT suggests that the deoxyribose moiety of 2'-deoxycytidine is stabilized by polar residues in a similar fashion as in *DmdNK*-WT (Johansson et al., 2001). As depicted in **Figure 43b**, the 3'-hydroxy group is believed to form hydrogen bonds with residues Y52 and E156 and the 5'-hydroxy group should interact with the neighbouring residues E40 and R153. In addition, a hydrophobic residue V18 is found approximately 3.6 Å away from the C3' carbon atom. The spatial limitations provided by this residue might explain why *BsdCK*-WT displayed higher activity towards 2'-modified nucleosides compared to 3'-modified ones. As can be seen from the predicted active site of *BsdCK*-WT, there is some space near 2'- and 3'-positions of ribose moiety to allow accommodation of nucleosides, bearing modifications at the said positions. However, size and polarity of the modifications are important, as both polar (Y52, E156) and hydrophobic (V18) residues are neighbouring C2' and C3' atoms. Hence, only substrates that are small enough and form favourable interactions with the residues can bind the active centre.

### 3.8. Enhancing *BsdCK* substrate diversity via single-site mutagenesis

The study on substrate specificity of *BsdCK*-WT has proven that the kinase can phosphorylate a much broader spectrum of pyrimidine nucleoside analogues than initially believed (Andersen and Neuhard, 2001; Møllgaard, 1980). However, there were certain substrates that were not phosphorylated by the kinase or phosphorylated very inefficiently. To investigate whether it is possible to expand the substrate scope of *BsdCK*, we have created 3 mutant variants of *BsdCK* and tested them towards  $N^4$ -modified cytidine nucleosides. Substrates (**Figure 36**), used for the study, were the same as those that were utilized in the assessment of substrate specificity of *DmdNK* mutant variants and are provided in Section 3.6.2.

#### 3.8.1. Synthesis and application of the mutant *BsdCK* variants

Mutant variants of *BsdCK* were generated via single-site mutagenesis. The enzymes were obtained with (His)<sub>6</sub>-tags at the C-termini and utilized without further removal of the tags. The preparation of the proteins is described in Section 2.3. In total, 3 mutant variants of *BsdCK* were generated: 2 of them carried a single mutation (*BsdCK*-R70M and *BsdCK*-D93A) and one was a double-mutant (*BsdCK*-R70M+D93A). The kinases were applied for the phosphorylation of cytosine nucleosides, listed in Section 3.6.1. The conditions for the phosphorylation reactions are provided in Section 2.3.5.

#### 3.8.2. Impact of the *BsdCK* active site mutations

As mentioned in the literature overview, *BsdCK*-WT is known to favour nucleosides of adenine and cytosine with a preference towards 2'-deoxy-nucleosides over ribonucleosides (Andersen and Neuhard, 2001; Møllgaard, 1980). However, as we have learned, the kinase can phosphorylate a much wider array of pyrimidine nucleosides with various modifications at the nucleobase or sugar. Even though *BsdCK*-WT performed relatively well in terms of substrate diversity, it was still outshined by *DmdNK*-WT, which possesses one of the broadest substrate specificities known for nucleoside kinases (Chen et al., 2017; Egeblad-Welin et al., 2007; Johansson et al., 1999; Knecht et al., 2009; Matsuura et al., 2017; Mikkelsen et al., 2008; Munch-Petersen et al., 2000; Solaroli et al., 2003). Certain nucleosides, such as  $N^4$ -glycinoyl-2'-deoxycytidine (**21**) or  $N^4$ -*sec*-butyl-2'-deoxycytidine (**27**),

were not phosphorylated by *BsdCK*-WT or were phosphorylated very inefficiently, whereas *DmdNK*-WT converted the compounds to their monophosphates considerably better. As discussed in the literature overview, one of the reasons for the broad substrate specificity of *DmdNK*-WT is the hydrophobic cavity in its active centre, which is lined with residues V84, M88, and A110 (Johansson et al., 1999). As was learned from the structural analysis of *BsdCK*-WT in the previous chapter, the corresponding residues in *BsdCK*-WT are F66, R70, and D93, respectively. To investigate whether replacement of the aforementioned residues would make *BsdCK* more similar to *DmdNK* in terms of substrate scope, mutants, where residues R70 and D93 were modified to mimic the ones found in *DmdNK*-WT, were created. According to the *in silico* model of *BsdCK*-WT, residue F66, which corresponds to V84 in *DmdNK*-WT, is expected to form stabilizing aromatic-aromatic interactions with cytosine nucleobase, hence the residue was left untouched. Utilizing single-site mutagenesis, 3 mutant variants of *BsdCK* were generated: two single-mutants *BsdCK*-R70M and *BsdCK*-D93A, and a double-mutation carrying variant *BsdCK*-R70M+D93A. The mutants were applied for the phosphorylation of *N*<sup>4</sup>-modified cytidine nucleosides (**Figure 36**). The results are provided in **Table 11**.

**Table 11.** Phosphorylation efficiencies of pyrimidine nucleosides by *BsdCK* wild-type and mutant variants. Number is the phosphorylation efficiency (%) calculated using HPLC-MS chromatogram areas. Cells are coloured based on mutant performance in comparison to the wild-type kinase with the particular substrate (a margin of error of  $\pm 3$  was applied). Rose – phosphorylation efficiency decreased  $\geq 2$ -fold compared to *BsdCK*-WT; orange – phosphorylation efficiency decreased  $\geq 1.5$ -fold but  $< 2$ -fold compared to *BsdCK*-WT; lime – phosphorylation efficiency increased  $\geq 1.5$ -fold but  $< 2$ -fold compared to *BsdCK*-WT; green – phosphorylation efficiency increased  $\geq 2$ -fold compared to *BsdCK*-WT; white – phosphorylation efficiency was similar to *BsdCK*-WT.

<i>BsdCK</i> \ Substrate	1	2	14	15	19	20	21	22	25	58	59	16	61	62
WT	100	93	95	2	0	0	11	0	0	0	0	18	1	7
R70M	7	2	0	0	0	0	2	0	0	0	0	0	0	0
R70M+D93A	100	55	99	98	37	0	98	0	0	0	0	9	0	1
D93A	100	5	97	79	16	0	20	0	0	0	0	2	0	0

The mutant variant *BsdCK*-R70M, where arginine was replaced with methionine, as is natively found in *DmdNK*-WT, exhibited extremely low overall activity. Compared to *BsdCK*-WT, the phosphorylation efficiency of canonical nucleosides 2'-deoxycytidine (**1**) and cytidine (**2**) decreased from

93–100% to 2–7%. Even though traces of *N*<sup>4</sup>-glycinoyl-2'-deoxycytidine (**21**) monophosphate were detected in the reaction mixture, the calculated phosphorylation efficiency was 5-fold lower than that of *BsdCK*-WT (2% compared to 11%). No other activity towards the remainder of the *N*<sup>4</sup>-modified cytidines was observed, thus *BsdCK*-R70M variant will not be further discussed.

The other single-mutant, *BsdCK*-D93A, which had alanine instead of aspartate in position 93, performed significantly better than *BsdCK*-R70M. Variant *BsdCK*-D93A retained similar activity towards 2'-deoxycytidine (**1**) and *N*<sup>4</sup>-acetyl-2'-deoxycytidine (**14**) as the wild-type variant and phosphorylated the compounds with 97–100% efficiency. Even though its activity towards cytidine decreased almost 20-fold compared to that of *BsdCK*-WT, a big improvement in phosphorylation of *N*<sup>4</sup>-isobutyryl-2'-deoxycytidine (**15**) was observed. The substrate was phosphorylated with 79% efficiency, whereas *BsdCK*-WT converted only 2% of the compound. In addition, mutation D93A increased the activity of the kinase towards *N*<sup>4</sup>-aminoacid modified deoxycytidines. Variant *BsdCK*-D93A phosphorylated *N*<sup>4</sup>-alaninoyl-2'-deoxycytidine (**19**) and *N*<sup>4</sup>-glycinoyl-2'-deoxycytidine (**21**) with an efficiency of 16% and 20%, respectively, whereas the phosphorylation efficiency of the wild-type kinase reached up to 11%.

The most significant increase in activity, however, was exhibited by the double-mutant *BsdCK*-R70M+D93A. A possible explanation for the observed effect might be positive intragenic epistasis, in which two mutations yield a more favourable result than would be expected from their individual effects (Parera and Martinez, 2014). Similarly to *BsdCK*-WT and the single-mutant *BsdCK*-D93A, *BsdCK*-R70M+D93A retained the same activities towards 2'-deoxycytidine (**1**) and *N*<sup>4</sup>-acetyl-2'-deoxycytidine (**14**), but an almost 2-fold decrease in phosphorylation efficiency of cytidine (**2**) compared to that of *BsdCK*-WT was observed. Nucleosides *N*<sup>4</sup>-isobutyryl-2'-deoxycytidine (**15**) and *N*<sup>4</sup>-glycinoyl-2'-deoxycytidine (**21**) were phosphorylated almost fully (98%), whereas efficiencies of the wild-type kinase reached only 2–11%. In addition, *N*<sup>4</sup>-alaninoyl-2'-deoxycytidine (**19**), which was not accepted as a substrate by the wild-type kinase, was phosphorylated with 37% efficiency. Interestingly, the observed phosphorylation efficiencies of the double-mutant *BsdCK*-R70M+D93A were even higher than those of *DmdNK*-WT, after which the mutant was modelled, and were comparable to those of the best performing *DmdNK*-V84A and *DmdNK*-V84G variants, even though the corresponding residue of *BsdCK* (F66) was not modified.



Even though the introduced mutations in the active centre of *BsdCK* increased the activity of the kinase towards certain nucleosides, some compounds remained unphosphorylated. The mutations were not enough to overcome the spatial limitations of the active site and/or unfavourable interactions between the residues of the substrate pocket and the substrates. None of the *BsdCK* mutants were able to phosphorylate Boc-protecting group bearing  $N^4$ -amino acid modified 2'-deoxycytidines (**20**, **22**, **25**), or the acidic cytidines (**58**, **59**). In addition, a 2- to 7-fold decrease in activity towards  $N^4$ -hydroxy- (**16**) and  $N^4$ -alkoxy-modified cytidines (**60**, **61**) was observed. The best-performing *BsdCK*-R70M+D93A variant presented with 0–9% phosphorylation efficiency, while *BsdCK*-WT converted the compounds to their monophosphate forms with efficiencies of 1–18%.

Analysis of the generated active site models of *BsdCK* provides some insight on how the introduced mutations affected the activity of the kinase towards  $N^4$ -modified 2'-deoxycytidines **15**, **19**, and **21**. In the wild-type variant, residue D93 is predicted to be located around 2.2 Å away from the  $N^4$ -atom of 2'-deoxycytidines as illustrated in **Figure 44a**. Carboxyl group of the aspartate residue is expected to form hydrogen bonds with the  $N^4$ -atom and assist with stabilizing the substrate in place. While the carboxyl functional group of D93 positively impacts binding of canonical substrates such as cytidine or uridine, it does the opposite for pyrimidine nucleosides bearing substitutions at the  $N^4$ - or  $O^4$ -position. Since the aspartate residue is located so closely to the said positions, it creates spatial limitations and only nucleosides with substitutions up to a certain size can fit in the active centre of the kinase. In addition, the negatively charged carboxyl group of D93 forms unfavourable polar interactions with certain modifications and, in turn, prevents the substrates from binding (Larsen, 1980). Replacing the residue with alanine, as is natively found in *DmdNK*-WT, mitigates both issues. As depicted in **Figure 44b**, the distance between the  $N^4$ -atom of cytosine nucleobase is predicted to increase almost twice (from 2.2 Å to 4.3 Å) compared to that of *BsdCK*-WT, thus bulkier substrates should be able enter the active site. Furthermore, removal of the negative charge, provided by the aspartate residue, is expected to make the environment for binding nucleosides with polar substitutions more favourable.

As can be seen from the generated *BsdCK*-WT model in **Figure 44a**, residue R70 is expected to be 4.2 Å away from the C5 atom of cytosine nucleobase. The distance is big enough to accommodate canonical cytosine or uracil nucleosides, however, it might create some spatial hindrance when substitutions at the C5 position are introduced. For example, phosphorylation of canonical 2'-deoxythymidine by *BsdCK*-WT is significantly less efficient

compared to that of 2'-deoxyuridine, and the constraints provided by R70 are expected to be the determinant. In addition, the positive charge provided by guanidinium functional group of arginine might prevent certain pyrimidine nucleosides with modifications at the C5 or  $N^4/O^4$ -positions from binding in the substrate pocket (Larsen, 1980).

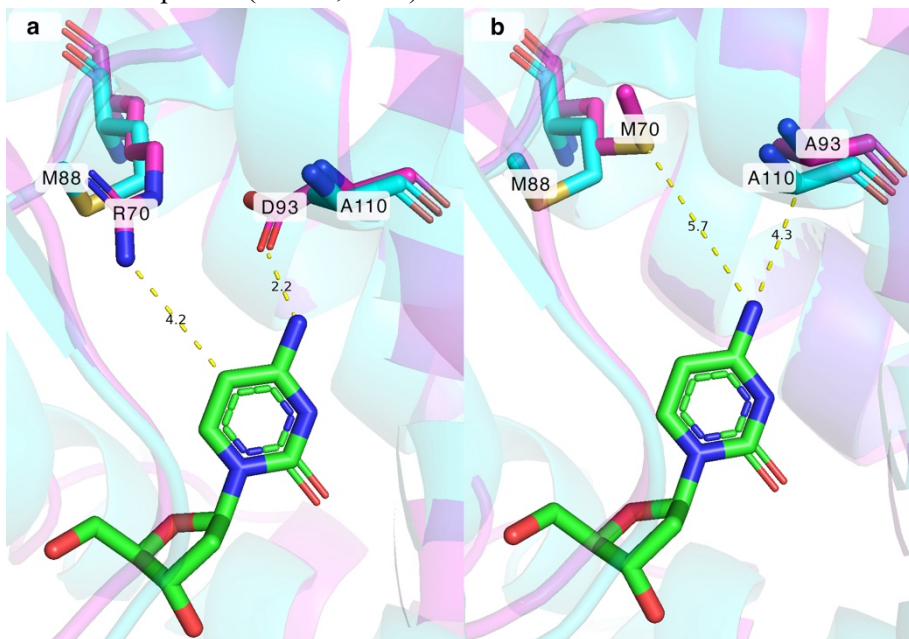


**Figure 44.** Superimposition of *BsdCK* (magenta) on *DmdNK* (cyan) with 2'-deoxycytidine (green) in the active centres. **a** M88 and A110 residues of *DmdNK*-WT, and corresponding R70 and D93 residues of *BsdCK*-WT near the  $N^4$  and C5 positions of 2'-deoxycytidine. **b** M88 and A110 residues of *DmdNK*-WT, and M70 and A93 residues of *BsdCK*-R70M+D93A mutant variant near the  $N^4$  and C5 positions of 2'-deoxycytidine. Yellow dashed lines show predicted distances between the residues of *BsdCK* and 2'-deoxycytidine. *DmdNK* PDB ID: 1j90. *BsdCK* models generated using ColabFold v1.5.5 software.

Replacing the R70 with a corresponding methionine residue from *DmdNK*-WT generates some additional space (**Figure 44b**) for nucleosides with bulkier modifications, as well as removes the positive charge provided by arginine. Even though a single R70M mutation did not increase the activity of *BsdCK* towards  $N^4$ -modified cytidines, a synergistic effect between R70M and D93A mutations was observed. The overall performance of the double mutant *BsdCK*-R70M+D93A was superior to that of the single mutant *BsdCK*-D93A. The hypothesis is that the extra space, in addition to the loss of the polar charges, allows for more mobility of the substrate in the active site. Hence, bulkier nucleosides can bind the substrate pocket more easily. In

conclusion, mimicking the active site of *DmdNK*-WT by replacing both R70 and D93 residues with corresponding methionine and alanine, respectively, has proven to be an effective strategy in increasing the activity of *BsdCK* towards  $N^4$ -modified cytidines.

### 3.9. Application of *DmdNK*-WT and *BsdCK*-WT for a larger-scale synthesis of nucleoside monophosphates

To explore the practical application side of nucleoside kinases, *DmdNK*-WT and *BsdCK*-WT were employed for a larger-scale synthesis of nucleoside 5'-monophosphates. The syntheses were executed via an enzymatic cascade, which consisted of two enzymes: a nucleoside kinase and an acetate kinase (**Figure 45**). *DmdNK*-WT was utilized for the phosphorylation of 2-thiouridine, and *BsdCK*-WT was used for the conversions of 2'-deoxycytidine and  $N^4$ -acetyl-2'-deoxycytidine into the corresponding 5'-monophosphates. During phosphorylation reactions, GTP is turned into GDP, which cannot be further used as a phosphate donor. To prevent the accumulation of GDP, the reaction mixture was supplemented with *EcACK*, which catalyses a phosphate group transfer from acetyl phosphate to a GDP molecule, forming GTP and acetic acid. Application of *EcACK* allows utilization of a lower amount of GTP, which, in addition to making the phosphorylation reactions more economical, also simplifies the purification of synthesized mononucleotides. The conditions for the syntheses are provided in Section 2.3.6.

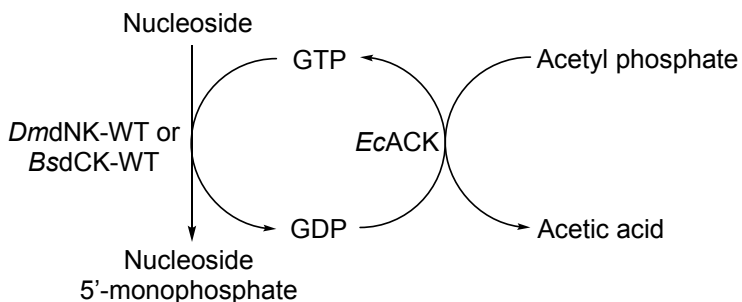


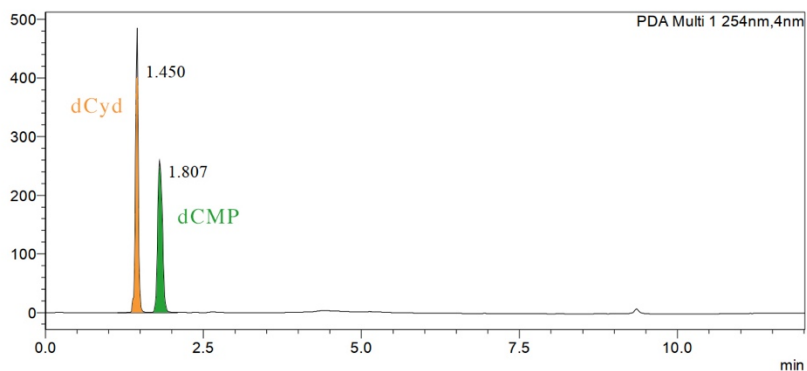
**Figure 45.** Nucleoside 5'-monophosphate synthesis using an enzymatic cascade that consists of *DmdNK*-WT or *BsdCK*-WT and *EcACK*.

The GTP regeneration system allowed using only 0.1 mol. eq. of GTP instead of the previously utilized 1.5 mol. eq. To ensure that the GTP regeneration was sufficient, the reaction mixtures were supplemented with 2 mol. eq. of acetyl phosphate every 24 h. The recurrent supplementation was

necessary because the half-life of acetyl phosphate at neutral pH and room temperature is known to be 21 h (Crans and Whitesides, 1983; Lipmann and Tuttle, 1944). Since the phosphorylation reactions took 72 h to complete, diminishing activities of the enzymes were inevitable. To overcome this issue, reaction mixtures were supplemented with the same initial amounts of *DmdNK*-WT or *BsdCK*-WT and *EcACK* every 24 h. The formed nucleoside monophosphates were purified twice: first by ion-exchange chromatography to separate all monophosphates, then – by reverse-phase chromatography, in which the remaining impurities were removed. The structures of the obtained compounds were confirmed by HPLC-MS and NMR analyses (provided in **Appendix 3**). The amounts of the mononucleotides were calculated using the UV spectra of their corresponding nucleosides and were as follows: 17 mg of 2'-deoxycytidine (4% final yield), 11 mg of *N*<sup>4</sup>-acetyl-2'-deoxycytidine (5% final yield), and 16 mg of 2-thiouridine (6% final yield).

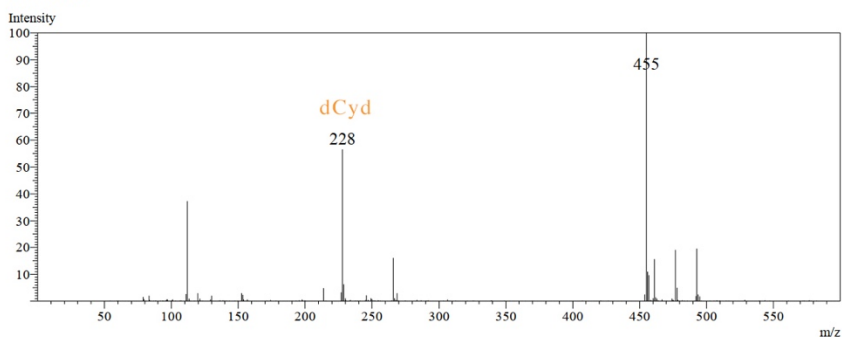
An example of HPLC-MS analysis of 2'-deoxycytidine phosphorylation by *BsdCK*-WT reaction mixture (before purification) is provided in **Figure 46** below. As can be seen from the HPLC chromatogram, the reaction mixture contains both 2'-deoxycytidine (yellow peak) and 2'-deoxycytidine 5'-monophosphate (green peak). As can be deduced from peak sizes, dCyd conversion to dCMP in the milligram-scale experiment is not as efficient as it was in microliter-scale experiments (detailed in Section 3.7). As is known from the previously discussed substrate specificity studies, both *DmdNK*-WT and *BsdCK*-WT can achieve phosphorylation efficiencies of up to 100%. However, the obtained mononucleotide yields in the larger-scale experiments were far from it, and the reasons are multifactorial. Firstly, in addition to the formation of acetic acid from GTP regeneration, the acetyl phosphate undergoes natural breakdown, as well (Lipmann and Tuttle, 1944). The resultant acetic acid lowers the pH of the reaction medium, creating a suboptimal environment for the kinases. The issue could be overcome by using a buffer of higher molarity. Secondly, enzyme precipitation was observed when utilizing automatic mixing. A milder approach, such as manual mixing, has been found to partially alleviate the problem. Thirdly, alternative purification methods for the nucleoside monophosphates should be explored. Retention of the mononucleotides in the purification columns was discovered to be poor and separation from impurities was problematic, which resulted in low final yields of the products. Fourth, the reaction optimization assay, described in Section 3.4, was executed in a microlitre-scale, and the optimal conditions required for the millilitre-scale synthesis are not necessarily the same. Hence additional optimisation assay might prove beneficial.

**a** <Chromatogram>  
mAU



**b**

R.Time:1.467



**c**

R.Time:1.833

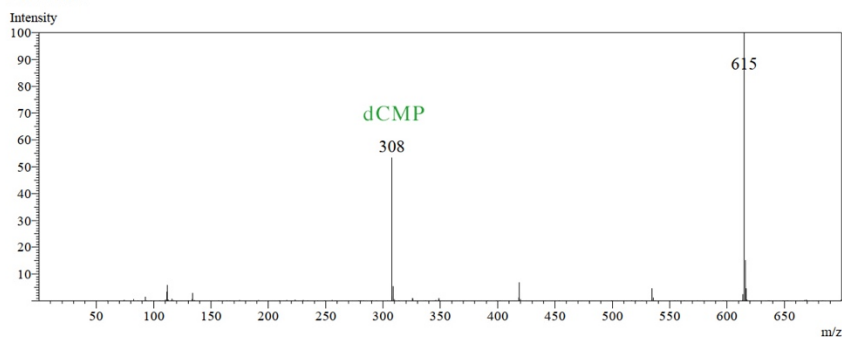


**Figure 46.** HPLC-MS analysis of dCyd phosphorylation by *BsdCK*-WT reaction mixture (before purification). **a** HPLC chromatogram of dCyd phosphorylation reaction mixture. The mixture contains dCyd (r. t. 1.450 min), dCMP (r. t. 1.807 min), and trace amounts of GTP (not visible). **b** MS spectrum of dCyd phosphorylation reaction mixture at 1.467 min. The peak at 228 m/z represents dCyd ( $M=227$  g/mol) at positive ionisation ( $[M+H]^+$ ). **c** MS spectrum of dCyd phosphorylation reaction mixture at 1.833 min. The peak at 308 m/z represents dCMP ( $M=307$  g/mol) at positive ionisation ( $[M+H]^+$ ).

Provided that the aforementioned issues are addressed, and a more efficient nucleoside monophosphate synthesis is attained, the mononucleotides could be further utilized in an enzymatic nucleoside 5'-triphosphate synthesis where the second and the third phosphorylation steps are performed by nucleoside monophosphate and diphosphate kinases (Bird et al., 2023; Ding et al., 2020; Fehlau et al., 2020). Similarly to nucleoside kinases, nucleoside monophosphate kinases (NMPKs) are relatively strict in their substrate preferences and should be selected thoughtfully. For example, mammalian uridylate-cytidylate kinase is known to phosphorylate CMP, dCMP, UMP, dUMP, AMP, and dAMP, while the isozymes of adenylate kinase accept AMP, dAMP, CMP, and dCMP as substrates (Van Rompay et al., 2000). In addition, viral thymidylate kinases from Herpes simplex virus-1 and varicella zoster virus phosphorylate 2'-deoxythymidine, dTMP, and dUMP (Deville-Bonne et al., 2010). The final phosphorylation step is performed by nucleoside diphosphate kinases (NDPKs). On the contrary to NMPKs, NDPKs are considered as non-specific enzymes. The wide substrate cleft enables NDPKs to phosphorylate a broad range of dinucleotides (Jong and Ma, 1991). For example, in addition to all canonical nucleoside diphosphates, *Homo sapiens* NDPK is known to phosphorylate various nucleotide analogues, such as azidothymidine or ribavirin diphosphates, or tenofovir monophosphate (Koch et al., 2009; Schaertl et al., 1998).

### Final remarks

The data presented in this thesis proposes an enzymatic alternative for chemical nucleoside monophosphate synthesis. Nucleoside kinases *DmdNK* and *BsdCK* were shown to be effective biocatalysts for the phosphorylation of canonical nucleosides and their analogues. The enzymes were discovered to have broad substrate acceptances as pyrimidine nucleosides bearing small- to moderate-sized modifications at the nucleobase or sugar were accepted as substrates. An enzymatic cascade, consisting of *DmdNK*-WT or *BsdCK*-WT and acetate kinase, which regenerates depleted GTP, was shown to be an option worth exploring for a milligram-scale synthesis of NMPs. Even though the final product yields were low, given that necessary optimisation steps are applied, the presented method could be employed as a more sustainable and less laborious alternative to chemical nucleoside phosphorylation. Furthermore, utilizing site-directed mutagenesis to alter the active centres of the kinases was shown to be an effective strategy to expand their accepted substrate scope. Certain modifications in the substrate pockets of *DmdNK* and

*BsdCK* significantly increased the activity of the enzymes towards *N*<sup>4</sup>-modified cytosine nucleosides.

The combined findings hold considerable significance from an industrial perspective. Traditional chemical nucleoside phosphorylation methods are known for their harsh conditions and by-product formation, they are labour-intensive and often result in inferior product yields. The presented enzymatic method provides a more sustainable and less laborious alternative to chemical phosphorylation. Compared to chemical methods, enzymatic NMP synthesis delivers a higher regio- and stereoselectivity, superior product yields and milder reaction conditions. In addition, the discoveries could be applied in the field of therapeutics. Nucleoside kinases play an important role in prodrug activation. Hence, the broad substrate acceptances of *DmdNK*-WT and *BsdCK*-WT suggest that the enzymes might be excellent candidates for suicide-gene therapy. Lastly, site-directed mutagenesis could be utilized to enhance the efficiency of the nucleoside kinases or even alter the enzymes to accommodate a specific substrate.

## CONCLUSIONS

1. A three-step synthesis can be applied for the synthesis of Boc-protected  $N^4$ -amino acid-modified deoxycytidines with medium to high final product yields (24–85%).
2. A catalyst-free deprotection of  $N^4$ -amino acid-modified deoxycytidines results in  $N$ -4-(2'-deoxycytidinyl)amino acid amides with final yields of 23–57%.
3. For the phosphorylation of 10 mM of 2'-deoxycytidine with a duration of 1 h at least 1.5 mol. eq. of GTP and 0.34 nmol/mL of *DmdNK*-WT or 47 nmol/mL of *BsdCK*-WT is necessary. The highest efficiencies are when temperatures and pH are 70 °C and 8.0 for *DmdNK*-WT, and 60 °C and 8.5 for *BsdCK*-WT.
4. *DmdNK*-WT phosphorylates all canonical nucleosides and pyrimidine nucleosides, bearing modifications at the nucleobase or sugar. *DmdNK*-WT displays high activity towards substrates with small- to medium-sized modifications at the  $N^4/O^4$  positions of the nucleobase. Its activity towards pyrimidine nucleosides bearing modifications at the C5-, 2'- and 3'-positions is low to moderate.
5. *BsdCK*-WT phosphorylates all canonical nucleosides and cytosine and uracil nucleosides with small  $N^4/O^4$ -substitutions. Conversions of C5-, 2'- and 3'-substituted pyrimidine nucleosides are less efficient.
6. Replacing *DmdNK* residues V84 and A110 with alanine or glycine increases the activity of the enzyme towards  $N^4$ -modified cytidines.
7. Mimicking the active site of *DmdNK*-WT by replacing *BsdCK* residues R70 and D93 with methionine and alanine, respectively, increases the activity of the kinase towards  $N^4$ -modified cytidines.
8. *DmdNK*-WT and *BsdCK*-WT can be employed for a milligram-scale synthesis of NMPs. Application of GTP regeneration system allows downscaling GTP concentration from 1.5 mol. eq. to 0.1 mol. eq. Since final yields of 2'-deoxycytidine,  $N^4$ -acetyl-2'-deoxycytidine, and 2-thiouridine 5'-monophosphates were low, additional optimisation is necessary for more satisfactory results.



## REFERENCES

1. Ahn, K., and Kornberg, A. (1990). Polyphosphate kinase from *Escherichia coli*. Purification and demonstration of a phosphoenzyme intermediate. *Journal of Biological Chemistry*, 265(20), 11734–11739. [https://doi.org/10.1016/S0021-9258\(19\)38459-5](https://doi.org/10.1016/S0021-9258(19)38459-5)
2. Akiyama, M., Crooke, E., and Kornberg, A. (1992). The polyphosphate kinase gene of *Escherichia coli*. Isolation and sequence of the ppk gene and membrane location of the protein. *The Journal of Biological Chemistry*, 267(31), 22556–22561.
3. Akola, J., and Jones, R. O. (2003). ATP hydrolysis in water – a density functional study. *The Journal of Physical Chemistry B*, 107(42), 11774–11783. <https://doi.org/10.1021/jp035538g>
4. An, C., Zhao, L., Wei, Z., and Zhou, X. (2017). Chemoenzymatic synthesis of 3'-phosphoadenosine-5'-phosphosulfate coupling with an ATP regeneration system. *Applied Microbiology and Biotechnology*, 101(20), 7535–7544. <https://doi.org/10.1007/s00253-017-8511-2>
5. Andersen, P. S., Smith, J. M., and Mygind, B. (1992). Characterization of the upp gene encoding uracil phosphoribosyltransferase of *Escherichia coli* K12. *European Journal of Biochemistry*, 204(1), 51–56. <https://doi.org/10.1111/j.1432-1033.1992.tb16604.x>
6. Andersen, R., and Neuhard, J. (2001). Deoxynucleoside kinases encoded by the yaaG and yaaF genes of *Bacillus subtilis*. *Journal of Biological Chemistry*, 276(8), 5518–5524. <https://doi.org/10.1074/jbc.M007918200>
7. Anderson, D. D., Quintero, C. M., and Stover, P. J. (2011). Identification of a de novo thymidylate biosynthesis pathway in mammalian mitochondria. *Proceedings of the National Academy of Sciences*, 108(37), 15163–15168. <https://doi.org/10.1073/pnas.1103623108>
8. Andexer, J. N., and Richter, M. (2015). Emerging Enzymes for ATP Regeneration in Biocatalytic Processes. *ChemBioChem*, 16(3), 380–386. <https://doi.org/10.1002/cbic.201402550>
9. Arcis, H., Ferguson, J. P., Cox, J. S., and Tremaine, P. R. (2020). The ionization constant of water at elevated temperatures and pressures: new data from direct conductivity measurements and revised formulations from  $T = 273$  K to 674 K and  $p = 0.1$  MPa to 31 MPa. *Journal of Physical and Chemical Reference Data*, 49(3). <https://doi.org/10.1063/1.5127662>

10. Arevalo, C. P., Bolton, M. J., Le Sage, V., Ye, N., Furey, C., Muramatsu, H., Alameh, M.-G., Pardi, N., Drapeau, E. M., Parkhouse, K., Garretson, T., Morris, J. S., Moncla, L. H., Tam, Y. K., Fan, S. H. Y., Lakdawala, S. S., Weissman, D., and Hensley, S. E. (2022). A multivalent nucleoside-modified mRNA vaccine against all known influenza virus subtypes. *Science*, 378(6622), 899–904. <https://doi.org/10.1126/science.abm0271>
11. Asano, Y., Mihara, Y., and Yamada, H. (1999). A novel selective nucleoside phosphorylating enzyme from *Morganella morganii*. *Journal of Bioscience and Bioengineering*, 87(6), 732–738. [https://doi.org/10.1016/S1389-1723\(99\)80145-5](https://doi.org/10.1016/S1389-1723(99)80145-5)
12. Ashihara, H., Takasawa, Y., and Suzuki, T. (1997). Metabolic fate of guanosine in higher plants. *Physiologia Plantarum*, 100(4), 909–916. <https://doi.org/10.1111/j.1399-3054.1997.tb00017.x>
13. Baddiley, J., Michelson, A. M., and Todd, A. R. (1948). Synthesis of adenosine triphosphate [3]. *Nature*, 161(4098), 761–762. <https://doi.org/10.1038/161761a0>
14. Balzarini, J., Liekens, S., Esnouf, R., and De Clercq, E. (2002). The A167Y mutation converts the herpes simplex virus type 1 thymidine kinase into a guanosine analogue kinase. *Biochemistry*, 41(20), 6517–6524. <https://doi.org/10.1021/bi0255930>
15. Barnadas-Carceller, B., Martinez-Peinado, N., Gómez, L. C., Ros-Lucas, A., Gabaldón-Figueira, J. C., Diaz-Mochon, J. J., Gascon, J., Molina, I. J., Pineda de las Infantas y Villatoro, M. J., and Alonso-Padilla, J. (2023). Identification of compounds with activity against *Trypanosoma cruzi* within a collection of synthetic nucleoside analogs. *Frontiers in Cellular and Infection Microbiology*, 12. <https://doi.org/10.3389/fcimb.2022.1067461>
16. Barré, A., Țințaș, M.-L., Levacher, V., Papamicaël, C., and Gembus, V. (2016). An overview of the synthesis of highly versatile N-hydroxysuccinimide esters. *Synthesis*, 49(03), 472–483. <https://doi.org/10.1055/s-0036-1588607>
17. Barroso, J. F., Elholm, M., and Flatmark, T. (2003). Tight binding of deoxyribonucleotide triphosphates to human thymidine kinase 2 expressed in *Escherichia coli*. Purification and partial characterization of its dimeric and tetrameric forms. *Biochemistry*, 42(51), 15158–15169. <https://doi.org/10.1021/bi035230f>
18. Batsanov, S. S. (2001). Van der Waals radii of elements. *Inorganic Materials*, 37(9), 871–885. <https://doi.org/10.1023/A:1011625728803>

19. Beigel, J. H., Tomashek, K. M., Dodd, L. E., Mehta, A. K., Zingman, B. S., Kalil, A. C., Hohmann, E., Chu, H. Y., Luetkemeyer, A., Kline, S., Lopez de Castilla, D., Finberg, R. W., Dierberg, K., Tapson, V., Hsieh, L., Patterson, T. F., Paredes, R., Sweeney, D. A., Short, W. R., ... Lane, H. C. (2020). Remdesivir for the treatment of Covid-19 — final report. *New England Journal of Medicine*, 383(19), 1813–1826. <https://doi.org/10.1056/NEJMoa2007764>
20. Bird, A. R., Molloy, J. C., and Hall, E. A. H. (2023). Biocatalytic synthesis of 2'-deoxynucleotide 5'-triphosphates from bacterial genomic DNA: Proof of principle. *Biotechnology and Bioengineering*, 120(6), 1531–1544. <https://doi.org/10.1002/bit.28374>
21. Bird, L. E., Ren, J., Wright, A., Leslie, K. D., Degreève, B., Balzarini, J., and Stammers, D. K. (2003). Crystal structure of Varicella zoster virus thymidine kinase. *Journal of Biological Chemistry*, 278(27), 24680–24687. <https://doi.org/10.1074/jbc.M302025200>
22. Bockamp, E.-O., Blasco, R., and Viñuela, E. (1991). *Escherichia coli* thymidine kinase: nucleotide sequence of the gene and relationships to other thymidine kinases. *Gene*, 101(1), 9–14. [https://doi.org/10.1016/0378-1119\(91\)90218-Z](https://doi.org/10.1016/0378-1119(91)90218-Z)
23. Bohman, C., and Eriksson, S. (1988). Deoxycytidine kinase from human leukemic spleen: preparation and characterization of the homogeneous enzyme. *Biochemistry*, 27(12), 4258–4265. <https://doi.org/10.1021/bi00412a009>
24. Burgess, K., and Cook, D. (2000). Syntheses of nucleoside triphosphates. *Chemical Reviews*, 100(6), 2047–2060. <https://doi.org/10.1021/cr990045m>
25. Cao, H., Li, C., Zhao, J., Wang, F., Tan, T., and Liu, L. (2018). Enzymatic production of glutathione coupling with an ATP regeneration system based on polyphosphate kinase. *Applied Biochemistry and Biotechnology*, 185(2), 385–395. <https://doi.org/10.1007/s12010-017-2664-4>
26. Cappannini, A., Ray, A., Purta, E., Mukherjee, S., Boccaletto, P., Moafinejad, S. N., Lechner, A., Barchet, C., Klaholz, B. P., Stefaniak, F., and Bujnicki, J. M. (2024). MODOMICS: a database of RNA modifications and related information. 2023 update. *Nucleic Acids Research*, 52(D1), D239–D244. <https://doi.org/10.1093/nar/gkad1083>
27. Carell, T., Brandmayr, C., Hienzsch, A., Müller, M., Pearson, D., Reiter, V., Thoma, I., Thumbs, P., and Wagner, M. (2012). Structure and function of noncanonical nucleobases. *Angewandte Chemie*

- International Edition*, 51(29), 7110–7131.  
<https://doi.org/10.1002/anie.201201193>
28. Carmany, D. O., Hollingsworth, K., and McCleary, W. R. (2003). Genetic and biochemical studies of phosphatase activity of PhoR. *Journal of Bacteriology*, 185(3), 1112–1115.  
<https://doi.org/10.1128/JB.185.3.1112-1115.2003>
  29. Caton-Williams, J., Lin, L., Smith, M., and Huang, Z. (2011). Convenient synthesis of nucleoside 5'-triphosphates for RNA transcription. *Chemical Communications*, 47(28), 8142.  
<https://doi.org/10.1039/c1cc12201k>
  30. Chen, F., Zhang, Y., Daugherty, A. B., Yang, Z., Shaw, R., Dong, M., Lutz, S., and Benner, S. A. (2017). Biological phosphorylation of an Unnatural Base Pair (UBP) using a *Drosophila melanogaster* deoxynucleoside kinase (DmdNK) mutant. *PLOS ONE*, 12(3), e0174163. <https://doi.org/10.1371/journal.pone.0174163>
  31. Chen, H., and Zhang, Y.-H. P. J. (2021). Enzymatic regeneration and conservation of ATP: challenges and opportunities. *Critical Reviews in Biotechnology*, 41(1), 16–33.  
<https://doi.org/10.1080/07388551.2020.1826403>
  32. Chu, M. Y., and Fischer, G. A. (1962). A proposed mechanism of action of 1-β-d-arabinofuranosyl-cytosine as an inhibitor of the growth of leukemic cells. *Biochemical Pharmacology*, 11(6), 423–430.  
[https://doi.org/10.1016/0006-2952\(62\)90225-3](https://doi.org/10.1016/0006-2952(62)90225-3)
  33. Clausen, A. R., Girandon, L., Ali, A., Knecht, W., Rozpedowska, E., Sandrini, M. P. B., Andreasson, E., Munch-Petersen, B., and Piškur, J. (2012). Two thymidine kinases and one multisubstrate deoxyribonucleoside kinase salvage DNA precursors in *Arabidopsis thaliana*. *The FEBS Journal*, 279(20), 3889–3897.  
<https://doi.org/10.1111/j.1742-4658.2012.08747.x>
  34. Crans, D. C., and Whitesides, G. M. (1983). A convenient synthesis of disodium acetyl phosphate for use in in situ ATP cofactor regeneration. *The Journal of Organic Chemistry*, 48(18), 3130–3132.  
<https://doi.org/10.1021/jo00166a048>
  35. Cristalli, G., Costanzi, S., Lambertucci, C., Lupidi, G., Vittori, S., Volpini, R., and Camaioni, E. (2001). Adenosine deaminase: Functional implications and different classes of inhibitors. *Medicinal Research Reviews*, 21(2), 105–128. [https://doi.org/10.1002/1098-1128\(200103\)21:2<105::AID-MED1002>3.0.CO;2-U](https://doi.org/10.1002/1098-1128(200103)21:2<105::AID-MED1002>3.0.CO;2-U)
  36. Crotty, S., Maag, D., Arnold, J. J., Zhong, W., Lau, J. Y. N., Hong, Z., Andino, R., and Cameron, C. E. (2000). The broad-spectrum antiviral

- ribonucleoside ribavirin is an RNA virus mutagen. *Nature Medicine*, 6(12), 1375–1379. <https://doi.org/10.1038/82191>
37. Dahl, C., Grønbaek, K., and Guldborg, P. (2011). Advances in DNA methylation: 5-hydroxymethylcytosine revisited. *Clinica Chimica Acta*, 412(11–12), 831–836. <https://doi.org/10.1016/j.cca.2011.02.013>
  38. Daniel, R., Danson, M., Eissenthal, R., Lee, C., and Peterson, M. (2008). The effect of temperature on enzyme activity: new insights and their implications. *Extremophiles*, 12(1), 51–59. <https://doi.org/10.1007/s00792-007-0089-7>
  39. De Clercq, E., and Shugar, D. (1975). Antiviral activity of 5-ethyl pyrimidine deoxynucleosides. *Biochemical Pharmacology*, 24(10), 1073–1078. [https://doi.org/10.1016/0006-2952\(75\)90192-6](https://doi.org/10.1016/0006-2952(75)90192-6)
  40. del Arco, J., and Fernandez-Lucas, J. (2018). Purine and pyrimidine phosphoribosyltransferases: a versatile tool for enzymatic synthesis of nucleoside-5'-monophosphates. *Current Pharmaceutical Design*, 23(45), 6898–6912. <https://doi.org/10.2174/1381612823666171017165707>
  41. del Arco, J., Galindo, J., Clemente-Suárez, V. J., Corrales, A., and Fernández-Lucas, J. (2020). Sustainable synthesis of uridine-5'-monophosphate analogues by immobilized uracil phosphoribosyltransferase from *Thermus thermophilus*. *Biochimica et Biophysica Acta (BBA) - Proteins and Proteomics*, 1868(1), 140251. <https://doi.org/10.1016/j.bbapap.2019.07.004>
  42. del Arco, J., Acosta, J., Pereira, H. M., Perona, A., Lokanath, N. K., Kunishima, N., and Fernández-Lucas, J. (2018). Enzymatic production of non-natural nucleoside-5'-monophosphates by a thermostable uracil phosphoribosyltransferase. *ChemCatChem*, 10(2), 439–448. <https://doi.org/10.1002/cctc.201701223>
  43. Deville-Bonne, D., El Amri, C., Meyer, P., Chen, Y., Agrofoglio, L. A., and Janin, J. (2010). Human and viral nucleoside/nucleotide kinases involved in antiviral drug activation: Structural and catalytic properties. *Antiviral Research*, 86(1), 101–120. <https://doi.org/10.1016/j.antiviral.2010.02.001>
  44. Ding, Y., Ou, L., and Ding, Q. (2020). Enzymatic synthesis of nucleoside triphosphates and deoxynucleoside triphosphates by surface-displayed kinases. *Applied Biochemistry and Biotechnology*, 190(4), 1271–1288. <https://doi.org/10.1007/s12010-019-03138-3>
  45. Domínguez-González, C., Hernández-Lain, A., Rivas, E., Hernández-Voth, A., Sayas Catalán, J., Fernández-Torrón, R., Fuiza-Luces, C., García García, J., Morís, G., Olivé, M., Miralles, F., Díaz-Manera, J.,

- Caballero, C., Méndez-Ferrer, B., Martí, R., García Arumi, E., Badosa, M. C., Esteban, J., Jimenez-Mallebrera, C., ... Paradas, C. (2019). Late-onset thymidine kinase 2 deficiency: a review of 18 cases. *Orphanet Journal of Rare Diseases*, 14(1), 100. <https://doi.org/10.1186/s13023-019-1071-z>
46. Dower, W. J., Miller, J. F., and Ragsdale, C. W. (1988). High efficiency transformation of *E. coli* by high voltage electroporation. *Nucleic Acids Research*, 16(13), 6127–6145. <https://doi.org/10.1093/nar/16.13.6127>
  47. Duarte, S., Carle, G., Faneca, H., Lima, M. C. P. de, and Pierrefite-Carle, V. (2012). Suicide gene therapy in cancer: Where do we stand now? *Cancer Letters*, 324(2), 160–170. <https://doi.org/10.1016/j.canlet.2012.05.023>
  48. Dunn, J., and Grider, M. H. (2023). *Physiology, Adenosine Triphosphate*. StatPearls.
  49. Durham, J. P., and Ives, D. H. (1971). The metabolism of deoxyribonucleosides in *Lactobacillus acidophilus*: Regulation of deoxyadenosine, deoxycytidine, deoxyguanosine and deoxythymidine kinase activities by nucleotides. *Biochimica et Biophysica Acta (BBA) - Nucleic Acids and Protein Synthesis*, 228(1), 9–25. [https://doi.org/10.1016/0005-2787\(71\)90542-9](https://doi.org/10.1016/0005-2787(71)90542-9)
  50. Dutta, N., Deb, I., Sarzynska, J., and Lahiri, A. (2022). Inosine and its methyl derivatives: Occurrence, biogenesis, and function in RNA. *Progress in Biophysics and Molecular Biology*, 169–170, 21–52. <https://doi.org/10.1016/j.pbiomolbio.2022.01.001>
  51. Egan, S. M., and Schleif, R. F. (1993). A regulatory cascade in the induction of rhaBAD. *Journal of Molecular Biology*, 234(1), 87–98. <https://doi.org/10.1006/jmbi.1993.1565>
  52. Egeblad-Welin, L., Sonntag, Y., Eklund, H., and Munch-Petersen, B. (2007). Functional studies of active-site mutants from *Drosophila melanogaster* deoxyribonucleoside kinase. *The FEBS Journal*, 274(6), 1542–1551. <https://doi.org/10.1111/j.1742-4658.2007.05701.x>
  53. El Omari, K., Solaroli, N., Karlsson, A., Balzarini, J., and Stammers, D. K. (2006). Structure of vaccinia virus thymidine kinase in complex with dTTP: insights for drug design. *BMC Structural Biology*, 6(1), 22. <https://doi.org/10.1186/1472-6807-6-22>
  54. Eriksson, S., Kierdaszuk, B., Munch-Petersen, B., Oberg, B., and Gunnar Johansson, N. (1991). Comparison of the substrate specificities of human thymidine kinase 1 and 2 and deoxycytidine kinase toward antiviral and cytostatic nucleoside analogs. *Biochemical and*

- Biophysical Research Communications*, 176(2), 586–592.  
[https://doi.org/10.1016/S0006-291X\(05\)80224-4](https://doi.org/10.1016/S0006-291X(05)80224-4)
55. Eriksson, S., Munch-Petersen, B., Johansson, K., and Ecklund, H. (2002). Structure and function of cellular deoxyribonucleoside kinases. *Cellular and Molecular Life Sciences CMLS*, 59(8), 1327–1346.  
<https://doi.org/10.1007/s00018-002-8511-x>
56. Esipov, R. S., Abramchik, Y. A., Fateev, I. V., Konstantinova, I. D., Kostromina, M. A., Muravyova, T. I., Artemova, K. G., and Miroshnikov, A. I. (2016). A cascade of thermophilic enzymes as an approach to the synthesis of modified nucleotides. *Acta Naturae*, 8(4), 82–90.
57. Fandilolu, P. M., Kamble, A. S., Dound, A. S., and Sonawane, K. D. (2019). Role of wybutosine and Mg<sup>+</sup> ions in modulating the structure and function of tRNA Phe: a molecular dynamics study. *ACS Omega*, 4(25), 21327–21339. <https://doi.org/10.1021/acsomega.9b02238>
58. Fehlau, M., Kaspar, F., Hellendahl, K. F., Schollmeyer, J., Neubauer, P., and Wagner, A. (2020). Modular enzymatic cascade synthesis of nucleotides using a (d)ATP regeneration system. *Frontiers in Bioengineering and Biotechnology*, 8.  
<https://doi.org/10.3389/fbioe.2020.00854>
59. Fillat, C., Carrio, M., Cascante, A., and Sangro, B. (2003). Suicide gene therapy mediated by the herpes simplex virus thymidine kinase gene / ganciclovir system: Fifteen years of application. *Current Gene Therapy*, 3(1), 13–26. <https://doi.org/10.2174/1566523033347426>
60. Fischer, M. (2010). *Amine coupling through EDC/NHS: A practical approach* (pp. 55–73). [https://doi.org/10.1007/978-1-60761-670-2\\_3](https://doi.org/10.1007/978-1-60761-670-2_3)
61. Fyfe, J. A. (1982). Differential phosphorylation of (E)-5-(2-bromovinyl)-2'-deoxyuridine monophosphate by thymidylate kinases from herpes simplex viruses types 1 and 2 and varicella zoster virus. *Molecular Pharmacology*, 21(2), 432–437.
62. Fyfe, J. A., Keller, P. M., Furman, P. A., Miller, R. L., and Elion, G. B. (1978). Thymidine kinase from herpes simplex virus phosphorylates the new antiviral compound, 9-(2-hydroxyethoxymethyl)guanine. *The Journal of Biological Chemistry*, 253(24), 8721–8727.
63. Garibyan, L., and Avashia, N. (2013). Polymerase chain reaction. *Journal of Investigative Dermatology*, 133(3), 1–4.  
<https://doi.org/10.1038/jid.2013.1>
64. Gentry, G. A. (1992). Viral thymidine kinases and their relatives. *Pharmacology & Therapeutics*, 54(3), 319–355.  
[https://doi.org/10.1016/0163-7258\(92\)90006-L](https://doi.org/10.1016/0163-7258(92)90006-L)

65. Geraghty, R., Aliota, M., and Bonnac, L. (2021). Broad-spectrum antiviral strategies and nucleoside analogues. *Viruses*, 13(4), 667. <https://doi.org/10.3390/v13040667>
66. Giacomello, A., and Salerno, C. (1978). Human hypoxanthine-guanine phosphoribosyltransferase. Steady state kinetics of the forward and reverse reactions. *Journal of Biological Chemistry*, 253(17), 6038–6044. [https://doi.org/10.1016/S0021-9258\(17\)34576-3](https://doi.org/10.1016/S0021-9258(17)34576-3)
67. Gillerman, I., and Fischer, B. (2010). An improved one-pot synthesis of nucleoside 5'-triphosphate analogues. *Nucleosides, Nucleotides and Nucleic Acids*, 29(3), 245–256. <https://doi.org/10.1080/15257771003709569>
68. Gomelsky, M. (2011). cAMP, c-di-GMP, c-di-AMP and now cGMP: bacteria use them all! *Molecular Microbiology*, 79(3), 562–565. <https://doi.org/10.1111/j.1365-2958.2010.07514.x>
69. Gross, A., Abril, O., Lewis, J. M., Geresh, S., and Whitesides, G. M. (1983). Practical synthesis of 5-phospho-D-ribose alpha-1-pyrophosphate (PRPP): enzymatic routes from ribose 5-phosphate or ribose. *Journal of the American Chemical Society*, 105(25), 7428–7435. <https://doi.org/10.1021/ja00363a037>
70. Guinan, M., Benckendorff, C., Smith, M., and Miller, G. J. (2020). Recent advances in the chemical synthesis and evaluation of anticancer nucleoside analogues. *Molecules*, 25(9), 2050. <https://doi.org/10.3390/molecules25092050>
71. Gulick, R. M., Mellors, J. W., Havlir, D., Eron, J. J., Gonzalez, C., McMahon, D., Richman, D. D., Valentine, F. T., Jonas, L., Meibohm, A., Emimi, E. A., Chodakewitz, J. A., Deutsch, P., Holder, D., Schleif, W. A., and Condra, J. H. (1997). Treatment with indinavir, zidovudine, and lamivudine in adults with human immunodeficiency virus infection and prior antiretroviral therapy. *New England Journal of Medicine*, 337(11), 734–739. <https://doi.org/10.1056/NEJM199709113371102>
72. Hanan, S., Jagarlamudi, K. K., Liya, W., Ellen, H., and Staffan, E. (2012). Quaternary structures of recombinant, cellular, and serum forms of Thymidine Kinase 1 from dogs and humans. *BMC Biochemistry*, 13(1), 12. <https://doi.org/10.1186/1471-2091-13-12>
73. Harlow, K. W., Nygaard, P., and Hove-Jensen, B. (1995). Cloning and characterization of the gsk gene encoding guanosine kinase of *Escherichia coli*. *Journal of Bacteriology*, 177(8), 2236–2240. <https://doi.org/10.1128/jb.177.8.2236-2240.1995>
74. Hazra, S., Ort, S., Konrad, M., and Lavie, A. (2010). Structural and kinetic characterization of human deoxycytidine kinase variants able to



- phosphorylate 5-substituted deoxycytidine and thymidine analogues. *Biochemistry*, 49(31), 6784–6790. <https://doi.org/10.1021/bi100839e>
75. Headen, T. F., Howard, C. A., Skipper, N. T., Wilkinson, M. A., Bowron, D. T., and Soper, A. K. (2010). Structure of  $\pi$ - $\pi$  interactions in aromatic liquids. *Journal of the American Chemical Society*, 132(16), 5735–5742. <https://doi.org/10.1021/ja909084e>
76. Heather, J. M., and Chain, B. (2016). The sequence of sequencers: The history of sequencing DNA. *Genomics*, 107(1), 1–8. <https://doi.org/10.1016/j.ygeno.2015.11.003>
77. Hellendahl, K. F., Kamel, S., Wetterwald, A., Neubauer, P., and Wagner, A. (2019). Human deoxycytidine kinase is a valuable biocatalyst for the synthesis of nucleotide analogues. *Catalysts*, 9(12), 997. <https://doi.org/10.3390/catal9120997>
78. Hennig, M., Scott, L. G., Sperling, E., Bermel, W., and Williamson, J. R. (2007). Synthesis of 5-fluoropyrimidine nucleotides as sensitive NMR probes of RNA structure. *Journal of the American Chemical Society*, 129(48), 14911–14921. <https://doi.org/10.1021/ja073825i>
79. Higgins, C. F., and Linton, K. J. (2004). The ATP switch model for ABC transporters. *Nature Structural & Molecular Biology*, 11(10), 918–926. <https://doi.org/10.1038/nsmb836>
80. Hirschbein, B. L., Mazenod, F. P., and Whitesides, G. M. (1982). Synthesis of phosphoenolpyruvate and its use in ATP cofactor regeneration. *The Journal of Organic Chemistry*, 47(19), 3765–3766. <https://doi.org/10.1021/jo00140a036>
81. Hoard, D. E., and Ott, D. G. (1965). Conversion of Mono- and Oligodeoxyribonucleotides to 5'-Triphosphates 1. *Journal of the American Chemical Society*, 87(8), 1785–1788. <https://doi.org/10.1021/ja01086a031>
82. Hoffman, M. A., Janson, D., Rose, E., and Rai, K. R. (1997). Treatment of hairy-cell leukemia with cladribine: response, toxicity, and long-term follow-up. *Journal of Clinical Oncology*, 15(3), 1138–1142. <https://doi.org/10.1200/JCO.1997.15.3.1138>
83. Holec, A. D., Mandal, S., Prathipati, P. K., and Destache, C. J. (2018). Nucleotide reverse transcriptase inhibitors: A thorough review, present status and future perspective as HIV therapeutics. *Current HIV Research*, 15(6). <https://doi.org/10.2174/1570162X15666171120110145>
84. Holmes, K. C., and Geeves, M. A. (2000). The structural basis of muscle contraction. *Philosophical Transactions of the Royal Society of*

- London. *Series B: Biological Sciences*, 355(1396), 419–431.  
<https://doi.org/10.1098/rstb.2000.0583>
85. Hottin, A., and Marx, A. (2016). Structural insights into the processing of nucleobase-modified nucleotides by DNA polymerases. *Accounts of Chemical Research*, 49(3), 418–427.  
<https://doi.org/10.1021/acs.accounts.5b00544>
86. Huang, M., and Graves, L. M. (2003). De novo synthesis of pyrimidine nucleotides; emerging interfaces with signal transduction pathways. *Cellular and Molecular Life Sciences CMLS*, 60(2), 321–336.  
<https://doi.org/10.1007/s000180300027>
87. Huang, Y., and Zhang, L. (2017). *An in vitro single-primer site-directed mutagenesis method for use in biotechnology* (pp. 375–383).  
[https://doi.org/10.1007/978-1-4939-6472-7\\_26](https://doi.org/10.1007/978-1-4939-6472-7_26)
88. Hulett, H. R. (1970). Non-enzymatic hydrolysis of adenosine phosphates. *Nature*, 225(5239), 1248–1249.  
<https://doi.org/10.1038/2251248a0>
89. Hulpia, F., Noppen, S., Schols, D., Andrei, G., Snoeck, R., Liekens, S., Vervaeke, P., and Van Calenbergh, S. (2018). Synthesis of a 3'-C-ethynyl- $\beta$ -d-ribofuranose purine nucleoside library: Discovery of C7-deazapurine analogs as potent antiproliferative nucleosides. *European Journal of Medicinal Chemistry*, 157, 248–267.  
<https://doi.org/10.1016/j.ejmech.2018.07.062>
90. Hult, K., and Berglund, P. (2003). Engineered enzymes for improved organic synthesis. *Current Opinion in Biotechnology*, 14(4), 395–400.  
[https://doi.org/10.1016/S0958-1669\(03\)00095-8](https://doi.org/10.1016/S0958-1669(03)00095-8)
91. Hurley, M. C., Lin, B., and Fox, I. H. (1986). *Regulation of deoxyadenosine and nucleoside analog phosphorylation by human placental adenosine kinase* (pp. 141–149). [https://doi.org/10.1007/978-1-4684-1248-2\\_22](https://doi.org/10.1007/978-1-4684-1248-2_22)
92. Illes, P., Klotz, K.-N., and Lohse, M. J. (2000). Signaling by extracellular nucleotides and nucleosides. *Naunyn-Schmiedeberg's Archives of Pharmacology*, 362(4–5), 295–298.  
<https://doi.org/10.1007/s002100000308>
93. Ishido, T., Yamazaki, N., Ishikawa, M., and Hirano, K. (2011). Characterization of DNA polymerase  $\beta$  from *Danio rerio* by overexpression in *E. coli* using the in vivo/in vitro compatible pIVEX plasmid. *Microbial Cell Factories*, 10(1), 84.  
<https://doi.org/10.1186/1475-2859-10-84>
94. Ishige, K., Zhang, H., and Kornberg, A. (2002). Polyphosphate kinase (PPK2), a potent, polyphosphate-driven generator of GTP. *Proceedings*

- of the National Academy of Sciences, 99(26), 16684–16688.  
<https://doi.org/10.1073/pnas.262655299>
95. Ives, D. H., and Ikeda, S. (1997). *Life on the salvage path: The deoxynucleoside kinases of Lactobacillus acidophilus R-26* (pp. 205–255). [https://doi.org/10.1016/S0079-6603\(08\)61033-8](https://doi.org/10.1016/S0079-6603(08)61033-8)
96. Jahani, F., Tajbakhsh, M., Khaksar, S., and Azizi, M. R. (2011). An efficient and highly chemoselective N-Boc protection of amines, amino acids, and peptides under heterogeneous conditions. *Monatshefte Für Chemie - Chemical Monthly*, 142(10), 1035–1043.  
<https://doi.org/10.1007/s00706-011-0534-2>
97. Jakubovska, J., Tauraitė, D., Birštonas, L., and Meškys, R. (2018). N4-Acyl-2'-deoxycytidine-5'-triphosphates for the enzymatic synthesis of modified DNA. *Nucleic Acids Research*, 46(12), 5911–5923.  
<https://doi.org/10.1093/nar/gky435>
98. Johansson, K., Ramaswamy, S., Ljungcrantz, C., Knecht, W., Piskur, J., Munch-Petersen, B., Eriksson, S., and Eklund, H. (2001). Structural basis for substrate specificities of cellular deoxyribonucleoside kinases. *Nature Structural Biology*, 8(7), 616–620.  
<https://doi.org/10.1038/89661>
99. Johansson, M., Van Rompay, A. R., Degève, B., Balzarini, J., and Karlsson, A. (1999). Cloning and characterization of the multisubstrate deoxyribonucleoside kinase of *Drosophila melanogaster*. *Journal of Biological Chemistry*, 274(34), 23814–23819.  
<https://doi.org/10.1074/jbc.274.34.23814>
100. Jong, A. Y., and Ma, J. J. (1991). *Saccharomyces cerevisiae* nucleoside-diphosphate kinase: Purification, characterization, and substrate specificity. *Archives of Biochemistry and Biophysics*, 291(2), 241–246. [https://doi.org/10.1016/0003-9861\(91\)90129-7](https://doi.org/10.1016/0003-9861(91)90129-7)
101. Jordheim, L. P., Durantel, D., Zoulim, F., and Dumontet, C. (2013). Advances in the development of nucleoside and nucleotide analogues for cancer and viral diseases. *Nature Reviews Drug Discovery*, 12(6), 447–464. <https://doi.org/10.1038/nrd4010>
102. Kamatani, N., Jinnah, H. A., Hennekam, R. C. M., and van Kuilenburg, A. B. P. (2021). Purine and pyrimidine metabolism. In *Emery and Rimoin's Principles and Practice of Medical Genetics and Genomics* (pp. 183–234). Elsevier. <https://doi.org/10.1016/B978-0-12-812535-9.00006-6>
103. Kawasaki, H., Usuda, Y., Shimaoka, M., and Utagawa, T. (2000). Phosphorylation of guanosine using guanosine-inosine kinase from *Exiguobacterium acetylicum* coupled with ATP regeneration.

- Bioscience, Biotechnology, and Biochemistry*, 64(10), 2259–2261.  
<https://doi.org/10.1271/bbb.64.2259>
104. Kesson, A. (1998). Use of aciclovir in herpes simplex virus infections. *Journal of Paediatrics and Child Health*, 34(1), 9–13.  
<https://doi.org/10.1046/j.1440-1754.1998.00440.x>
105. Khavari, D. A., Sen, G. L., and Rinn, J. L. (2010). DNA methylation and epigenetic control of cellular differentiation. *Cell Cycle*, 9(19), 3880–3883. <https://doi.org/10.4161/cc.9.19.13385>
106. Kigawa, T., Yabuki, T., Yoshida, Y., Tsutsui, M., Ito, Y., Shibata, T., and Yokoyama, S. (1999). Cell-free production and stable-isotope labeling of milligram quantities of proteins. *FEBS Letters*, 442(1), 15–19. [https://doi.org/10.1016/S0014-5793\(98\)01620-2](https://doi.org/10.1016/S0014-5793(98)01620-2)
107. Kim, D.-M., and Swartz, J. R. (1999). Prolonging cell-free protein synthesis with a novel ATP regeneration system. *Biotechnology and Bioengineering*, 66(3), 180–188. [https://doi.org/10.1002/\(SICI\)1097-0290\(1999\)66:3<180::AID-BIT6>3.0.CO;2-S](https://doi.org/10.1002/(SICI)1097-0290(1999)66:3<180::AID-BIT6>3.0.CO;2-S)
108. Knecht, W. (2002). A few amino acid substitutions can convert deoxyribonucleoside kinase specificity from pyrimidines to purines. *The EMBO Journal*, 21(7), 1873–1880.  
<https://doi.org/10.1093/emboj/21.7.1873>
109. Knecht, W. (2003). Mosquito has a single multisubstrate deoxyribonucleoside kinase characterized by unique substrate specificity. *Nucleic Acids Research*, 31(6), 1665–1672.  
<https://doi.org/10.1093/nar/gkg257>
110. Knecht, W., Mikkelsen, N. E., Clausen, A. R., Willer, M., Eklund, H., Gojković, Z., and Piškur, J. (2009). *Drosophila melanogaster* deoxyribonucleoside kinase activates gemcitabine. *Biochemical and Biophysical Research Communications*, 382(2), 430–433.  
<https://doi.org/10.1016/j.bbrc.2009.03.041>
111. Knecht, W., Munch-Petersen, B., and Piškur, J. (2000). Identification of residues involved in the specificity and regulation of the highly efficient multisubstrate deoxyribonucleoside kinase from *Drosophila melanogaster*. *Journal of Molecular Biology*, 301(4), 827–837.  
<https://doi.org/10.1006/jmbi.2000.3990>
112. Knecht, W., Petersen, G. E., Munch-Petersen, B., and Piškur, J. (2002). Deoxyribonucleoside kinases belonging to the thymidine kinase 2 (TK2)-like group vary significantly in substrate specificity, kinetics and feed-back regulation. *Journal of Molecular Biology*, 315(4), 529–540. <https://doi.org/10.1006/jmbi.2001.5257>

113. Knecht, W., Rozpedowska, E., Le Breton, C., Willer, M., Gojkovic, Z., Sandrini, M. P. B., Joergensen, T., Hasholt, L., Munch-Petersen, B., and Piskur, J. (2007). *Drosophila* deoxyribonucleoside kinase mutants with enhanced ability to phosphorylate purine analogs. *Gene Therapy*, *14*(17), 1278–1286. <https://doi.org/10.1038/sj.gt.3302982>
114. Koch, K., Chen, Y., Feng, J. Y., Borroto-Esoda, K., Deville-Bonne, D., Janin, J., and Moréra, S. (2009). Nucleoside diphosphate kinase and the activation of antiviral phosphonate analogs of nucleotides: binding mode and phosphorylation of tenofovir derivatives. *Nucleosides, Nucleotides and Nucleic Acids*, *28*(8), 776–792. <https://doi.org/10.1080/15257770903155899>
115. Koizumi, K., Shimamoto, Y., Azuma, A., Wataya, Y., Matsuda, A., Sasaki, T., and Fukushima, M. (2001). Cloning and expression of uridine/cytidine kinase cDNA from human fibrosarcoma cells. *International Journal of Molecular Medicine*, *8*(3), 273–278.
116. Koplūnaitė, M., Butkutė, K., Stankevičiūtė, J., and Meškys, R. (2024). Exploring the mutated kinases for chemoenzymatic synthesis of N4-modified cytidine monophosphates. *Molecules*, *29*(16), 3767. <https://doi.org/10.3390/molecules29163767>
117. Kore, A. R., Shanmugasundaram, M., Senthilvelan, A., and Srinivasan, B. (2012). An improved protection-free one-pot chemical synthesis of 2'-deoxynucleoside-5'-triphosphates. *Nucleosides, Nucleotides and Nucleic Acids*, *31*(5), 423–431. <https://doi.org/10.1080/15257770.2012.670739>
118. Kovács, T., and Ötvös, L. (1988). Simple synthesis of 5-vinyl- and 5-ethynyl-2'-deoxyuridine-5'-triphosphates. *Tetrahedron Letters*, *29*(36), 4525–4528. [https://doi.org/10.1016/S0040-4039\(00\)80537-7](https://doi.org/10.1016/S0040-4039(00)80537-7)
119. Krapcho, A., and Kuell, C. (1990). Mono-protected diamines. N-tert-butoxycarbonyl- $\alpha,\omega$ -alkanediamines from  $\alpha,\omega$ -alkanediamines. *Synthetic Communications*, *20*(16), 2559–2564. <https://doi.org/10.1080/00397919008053205>
120. Krüger, D. H., and Bickle, T. A. (1983). Bacteriophage survival: multiple mechanisms for avoiding the deoxyribonucleic acid restriction systems of their hosts. *Microbiological Reviews*, *47*(3), 345–360. <https://doi.org/10.1128/mr.47.3.345-360.1983>
121. Kuś, P., Kusz, J., and Książek, M. (2020). Aromatic C–H $\cdots$  $\pi$ , C–H $\cdots$ O and parallel aromatic–aromatic interactions in the crystal structure of meso-tetrakis[4-(benzyloxy)phenyl]porphyrin. *Journal of Chemical Crystallography*, *50*(1), 21–27. <https://doi.org/10.1007/s10870-018-0752-0>

122. Lapponi, M. J., Rivero, C. W., Zinni, M. A., Britos, C. N., and Trelles, J. A. (2016). New developments in nucleoside analogues biosynthesis: A review. *Journal of Molecular Catalysis B: Enzymatic*, 133, 218–233. <https://doi.org/10.1016/j.molcatb.2016.08.015>
123. Larsen, P. O. (1980). Physical and chemical properties of amino acids. In *Amino Acids and Derivatives* (pp. 225–269). Elsevier. <https://doi.org/10.1016/B978-0-12-675405-6.50012-7>
124. Ledesma-Amaro, R., Jiménez, A., Santos, M. A., and Revuelta, J. L. (2013). Biotechnological production of feed nucleotides by microbial strain improvement. *Process Biochemistry*, 48(9), 1263–1270. <https://doi.org/10.1016/j.procbio.2013.06.025>
125. Leija, C., Rijo-Ferreira, F., Kinch, L. N., Grishin, N. V., Nischan, N., Kohler, J. J., Hu, Z., and Phillips, M. A. (2016). Pyrimidine salvage enzymes are essential for de novo biosynthesis of deoxypyrimidine nucleotides in *Trypanosoma brucei*. *PLOS Pathogens*, 12(11), e1006010. <https://doi.org/10.1371/journal.ppat.1006010>
126. Lelièvre, C. M., Balandras, M., Petit, J., Vergne-Vaxelaire, C., and Zaparucha, A. (2020). ATP regeneration system in chemoenzymatic amide bond formation with thermophilic CoA ligase. *ChemCatChem*, 12(4), 1184–1189. <https://doi.org/10.1002/cctc.201901870>
127. Li, B., Li, R., Dorff, P., McWilliams, J., Guinn, R., Guinness, S., Han, L., Wang, K., and Yu, S. (2019). Deprotection of N-Boc groups under continuous-flow high-temperature conditions. *The Journal of Organic Chemistry*, 84(8), 4846–4855. <https://doi.org/10.1021/acs.joc.8b02909>
128. Li, X., Ma, S., and Yi, C. (2016). Pseudouridine: the fifth RNA nucleotide with renewed interests. *Current Opinion in Chemical Biology*, 33, 108–116. <https://doi.org/10.1016/j.cbpa.2016.06.014>
129. Li, Z., Ning, X., Zhao, Y., Zhang, X., Xiao, C., and Li, Z. (2020). Efficient one-pot dyntesis of vtyidine 5'-monophosphate using an extremophilic enzyme cascade system. *Journal of Agricultural and Food Chemistry*, 68(34), 9188–9194. <https://doi.org/10.1021/acs.jafc.0c04055>
130. Lipmann, F., and Tuttle, L. C. (1944). Acetyl phosphate: Chemistry, determination, and synthesis. *Journal of Biological Chemistry*, 153(2), 571–582. [https://doi.org/10.1016/S0021-9258\(18\)72001-2](https://doi.org/10.1016/S0021-9258(18)72001-2)
131. Liu, Z.-Q., Zhang, L., Sun, L.-H., Li, X.-J., Wan, N.-W., and Zheng, Y.-G. (2012). Enzymatic production of 5'-inosinic acid by a newly synthesised acid phosphatase/phosphotransferase. *Food Chemistry*, 134(2), 948–956. <https://doi.org/10.1016/j.foodchem.2012.02.213>

132. Ludwig, J. (1981). A new route to nucleoside 5'-triphosphates. *Acta Biochimica et Biophysica; Academiae Scientiarum Hungaricae*, 16(3–4), 131–133. <http://www.ncbi.nlm.nih.gov/pubmed/7347985>
133. Ludwig, J., and Eckstein, F. (1989). Rapid and efficient synthesis of nucleoside 5'-0-(1-thiotriphosphates), 5'-triphosphates and 2',3'-cyclophosphorothioates using 2-chloro-4H-1,3,2-benzodioxaphosphorin-4-one. *The Journal of Organic Chemistry*, 54(3), 631–635. <https://doi.org/10.1021/jo00264a024>
134. Ma, J., Zhong, M., Xiong, Y., Gao, Z., Wu, Z., Liu, Y., and Hong, X. (2021). Emerging roles of nucleotide metabolism in cancer development: progress and prospect. *Aging*, 13(9), 13349–13358. <https://doi.org/10.18632/aging.202962>
135. Ma, S., Zhao, L., Zhu, Z., Liu, Q., Xu, H., Johansson, M., Karlsson, A., and Zheng, X. (2011). The multisubstrate deoxyribonucleoside kinase of *Drosophila melanogaster* as a therapeutic suicide gene of breast cancer cells. *The Journal of Gene Medicine*, 13(6), 305–311. <https://doi.org/10.1002/jgm.1573>
136. Makarov, M., Meng, J., Tretyachenko, V., Srb, P., Březinová, A., Giacobelli, V. G., Bednárová, L., Vondrášek, J., Dunker, A. K., and Hlouchová, K. (2021). Enzyme catalysis prior to aromatic residues: Reverse engineering of a dephospho-CoA kinase. *Protein Science*, 30(5), 1022–1034. <https://doi.org/10.1002/pro.4068>
137. Mathews, C. K. (2015). Deoxyribonucleotide metabolism, mutagenesis and cancer. *Nature Reviews Cancer*, 15(9), 528–539. <https://doi.org/10.1038/nrc3981>
138. Mathews, I. I., Erion, M. D., and Ealick, S. E. (1998). Structure of human adenosine kinase at 1.5 Å resolution. *Biochemistry*, 37(45), 15607–15620. <https://doi.org/10.1021/bi9815445>
139. Matsuura, M. F., Winiger, C. B., Shaw, R. W., Kim, M.-J., Kim, M.-S., Daugherty, A. B., Chen, F., Moussatche, P., Moses, J. D., Lutz, S., and Benner, S. A. (2017). A single deoxynucleoside kinase variant from *Drosophila melanogaster* synthesizes monophosphates of nucleosides that are components of an expanded genetic system. *ACS Synthetic Biology*, 6(3), 388–394. <https://doi.org/10.1021/acssynbio.6b00228>
140. Menéndez-Arias, L., Álvarez, M., and Pacheco, B. (2014). Nucleoside/nucleotide analog inhibitors of hepatitis B virus polymerase: mechanism of action and resistance. *Current Opinion in Virology*, 8, 1–9. <https://doi.org/10.1016/j.coviro.2014.04.005>

141. Meng, Q., Zhang, Y., Ju, X., Ma, C., Ma, H., Chen, J., Zheng, P., Sun, J., Zhu, J., Ma, Y., Zhao, X., and Chen, T. (2016). Production of 5-aminolevulinic acid by cell free multi-enzyme catalysis. *Journal of Biotechnology*, 226, 8–13. <https://doi.org/10.1016/j.jbiotec.2016.03.024>
142. Micozzi, D., Carpi, F. M., Pucciarelli, S., Polzonetti, V., Polidori, P., Vilar, S., Williams, B., Costanzi, S., and Vincenzetti, S. (2014). Human cytidine deaminase: A biochemical characterization of its naturally occurring variants. *International Journal of Biological Macromolecules*, 63, 64–74. <https://doi.org/10.1016/j.ijbiomac.2013.10.029>
143. Mihara, Y., Utagawa, T., Yamada, H., and Asano, Y. (2000). Phosphorylation of nucleosides by the mutated acid phosphatase from *Morganella morganii*. *Applied and Environmental Microbiology*, 66(7), 2811–2816. <https://doi.org/10.1128/AEM.66.7.2811-2816.2000>
144. Mikkelsen, N. E., Johansson, K., Karlsson, A., Knecht, W., Andersen, G., Piškur, J., Munch-Petersen, B., and Eklund, H. (2003). Structural basis for feedback inhibition of the deoxyribonucleoside salvage pathway: Studies of the *Drosophila* deoxyribonucleoside kinase. *Biochemistry*, 42(19), 5706–5712. <https://doi.org/10.1021/bi0340043>
145. Mikkelsen, N. E., Munch-Petersen, B., and Eklund, H. (2008). Structural studies of nucleoside analog and feedback inhibitor binding to *Drosophila melanogaster* multisubstrate deoxyribonucleoside kinase. *The FEBS Journal*, 275(9), 2151–2160. <https://doi.org/10.1111/j.1742-4658.2008.06369.x>
146. Mikkola, S. (2020). Nucleotide sugars in chemistry and biology. *Molecules*, 25(23), 5755. <https://doi.org/10.3390/molecules25235755>
147. Mirdita, M., Schütze, K., Moriwaki, Y., Heo, L., Ovchinnikov, S., and Steinegger, M. (2022). ColabFold: making protein folding accessible to all. *Nature Methods*, 19(6), 679–682. <https://doi.org/10.1038/s41592-022-01488-1>
148. Moffatt, J. G., and Khorana, H. G. (1961). Nucleoside Polyphosphates. X. 1 The Synthesis and Some Reactions of Nucleoside-5' Phosphoromorpholidates and Related Compounds. Improved Methods for the Preparation of Nucleoside-5' Polyphosphates 1. *Journal of the American Chemical Society*, 83(3), 649–658. <https://doi.org/10.1021/ja01464a034>
149. Møllgaard, H. (1980). Deoxyadenosine/deoxycytidine kinase from *Bacillus subtilis*. Purification, characterization, and physiological function. *The Journal of Biological Chemistry*, 255(17), 8216–8220. <http://www.ncbi.nlm.nih.gov/pubmed/6251049>



150. Moore, L. D., Le, T., and Fan, G. (2013). DNA methylation and its basic function. *Neuropsychopharmacology*, 38(1), 23–38.  
<https://doi.org/10.1038/npp.2012.112>
151. Morgenroth, A., Vogg, A. T., Mottaghy, F. M., and Schmaljohann, J. (2011). Targeted endoradiotherapy using nucleotides. *Methods*, 55(3), 203–214. <https://doi.org/10.1016/j.ymeth.2011.06.009>
152. Mori, H., Iida, A., Teshiba, S., and Fujio, T. (1995). Cloning of a guanosine-inosine kinase gene of *Escherichia coli* and characterization of the purified gene product. *Journal of Bacteriology*, 177(17), 4921–4926. <https://doi.org/10.1128/jb.177.17.4921-4926.1995>
153. Motomura, K., Hirota, R., Okada, M., Ikeda, T., Ishida, T., and Kuroda, A. (2014). A new subfamily of polyphosphate kinase 2 (class III PPK2) catalyzes both nucleoside monophosphate phosphorylation and nucleoside diphosphate phosphorylation. *Applied and Environmental Microbiology*, 80(8), 2602–2608.  
<https://doi.org/10.1128/AEM.03971-13>
154. Munch-Petersen, B., Cloos, L., Jensen, H. K., and Tyrsted, G. (1995). Human thymidine kinase 1. Regulation in normal and malignant cells. *Advances in Enzyme Regulation*, 35, 69–89.  
[https://doi.org/10.1016/0065-2571\(94\)00014-T](https://doi.org/10.1016/0065-2571(94)00014-T)
155. Munch-Petersen, B., Cloos, L., Tyrsted, G., and Eriksson, S. (1991). Diverging substrate specificity of pure human thymidine kinases 1 and 2 against antiviral dideoxynucleosides. *The Journal of Biological Chemistry*, 266(14), 9032–9038.
156. Munch-Petersen, B., Knecht, W., Lenz, C., Søndergaard, L., and Piškur, J. (2000). Functional expression of a multisubstrate deoxyribonucleoside kinase from *Drosophila melanogaster* and its C-terminal deletion mutants. *Journal of Biological Chemistry*, 275(9), 6673–6679. <https://doi.org/10.1074/jbc.275.9.6673>
157. Naesens, L., Guddat, L. W., Keough, D. T., van Kuilenburg, A. B. P., Meijer, J., Vande Voorde, J., and Balzarini, J. (2013). Role of human hypoxanthine guanine phosphoribosyltransferase in activation of the antiviral agent T-705 (favipiravir). *Molecular Pharmacology*, 84(4), 615–629. <https://doi.org/10.1124/mol.113.087247>
158. Nainar, S., Cuthbert, B. J., Lim, N. M., England, W. E., Ke, K., Sophal, K., Quechol, R., Mobley, D. L., Goulding, C. W., and Spitale, R. C. (2020). An optimized chemical-genetic method for cell-specific metabolic labeling of RNA. *Nature Methods*, 17(3), 311–318.  
<https://doi.org/10.1038/s41592-019-0726-y>

159. Nakajima, H., Nagata, K., Kondo, H., and Imahori, K. (1984). Continuous ATP regeneration process with stable acetate kinase. *Journal of Applied Biochemistry*, 6(1–2), 19–28.
160. Nelson, D. L., Cox, M. M., and Hoskins, A. A. (2021). *Lehninger Principles of Biochemistry. Eighth Edition*. W. H. Freeman and Company.
161. Neri, F., Incarnato, D., Krepelova, A., Rapelli, S., Anselmi, F., Parlato, C., Medana, C., Dal Bello, F., and Oliviero, S. (2015). Single-base resolution analysis of 5-formyl and 5-carboxyl cytosine reveals promoter DNA methylation dynamics. *Cell Reports*, 10(5), 674–683. <https://doi.org/10.1016/j.celrep.2015.01.008>
162. Neville, N., Roberge, N., and Jia, Z. (2022). Polyphosphate kinase 2 (PPK2) enzymes: Structure, function, and roles in bacterial physiology and virulence. *International Journal of Molecular Sciences*, 23(2), 670. <https://doi.org/10.3390/ijms23020670>
163. Noguchi, T., and Shiba, T. (1998). Use of *Escherichia coli* polyphosphate kinase for oligosaccharide synthesis. *Bioscience, Biotechnology, and Biochemistry*, 62(8), 1594–1596. <https://doi.org/10.1271/bbb.62.1594>
164. Nyhan, W. L. (1973). The Lesch-Nyhan syndrome. *Annual Review of Medicine*, 24(1), 41–60. <https://doi.org/10.1146/annurev.me.24.020173.000353>
165. Nyhan, W. L. (2014). Nucleotide synthesis via salvage pathway. In *Encyclopedia of Life Sciences*. Wiley. <https://doi.org/10.1002/9780470015902.a0001399.pub3>
166. Parera, M., and Martinez, M. (2014). Strong epistatic interactions within a single protein. *Molecular Biology and Evolution*, 31(6), 1546–1553. <https://doi.org/10.1093/molbev/msu113>
167. Parker, W. B., Allan, P. W., Waud, W. R., Hong, J. S., and Sorscher, E. J. (2011). Effect of expression of adenine phosphoribosyltransferase on the in vivo anti-tumor activity of prodrugs activated by *E. coli* purine nucleoside phosphorylase. *Cancer Gene Therapy*, 18(6), 390–398. <https://doi.org/10.1038/cgt.2011.4>
168. Partridge, L., Barrie, B., Fowler, K., and French, V. (1994). Evolution and development of body size and cell size in *Drosophila melanogaster* in response to temperature. *Evolution*, 48(4), 1269–1276. <https://doi.org/10.1111/j.1558-5646.1994.tb05311.x>
169. Phizicky, E. M., and Alfonzo, J. D. (2010). Do all modifications benefit all tRNAs? *FEBS Letters*, 584(2), 265–271. <https://doi.org/10.1016/j.febslet.2009.11.049>

170. Piškur, J., Sandrini, M. P. B., Knecht, W., and Munch-Petersen, B. (2004). Animal deoxyribonucleoside kinases: ‘forward’ and ‘retrograde’ evolution of their substrate specificity. *FEBS Letters*, *560*(1–3), 3–6. [https://doi.org/10.1016/S0014-5793\(04\)00081-X](https://doi.org/10.1016/S0014-5793(04)00081-X)
171. Prichard, M. N., Keith, K. A., Johnson, M. P., Harden, E. A., McBrayer, A., Luo, M., Qiu, S., Chattopadhyay, D., Fan, X., Torrence, P. F., and Kern, E. R. (2007). Selective phosphorylation of antiviral drugs by vaccinia virus thymidine kinase. *Antimicrobial Agents and Chemotherapy*, *51*(5), 1795–1803. <https://doi.org/10.1128/AAC.01447-06>
172. Pruijssers, A. J., and Denison, M. R. (2019). Nucleoside analogues for the treatment of coronavirus infections. *Current Opinion in Virology*, *35*, 57–62. <https://doi.org/10.1016/j.coviro.2019.04.002>
173. Pyle, J. D., Lund, S. R., O’Toole, K. H., and Saleh, L. (2024). Virus-encoded glycosyltransferases hypermodify DNA with diverse glycans. *Cell Reports*, *43*(8), 114631. <https://doi.org/10.1016/j.celrep.2024.114631>
174. Qian, Y., Ding, Q., Li, Y., Zou, Z., Yan, B., and Ou, L. (2014). Phosphorylation of uridine and cytidine by uridine–cytidine kinase. *Journal of Biotechnology*, *188*, 81–87. <https://doi.org/10.1016/j.jbiotec.2014.08.018>
175. Rao, N. N., Gómez-García, M. R., and Kornberg, A. (2009). Inorganic polyphosphate: Essential for growth and survival. *Annual Review of Biochemistry*, *78*(1), 605–647. <https://doi.org/10.1146/annurev.biochem.77.083007.093039>
176. Rist, M., and Marino, J. (2002). Fluorescent nucleotide base analogs as probes of nucleic acid structure, dynamics and interactions. *Current Organic Chemistry*, *6*(9), 775–793. <https://doi.org/10.2174/1385272023373914>
177. Roberts, G. B., Fyfe, J. A., McKee, S. A., Rahim, S. G., Daluge, S. M., Almond, M. R., Rideout, J. L., Koszalka, G. W., and Krenitsky, T. A. (1993). Varicella-Zoster virus thymidine kinase. *Biochemical Pharmacology*, *46*(12), 2209–2218. [https://doi.org/10.1016/0006-2952\(93\)90611-Y](https://doi.org/10.1016/0006-2952(93)90611-Y)
178. Robescu, M. S., Serra, I., Terreni, M., Ubiali, D., and Bavaro, T. (2020). A multi-enzymatic cascade reaction for the synthesis of vidarabine 5'-monophosphate. *Catalysts*, *10*(1), 60. <https://doi.org/10.3390/catal10010060>
179. Rossolini, G. M., Schippa, S., Riccio, M. L., Berlutti, F., Macaskie, L. E., and Thaller, M. C. (1998). Bacterial nonspecific acid

- phosphohydrolases: physiology, evolution and use as tools in microbial biotechnology. *Cellular and Molecular Life Sciences (CMLS)*, 54(8), 833–850. <https://doi.org/10.1007/s000180050212>
180. Roy, B., Depaix, A., Périgaud, C., and Peyrottes, S. (2016). Recent trends in nucleotide synthesis. *Chemical Reviews*, 116(14), 7854–7897. <https://doi.org/10.1021/acs.chemrev.6b00174>
181. Rudolph, F. B. (1994). The biochemistry and physiology of nucleotides. *The Journal of Nutrition*, 124(13), 124S-127S. [https://doi.org/10.1093/jn/124.suppl\\_1.124S](https://doi.org/10.1093/jn/124.suppl_1.124S)
182. Sabini, E., Hazra, S., Konrad, M., and Lavie, A. (2007). Nonenantioselectivity property of human deoxycytidine kinase explained by structures of the enzyme in complex with L- and D-nucleosides. *Journal of Medicinal Chemistry*, 50(13), 3004–3014. <https://doi.org/10.1021/jm0700215>
183. Sabini, E., Ort, S., Monnerjahn, C., Konrad, M., and Lavie, A. (2003). Structure of human dCK suggests strategies to improve anticancer and antiviral therapy. *Nature Structural & Molecular Biology*, 10(7), 513–519. <https://doi.org/10.1038/nsb942>
184. Saeb, S., Assche, J. Van, Loustau, T., Rohr, O., Wallet, C., and Schwartz, C. (2022). Suicide gene therapy in cancer and HIV-1 infection: An alternative to conventional treatments. *Biochemical Pharmacology*, 197, 114893. <https://doi.org/10.1016/j.bcp.2021.114893>
185. Sahlin, K., and Harris, R. C. (2011). The creatine kinase reaction: a simple reaction with functional complexity. *Amino Acids*, 40(5), 1363–1367. <https://doi.org/10.1007/s00726-011-0856-8>
186. Saito, Y., and Hudson, R. H. E. (2018). Base-modified fluorescent purine nucleosides and nucleotides for use in oligonucleotide probes. *Journal of Photochemistry and Photobiology C: Photochemistry Reviews*, 36, 48–73. <https://doi.org/10.1016/j.jphotochemrev.2018.07.001>
187. Sandrini, M. P. B., Clausen, A. R., Munch-Petersen, B., and Piškur, J. (2006). Thymidine kinase diversity in bacteria. *Nucleosides, Nucleotides and Nucleic Acids*, 25(9–11), 1153–1158. <https://doi.org/10.1080/15257770600894469>
188. Sandrini, M. P. B., Clausen, A. R., On, S. L. W., Aarestrup, F. M., Munch-Petersen, B., and Piškur, J. (2007). Nucleoside analogues are activated by bacterial deoxyribonucleoside kinases in a species-specific manner. *Journal of Antimicrobial Chemotherapy*, 60(3), 510–520. <https://doi.org/10.1093/jac/dkm240>

189. Sandrini, M. P. B., and Piškur, J. (2005). Deoxyribonucleoside kinases: two enzyme families catalyze the same reaction. *Trends in Biochemical Sciences*, 30(5), 225–228.  
<https://doi.org/10.1016/j.tibs.2005.03.003>
190. Sanger, F., Nicklen, S., and Coulson, A. R. (1977). DNA sequencing with chain-terminating inhibitors. *Proceedings of the National Academy of Sciences*, 74(12), 5463–5467.  
<https://doi.org/10.1073/pnas.74.12.5463>
191. Schaertl, S., Konrad, M., and Geeves, M. A. (1998). Substrate specificity of human nucleoside-diphosphate kinase revealed by transient kinetic analysis. *Journal of Biological Chemistry*, 273(10), 5662–5669. <https://doi.org/10.1074/jbc.273.10.5662>
192. Scism, R. A., Stec, D. F., and Bachmann, B. O. (2007). Synthesis of nucleotide analogues by a promiscuous phosphoribosyltransferase. *Organic Letters*, 9(21), 4179–4182. <https://doi.org/10.1021/ol7016802>
193. Scraba, D. G., Bradley, R. D., Leyritz-Wills, M., and Warren, R. A. J. (1983). Bacteriophage  $\phi$ W-14: The contribution of covalently bound putrescine to DNA packing in the phage head. *Virology*, 124(1), 152–160. [https://doi.org/10.1016/0042-6822\(83\)90298-2](https://doi.org/10.1016/0042-6822(83)90298-2)
194. Seifert, R. (2015). cCMP and cUMP: emerging second messengers. *Trends in Biochemical Sciences*, 40(1), 8–15.  
<https://doi.org/10.1016/j.tibs.2014.10.008>
195. Serra, I., Conti, S., Piškur, J., Clausen, A. R., Munch-Petersen, B., Terreni, M., and Ubiali, D. (2014). Immobilized *Drosophila melanogaster* deoxyribonucleoside kinase (*DmdNK*) as a high performing biocatalyst for the synthesis of purine arabinonucleotides. *Advanced Synthesis & Catalysis*, 356(2–3), 563–570.  
<https://doi.org/10.1002/adsc.201300649>
196. Serra, I., Ubiali, D., Piškur, J., Munch-Petersen, B., Bavaro, T., and Terreni, M. (2017). Immobilization of deoxyadenosine kinase from *Dictyostelium discoideum* (*DddAK*) and its application in the 5'-phosphorylation of arabinosyladenine and arabinosyl-2-fluoroadenine. *ChemistrySelect*, 2(19), 5403–5408.  
<https://doi.org/10.1002/slct.201700558>
197. Shanmugasundaram, M., Senthilvelan, A., and Kore, A. R. (2019). C-5 substituted pyrimidine nucleotides/nucleosides: Recent progress in synthesis, functionalization, and applications. *Current Organic Chemistry*, 23(13), 1439–1468.  
<https://doi.org/10.2174/1385272823666190809124310>

198. Shelton, J., Lu, X., Hollenbaugh, J. A., Cho, J. H., Amblard, F., and Schinazi, R. F. (2016). Metabolism, biochemical actions, and chemical synthesis of anticancer nucleosides, nucleotides, and base analogs. *Chemical Reviews*, *116*(23), 14379–14455. <https://doi.org/10.1021/acs.chemrev.6b00209>
199. Shimane, M., Sugai, Y., Kainuma, R., Natsume, M., and Kawaide, H. (2012). Mevalonate-dependent enzymatic synthesis of amorphadiene driven by an ATP-regeneration system using polyphosphate kinase. *Bioscience, Biotechnology, and Biochemistry*, *76*(8), 1558–1560. <https://doi.org/10.1271/bbb.120177>
200. Sinokrot, H., Smerat, T., Najjar, A., and Karaman, R. (2017). Advanced prodrug strategies in nucleoside and non-nucleoside antiviral agents: A review of the recent five years. *Molecules*, *22*(10), 1736. <https://doi.org/10.3390/molecules22101736>
201. Sjöberg, A. H., Wang, L., and Eriksson, S. (1998). Substrate specificity of human recombinant mitochondrial deoxyguanosine kinase with cytostatic and antiviral purine and pyrimidine analogs. *Molecular Pharmacology*, *53*(2), 270–273. <https://doi.org/10.1124/mol.53.2.270>
202. Slot Christiansen, L., Munch-Petersen, B., and Knecht, W. (2015). Non-viral deoxyribonucleoside kinases – diversity and practical use. *Journal of Genetics and Genomics*, *42*(5), 235–248. <https://doi.org/10.1016/j.jgg.2015.01.003>
203. Solaroli, N., Bjerke, M., Amiri, M. H., Johansson, M., and Karlsson, A. (2003). Active site mutants of *Drosophila melanogaster* multisubstrate deoxyribonucleoside kinase. *European Journal of Biochemistry*, *270*(13), 2879–2884. <https://doi.org/10.1046/j.1432-1033.2003.03666.x>
204. Solaroli, N., Johansson, M., Balzarini, J., and Karlsson, A. (2007). Enhanced toxicity of purine nucleoside analogs in cells expressing *Drosophila melanogaster* nucleoside kinase mutants. *Gene Therapy*, *14*(1), 86–92. <https://doi.org/10.1038/sj.gt.3302835>
205. Solaroli, N., Johansson, M., Persoons, L., Balzarini, J., and Karlsson, A. (2008). Substrate specificity of feline and canine herpesvirus thymidine kinase. *Antiviral Research*, *79*(2), 128–132. <https://doi.org/10.1016/j.antiviral.2008.03.003>
206. Spadari, S., Maga, G., Focher, F., Ciarrocchi, G., Manservigi, R., Arcamone, F., Capobianco, M., Carcuro, A., and Colonna, F. (1992). L-Thymidine is phosphorylated by herpes simplex virus type 1

- thymidine kinase and inhibits viral growth. *Journal of Medicinal Chemistry*, 35(22), 4214–4220. <https://doi.org/10.1021/jm00100a029>
207. Spychala, J., Datta, N. S., Takabayashi, K., Datta, M., Fox, I. H., Gribbin, T., and Mitchell, B. S. (1996). Cloning of human adenosine kinase cDNA: sequence similarity to microbial ribokinases and fructokinases. *Proceedings of the National Academy of Sciences*, 93(3), 1232–1237. <https://doi.org/10.1073/pnas.93.3.1232>
208. Stauffer, C. S., Bhaket, P., Fothergill, A. W., Rinaldi, M. G., and Datta, A. (2007). Total synthesis and antifungal activity of a carbohydrate ring-expanded pyranosyl nucleoside analogue of nikkomycin B. *The Journal of Organic Chemistry*, 72(26), 9991–9997. <https://doi.org/10.1021/jo701814b>
209. Sternberg, N., and Coulby, J. (1990). Cleavage of the bacteriophage P1 packaging site (pac) is regulated by adenine methylation. *Proceedings of the National Academy of Sciences*, 87(20), 8070–8074. <https://doi.org/10.1073/pnas.87.20.8070>
210. Studier, F. W., and Moffatt, B. A. (1986). Use of bacteriophage T7 RNA polymerase to direct selective high-level expression of cloned genes. *Journal of Molecular Biology*, 189(1), 113–130. [https://doi.org/10.1016/0022-2836\(86\)90385-2](https://doi.org/10.1016/0022-2836(86)90385-2)
211. Su, W., Weng, Y., Jiang, L., Yang, Y., Zhao, L., Chen, Z., Li, Z., and Li, J. (2010). Recent progress in the use of Vilsmeier-type reagents. *Organic Preparations and Procedures International*, 42(6), 503–555. <https://doi.org/10.1080/00304948.2010.513911>
212. Suzuki, N. N., Koizumi, K., Fukushima, M., Matsuda, A., and Inagaki, F. (2004). Structural basis for the specificity, catalysis, and regulation of human uridine-cytidine kinase. *Structure*, 12(5), 751–764. <https://doi.org/10.1016/j.str.2004.02.038>
213. Tamura, R., Miyoshi, H., Yoshida, K., Okano, H., and Toda, M. (2021). Recent progress in the research of suicide gene therapy for malignant glioma. *Neurosurgical Review*, 44(1), 29–49. <https://doi.org/10.1007/s10143-019-01203-3>
214. Tao, J., and Xu, J.-H. (2009). Biocatalysis in development of green pharmaceutical processes. *Current Opinion in Chemical Biology*, 13(1), 43–50. <https://doi.org/10.1016/j.cbpa.2009.01.018>
215. Teng, F., Wang, L., Hu, M., and Tao, Y. (2023). Cell-free regeneration of ATP based on polyphosphate kinase 2 facilitates cytidine 5'-monophosphate production. *Enzyme and Microbial Technology*, 165, 110211. <https://doi.org/10.1016/j.enzmictec.2023.110211>

216. Torres, R. J., and Puig, J. G. (2007). Hypoxanthine-guanine phosphoribosyltransferase (HPRT) deficiency: Lesch-Nyhan syndrome. *Orphanet Journal of Rare Diseases*, 2(1), 48. <https://doi.org/10.1186/1750-1172-2-48>
217. Tzeng, C.-M., and Kornberg, A. (2000). The multiple activities of polyphosphate kinase of *Escherichia coli* and their subunit structure determined by radiation target analysis. *Journal of Biological Chemistry*, 275(6), 3977–3983. <https://doi.org/10.1074/jbc.275.6.3977>
218. Urbelienė, N., Tiškus, M., Tamulaitienė, G., Gasparavičiūtė, R., Lapinskaitė, R., Jauniškis, V., Sūdžius, J., Meškienė, R., Tauraitė, D., Skrodenytė, E., Urbelis, G., Vaitekūnas, J., and Meškys, R. (2023). Cytidine deaminases catalyze the conversion of N(S,O)<sup>4</sup>-substituted pyrimidine nucleosides. *Science Advances*, 9(5). <https://doi.org/10.1126/sciadv.ade4361>
219. van de Vossenberg, J., Driessen, A., da Costa, M., and Konings, W. (1999). Homeostasis of the membrane proton permeability in *Bacillus subtilis* grown at different temperatures. *Biochimica et Biophysica Acta (BBA) - Biomembranes*, 1419(1), 97–104. [https://doi.org/10.1016/S0005-2736\(99\)00063-2](https://doi.org/10.1016/S0005-2736(99)00063-2)
220. Van Rompay, A. R., Johansson, M., and Karlsson, A. (2000). Phosphorylation of nucleosides and nucleoside analogs by mammalian nucleoside monophosphate kinases. *Pharmacology & Therapeutics*, 87(2–3), 189–198. [https://doi.org/10.1016/S0163-7258\(00\)00048-6](https://doi.org/10.1016/S0163-7258(00)00048-6)
221. Van Rompay, A. R., Johansson, M., and Karlsson, A. (2003). Substrate specificity and phosphorylation of antiviral and anticancer nucleoside analogues by human deoxyribonucleoside kinases and ribonucleoside kinases. *Pharmacology & Therapeutics*, 100(2), 119–139. <https://doi.org/10.1016/j.pharmthera.2003.07.001>
222. Van Rompay, A. R., Norda, A., Lindén, K., Johansson, M., and Karlsson, A. (2001). Phosphorylation of uridine and cytidine nucleoside analogs by two human uridine-cytidine kinases. *Molecular Pharmacology*, 59(5), 1181–1186. <https://doi.org/10.1124/mol.59.5.1181>
223. Veech, R. L., Todd King, M., Pawlosky, R., Kashiwaya, Y., Bradshaw, P. C., and Curtis, W. (2019). The “great” controlling nucleotide coenzymes. *IUBMB Life*, 71(5), 565–579. <https://doi.org/10.1002/iub.1997>
224. Vernis, L. (2003). Reconstitution of an efficient thymidine salvage pathway in *Saccharomyces cerevisiae*. *Nucleic Acids Research*, 31(19), 120e–1120. <https://doi.org/10.1093/nar/gng121>



225. Villela, D., Sanchez-Quitian, A., Ducati, G., Santos, S., and Basso, A. (2011). Pyrimidine salvage pathway in *Mycobacterium tuberculosis*. *Current Medicinal Chemistry*, 18(9), 1286–1298. <https://doi.org/10.2174/092986711795029555>
226. Viswanadham, B., Mahomed, A., Friedrich, H., and Singh, S. (2017). Efficient and expeditious chemoselective BOC protection of amines in catalyst and solvent-free media. *Research on Chemical Intermediates*, 43(3), 1355–1363. <https://doi.org/10.1007/s11164-016-2702-9>
227. Walko, C. M., and Lindley, C. (2005). Capecitabine: A review. *Clinical Therapeutics*, 27(1), 23–44. <https://doi.org/10.1016/j.clinthera.2005.01.005>
228. Wang, D., Zhang, Y., and Kleiner, R. E. (2020). Cell- and polymerase-selective metabolic labeling of cellular RNA with 2'-azidocytidine. *Journal of the American Chemical Society*, 142(34), 14417–14421. <https://doi.org/10.1021/jacs.0c04566>
229. Wang, J., Liang, Y.-L., and Qu, J. (2009). Boiling water-catalyzed neutral and selective N-Boc deprotection. *Chemical Communications*, 34, 5144. <https://doi.org/10.1039/b910239f>
230. Wang, L., Karlsson, A., Arnér, E. S., and Eriksson, S. (1993). Substrate specificity of mitochondrial 2'-deoxyguanosine kinase. Efficient phosphorylation of 2-chlorodeoxyadenosine. *The Journal of Biological Chemistry*, 268(30), 22847–22852.
231. Wang, L., Munch-Petersen, B., Herrström Sjöberg, A., Hellman, U., Bergman, T., Jörnvall, H., and Eriksson, S. (1999). Human thymidine kinase 2: molecular cloning and characterisation of the enzyme activity with antiviral and cytostatic nucleoside substrates. *FEBS Letters*, 443(2), 170–174. [https://doi.org/10.1016/S0014-5793\(98\)01711-6](https://doi.org/10.1016/S0014-5793(98)01711-6)
232. Wang, Y., Canine, B. F., and Hatefi, A. (2011). HSV-TK/GCV cancer suicide gene therapy by a designed recombinant multifunctional vector. *Nanomedicine: Nanotechnology, Biology and Medicine*, 7(2), 193–200. <https://doi.org/10.1016/j.nano.2010.08.003>
233. Weigele, P., and Raleigh, E. A. (2016). Biosynthesis and function of modified bases in bacteria and their viruses. *Chemical Reviews*, 116(20), 12655–12687. <https://doi.org/10.1021/acs.chemrev.6b00114>
234. Welin, M., Kosinska, U., Mikkelsen, N.-E., Carnrot, C., Zhu, C., Wang, L., Eriksson, S., Munch-Petersen, B., and Eklund, H. (2004). Structures of thymidine kinase 1 of human and mycoplasmic origin. *Proceedings of the National Academy of Sciences*, 101(52), 17970–17975. <https://doi.org/10.1073/pnas.0406332102>

235. Welin, M., Skovgaard, T., Knecht, W., Zhu, C., Berenstein, D., Munch-Petersen, B., Piškur, J., and Eklund, H. (2005). Structural basis for the changed substrate specificity of *Drosophila melanogaster* deoxyribonucleoside kinase mutant N64D. *The FEBS Journal*, 272(14), 3733–3742. <https://doi.org/10.1111/j.1742-4658.2005.04803.x>
236. Wilkinson, E., Cui, Y.-H., and He, Y.-Y. (2022). Roles of RNA modifications in diverse cellular functions. *Frontiers in Cell and Developmental Biology*, 10. <https://doi.org/10.3389/fcell.2022.828683>
237. Wu, Y., Fa, M., Tae, E. L., Schultz, P. G., and Romesberg, F. E. (2002). Enzymatic phosphorylation of unnatural nucleosides. *Journal of the American Chemical Society*, 124(49), 14626–14630. <https://doi.org/10.1021/ja028050m>
238. Xu, W., Chan, K. M., and Kool, E. T. (2017). Fluorescent nucleobases as tools for studying DNA and RNA. *Nature Chemistry*, 9(11), 1043–1055. <https://doi.org/10.1038/nchem.2859>
239. Yamada, Y., Goto, H., and Ogasawara, N. (1981). Adenosine kinase from human liver. *Biochimica et Biophysica Acta (BBA) - Enzymology*, 660(1), 36–43. [https://doi.org/10.1016/0005-2744\(81\)90105-4](https://doi.org/10.1016/0005-2744(81)90105-4)
240. Yoshikawa, M., Kato, T., and Takenishi, T. (1967). A novel method for phosphorylation of nucleosides to 5'-nucleotides. *Tetrahedron Letters*, 8(50), 5065–5068. [https://doi.org/10.1016/S0040-4039\(01\)89915-9](https://doi.org/10.1016/S0040-4039(01)89915-9)
241. Yu, L., Xu, L., Xu, M., Wan, B., Yu, L., and Huang, Q. (2011). Role of Mg<sup>2+</sup> ions in protein kinase phosphorylation: insights from molecular dynamics simulations of ATP-kinase complexes. *Molecular Simulation*, 37(14), 1143–1150. <https://doi.org/10.1080/08927022.2011.561430>
242. Zalkin, H., and Dixon, J. E. (1992). *De novo purine nucleotide biosynthesis* (pp. 259–287). [https://doi.org/10.1016/S0079-6603\(08\)60578-4](https://doi.org/10.1016/S0079-6603(08)60578-4)
243. Zenchenko, A. A., Drenichev, M. S., Il'icheva, I. A., and Mikhailov, S. N. (2021). Antiviral and antimicrobial nucleoside derivatives: structural features and mechanisms of action. *Molecular Biology*, 55(6), 786–812. <https://doi.org/10.1134/S0026893321040105>
244. Zhang, D., Bender, D. M., Victor, F., Peterson, J. A., Boyer, R. D., Stephenson, G. A., Azman, A., and McCarthy, J. R. (2008). Facile rearrangement of N4-( $\alpha$ -aminoacyl)cytidines to N-(4-cytidinyl)amino acid amides. *Tetrahedron Letters*, 49(13), 2052–2055. <https://doi.org/10.1016/j.tetlet.2008.02.015>

245. Zhang, J., Wu, B., Zhang, Y., Kowal, P., and Wang, P. G. (2003). Creatine phosphate–creatine kinase in enzymatic synthesis of glycoconjugates. *Organic Letters*, 5(15), 2583–2586. <https://doi.org/10.1021/ol034319a>
246. Zhulai, G., Oleinik, E., Shibaev, M., and Ignatev, K. (2022). Adenosine-metabolizing enzymes, adenosine kinase and adenosine deaminase, in cancer. *Biomolecules*, 12(3), 418. <https://doi.org/10.3390/biom12030418>
247. Zou, Z., Ding, Q., Ou, L., and Yan, B. (2013). Efficient production of deoxynucleoside-5'-monophosphates using deoxynucleoside kinase coupled with a GTP-regeneration system. *Applied Microbiology and Biotechnology*, 97(21), 9389–9395. <https://doi.org/10.1007/s00253-013-5173-6>

## APPENDICES

### Appendix 1. Synthesized *N*<sup>4</sup> amino acid-acylated nucleosides.

#### ***tert*-Butyl ((*S*)-1-((1-((2*R*,4*S*,5*R*)-4-hydroxy-5-(hydroxymethyl)tetrahydrofuran-2-yl)-2-oxo-1,2-dihydropyrimidin-4-yl)amino)-1-oxopropan-2-yl)carbamate**

Yield 1.32 g (50%), white solid, mp 110–113 °C.

$R_f = 0.61$  ( $\text{CHCl}_3:\text{CH}_3\text{OH} - 5:1$ ).

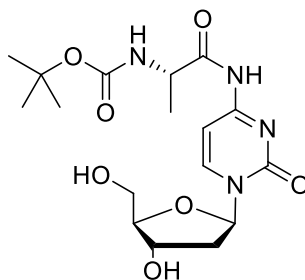
MS (ESI<sup>+</sup>):  $m/z$  399.15  $[\text{M}+\text{H}]^+$ , 397.15  $[\text{M}-\text{H}]^-$ .

UV( $\text{CH}_3\text{OH}$ )  $\lambda_{\text{max}}=246; 299$  nm.

$\epsilon_{246}=15842 \text{ M}^{-1}\text{cm}^{-1}$ ,  $\epsilon_{299}=8515 \text{ M}^{-1}\text{cm}^{-1}$ .

<sup>1</sup>H NMR (DMSO-*d*<sub>6</sub>, 400 MHz):  $\delta = 1.22$  (d,  $J = 7.2$  Hz, 3H, CH<sub>3</sub>), 1.38 (s, 9H, 3CH<sub>3</sub>), 2.02 (dt,  $J = 13.0, 6.2$  Hz, 1H, CH<sub>2</sub>), 2.25–2.34 (m, 1H, CH<sub>2</sub>), 3.54–3.67 (m, 2H, CH<sub>2</sub>), 3.87 (q,  $J = 3.7$  Hz, 1H, CH), 4.13–4.20 (m, 1H, CH), 4.19–4.25 (m, 1H, CH), 5.06 (t,  $J = 5.2$  Hz, 1H, OH), 5.28 (d,  $J = 4.3$  Hz, 1H, OH), 6.11 (t,  $J = 6.2$  Hz, 1H, CH), 7.20 (d,  $J = 7.3$  Hz, 2H, CH=CH and NH), 8.35 (d,  $J = 7.5$  Hz, 1H, CH=CH), 10.86 (s, 1H, NH).

<sup>13</sup>C NMR (DMSO-*d*<sub>6</sub>, 101 MHz):  $\delta = 17.74, 28.65, 41.38, 51.06, 61.38, 70.34, 79.64, 86.70, 88.41, 95.66, 145.65, 154.85, 155.69, 162.76, 175.00$ .



#### ***tert*-Butyl (2-((1-((2*R*,4*S*,5*R*)-4-hydroxy-5-(hydroxymethyl)tetrahydrofuran-2-yl)-2-oxo-1,2-dihydropyrimidin-4-yl)amino)-2-oxoethyl)carbamate**

Yield 1.36 g (53%), white solid, mp 110–112 °C.

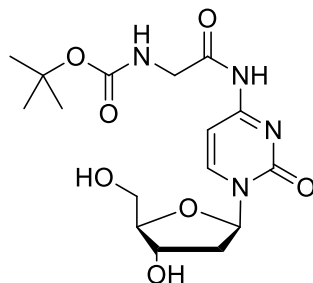
$R_f = 0.60$  ( $\text{CHCl}_3:\text{CH}_3\text{OH} - 5:1$ ).

MS (ESI<sup>+</sup>):  $m/z$  385.10  $[\text{M}+\text{H}]^+$ , 383.10  $[\text{M}-\text{H}]^-$ .

UV ( $\text{CH}_3\text{OH}$ )  $\lambda_{\text{max}}=246; 299$  nm.

$\epsilon_{246}=15600 \text{ M}^{-1}\text{cm}^{-1}$ ,  $\epsilon_{299}=7800 \text{ M}^{-1}\text{cm}^{-1}$ .

<sup>1</sup>H NMR (DMSO-*d*<sub>6</sub>, 400 MHz):  $\delta = 1.39$  (s, 9H, 3CH<sub>3</sub>), 2.03 (dt,  $J = 13.0, 6.3$  Hz, 1H, CH<sub>2</sub>), 2.30 (ddd,  $J = 13.3, 6.1, 3.8$  Hz, 1H, CH<sub>2</sub>), 3.53–3.70 (m, 2H, CH<sub>2</sub>), 3.79 (d,  $J = 6.1$  Hz, 2H, CH<sub>2</sub>), 3.87 (q,  $J = 3.7$  Hz, 1H, CH), 4.23 (dq,  $J = 7.6, 4.0$  Hz, 1H, CH), 5.06 (t,  $J = 5.2$  Hz, 1H, OH), 5.28 (d,  $J = 4.3$  Hz, 1H, OH), 6.11 (t,  $J = 6.3$  Hz, 1H, CH), 7.09 (t,  $J = 6.1$  Hz, 1H, NH),



7.17 (d,  $J = 7.5$  Hz, 1H, CH=CH), 8.35 (d,  $J = 7.5$  Hz, 1H, CH=CH), 10.87 (s, 1H, NH).

$^{13}\text{C}$  NMR (DMSO- $d_6$ , 101 MHz):  $\delta = 25.70, 28.63, 41.37, 44.60, 61.41, 70.39, 78.67, 79.64, 86.67, 88.39, 95.66, 145.62, 154.86, 156.35$ .

***tert*-Butyl (3-((1-((2R,4S,5R)-4-hydroxy-5-(hydroxymethyl)tetrahydrofuran-2-yl)-2-oxo-1,2-dihydropyrimidin-4-yl)amino)-3-oxopropyl)carbamate**

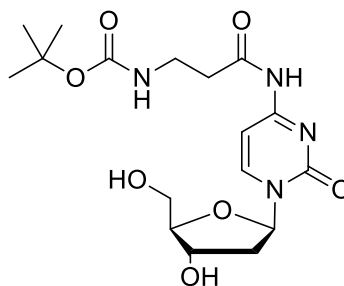
Yield 1.55 g (59%), white solid, mp 108–111 °C.  $R_f = 0.59$  (CHCl<sub>3</sub>:CH<sub>3</sub>OH – 5:1).

MS (ESI<sup>+</sup>):  $m/z$  399.10 [M+H]<sup>+</sup>; 397.10 [M-H]<sup>-</sup>. UV(CH<sub>3</sub>OH)  $\lambda_{\text{max}} = 247; 298$  nm.  $\epsilon_{247} = 15300 \text{ M}^{-1}\text{cm}^{-1}$ ,  $\epsilon_{298} = 7905 \text{ M}^{-1}\text{cm}^{-1}$ .

$^1\text{H}$  NMR (DMSO- $d_6$ , 400 MHz):  $\delta = 1.36$  (s, 9H, CH<sub>3</sub>), 1.93–2.07 (m, 1H, CH<sub>2</sub>), 2.29

(ddd,  $J = 13.2, 6.0, 3.9$  Hz, 1H, CH<sub>2</sub>), 2.54 (t,  $J = 7.6$  Hz, 2H, CH<sub>2</sub>), 3.19 (dd,  $J = 11.6, 5.8$  Hz, 2H, CH<sub>2</sub>), 3.47–3.66 (m, 2H, CH<sub>2</sub>), 3.86 (dd,  $J = 7.1, 3.5$  Hz, 1H, CH), 4.17–4.29 (m, 1H, CH), 5.04 (t,  $J = 4.9$  Hz, 1H, OH), 5.26 (d,  $J = 4.0$  Hz, 1H, OH), 6.11 (t, 1H,  $J = 6.3$  Hz, CH), 6.83 (bs, 1H, NH), 7.20 (d, 1H,  $J = 7.4$  Hz, CH=CH), 8.33 (d, 1H,  $J = 7.5$  Hz, CH=CH), 10.84 (s, 1H, NH).

$^{13}\text{C}$  NMR (DMSO- $d_6$ , 101 MHz):  $\delta = 25.69, 28.68, 36.38, 37.40, 61.40, 70.39, 78.10, 86.59, 88.36, 95.83, 145.38, 154.91, 155.94, 162.67, 172.64$ .



***tert*-Butyl ((*S*)-1-((1-((2*R*,4*S*,5*R*)-4-hydroxy-5-(hydroxymethyl)tetrahydrofuran-2-yl)-2-oxo-1,2-dihydropyrimidin-4-yl)amino)-4-methyl-1-oxopentan-2-yl)carbamate**

Yield 1.91 g (65%), white solid, mp 113–115 °C.

$R_f = 0.68$  (CHCl<sub>3</sub>:CH<sub>3</sub>OH – 5:1).

MS (ESI<sup>+</sup>):  $m/z$  441.20 [M+H]<sup>+</sup>; 439.20 [M-H]<sup>-</sup>.

UV (CH<sub>3</sub>OH)  $\lambda_{max} = 246$ ; 299 nm

$\epsilon_{246} = 13700 \text{ M}^{-1}\text{cm}^{-1}$ ,  $\epsilon_{299} = 6900 \text{ M}^{-1}\text{cm}^{-1}$ .

<sup>1</sup>H NMR (DMSO-*d*<sub>6</sub>, 400 MHz):  $\delta = 0.84$ –0.90

(m, 6H, 2CH<sub>3</sub>), 1.28–1.33 (m, 1H, CH), 1.38 (s,

9H, 3CH<sub>3</sub>), 1.42–1.56 (m, 2H, CH<sub>2</sub>), 1.58–1.73

(m, 1H, CH), 1.98–2.07 (m, 1H, CH<sub>2</sub>), 2.25–2.34

(m, 1H, CH<sub>2</sub>), 3.49–3.69 (m, 2H, CH<sub>2</sub>), 3.86 (q,

$J = 3.5$  Hz, 1H, CH), 4.15–4.27 (m, 1H, CH), 5.05 (t,  $J = 5.0$  Hz, 1H, OH),

5.27 (d,  $J = 4.1$  Hz, 1H, OH), 6.11 (t,  $J = 6.2$  Hz, 1H, CH), 7.13 (d,  $J = 7.7$

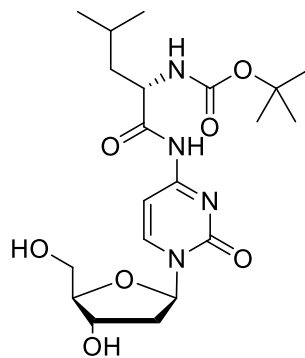
Hz, 1H, NH), 7.19 (d,  $J = 7.4$  Hz, 1H, CH=CH), 8.34 (d,  $J = 7.4$  Hz, 1H,

CH=CH), 10.91 (s, 1H, NH).

<sup>13</sup>C NMR (DMSO-*d*<sub>6</sub>, 101 MHz):  $\delta = 21.63$ , 23.53, 24.84, 25.69, 28.64, 54.26,

61.37, 70.34, 78.66, 79.64, 86.69, 88.40, 95.68, 145.64, 154.84, 155.40,

173.23.



***tert*-Butyl ((2*S*,3*S*)-1-((1-((2*R*,4*S*,5*R*)-4-hydroxy-5-(hydroxymethyl)tetrahydrofuran-2-yl)-2-oxo-1,2-dihydropyrimidin-4-yl)amino)-3-methyl-1-oxopentan-2-yl)carbamate**

Yield 1.17 g (40%), white solid, mp 112–114 °C.

$R_f = 0.68$  (CHCl<sub>3</sub>:CH<sub>3</sub>OH – 5:1).

MS (ESI<sup>+</sup>):  $m/z$  441.20 [M+H]<sup>+</sup>; 439.20 [M-H]<sup>-</sup>.

UV (CH<sub>3</sub>OH)  $\lambda_{max} = 247$ ; 299 nm.

$\epsilon_{247} = 14300 \text{ M}^{-1}\text{cm}^{-1}$ ,  $\epsilon_{299} = 7780 \text{ M}^{-1}\text{cm}^{-1}$ .

<sup>1</sup>H NMR (DMSO-*d*<sub>6</sub>, 400 MHz):  $\delta = 0.76$ –0.91

(m, 6H, 2CH<sub>3</sub>), 1.09–1.22 (m, 1H, CH), 1.38 (s,

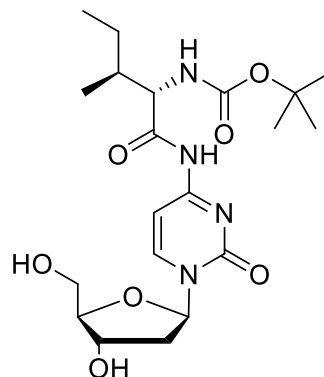
9H, 3CH<sub>3</sub>), 1.67–1.79 (m, 2H, CH<sub>2</sub>), 2.03 (dt,  $J =$

12.9, 6.2 Hz, 1H, CH<sub>2</sub>), 2.24–2.35 (m, 1H,

CH<sub>2</sub>), 3.51–3.69 (m, 2H, CH<sub>2</sub>), 3.87 (q,  $J = 3.6$

Hz, 1H, CH), 4.06 (t,  $J = 7.9$  Hz, 1H, CH), 4.17–

4.31 (m, 1H, CH), 5.07 (t,  $J = 5.2$  Hz, 1H, OH), 5.28 (d,  $J = 4.2$  Hz, 1H, OH),



6.11 (t,  $J = 6.2$  Hz, 1H, CH), 7.05 (d,  $J = 8.2$  Hz, 1H, NH), 7.23 (d,  $J = 7.4$  Hz, 1H, CH=CH), 8.36 (d,  $J = 7.5$  Hz, 1H, CH=CH), 10.86 (s, 1H, NH).

$^{13}\text{C}$  NMR (DMSO- $d_6$ , 101 MHz):  $\delta = 11.32, 15.72, 24.86, 28.63, 36.47, 41.35, 60.12, 61.38, 70.34, 78.70, 86.72, 88.40, 95.68, 145.74, 154.88, 156.00, 162.53, 173.23$ .

***tert*-Butyl ((S)-1-((1-((2R,4S,5R)-4-hydroxy-5-(hydroxymethyl)tetrahydrofuran-2-yl)-2-oxo-1,2-dihydropyrimidin-4-yl)amino)-4-(methylthio)-1-oxobutan-2-yl)carbamate**

Yield 1.03 g (34%), white solid, mp 104–106 °C.

$R_f = 0.60$  (CHCl<sub>3</sub>:CH<sub>3</sub>OH – 5:1).

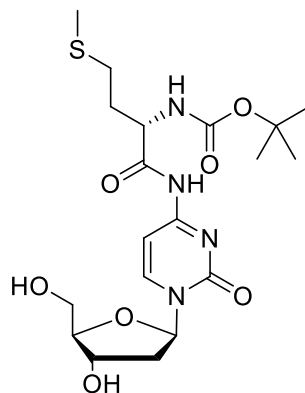
MS (ESI<sup>+</sup>):  $m/z$  459.15 [M+H]<sup>+</sup>, 457.15 [M-H]<sup>-</sup>.

UV (CH<sub>3</sub>OH)  $\lambda_{\text{max}} = 246; 299$  nm.

$\epsilon_{246} = 15100 \text{ M}^{-1}\text{cm}^{-1}$ ,  $\epsilon_{299} = 8100 \text{ M}^{-1}\text{cm}^{-1}$ .

$^1\text{H}$  NMR (DMSO- $d_6$ , 400 MHz):  $\delta = 1.38$  (s, 9H, 3CH<sub>3</sub>), 1.73–1.98 (m, 1H, CH<sub>2</sub>), 1.98–2.05 (m, 1H, CH), 2.05 (s, 3H, CH<sub>3</sub>), 2.26–2.35 (m, 1H, CH<sub>2</sub>), 2.39–2.51 (m, 4H, 2CH<sub>2</sub>), 3.53–3.69 (m, 2H, CH<sub>2</sub>), 3.87 (q,  $J = 3.8$  Hz, 1H, CH), 4.22 (dd,  $J = 8.7, 5.1$  Hz, 1H, CH), 5.06 (t,  $J = 5.2$  Hz, 1H, OH), 5.28 (d,  $J = 4.3$  Hz, 1H, OH), 6.11 (t,  $J = 6.2$  Hz, 1H, CH), 7.20 (d,  $J = 7.4$  Hz, 1H, CH=CH), 7.25 (d,  $J = 7.7$  Hz, 1H, NH), 8.36 (d,  $J = 7.4$  Hz, 1H, CH=CH), 10.92 (s, 1H, NH).

$^{13}\text{C}$  NMR (DMSO- $d_6$ , 101 MHz):  $\delta = 15.02, 25.70, 28.63, 30.25, 55.27, 61.38, 70.34, 78.84, 86.72, 88.41, 95.71, 145.69, 154.85, 156.03, 162.70, 173.23, 173.92$ .



***tert*-Butyl ((S)-1-((1-((2R,4S,5R)-4-hydroxy-5-(hydroxymethyl)tetrahydrofuran-2-yl)-2-oxo-1,2-dihydropyrimidin-4-yl)amino)-1-oxo-3-phenylpropan-2-yl)carbamate**

Yield 2.66 g (85%), white solid, mp 119–122 °C.

R<sub>f</sub> = 0.65 (CHCl<sub>3</sub>:CH<sub>3</sub>OH – 5:1).

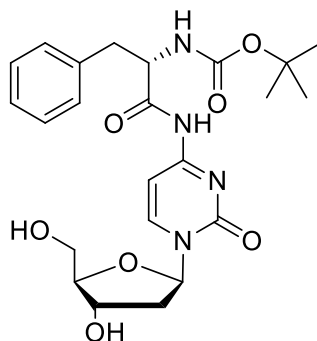
MS (ESI<sup>+</sup>): *m/z* 475.20 [M+H]<sup>+</sup>; 473.20 [M-H]<sup>-</sup>.

UV (CH<sub>3</sub>OH) λ<sub>max</sub>=247; 300 nm.

ε<sub>247</sub>=13658 M<sup>-1</sup>cm<sup>-1</sup>, ε<sub>300</sub>=7617 M<sup>-1</sup>cm<sup>-1</sup>.

<sup>1</sup>H NMR (DMSO-d<sub>6</sub>, 400 MHz): δ = 1.31 (s, 9H, 3CH<sub>3</sub>), 2.03 (dt, *J* = 12.9, 6.2 Hz, 1H, CH<sub>2</sub>), 2.31 (ddd, *J* = 13.2, 5.9, 4.0 Hz, 1H, CH<sub>2</sub>), 2.67–2.84 (m, 1H, CH<sub>2</sub>), 3.00 (dd, *J* = 13.5, 3.5 Hz, 1H, CH<sub>2</sub>), 3.61 (dt, *J* = 11.8, 4.6 Hz, 2H, CH<sub>2</sub>), 3.88 (q, *J* = 3.6 Hz, 1H, CH), 4.23 (dq, *J* = 7.9, 3.9 Hz, 1H, CH), 4.32–4.48 (m, 1H, CH), 5.07 (t, *J* = 5.2 Hz, 1H, OH), 5.29 (d, *J* = 4.2 Hz, 1H, OH), 6.12 (t, *J* = 6.2 Hz, 1H, CH), 7.21 (t, *J* = 7.6 Hz, 3H, 3CH), 7.25–7.35 (m, 2H, CH=CH and NH), 7.39 (d, *J* = 7.2 Hz, 2H, 2CH), 8.37 (d, *J* = 7.5 Hz, 1H, CH=CH), 11.17 (s, 1H, NH).

<sup>13</sup>C NMR (DMSO-d<sub>6</sub>, 101 MHz): δ = 28.58, 36.99, 41.39, 57.38, 61.39, 70.36, 79.64, 86.74, 88.42, 95.74, 126.84, 128.49, 129.83, 138.13, 145.72, 154.86, 155.98, 162.75, 173.23.



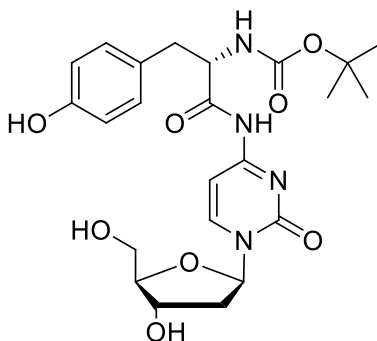
***tert*-Butyl ((S)-1-((1-((2R,4S,5R)-4-hydroxy-5-(hydroxymethyl)tetrahydrofuran-2-yl)-2-oxo-1,2-dihydropyrimidin-4-yl)amino)-3-(4-hydroxyphenyl)-1-oxopropan-2-yl)carbamate**

Yield 1.72 g (53%), white solid, mp 137–140 °C. R<sub>f</sub> = 0.50 (CHCl<sub>3</sub>:CH<sub>3</sub>OH – 5:1).

MS (ESI<sup>+</sup>): *m/z* 491.20 [M+H]<sup>+</sup>, 489.20 [M-H]<sup>-</sup>. UV (CH<sub>3</sub>OH) λ<sub>max</sub>=248; 300 nm.

ε<sub>248</sub>=19300 M<sup>-1</sup>cm<sup>-1</sup>, ε<sub>300</sub>=9700 M<sup>-1</sup>cm<sup>-1</sup>.

<sup>1</sup>H NMR (DMSO-d<sub>6</sub>, 400 MHz): δ = 1.32 (s, 9H, 3CH<sub>3</sub>), 2.03 (dt, *J* = 12.9, 6.0 Hz, 1H, CH<sub>2</sub>), 2.24–2.36 (m, 1H, CH<sub>2</sub>), 2.57–2.68 (m, 1H, CH<sub>2</sub>), 2.87 (dd, *J* = 13.8, 4.2 Hz, 1H, CH<sub>2</sub>), 3.53–3.67 (m, 2H, CH<sub>2</sub>), 3.87 (q, *J* = 3.9 Hz, 1H, CH), 4.22 (dt, *J* = 8.2, 4.0 Hz, 1H, CH), 4.26–





4.39 (m, 1H, CH), 5.06 (t,  $J = 5.3$  Hz, 1H, OH), 5.28 (d,  $J = 4.3$  Hz, 1H, OH), 6.12 (t,  $J = 6.3$  Hz, 1H, CH), 6.65 (d,  $J = 8.4$  Hz, 2H, 2CH), 6.99–7.26 (m, 4H, 2CH, OH and CH=CH), 8.36 (d,  $J = 7.5$  Hz, 1H, CH=CH), 9.2 (s, 1H, NH), 11.09 (s, 1H, NH).

$^{13}\text{C}$  NMR (DMSO- $d_6$ , 101 MHz):  $\delta = 24.81, 28.60, 36.28, 41.37, 57.69, 61.40, 70.37, 78.72, 86.73, 88.41, 95.74, 115.28, 128.06, 130.74, 145.68, 154.87, 156.33, 162.74, 174.25$ .

**Appendix 2.** Synthesized *N*-4-(2'-deoxycytidinyl)amino acid amides.

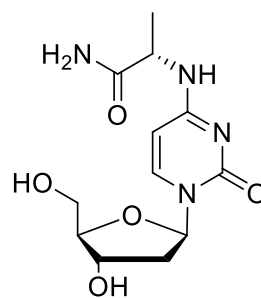
**(S)-2-((1-((2R,4S,5R)-4-Hydroxy-5-(hydroxymethyl)tetrahydrofuran-2-yl)-2-oxo-1,2-dihydropyrimidin-4-yl)amino)propanamide**

Yield 0.11 g (37%), white solid, mp 155–158 °C.  $R_f = 0.72$  (1,4-dioxane:isopropanol:H<sub>2</sub>O:NH<sub>4</sub>OH – 4:2:2:1).

MS (ESI<sup>+</sup>):  $m/z$  299.10 [M+H]<sup>+</sup>, 297.10 [M-H]<sup>-</sup>. UV (CH<sub>3</sub>OH)  $\lambda_{\text{max}}=273$  nm.  $\epsilon_{273}=12895$  M<sup>-1</sup>cm<sup>-1</sup>.

$^1\text{H}$  NMR (DMSO- $d_6$ , 400 MHz):  $\delta = 1.26$  (d,  $J = 7.1$  Hz, 3H, CH<sub>3</sub>), 1.93 (dt,  $J = 13.2, 6.3$  Hz, 1H, CH<sub>2</sub>), 2.07–2.13 (m, 1H, CH<sub>2</sub>), 3.55 (q,  $J = 5.3$  Hz, 2H, CH<sub>2</sub>), 3.76 (q, 1H,  $J = 3.6$  Hz, CH), 4.20 (dd,  $J = 5.6, 3.1$  Hz, 1H, CH), 4.48 (p,  $J = 7.1$  Hz, 1H, CH), 4.99 (t,  $J = 5.2$  Hz, 1H, OH), 5.21 (d,  $J = 4.1$  Hz, 1H, OH), 5.90 (d,  $J = 7.5$  Hz, 1H, CH=CH), 6.15 (t,  $J = 6.7$  Hz, 1H, CH), 7.02 (s, 1H, NH<sub>2</sub>), 7.48 (s, 1H, NH<sub>2</sub>), 7.74–7.81 (m, 2H, CH=CH and NH).

$^{13}\text{C}$  NMR (DMSO- $d_6$ , 101 MHz):  $\delta = 18.96, 40.81, 49.07, 61.83, 70.86, 85.33, 87.65, 95.29, 140.37, 155.40, 163.22, 174.62$ .

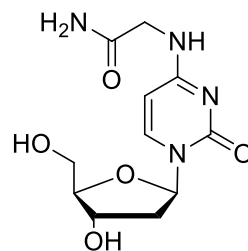


**2-((1-((2R,4S,5R)-4-Hydroxy-5-(hydroxymethyl)tetrahydrofuran-2-yl)-2-oxo-1,2-dihydropyrimidin-4-yl)amino)acetamide**

Yield 0.18 g (48%), white solid, mp 150–153 °C.  $R_f = 0.70$  (1,4-dioxane:isopropanol:H<sub>2</sub>O:NH<sub>4</sub>OH – 4:2:2:1).

MS (ESI<sup>+</sup>):  $m/z$  285.05 [M+H]<sup>+</sup>, 283.05 [M-H]<sup>-</sup>. UV (CH<sub>3</sub>OH)  $\lambda_{\text{max}}=273$  nm.  $\epsilon_{273}=11100$  M<sup>-1</sup>cm<sup>-1</sup>.

$^1\text{H}$  NMR (DMSO- $d_6$ , 400 MHz):  $\delta = 1.89$ – $1.97$  (m, 1H, CH<sub>2</sub>), 2.10 (ddd,  $J = 13.1, 5.9, 3.2$  Hz, 1H, CH<sub>2</sub>), 3.17 (d,  $J = 5.2$  Hz, 2H, CH<sub>2</sub>), 3.49–3.60 (m, 2H, CH<sub>2</sub>), 3.77 (dd,  $J = 6.9, 3.7$  Hz, 1H, CH), 3.85 (dd,  $J = 5.6, 1.5$  Hz, 1H, CH), 4.98



(t,  $J = 5.2$  Hz, 1H, OH), 5.20 (d,  $J = 4.1$  Hz, 1H, OH), 5.90 (d,  $J = 7.5$  Hz, 1H, CH=CH), 6.16 (t,  $J = 6.7$  Hz, 1H, CH), 7.07 (s, 1H, NH<sub>2</sub>), 7.43 (s, 1H, NH<sub>2</sub>), 7.78 (d,  $J = 7.5$  Hz, 1H, CH=CH), 7.83 (t,  $J = 5.6$  Hz, 1H, NH).

<sup>13</sup>C NMR (DMSO-d<sub>6</sub>, 101 MHz):  $\delta = 43.20, 49.06, 61.83, 70.87, 85.34, 87.66, 95.24, 140.42, 155.49, 163.90, 171.12$ .

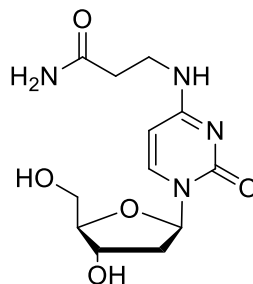
**3-((1-((2R,4S,5R)-4-Hydroxy-5-(hydroxymethyl)tetrahydrofuran-2-yl)-2-oxo-1,2-dihydropyrimidin-4-yl)amino)propanamide**

Yield 0.17 mg (57%), white solid, mp 145–149 °C.  $R_f = 0.71$  (1,4-dioxane:isopropanol:H<sub>2</sub>O:NH<sub>4</sub>OH – 4:2:2:1).

MS (ESI<sup>+</sup>):  $m/z$  299.10 [M+H]<sup>+</sup>, 297.10 [M-H]<sup>-</sup>. UV (CH<sub>3</sub>OH)  $\lambda_{max} = 275$  nm.  $\epsilon_{275} = 11600$  M<sup>-1</sup>cm<sup>-1</sup>.

<sup>1</sup>H NMR (DMSO-d<sub>6</sub>, 400 MHz):  $\delta = 1.87$ – $1.97$  (m, 1H, CH<sub>2</sub>), 2.09 (ddd,  $J = 13.0, 5.9, 3.2$  Hz, 1H, CH<sub>2</sub>), 2.31 (t,  $J = 6.7$  Hz, 2H, CH<sub>2</sub>), 3.42 (dd,  $J = 12.7, 6.6$  Hz, 2H, CH<sub>2</sub>), 3.48– $3.59$  (m, 2H, CH<sub>2</sub>), 3.76 (dd,  $J = 6.9, 3.8$  Hz, 1H, CH), 4.19 (dd,  $J = 5.6, 3.0$  Hz, 1H, CH), 4.98 (t,  $J = 5.1$  Hz, 1H, OH), 5.21 (d,  $J = 4.0$  Hz, 1H, OH), 5.77 (d,  $J = 7.5$  Hz, 1H, CH=CH), 6.12– $6.20$  (m, 1H, CH), 6.86 (s, 1H, NH<sub>2</sub>), 7.38 (s, 1H, NH<sub>2</sub>), 7.66– $7.85$  (m, 2H, CH=CH and NH).

<sup>13</sup>C NMR (DMSO-d<sub>6</sub>, 101 MHz):  $\delta = 34.84, 36.64, 49.06, 61.85, 70.89, 85.28, 87.61, 95.18, 140.20, 155.52, 163.74, 173.00$ .

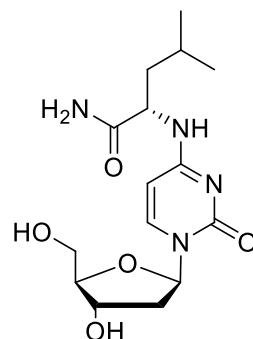


**(S)-2-((1-((2R,4S,5R)-4-Hydroxy-5-(hydroxymethyl)tetrahydrofuran-2-yl)-2-oxo-1,2-dihydropyrimidin-4-yl)amino)-4-methylpentanamide**

Yield 0.1 g (29%), white solid, mp 157–160 °C.  $R_f = 0.79$  (1,4-dioxane:isopropanol:H<sub>2</sub>O:NH<sub>4</sub>OH – 4:2:2:1).

MS (ESI<sup>+</sup>):  $m/z$  341.10 [M+H]<sup>+</sup>, 339.10 [M-H]<sup>-</sup>. UV (CH<sub>3</sub>OH)  $\lambda_{max} = 273$  nm.  $\epsilon_{273} = 10300$  M<sup>-1</sup>cm<sup>-1</sup>.

<sup>1</sup>H NMR (DMSO-d<sub>6</sub>, 400 MHz):  $\delta = 0.88$  (dd,  $J = 15.3, 6.5$  Hz, 6H, 2CH<sub>3</sub>), 1.44– $1.55$  (m, 2H, CH<sub>2</sub>), 1.55– $1.70$  (m, 1H, CH), 1.93 (dq,  $J = 13.2, 6.3$  Hz, 1H, CH<sub>2</sub>), 2.10 (ddd,  $J = 13.0, 5.9, 3.3$  Hz, 1H, CH<sub>2</sub>), 3.17 (s, 1H, CH), 3.49– $3.59$  (m, 2H, CH<sub>2</sub>), 3.71– $3.82$  (m, 1H, CH), 4.20 (dt,  $J = 5.9, 3.0$  Hz, 1H, CH), 4.44– $4.55$  (m, 1H, CH), 5.03 (bs, 1H, OH), 5.22 (bs, 1H, OH), 5.87 (d,  $J = 7.6$  Hz, 1H, CH=CH), 6.15 (t,  $J = 6.7$  Hz, 1H, CH), 6.97 (s, 1H, NH<sub>2</sub>), 7.50 (s, 1H, NH<sub>2</sub>), 7.68– $7.86$  (m, 2H, CH=CH and NH).



$^{13}\text{C}$  NMR (DMSO- $d_6$ , 101 MHz):  $\delta$  = 22.05, 23.53, 24.89, 49.06, 52.03, 61.83, 70.85, 85.30, 87.66, 95.27, 140.33, 155.42, 163.68, 174.63.

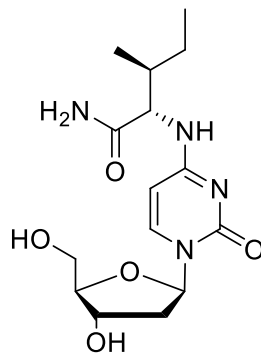
**(2S,3S)-2-((1-((2R,4S,5R)-4-Hydroxy-5-(hydroxymethyl)tetrahydrofuran-2-yl)-2-oxo-1,2-dihydropyrimidin-4-yl)amino)-3-methylpentanamide**

Yield 0.09 g (26%), white solid, mp 156–159 °C.  $R_f$  = 0.79 (1,4-dioxane:isopropanol:H<sub>2</sub>O:NH<sub>4</sub>OH – 4:2:2:1).

MS (ESI<sup>+</sup>):  $m/z$  341.15 [M+H]<sup>+</sup>; 339.15 [M-H]<sup>-</sup>. UV (CH<sub>3</sub>OH)  $\lambda_{\text{max}}$ =274 nm.  $\epsilon_{274}$ =12273 M<sup>-1</sup>cm<sup>-1</sup>.

$^1\text{H}$  NMR (DMSO- $d_6$ , 400 MHz):  $\delta$  = 0.74–0.97 (m, 6H, 2CH<sub>3</sub>), 1.05–1.55 (m, 2H, CH<sub>2</sub>), 1.77 (ddt,  $J$  = 12.9, 6.8, 3.4 Hz, 1H, CH), 1.89–2.01 (m, 1H, CH<sub>2</sub>), 2.10 (ddd,  $J$  = 12.9, 5.7, 3.2 Hz, 1H, CH<sub>2</sub>), 3.48–3.62 (m, 2H, CH<sub>2</sub>), 3.69–3.82 (m, 1H, CH), 4.13–4.27 (m, 1H, CH), 4.41–4.55 (m, 1H, CH), 5.01 (bs, 1H, OH), 5.21 (bs, 1H, OH), 5.98 (d,  $J$  = 7.5 Hz, 1H, CH=CH), 6.16 (t,  $J$  = 6.6 Hz, 1H, CH), 7.05 (s, 1H, NH<sub>2</sub>), 7.53 (s, 1H, NH<sub>2</sub>), 7.69 (d,  $J$  = 9.0 Hz, 1H, NH), 7.76 (d,  $J$  = 7.5 Hz, 1H, CH=CH).

$^{13}\text{C}$  NMR (DMSO- $d_6$ , 101 MHz):  $\delta$  = 11.73, 15.91, 24.91, 26.30, 37.29, 57.63, 61.85, 70.87, 85.30, 87.64, 95.34, 140.29, 155.44, 163.92, 173.38.



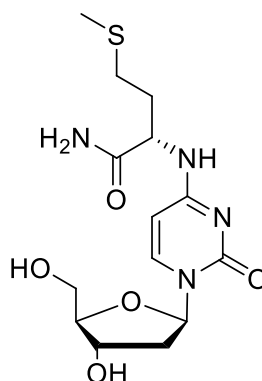
**(S)-2-((1-((2R,4S,5R)-4-Hydroxy-5-(hydroxymethyl)tetrahydrofuran-2-yl)-2-oxo-1,2-dihydropyrimidin-4-yl)amino)-4-(methylthio)butanamide**

Yield 0.21 g (51%), mp 146–148 °C.  $R_f$  = 0.80 (1,4-dioxane:isopropanol:H<sub>2</sub>O:NH<sub>4</sub>OH – 4:2:2:1).

MS (ESI<sup>+</sup>):  $m/z$  359.10 [M+H]<sup>+</sup>; 357.10 [M-H]<sup>-</sup>. UV (CH<sub>3</sub>OH)  $\lambda_{\text{max}}$ =273 nm.  $\epsilon_{273}$ =11600 M<sup>-1</sup>cm<sup>-1</sup>.

$^1\text{H}$  NMR (DMSO- $d_6$ , 400 MHz):  $\delta$  = 1.781.90 (m, 1H, CH<sub>2</sub>), 1.88–2.03 (m, 2H, CH<sub>2</sub>), 2.05 (s, 3H, CH<sub>3</sub>), 2.07–2.17 (m, 1H, CH<sub>2</sub>), 2.40–2.51 (m, 2H, CH<sub>2</sub>), 3.55 (q,  $J$  = 5.3 Hz, 2H, CH<sub>2</sub>), 3.77 (q,  $J$  = 3.7 Hz, 1H, CH), 4.20 (dq,  $J$  = 6.7, 3.3 Hz, 1H, CH), 4.55 (td,  $J$  = 8.4, 4.8 Hz, 1H, CH), 5.00 (t,  $J$  = 5.3 Hz, 1H, OH), 5.22 (d,  $J$  = 4.2 Hz, 1H, OH), 5.90 (d,  $J$  = 7.5 Hz, 1H, CH=CH), 6.15 (t,  $J$  = 6.7 Hz, 1H, CH), 7.08 (s, 1H, NH<sub>2</sub>), 7.51 (s, 1H, NH<sub>2</sub>), 7.78 (d,  $J$  = 7.5 Hz, 1H, CH=CH), 7.83 (d,  $J$  = 8.0 Hz, 1H, NH).

$^{13}\text{C}$  NMR (DMSO- $d_6$ , 101 MHz):  $\delta$  = 15.09, 30.10, 32.38, 40.80, 52.87, 61.83, 70.87, 85.37, 87.67, 95.31, 140.50, 155.38, 163.73, 173.56.



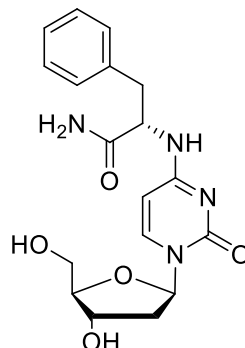
**(S)-2-((1-((2R,4S,5R)-4-Hydroxy-5-(hydroxymethyl)tetrahydrofuran-2-yl)-2-oxo-1,2-dihydropyrimidin-4-yl)amino)-3-phenylpropanamide**

Yield 0.09 g (23%), white solid, mp 165–168 °C.  $R_f = 0.90$  (1,4-dioxane:isopropanol:H<sub>2</sub>O:NH<sub>4</sub>OH – 4:2:2:1).

MS (ESI<sup>+</sup>):  $m/z$  375.10 [M+H]<sup>+</sup>, 373.10 [M-H]<sup>-</sup>. UV (CH<sub>3</sub>OH)  $\lambda_{max} = 276$  nm.  $\epsilon_{276} = 10900$  M<sup>-1</sup>cm<sup>-1</sup>.

<sup>1</sup>H NMR (DMSO-d<sub>6</sub>, 400 MHz):  $\delta = 1.91$  (dt,  $J = 13.1, 6.4$  Hz, 1H, CH<sub>2</sub>), 2.00–2.18 (m, 1H, CH<sub>2</sub>), 2.84 (dd,  $J = 13.8, 9.7$  Hz, 1H, CH<sub>2</sub>), 3.08 (dd,  $J = 13.8, 4.3$  Hz, 1H, CH<sub>2</sub>), 3.48–3.58 (m, 2H, CH<sub>2</sub>), 3.75 (q,  $J = 3.5$  Hz, 1H, CH), 4.11–4.26 (m, 1H, CH), 4.73 (td,  $J = 9.3, 4.4$  Hz, 1H, CH), 5.02 (bs, 1H, OH), 5.25 (bs, 1H, OH), 5.86 (d,  $J = 7.6$  Hz, 1H, CH=CH), 6.08–6.17 (m, 1H, CH), 7.12 (s, 1H, NH<sub>2</sub>), 7.13–7.36 (m, 5H, 5CH), 7.64 (s, 1H, NH<sub>2</sub>), 7.73 (d,  $J = 7.6$  Hz, 1H, CH=CH), 7.94 (d,  $J = 8.3$  Hz, 1H, NH).

<sup>13</sup>C NMR (DMSO-d<sub>6</sub>, 101 MHz):  $\delta = 38.12, 54.99, 61.80, 70.84, 85.31, 87.66, 95.26, 126.72, 128.52, 128.60, 129.59, 138.53, 140.44, 155.33, 163.63, 173.51$ .



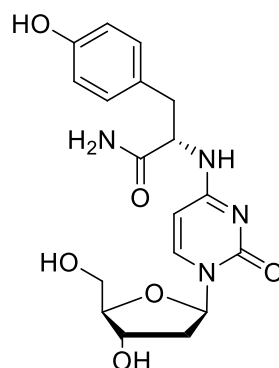
**(S)-2-((1-((2R,4S,5R)-4-Hydroxy-5-(hydroxymethyl)tetrahydrofuran-2-yl)-2-oxo-1,2-dihydropyrimidin-4-yl)amino)-3-(4-hydroxyphenyl)propanamide**

Yield 0.18 g (46%), white solid, mp 170–173 °C.  $R_f = 0.85$  (1,4-dioxane:isopropanol:H<sub>2</sub>O:NH<sub>4</sub>OH – 4:2:2:1).

MS (ESI<sup>+</sup>):  $m/z$  391.15 [M+H]<sup>+</sup>, 389.15 [M-H]<sup>-</sup>. UV (CH<sub>3</sub>OH)  $\lambda_{max} = 276$  nm.  $\epsilon_{276} = 13500$  M<sup>-1</sup>cm<sup>-1</sup>.

<sup>1</sup>H NMR (DMSO-d<sub>6</sub>, 400 MHz):  $\delta = 1.87$ –1.97 (m, 1H, CH<sub>2</sub>), 1.97–2.15 (m, 1H, CH<sub>2</sub>), 2.72 (dd,  $J = 13.8, 9.5$  Hz, 1H, CH<sub>2</sub>), 2.95 (dd,  $J = 13.9, 4.5$  Hz, 1H, CH<sub>2</sub>), 3.51–3.57 (m, 2H, CH<sub>2</sub>), 3.75 (q,  $J = 3.7$  Hz, 1H, CH), 4.16–4.23 (m, 1H, CH), 4.60–4.69 (m, 1H, CH), 5.86 (d,  $J = 7.5$  Hz, 1H, CH=CH), 6.12 (t,  $J = 6.6$  Hz, 1H, CH), 6.64 (d,  $J = 8.5$  Hz, 2H, 2CH), 7.05 (d,  $J = 8.6$  Hz, 3H, 2CH and OH), 7.55 (s, 1H, NH<sub>2</sub>), 7.73 (d,  $J = 7.5$  Hz, 1H, CH=CH), 7.81 (d,  $J = 8.2$  Hz, 1H, NH), 8.23 (s, 1H, NH<sub>2</sub>).

<sup>13</sup>C NMR (DMSO-d<sub>6</sub>, 101 MHz):  $\delta = 24.82, 37.36, 55.27, 61.82, 70.85, 85.34, 87.65, 95.27, 115.33, 128.49, 130.48, 140.38, 155.34, 156.23, 163.61, 173.62$ .



### Appendix 3. Synthesized nucleoside 5'-monophosphates.

#### 2'-Deoxycytidine 5'-monophosphate

Yield 17 mg (4%), white solid.

MS (ESI<sup>+</sup>): m/z 307.75 [M+H]<sup>+</sup>, 305.75

[M-H]<sup>-</sup>. UV (H<sub>2</sub>O) λ<sub>max</sub>=279 nm.

ε<sub>279</sub>=12100 M<sup>-1</sup>cm<sup>-1</sup>.

<sup>1</sup>H NMR (D<sub>2</sub>O, 400 MHz): δ = 2.22–2.30

(m, 1H, CH<sub>2</sub>), 2.31–2.39 (m, 1H, CH<sub>2</sub>),

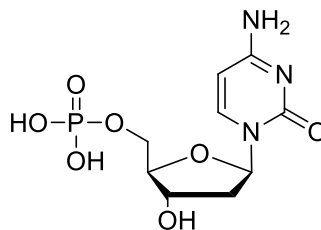
3.92 (h, *J* = 7.2 Hz, 2H, CH<sub>2</sub>), 4.11 (q, *J* =

3.9 Hz, 1H, CH), 4.49 (dt, *J* = 6.9, 3.6 Hz, 1H, CH), 6.06 (d, *J* = 7.5 Hz, 1H,

CH=CH), 6.27 (t, *J* = 6.7 Hz, 1H, CH), 7.95 (d, *J* = 7.6 Hz, 1H, CH=CH).

<sup>13</sup>C NMR (D<sub>2</sub>O, 101 MHz): δ = 39.38, 63.98, 71.06, 85.97, 96.62, 129.37, 141.97, 157.60, 166.17.

<sup>31</sup>P NMR (D<sub>2</sub>O, 162 Hz): δ = 2.05 (s, P<sub>α</sub>).



#### N<sup>4</sup>-Acetyl-2'-deoxycytidine 5'-monophosphate

Yield 11 mg (5%), white solid.

MS (ESI<sup>+</sup>): m/z 349.75 [M+H]<sup>+</sup>, 347.85

[M-H]<sup>-</sup>. UV (H<sub>2</sub>O) λ<sub>max</sub>=243; 296 nm.

ε<sub>243</sub>=11200 M<sup>-1</sup>cm<sup>-1</sup>, ε<sub>296</sub>=6500 M<sup>-1</sup>cm<sup>-1</sup>.

<sup>1</sup>H NMR (D<sub>2</sub>O, 400 MHz): δ = 2.14 (s,

3H, CH<sub>3</sub>), 2.20–2.31 (m, 1H, CH<sub>2</sub>),

2.51–2.64 (m, 1H, CH<sub>2</sub>), 3.66–3.86 (m,

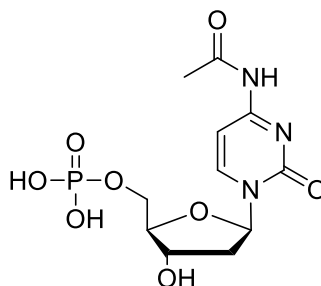
2H, CH<sub>2</sub>), 4.14 (q, *J* = 4.2 Hz, 1H, CH),

4.55 (tt, *J* = 7.8, 4.4 Hz, 1H, CH), 6.17

(t, *J* = 6.3 Hz, 1H, CH), 7.26 (d, *J* = 7.5 Hz, 1H, CH=CH), 8.26 (d, *J* = 7.5 Hz, 1H, CH=CH).

<sup>13</sup>C NMR (D<sub>2</sub>O, 101 MHz): δ = 23.66, 39.40, 61.17, 72.60, 86.81, 87.39, 98.12, 145.68, 157.07, 162.62, 174.10.

<sup>31</sup>P NMR (D<sub>2</sub>O, 162 Hz): δ = 3.34 (s, P<sub>α</sub>).



## 2-Thiouridine 5'-monophosphate

Yield 16 mg (6%), white solid.

MS (ESI<sup>+</sup>): m/z 340.70 [M+H]<sup>+</sup>, 338.75

[M-H]<sup>-</sup>. UV (H<sub>2</sub>O) λ<sub>max</sub>=257 nm.

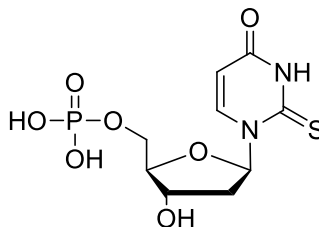
ε<sub>257</sub>=13500 M<sup>-1</sup>cm<sup>-1</sup>.

<sup>1</sup>H NMR (D<sub>2</sub>O, 400 MHz): δ = 4.13 (d, *J* = 13.2 Hz, 1H, CH), 4.29 (d, *J* = 11.9 Hz, 1H, CH), 4.40 (d, *J* = 5.8 Hz, 1H, CH), 4.43–

4.54 (m, 2H, CH<sub>2</sub>), 6.39 (d, *J* = 8.2 Hz, 1H, CH=CH), 6.69 (s, 1H, CH), 8.29 (d, *J* = 8.1 Hz, 1H, CH=CH).

<sup>13</sup>C NMR (D<sub>2</sub>O, 400 MHz): δ = 24.29, 68.95, 74.79, 77.93, 83.46, 118.64, 142.36, 163.16, 181.96.

<sup>31</sup>P NMR (D<sub>2</sub>O, 162 Hz): δ = 2.50 (s, P<sub>α</sub>).



**Appendix 4.** Primers employed for gene amplification of *Dmd*NK-WT, *Bsd*CK-WT and *Ec*ACK by PCR.

Gene Name	Gene Source	Primer Name	Primer Sequence 5'→3'
<i>dNK</i>	pOpen-dromedNK	dNK_F	AGAAGGAGATATAACTATGGCGGAAGCAGCAAGCTG
		dNK_R	GTGGTGGTGATGGTGATGGCCGCGTGCAACACGCTGACG
<i>dCK</i>	<i>B. subtilis</i> 168	dCK_F	AGAAGGAGATATAACTATGAAGGAACATCATATC
		dCK_R	GTGGTGGTGATGGTGATGGCCCTTTTTTTGATTATCATG
<i>ACK</i>	<i>E. coli</i> DH5 $\alpha$	ACK_F	AGAAGGAGATATAACTATGTCGAGTAAGTTAGTAC
		ACK_R	GTGGTGGTGATGGTGATGGCCGGCAGTCAGGCGGCTC

**Appendix 5.** Templates and primers used for site-directed mutagenesis of *Dmd*NK and *Bsd*CK.

Variant	Template	Primer name	Primer Sequence 5'→3'
dNK-W57F	pLATE31-dNK	dNK-W57F-F	GAGCCGGTTGAAAAAttcCGTAATGTTAATGGTG
dNK-W57V	pLATE31-dNK	dNK-W57V-F	GAGCCGGTTGAAAAAgtgCGTAATGTTAATGGTG
dNK-Q81A	pLATE31-dNK	dNK-Q81A-F	GCAATGCCGTTTgegAGCTATGTTACCCTGAC
dNK-Q81A+V84G	pLATE31-dNK-Q81A	dNK-Q81A+V84G-F	GTTTgcgAGCTATGgTACCCTGACCATGCTGCAG
dNK-Q81A+M88G	pLATE31-dNK-Q81A	dNK-M88G-F	GTTACCCTGACCgggCTGCAGAGCCATACCGCACCGAC
dNK-Q81A+A110G	pLATE31-dNK-Q81A	dNK-A110G-F	GAACGCAGCATCTTCAGCggaCGTTATTGTTTTG
dNK-V84A	pLATE31-dNK	dNK-V84A-F	CAGAGCTATgcgACCCTGACCATGCTGCAG
		dNK-V84A-R	GTCAGGGTcgCATAGCTCTGAAACGGCATTG
dNK-V84G	pLATE31-dNK	dNK-V84G-F	GTTTCAGAGCTATggtACCCTGACCATGCTGCAG
dNK-V84A+M88A	pLATE31-dNK-V84A	dNK-V84A+M88A-F	GCTATgegACCCTGACCcgCTGCAGAGCCATACCGCAC
		dNK-V84A+M88A-R	cgCGGTCAGGGTcgCATAGCTCTGAAACGGCATTGC

**Appendix 5 continued.** Templates and primers used for site-directed mutagenesis of *DmdNK* and *BsdCK*.

Variant	Template	Primer name	Primer Sequence 5'→3'
dNK-V84A+A110D	pLATE31-dNK-V84A	dNK-A110D-F	CATCTTCAGCgatCGTTATTGTTTTGTTGAAAATATG
		dNK-A110D-R	CAAAACAATAACGatcGCTGAAGATGCTGCGTTC
dNK-M88A	pLATE31-dNK	dNK-M88A-F	gcgCTGCAGAGCCATACCGCACCGACCAACAAAAAACT
		dNK-M88A-R	ATAGCTCTGAAACGGCATTGCCCATTTTTTCGGATC
dNK-M88G	pLATE31-dNK	dNK-M88G-F	GTTACCCTGACCgggCTGCAGAGCCATACCGCACCGAC
dNK-M88R	pLATE31-dNK	dNK-M88R-F	GTTACCCTGACCaggCTGCAGAGCCATACCGCAC
		dNK-M88R-R	GCTCTGCAGcctGGTCAGGGTAACATAGC
dNK-M88R-A110D	pLATE31-dNK-M88R	dNK-A110D-F	CATCTTCAGCgatCGTTATTGTTTTGTTGAAAATATG
		dNK-A110D-R	CAAAACAATAACGatcGCTGAAGATGCTGCGTTC
dNK-A110D	pLATE31-dNK	dNK-A110D-F	CATCTTCAGCgatCGTTATTGTTTTGTTGAAAATATG
		dNK-A110D-R	CAAAACAATAACGatcGCTGAAGATGCTGCGTTC
dNK-A110G	pLATE31-dNK	dNK-A110G-F	GAACGCAGCATCTTCAGCggaCGTTATTGTTTTG
dCK-R70M	pLATE31-dCK	dCK-R70M-F	atgTTCAAAGAACAGAAAACAATTTTTGAAGC
		dCK-R70M-R	AAGTAAATTTGAAGGTGAAAGCTCCAACG
dCK-R70M+D93M	pLATE31-dCK-R70M	dCK-D93M-F	GATTTATGAAgcgACAGGAATTTTCGCAAAAATG
		dCK-D93M-R	GAAAATTCCTGTcgcTTCATAAATCGAACGATC
dCK-D93M	pLATE31-dCK	dCK-D93M-F	GATTTATGAAgcgACAGGAATTTTCGCAAAAATG
		dCK-D93M-R	GAAAATTCCTGTcgcTTCATAAATCGAACGATC



## SANTRAUKA

Nukleozidai ir nukleotidai yra itin svarbi junginių grupė, atliekanti daugybę gyvybiškai svarbių vaidmenų ląstelėje. Nukleotidai sudaro DNR ir RNR, kurios vykdo genetinės informacijos saugojimo bei pernašos funkcijas, šie junginiai dalyvauja ląsteliniame signalo perdavime, atlieka kofaktorių vaidmenį bei yra pagrindinis energijos šaltinis įvairiuose metaboliniuose procesuose ląstelėse. Dėl nenuginčijamos svarbos minėti junginiai susilaukia daug dėmesio molekulinės biologijos, biotechnologijos bei farmakologijos srityse. Nukleozidų ir nukleotidų analogai dažnai pasitelkiami fermentiniuose tyrimuose, kur jie yra naudojami kaip substratai ar slopikliai kinazėms, polimerazėms, hidrolazėms ir kitiems fermentams. Radioaktyviai ar fluorescenciškai žymėti nukleotidai naudojami kaip zondai nukleorūgščių tyrimuose. Taip pat, tam tikri nukleozidų ir nukleotidų analogai pasižymi priešvėžinėmis ar priešvirusinėmis savybėmis bei įeina į modernių RNR vakcinų sudėtį.

Įprastai, norint gauti modifikuotus nukleotidus yra pasitelkiamas cheminis fosforilinimas, tačiau net ir praėjus keliasdešimčiai metų nuo pirmųjų fosforilinimo metodų sukūrimo, kol kas neegzistuoja vienas, universalus metodas, tinkantis visiems substratams. Cheminis fosforilinimas dažniausiai remiasi fosfochlorido reagentų naudojimu. Šie junginiai yra itin reaktyvūs, higroskopiški bei kenksmingi aplinkai. Cheminis fosforilinimas paprastai atliekamas keliais žingsniais, reikalauja apsauginių grupių naudojimo bei neretai pasižymi žemomis – vidutinėmis galutinio produkto išeigomis. Dėl minėtųjų trūkumų yra ieškoma naujų būdų gauti modifikuotiems nukleotidams. Vienas tokių – fermentinis fosforilinimas, atliekamas nukleozidų kinazių.

Nukleozidų kinazės, skirstomos į ribonukleozidų kinazes (rNK) ir deoksinukleozidų kinazes (dNK), katalizuoja negrįžtamą fosfato grupės pernašą nuo nukleozido trifosfato, dažniausiai ATP ar GTP, ant nukleozido 5'-OH grupės, susidarant nukleozido difosfatui ir nukleozido monofosfatui. Be to, kad nukleozidų kinazės katalizuoja pirmąjį nukleotidų sintezės etapo žingsnį, rNK ir dNK taip pat atlieka įvairių priešvirusinių ir priešvėžinių provaistų aktyvumą *in vivo*. Nukleozidų kinazės yra substratams specifiški fermentai, o jų specifiskumas priklauso nuo aminorūgščių, esančių substrato prijungimo vietose. Šių aminorūgščių dydis ir poliškumas lemia kokie substratai į fermento aktyvųjų centrą prisijungia, o kurie – ne. Prisijungimas yra galimas tik tuomet, kai tarp minėtų aminorūgščių bei nukleozido susidaro palankios sąveikos. Dauguma nukleozidų kinazių pasižymi ganėtinai

kompaktiškoms substratų prisijungimo vietoms ir gali prisijungti tik kanoninius ar nedaug modifikuotus nukleozidus, pavyzdžiui, nukleozidus su metilinta ar fluorinta nukleobaze.

Visi gyvi organizmai, išskyrus grybus, turi bent vieną deoksinukleozidų kinazę. Žinduolių ląstelėse yra keturios dNK, kurių substratiniai selektyvumai šiek tiek persidengia. Deoksicitidino kinazė (dCK) efektyviausiai fosforilina deoksicitidiną, tačiau substratais tinka ir deoksiadenozinas, deoksiguanozinas bei keletas nukleozidų analogų, tokių kaip gemcitabinas, citarabinas ir fludarabinas. Timidino kinazė 2 (TK2) fosforilina kanoninius nukleozidus deoksitimidiną, deoksicitidiną ir deoksiuridiną, bei tam tikrus pirimidino analogus, kaip azidotimidinas, 3'-fluor-2',3'-deoksitimidinas, 5-(2-bromvinil)-2'-deoksiuridinas ir 1-(2'-deoksi-2'-fluor-1-β-D-arabinofuranozil)-5-joduracilas. Deoksiguanozino kinazė (dGK) fosforilina natūralius purino deoksinukleozidus, tokius kaip deoksiguanozinas, deoksiadenozinas ir deoksiinozinas. Šiai kinazei substratais taip pat tinka ir tam tikri purino nukleozidų analogai, tokie kaip 9-β-D-arabinofuranozilguaninas ar 2',2'-difluordeoksiguanozinas. Timidino kinazė 1 (TK1) pasižymi labiausiai apribotu substratiniu spektru – fermentas fosforilina tik deoksitimidiną, deoksiuridiną, azidotimidiną ir 5-halogen-deoksiuridinus.

Lyginant su dNK, rNK yra mažiau ištirti fermentai. Žinduoliuose aptinkami trys rNK variantai: uridino-citidino kinazė 1 (UCK1), uridino-citidino kinazė 2 (UCK2) ir adenzino kinazė (ADK). UCK1 ir UCK2 pasižymi panašiu substratiniu spektru ir fosforilina uridiną ir citidiną bei pirimidino nukleozidų analogus, tokius kaip 6-azauridinas, 5-fluoruridinas ir N<sup>4</sup>-acetilcitidinas. Šios kinazės nefosforilina deoksinukleozidų ar purino nukleozidų. Priešingai, ADK fosforilina tiek ribo-, tiek deoksiadenoziną.

Kitaip nei žinduoliai, vabzdžiai turi tik vieną dNK, fosforilinančią visus kanoninius deoksinukleozidus. Pavyzdžiui, *Anopheles gambiae* turi daugiasubstratę kinazę, gebančią fosforilinti visus keturis kanoninius deoksinukleozidus, pirmenybę teikdama purino nukleozidams. Be natūralių substratų ši kinazė taip pat fosforilina ir nukleozidų analogus, tokius kaip stavudinas, 5-fluor-2'-deoksiuridinas, 2-chlor-2'-deoksiadenozinas ir 5-bromvinil-2'-deoksiuridinas. *Drosophila melanogaster* dNK (*DmdNK*) ir *Bombyx mori* dNK, priešingai, pirmenybę teikia pirimidino nukleozidams, tačiau fosforilinami ir purinai. Be kanoninių nukleozidų šios kinazės taip pat yra aktyvios ir įvairių nukleozidų analogų, tokių kaip 5-fluor-2'-deoksiuridinas, 2',3'-dideoksicitidinas, arabinozilcitozinas, 3'-deoksiadenozinas ir fludarabinas, atžvilgiu. Minėtoji *DmdNK* iš nukleozidų kinazių išsiskiria ne tik itin plačiu substratiniu spektru, bet ir ypač dideliu kataliziniu našumu – tai yra greičiausia žinoma nukleozidų kinazė.

Dauguma bakterijų turi TK, tačiau dCK, dAK ar dGK aktyvumai nėra aptinkami. Dabartinėmis žiniomis tik *Lactobacillus* ir *Bacillus* genčių bakterijos geba fosforilinti visus keturis kanoninius deoksinukleozidus. Pavyzdžiui, *Lactobacillus acidophilus* R26 kamiene, neturinčiame ribonukleotidų reduktazinio aktyvumo, yra aptinkamos dvi papildomos dNK, taip patenkinant ląstelės deoksinukleotidų poreikius. Heterodimeriniai dAK/dGK ir dAK/dCK yra atsakingi už deoksiadenozino, deoksiguanozino ir deoksicitidino monofosfatų sintezę. *Bacillus subtilis* ląstelėse taip pat aptinkamos dvi papildomos dNK: dGK ir dACK/dCK. Fermentas dGK yra aktyvus deoksiguanozino ir deoksiinozino atžvilgiu, o dACK/dCK, dar vadinamas dCK, fosforilina citozino ir adenino nukleozidus su įvairiais cukrumis, tokiais kaip ribozė, deoksiribozė ar arabinozė. Nors ši kinazė ir nėra gerai ištirta, turimi duomenys leidžia manyti, jog ši kinazė pasižymi ganėtinai aukštu kataliziniu našumu.

Nukleozidų kinazės yra sėkmingai pritaikomos fermentinei nukleozidų monofosfatų sintezei. Pavyzdžiui, imobilizuota žmogaus dCK panaudota fludarabino monofosfato gavimui su galutine 55 % išeiga, o imobilizuota dAK iš dirvožemio amebos *Dictostelium discoideum* pritaikyta vidarabino ir fludarabino monofosfatų sintezėms su išeigomis, siekiančiomis 99 %. Nukleozidų kinazės neretai naudojamos ir daugiafermentinėse sistemose. Pavyzdžiui, fermentinė sistema, sudaryta iš *Clostridium perfringens* uridino fosforilazės, *Aeromonas hydrophila* purino nukleozidų fosforilazės ir *Dictyostelium discoideum* deoksiadenozino kinazės buvo sėkmingai panaudota mililitrų-skalės vidarabino monofosfato sintezei, pasiekiant 95 % vidarabino monofosfato išeigą. DmdNK, kartu su uridino monofosfatocitidino monofosfato kinaze ir nukleozidų difosfatų kinaze buvo pasitelkta nukleozidų trifosfatų sintezėms su 75-99 % išeigomis, pradiniais junginiais naudojant citidiną, deoksicitidiną, arabinozilcitoziną bei 5-fluorcitidiną. Ši sistema taip pat buvo papildyta ir piruvato kinaze, kuri atliko ATP regeneravimo funkciją panaudojant fosfoenolpiruvatą. Taip pat, dCK iš *Bacillus subtilis* (BsdCK) kartu su *Lactobacillus delbrueckii* N-deoksi-riboziltransferaze ir *Escherichia coli* acetato kinaze buvo panaudota vieno indo deoksinukleozidų monofosfatų sintezei. Šioje sistemoje N-deoksi-riboziltransferazė katalizavo deoksiribozės perkėlimą nuo deoksitimidino ant adenozino, 2-aminoadenozino bei citozino. Panaudojant GTP kaip fosfato donorą, susidariusį nukleozidą fosforilino BsdCK, o acetato kinazė regeneravo sunaudotą GTP panaudojant acetilfosfatą. Sistemos efektyvumas siekė 62–90 %.

Fermentinio fosforilinimo reakcijoms svarbu pasirinkti su substratu suderinamą nukleozidų kinazę, siekiant užtikrinti geriausią rezultatą. Šių

fermentų siūlomos švelnios reakcijų sąlygos, aukštas regio- bei stereoselektyvumas daro fermentinį nukleozidų fosforilinimą patrauklia alternatyva cheminiams fosforilinimo metodams.

Šio **darbo tikslas** buvo ištirti *DmdNK* ir *BsdCK* panaudojimo fermentinei nukleozidų 5'-monofosfatų sintezei galimybes. Tikslui pasiekti iškelti šie uždaviniai:

- Cheminiais metodais susintetinti  $N^4$ -aminorūgštimis modifikuotus 2'-deoksicitidino nukleozidus, kurie bus panaudojami kaip substratai nukleozidų kinazėms.
- Rasti optimalias reakcijų sąlygas laukinio tipo fermentams *DmdNK* (*DmdNK*-WT) ir *BsdCK* (*BsdCK*-WT).
- Ištirti *DmdNK*-WT ir *BsdCK*-WT substratinius atrankumus.
- Ištirti *DmdNK* aktyviojo centro mutacijų poveikį fermento aktyvumui.
- Praplėsti *BsdCK* tinkamų substratų spektrą pasitelkiant tikslinę mutagenezę.
- Panaudoti *DmdNK*-WT ir *BsdCK*-WT didesnės skalės nukleozidų 5'-monofosfatų sintezei.

Įprastai nukleozidų bazės yra modifikuojamos pirimidinų C5 arba 7-deazapurinų C7 pozicijose, nes šios turi mažiausiai įtakos Vatsono-Kriko porų susidarymui. Kiek mažiau žinoma apie modifikacijas pirimidinų  $N^4$  ir  $O^4$ , bei purinų  $N^6$  ir  $O^6$  pozicijose. Darbo metu susintetinti literatūroje neaprašyti  $N^4$  pozicijoje aminorūgštimis modifikuoti 2'-deoksicitidino nukleozidai. Trijų žingsnių sintezės metu gauti aštuoni Boc apsauginę grupę turintys  $N^4$ -aminorūgštimis acilinti 2'-deoksicitidino dariniai, kurių išeigos siekė iki 85 %. Apsauginės grupės pašalinimo reakcijos metu susintetinti junginiai persitvarkė į *N*-(4-(2'-deoksicitidinil))aminorūgščių amidus, kurie buvo išskirti su 23–57 % galutinėmis išeigomis. Aminorūgščių prijungimas prie deoksicitidino padidina šio nukleozido funkcinę įvairovę ir taip praplečia jo panaudojimo galimybes. Tokie junginiai papildo jau egzistuojančių nukleozidų analogų biblioteką bei gali būti panaudojami kaip substratai įvairių fermentų tokių, kaip nukleozidų fosforilazės, deaminazės ar *N*-deoksiriboziltransferazės, tyrimams. Junginius taip pat galima panaudoti kaip pradinius junginius cheminei ar fermentinei nukleotidų sintezei. Susintetinti deoksicitidino analogai, kartu su papildomais kanoniniais ir modifikuotais nukleozidais, buvo tirti kaip substratai nukleozidų kinazių *DmdNK* ir *BsdCK* substratinių selektyvumų charakterizavimui.

Prieš atliekant nukleozidų kinazių substratinio selektyvumo tyrimus, buvo įvertinta, kokios sąlygos yra optimalios šių kinazių katalizuojamoms reakcijoms vykti. Įvertinti šie parametrai: reakcijos trukmė, temperatūra, reakcijos mišinio pH, nukleozido, fosfato donoro GTP bei nukleozidų kinazių koncentracijos. Nustatyta, jog 10 mM 2'-deoksicitidino fosforiliniui reikia bent 15 mM GTP ir 0,34 nmol/ml *DmdNK*-WT arba 47 nmol/ml *BsdCK*-WT. Didžiausias katalizinis efektyvumas pasiekiamas, kai temperatūra ir mišinio pH yra 70 °C ir 8,0 *DmdNK* atveju arba 60 °C ir 8,5 *BsdCK* atveju. Visgi, siekiant išvengti nukleozidų ir nukleotidų degradacijos bei galimo fermentų denatūravimo reakcijoms vykstant ilgiau nei 5 min, buvo pasirinktos kiek švelnesnės sąlygos: 37 °C ir pH 7,5. Esant tokioms sąlygoms, fermentinių reakcijų trukmė yra 1 val.

Nors *DmdNK*-WT substratinis selektyvumas tyrinėtas nemažai, dauguma eksperimentų atlikti naudojant kanoninius nukleozidus arba nukleozidinius provaistus, kurie dažniausiai turi fluorintą nukleobazę arba ribozei alternatyvų cukrų. Informacijos apie *DmdNK*-WT aktyvumą  $N^4$ - ar  $O^4$ -modifikuotų pirimidino nukleozidu atžvilgiu žinoma nedaug. Priešingai nei *DmdNK*-WT, *BsdCK*-WT yra mažai iširta kinazė. Šis fermentas fosforilina adenino ir citozino 2'-deoksi- ir ribonukleozidus, tačiau nukleozidų analogų fosforilimo galimybės nėra žinomos. Kinazių charakterizavimui buvo pasirinkti pirimidino nukleozidai, turintys įvairaus poliškumo ir dydžio modifikacijas nukleobazėje ar cukruje.

Darbo metu nustatyta, jog *DmdNK*-WT fosforilina ne tik visus kanoninius nukleozidus, bet ir pirimidino nukleozidus, turinčius mažus ir vidutinio dydžio pakaitus  $N^4$  ir  $O^4$  pozicijose, tokius kaip acetil-, hidroksi- ar *sec*-butil-. Palyginus, C5 pozicijoje modifikuoti nukleozidai (su metil- ar fluor-pakaitais) fosforilami ne taip efektyviai. Taip pat atskleista, jog kinazė toleruoja nedideles modifikacijas, tokias kaip *O*-metil- ar amino-, ribozės 2'- ir 3'-pozicijose.

Tyrimai atskleidė, jog *BsdCK*-WT substratinis selektyvumas yra gerokai platesnis, nei galvota anksčiau. Kinazė efektyviai fosforilina ne tik visus kanoninius nukleozidus, bet ir citozino ir uracilo nukleozidus su nedideliais pakaitais  $N^4/O^4$  pozicijoje, tokiais kaip acetil-, hidroksi- ar tio-. Visgi, didesnius pakaitus turintys nukleozidai, pvz.:  $N^4$ -izobutiril- ar  $N^4$ -glicinoil-2'-deoksicitidinas, fosforilunami itin neefektyviai arba nefosforilunami visai. Kaip ir *DmdNK*-WT atveju, nukleozidų analogai, turintys pakaitus C5 pozicijoje, buvo prastesni substratai, lyginant su panašaus dydžio modifikacijas  $N^4/O^4$ -pozicijoje turinčiais nukleozidais. Nedidelės modifikacijos, tokios kaip *O*-metil- ar amino-, ribozės 2'-pozicijoje taip pat yra priimtinos.

Nors *DmdNK*-WT ir *BsdCK*-WT substratiniai spektrai viršijo lūkesčius, tam tikri substratai nebuvo fosforilinami. Tai lėmė tiek nukleozidų modifikacijų dydis, tiek jų poliškumas. Siekiant praplėsti tinkamų substratų spektrą, darbo metu pasitelkta tikslinė mutagenezė: sukurti *DmdNK* ir *BsdCK* mutantai, turintys taškines mutacijas aktyviuosiuose centruose. Viso sukurta šešiolika *DmdNK* mutantinių variantų. Mutagenezei parinktos aminorūgštys, dalyvaujančios nukleozido prisijungime. *DmdNK*-WT aktyviajame centre aminorūgštys V84, M88 ir A110 formuoja hidrofobinę kišenę, kuri, kaip manoma, lemia tokį platų fermento substratinį spektrą. Siekiant praplėsti hidrofobinę kišenę bei pašalinti hidrofobines aminorūgščių grandines, minėtos aminorūgštys buvo pakeistos mažesnėmis – alaninu ir glicinu. Tai ne tik praplėtė hidrofobinę kišenę, bet ir pašalino minėtųjų aminorūgščių hidrofobines grandines, kurios gali sudaryti nepalankias sąveikas su tam tikrais substratais. Taip pat žinoma, jog glutaminas, esantis 81-oje pozicijoje, formuoja vandenilinius ryšius su pirimidino nukleobaze ir taip stabilizuoja nukleozidą fermento aktyviajame centre. Siekiant pašalinti stabilizuojančias jėgas ir suteikti papildomo mobilumo prisijungusiam nukleozidui, Q81 buvo pakeista alaninu. Su prisijungusiu nukleozidu taip pat sąveikauja ir W57 aminorūgštis, sudarydama stekingo sąveiką su nukleobaze. Siekiant nustatyti, ar šios stabilizuojančios sąveikos pašalinimas leis kinazės aktyviajame centre prisijungti stambesniems nukleozidams, W57 buvo pakeista hidrofobinėmis aminorūgštimis fenilalaninu ir valinu.

Nustatyta, jog didžiausi *DmdNK* aktyvumo pokyčiai yra pasiekiami aminorūgštis V84 ir A110 pakeičiant mažesnėmis aminorūgštimis glicinu arba alaninu, tokie *DmdNK* mutantai išsaugo aukštą aktyvumą kanoniniam 2'-deoksicitidinui, tačiau tampa gerokai aktyvesni  $N^4$ -pozicijoje modifikuotų citidinių atžvilgiu. Aminorūgštį W57 pakeitus valinu arba fenilalaninu bendras kinazės aktyvumas sumažėja, kaip ir M88 pakeitus alaninu, glicinu arba argininu. Aminorūgštį Q81 pakeitus alaninu nebuvo pastebėta reikšmingų kinazės aktyvumo pokyčių  $N^4$ -pozicijoje modifikuotų citidinių atžvilgiu.

Siekiant padaryti *BsdCK* panašesnę į *DmdNK* substratinio selektyvumo atžvilgiu, buvo sukurti *BsdCK* mutantiniai variantai, kuriuose *BsdCK* aktyvusis centras atkartoją *DmdNK*-WT aktyvųjų centrą. Nors *BsdCK*-WT kristalinė struktūra ir nėra nustatyta, atlikus kompiuterinį aktyvaus centro modeliavimą ir gautą modelį palyginus su *DmdNK*-WT aktyviuoju centru, buvo nustatytos potencialios aminorūgštys, lemiančios *BsdCK*-WT substratinį selektyvumą. Pagal *in silico* modelį, *BsdCK*-WT aminorūgštys R70 bei D93 atitinka *DmdNK*-WT M88 ir A110 aminorūgštis. Nustatyta, jog *DmdNK*-WT aktyviojo centro imitavimas *BsdCK*-WT aminorūgštis R70 ir D93 pakeičiant metioninu ir alaninu, atitinkamai, padidino kinazės aktyvumą

$N^4$ -pozicijoje modifikuotų citidinių atžvilgiu: *BsdCK* įgijo gebėjimą fosforilinti didesnius pakaitus (pvz.:  $N^4$ -izobutiril- ar  $N^4$ -alaninoil-) turinčius 2'-deoksicitidino nukleozidus, kurių laukinio tipo *BsdCK* nefosforilino.

Norint įvertinti kinazių praktinį pritaikomumą, šios buvo panaudotos didesnės skalės nukleozidų 5'-monofosfatų sintezei: *DmdNK-WT* pasitelkta 2'-tiouridino monofosfato, o *BsdCK-WT* – 2'-deoksicitidino bei  $N^4$ -acetil-2'-deoksicitidino monofosfatų sintezėms. Sintezių metu papildomai panaudota *Escherichia coli* acetato kinazė, kuri, pasitelkiant acetilfosfatą, regeneruoja fosfato donorą GTP iš susiformavusio GDP. Tokios regeneracinės sistemos dėka sintezės tapo tvaresnės ir ekonomiškesnės, nes buvo naudota tik 0,1 mol. ekv. GTP vietoje įprasto 1,5 mol. ekv. Nors galutiniai monofosfatų kiekiai siekė 11–17 mg (4–6 % galutinės išėigos), darbo metu parodyta, jog nukleozidų kinazes galima pritaikyti didesniems nukleotidų kiekiams gauti. Visgi, siekiant geresnių produktų išėigų būtina atlikti papildomus optimizavimo žingsnius.

Darbo metu gauti rezultatai yra svarbūs ne tik iš tiriamosios pusės, bet ir pramoniniu požiūriu. Pasauliui judant žaliosios chemijos link, nukleozidų kinazės gali būti naudojamos kaip katalizatoriai didelės skalės nukleotidų ir jų analogų sintezėje. Aukštas regio- bei stereoselektyvumas, didelės produktų išėigos bei švelnios reakcijų sąlygos, siūlomos nukleozidų kinazių yra patraukli alternatyva daug darbo ir laiko reikalaujantiems cheminiams metodams, kurie dažnai remiasi gamtai nedraugiškų reagentų naudojimu, dideliu atliekų generavimu ir neretai pasižymi žemomis ar vidutinėmis produktų išėigomis. Nukleozidų kinazės gali būti pritaikomos ne tik pramoniniais tikslais, bet ir terapijoje. Jau daugelį metų yra tiriamas tokių fermentų pritaikymas vėžio gydymui. Terapijos metu genas, koduojantis nukleozido kinazę, kartu su netoksišku provaistu yra pristatomas į vėžines ląsteles. Tuomet provaistas yra fosforilinamas į aktyvią formą ir taip selektyviai paveikiamos vėžinės ląstelės, nepažeidžiant aplink esančių sveikų audinių. Kol kas tokiai terapijai dažniausiai pasitelkiama timidino kinazė iš Herpes simplex 1 viruso, tačiau platus *DmdNK-WT* ir *BsdCK-WT* substratinis spektras leidžia manyti, jog šios kinazės taip pat galėtų turėti terapinį potencialą. Galiausiai, tikslinė mutagenezė gali būti panaudota kaip galingas įrankis, norint padidinti kinazių efektyvumą ir pritaikyti jas norimiems substratams.

Suformuluotos šios darbo **išvados**:

1. Trijų žingsnių sintezę galima pritaikyti Boc-apsaugine grupe apsaugotų  $N^4$ -aminorūgštimis modifikuotų deoksicitidino nukleozidų gavimui su vidutine ar didele galutine išėiga (24–85 %).

2. Apsauginės grupės pašalinimo metu  $N^4$ -aminorūgštimis modifikuotus deoksicitidino nukleozidai persitvarko į  $N$ -4-(2'-deoksicitidinil)aminorūgščių amidus, kurių galutinė išeiga 23–57 %.
3. Optimaliam 10 mM 2'-deoksicitidino fosforilnimui, trunkančiam 1 val., reikia bent 1,5 mol. ekv. GTP ir 0,34 nmol/ml *DmdNK*-WT arba 47 nmol/ml *BsdCK*-WT. Didžiausi fermentiniai aktyvumai pasiekiami temperatūrai ir pH esant 70 °C ir 8,0 *DmdNK*-WT atveju ir 60 °C ir 8,5 *BsdCK*-WT atveju.
4. *DmdNK*-WT fosforilina visus kanoninius nukleozidus bei įvairius pirimidino nukleozidų analogus. Substratais tinka uracilo ir citozino nukleozidai, turintys nedidelius-vidutinius pakaitus  $N^4/O^4$  ir C5 nukleobazių pozicijose bei nukleozidai, turintys mažas modifikacijas ribozės 2' ir 3' pozicijose.
5. *BsdCK*-WT fosforilina visus kanoninius nukleozidus ir įvairius uracilo ir citozino nukleozidus su nedideliais pakaitais  $N^4/O^4$  ir C5 nukleobazių arba ribozės 2' ir 3' pozicijose.
6. Aminorūgščių V84 ir A110 pakeitimas alaninu arba glicinu *DmdNK* aktyviajame centre padidina kinazės aktyvumą  $N^4$ -pozicijoje modifikuotų citidino nukleozidų atžvilgiu.
7. Aminorūgščių R70 ir D93 pakeitimas metioninu ir alaninu, atitinkamai, *BsdCK* aktyviajame centre padidina fermento aktyvumą  $N^4$ -pozicijoje modifikuotų citidino nukleozidų atžvilgiu.
8. *DmdNK*-WT ir *BsdCK*-WT kartu su GTP regeneravimo sistema gali būti panaudojamos didesnės skalės nukleozidų monofosfatų sintezei. Darbo metu susintetintų 2'-deoksicitidino,  $N^4$ -acetil-2'-deoksicitidino ir 2-tiouridino monofosfatų galutinė išeiga yra maža ir, norint, jog šių junginių išeiga būtų didesnė, būtinas papildomas reakcijų optimizavimas.



## ACKNOWLEDGEMENTS

I would like to express heartfelt appreciation to my wonderful supervisor Prof. Dr. Rolandas Meškys without whom this thesis would not be possible. I am forever grateful for the invaluable mentorship, infinite patience and unwavering support throughout my scientific journey.

I am also thankful to my former supervisor Dr. Daiva Tauraitė for guiding me throughout my bachelor's and master's studies, and the first year of my doctoral studies. If not for her, I would not be where I am today.

My amazing officemates, Roberta, Justas, and Kamilė, thank you for the numerous work-related “A-ha!” moments, amusing chit-chat and giggles.

I would like to thank my colleagues for the plentiful professional advice and entertaining coffee break conversations.

I could not be more grateful to my better half Simas, my parents and friends for the received support, encouragement, and faith.

## LIST OF PUBLICATIONS

1. **Koplūnaitė, M.**, Butkutė, K., Meškys, R., Tauraitė, D. Synthesis of pyrimidine nucleoside and amino acid conjugates. *Tetrahedron Letters*. 2020; 61(49): 152598. DOI: 10.1016/j.tetlet.2020.152598
2. **Koplūnaitė, M.**, Butkutė, K., Špelveris, D., Urbelienė, N., Meškys, R. Enzymatic synthesis of modified nucleoside 5'-monophosphates. *Catalysts*. 2022; 12(11): 1401. DOI: 10.3390/catal12111401
3. **Koplūnaitė, M.\***, Butkutė, K.\*, Stankevičiūtė, J., Meškys, R. Exploring the mutated kinases for chemoenzymatic synthesis of  $N^4$ -modified cytidine monophosphates. *Molecules*. 2024; 29(16): 3767. DOI: 10.3390/molecules29163767

\* The authors contributed equally to this work.

## SCIENTIFIC PARTICIPATION

### Conference presentations

1. **Koplūnaitė, M.**, Butkutė, K., Špelveris, D., Meškys, R. Enzymatic nucleoside 5'-monophosphate synthesis and substrate specificity comparison of *D. melanogaster* deoxynucleoside kinase and *B. subtilis* deoxycytidine kinase. 10<sup>th</sup> International Congress on Biocatalysis. Hamburg, Germany, 2022 August 28 – September 1.
2. **Koplūnaitė, M.**, Butkutė, K., Meškys, R. Enzymatic synthesis of modified nucleoside 5'-monophosphates. The 47<sup>th</sup> FEBS Congress. Tours, France, 2023 July 8 – 12.

### Patent and patent application

1. **Koplūnaitė, M.**, Urbelienė, N., Meškys, R., Iksalaitė, D., Zakrys, L., Karpus, L. C-Nucleoside monophosphate synthesis. UK patent GB2614570A.
2. **Koplūnaitė, M.**, Urbelienė, N., Meškys, R., Iksalaitė, D., Zakrys, L., Karpus, L., Ruggieri, F., Grobe, S. C-Nucleoside monophosphate synthesis. International patent WO2023131727A1.

## CURRICULUM VITAE

Martyna Koplūnaitė

Vilnius University Life Sciences Center

Sauletekio av. 7, LT-10257 Vilnius, Lithuania

Phone: +370 636 21957

E-mail: [martyna.koplunaite@gmc.vu.lt](mailto:martyna.koplunaite@gmc.vu.lt)

### Education

2014–2018 Bachelor's degree in Biochemistry, Vilnius University

2018–2020 Master's degree in Biochemistry, Vilnius University

### Scientific work experience

2020–2023 Junior scientist, Vilnius University, Institute of Biochemistry, Department of Molecular Microbiology and Biotechnology

2024–Present Junior scientist, Vilnius University, Institute of Biochemistry, Department of Molecular Microbiology and Biotechnology

### Published scientific research

1. Urbelienė, N., Kutanovas, S., Meškienė, R., Gasparavičiūtė, R., Tauraitė, D., **Koplūnaitė, M.**, Meškys, R. Application of the uridine auxotrophic host and synthetic nucleosides for a rapid selection of hydrolases from metagenomic libraries. *Microbial Biotechnology*. 2019; 12(1): 148-160. DOI: 10.1111/1751-7915.13316

2. **Koplūnaitė M.**, Butkutė K., Meškys R., Tauraitė D. Synthesis of pyrimidine nucleoside and amino acid conjugates. *Tetrahedron Letters*. 2020; 61(49): 152598. DOI: 10.1016/j.tetlet.2020.152598

3. **Koplūnaitė M.**, Butkutė K., Špelveris D., Urbelienė N., Meškys R. Enzymatic synthesis of modified nucleoside 5'-monophosphates. *Catalysts*. 2022; 12(11): 1401. DOI: 10.3390/catal12111401

4. Preitakaitė V., Barasa P., Aučynaitė A., Plakys G., **Koplūnaitė M.**, Zubavičiūtė S., Meškys R. Bacterial amidohydrolases and modified. 5-fluorocytidine compounds: Novel enzyme-prodrug pairs. *PLoS ONE*. 2023; 18(11): e0294696. DOI: 10.1371/journal.pone.0294696

5. **Koplūnaitė, M.\***, Butkutė, K.\*, Stankevičiūtė, J., Meškys, R. Exploring the mutated kinases for chemoenzymatic synthesis of  $N^4$ -modified cytidine monophosphates. *Molecules*. 2024; 29(16): 3767. DOI: 10.3390/molecules29163767

\* The authors contributed equally to this work.

## NOTES

## NOTES

## NOTES

Vilniaus universiteto leidykla  
Saulėtekio al. 9, III rūmai, LT-10222 Vilnius  
El. p. [info@leidykla.vu.lt](mailto:info@leidykla.vu.lt), [www.leidykla.vu.lt](http://www.leidykla.vu.lt)  
Tiražas 12 egz.